Profiling and Characterization of Different Propolis Samples and Their Activities Against *Trypanosoma brucei*, *Trypanosoma congolense* and *Crithidia fasciculata*

This Thesis Presented For

The Degree of Doctor of Philosophy in Pharmaceutical Sciences in Strathclyde Institute of Pharmacy and Biomedical Science

By

Samya S. Alenezi

B.Sc., M.Sc.

University of Strathclyde
161 Cathedral Street
Glasgow
G4 0RE
United Kingdom

Declaration

'I declare that, except where specifically indicated, all the work presented in this report is my own and I am the sole author of all parts.'

'The copyright of this thesis belongs to the author under the terms of the United Kingdom Copyright Acts as qualified by University of Strathclyde Regulation 3.50. Due acknowledgement must always be made of the use of any material contained in, or derived from, this thesis.'

Acknowledgements

Table of Contents

List of Tables

List of Figures

List of Abbreviations

^{13}C NMR	Carbon Nuclear Magnetic Resonance
^{1}H NMR	Proton Nuclear Magnetic Resonance
2D NMR	Two-Dimensional Nuclear Magnetic Resonance Spectroscopy
AAT	Animal African Trypanosomiasis
ACN	Acetonitrile
BSF	Bloodstream Form
Calc.	Calculated exact mass
CC	Column Chromatography
$CDCl_3$	Deuterated Chloroform
Conc.	Concentration
COSY	Correlation Spectroscopy (COSY)
D	Doublet
DMEM	Dulbecco's Modified Eagle's Medium
DCM	Dichloromethane
DEPT	Distortionless Enhancement by Polarization Transfer
DMSO	Dimethyl sulfoxide
DMSO-d6	Deuterated Dimethyl Sulfoxide
EC_{50}	Half Maximal Effective Concentration
EEP	Ethanol Extract of Propolis
FBS	Fetal Bovine Serum
ELSD	Evaporative Light Scattering Detector
ESI-MS	Electrospray Ionization Mass Spectrometry
EtOAc	Ethyl Acetate
GC-MS	Gas Chromatography Mass Spectrometry
HAT	Human African Trypanosomiasis
HSQC	Heteronuclear Single Quantum Coherence
HMBC	Heteronuclear Multiple Bond Correlation
HPLC	High Performance Liquid Chromatography
Hz	Hertz
IC_{50}	The half maximal Inhibitory Concentrations
IR	Infrared

LC	Liquid Chromatography
M	Multiple
MS/MS	Tandem Mass Spectrometry
MeOH	Methanol
mg	milligram
MHz	Megahertz
Min	Minute
ml	Millilitre
µl	Microlitre
MPLC	Medium Pressure Liquid Chromatography
MS	Mass Spectroscopy
NMR	Nuclear Magnetic Resonance
NO	Nitric Oxide
no.	Number
PNG	Papua New Guinea
PCA	Principal Component Analysis
PLS	Partial Least Squares
RDBE	Ring Double Bond Equivalent
RT	Retention Time
R_f	Retention Factor
rpm	Round Per Minute
RSD	Relative Standard Deviation
S	Singlet
SEC	Size-Exclusion Chromatography
SPE	Solid-Phase Extraction
SD	Standard Deviation
T	Triplet
T.b. brucei	Trypanosoma brucei brucei
T. congolense	Trypanosoma congolense
TLC	Thin Layer Chromatography
UV	Ultraviolet light
WT	Wild Type

Published Work

Chapter 5 of this thesis have been published

• Novel flavanones with anti-trypanosomal activity isolated from Zambian and Tanzanian propolis samples

Alenezi, S.S., Natto, M.J., Igoli, J.O., Gray, A.I., Fearnley, J., Fearnley, H., de Koning, H.P. and Watson, D.G., 2020 Oct 31. International Journal for Parasitology: Drugs and Drug Resistance

List of other Publication

• Antitrypanosomal and antileishmanial activity of chalcones and flavanones from polygonum salicifolium.

Zheoat, A.M., **Alenezi, S**., Elmahallawy, E.K., Ungogo, M.A., Alghamdi, A.H., Watson, D.G., Igoli, J.O., Gray, A.I., de Koning, H.P. and Ferro, V.A., 2021. Pathogens, 10(2), p.175.

• Antiparasitic and cytotoxic activity of bokkosin, a novel diterpene-substituted chromanyl benzoquinone from Calliandra portoricensis.

Nvau, J.B., **Alenezi, S.**, Ungogo, M.A., Alfayez, I.A., Natto, M.J., Gray, A.I., Ferro, V.A., Watson, D.G., De Koning, H.P. and Igoli, J.O., 2020. Frontiers in chemistry, 8.

• Contribution in writing chapter 7 of book Bee Products:

The Chemical and Biological Properties of Propolis. In Bee Products-Chemical and Biological Properties

Siheri, W., **Alenezi, S.**, Tusiimire, J. and Watson, D.G., 2017. Springer, Cham. (pp. 137-178).

• Preliminary studies: the potential anti-angiogenic activities of two Sulawesi Island (Indonesia) propolis and their chemical characterization

Iqbal, M., Fan, T.P., Watson, D., **Alenezi, S.,** Saleh, K. and Sahlan, M., 2019. Heliyon, 5(7), p.e01978

• European propolis is highly active against trypanosomatids including Crithidia fasciculata.

Alotaibi, A., Ebiloma, G.U., Williams, R., **Alenezi, S**., Donachie, A.M., Guillaume, S., Igoli, J.O., Fearnley, J., de Koning, H.P. and Watson, D.G., 2019. Scientific Reports (Nature Publisher Group), 9, pp.1-10.

• Isolation of a novel flavanonol and an alkylresorcinol with highly potent anti-trypanosomal activity from Libyan propolis.

Siheri, W., Ebiloma, G.U., Igoli, J.O., Gray, A.I., Biddau, M., Akrachalanont, P., **Alenezi, S**., Alwashih, M.A., Edrada-Ebel, R., Muller, S. and Lawrence, C.E., 2019. Molecules, 24(6), p.1041.

Abstract

It is becoming increasingly clear that one of the major biological activities of propolis is anti-protozoal activity. This study aimed to investigate the chemical profile of different propolis samples and examine their *in vitro* activity of against the protozoal parasites: *Crithidia fasciculata*, *Trypansoma congolense*, drug resistant *Trypansoma congolense* (6C3)*, Trypanosoma b. brucei* and pentamidine resistant *Trypanosoma brucei* (B48), which cause disease in humans and other animals as well as insects. In addition, the samples were assayed for their toxicity against human U937 cells and murine RAW 246.7 cells *in vitro*.

Chemical profiling was conducted by using negative ion spray ESI (LC-MS) with principal components analysis (PCA) of the data obtained and indicated that there was a wide variation in the composition of the propolis samples. The active principles were targeted for isolation by bioassay-led fractionation, using medium pressure chromatographic (MPLC) and/or other chromatographic methods, including column chromatography CC, Thin Layer Chromatography (TLC) and Size Exclusion Chromatography (SEC) and Solid-phase extraction (SPE). Twenty pure compounds were isolated, and their structures were elucidated by spectroscopic methods. Twelve triterpenoid compounds were identified from Papua New Guinea propolis as: mangiferonic acid (**1**), isomangiferolic acid (**2**), 27-hydroxyisomangiferolic acid (**3**), cycloartenol (**4**), ambonic acid (**5**), ambolic acid (**6**), 24-methylenecycloartenol (**7**), cycloeucalenol (**8**), 20-hydroxybetulin (**9**), botulin (**10**), betulinic acid (**11**) and madecassic acid (**12**). Three flavanones were isolated from Tanzanian and Zambian propolis, two of them were found to be novel compounds. They were characterized based on their spectral and physical data and identified as 6-(1,1-dimethylallyl) pinocembrin (**13**) and 5-hydroxy-4″,4″-dimethyl-5″-methyl-5″-*H*-dihydrofuranol [2″,3″,6,7] flavanone (**15**). While the other compound was a known compound 6-(1,1-dimethylallyl) eriodictyol (**14**). Fractionation of a Nigerian propolis sample yielded of five known flavanones, isoflavan and the isoflavonoids 7-O-methylvestitol (**16**), neovestitol (**17**), vestitol (**18**), medicarpin (**19**) and 7-hydroxyflavanone (**20**). The samples had high levels of activity against *T. congolense* and *T. b..brucei* and moderate activity against *Crithidia fasciculata.* The crude sample extracts displayed a high selectivity index against kinetoplastid parasites compared to mammalian cells. The Tanzanian, Zambian and Nigerian propolis extracts were found to be more active than their purified compounds in these assays. A growth curve of *T. brucei* at concentrations $\geq$ EC$_{50}$ of the most active purified compounds in these assays was conducted and found that 20-

hydroxybetuline was trypanostatic with an IC_{50} of 2.04 μg/ml against *T. b. brucei*. Overall, the propolis extracts showed lower toxicity than the purified compounds to both U937 and RAW 26.7 cells.

Chapter one

1 General Introduction

1.1   Overview of Propolis

Bees produce several different products, which have health benefits. There is no doubt that honey has a highly significant status in medical treatments, while other apian materials, such as wax, royal jelly and propolis have fewer medical applications, despite the fact that propolis has been used by people since ancient times (Ghisalberti, 1979, Burdock, 1998a). The term propolis comes from two Greek words, pro (which means for or in defence of) and polis (which means the city); thus, propolis means in defense of the city or beehive (Ghisalberti, 1979). Propolis is a sticky resinous substance, which is gathered from buds and the bark of trees. It is also known as "bee glue" as bees use it to cover surfaces, seal holes in their hives. This maintains a healthy environment in the hive and protects them from microbes, infections and spore-producing organisms, including fungi and molds (Wagh, 2013). It is therefore considered to be a potent chemical weapon against bacteria, viruses, and other pathogenic microorganisms that may invade the bee colony. Also, bees use propolis as an embalming substance, to mummify invaders, such as other insects, that have been killed and are too heavy to remove from the colony (Bankova, 2005, Wagh, 2013). Humans certainly have observed the behaviors of honeybees and how they use propolis in their hives, which might have inspired interest in the biological properties of bee glue. Therefore, it is not surprising that propolis has been an area of interest in natural products studies in recent times. The literature on propolis is very large and even a lengthy review cannot cover all of the literature but can only give an indication of the areas of interest in propolis research. There have been many reviews of the chemical and biological properties of propolis over the years and the most recent ones are listed here: (Sforcin and Bankova, 2011, Toreti et al., 2013, Wagh, 2013, Bankova et al., 2014, Chandna et al., 2014, Silva-Carvalho et al., 2015, Bankova et al., 2016, Sforcin, 2016, Pasupuleti et al., 2017). For a recent comprehensive review of the biological properties of propolis see (Santos, 2020)

1.2   Propolis in History

The ancient Greeks, Romans, and Egyptians, were the first to use propolis and they used it for wound healing and as a disinfection substance (Sforcin, 2007). The long history of the use of propolis as a medicine is claimed to be as old as the use of other honeybee products, with the former being used from at least 300 BC (Ghisalberti, 1979, Burdock, 1998b, Sforcin, 2007).

According to Egyptian history, propolis was one of the main ingredients used in an embalming recipe for mummification where it played the role of a preservative agent (Mejanelle et al., 1997, Kuropatnicki et al., 2013). Also, many other ancient civilizations, such as the Chinese, Indian, and Arabian, all believed in the power of propolis to treat medical conditions like sores, ulcers, and some skin lesions, so it was used both internally and externally. For a comprehensive review of the history of propolis use see (Kuropatnicki et al., 2013).

1.3   Propolis in Present Time: Problem of Standardization

In recent years, there has been renewed interest in the study of the beneficial therapeutic properties of propolis, via the study of chemical profiling and biological properties of numerous samples from different geographic regions as an attempt to set a general standardization of the composition of propolis in each single specific region. Despite being used from early times, propolis is often still counted as "folk medicine" and is still an unofficial drug in the field of pharmacy (Kuropatnicki et al., 2013, Toreti et al., 2013, Valenzuela-Barra et al., 2015). However, over the last two decades, its use has begun to have scientific backing. It is considered to be a promising natural source for the discovery of new pharmaceutical products to treat several types of diseases. Thus, it has been subjected to intensive studies, dealing with antioxidant, antimicrobial, anti-inflammatory, immune-modulatory, and anticancer properties (Banskota et al., 2001). Nevertheless, propolis is still not yet considered as an official conventional medicine in the health system because of a lack of standardization of its chemical composition, due to the variability of its chemical components and thus its biological activity, which varies according to the different geographic locations of its collection (Silva-Carvalho et al., 2015). In addition, there is presently inadequate data regarding therapeutic efficacy from clinical trial studies involving propolis. As a result, there are only a few propolis products, which have received Food and Drug Administration FDA approval (Fitzmaurice et al., 2011).

1.4   Propolis Characteristics
1.4.1   Chemical components of propolis

In general, propolis contains about 50% of resin and vegetable balms, around 30% wax, approximately 10% essential and aromatic oils, while the last 10% is composed of 5% pollen and 5% various biologically active organic compounds that derived from secondary metabolites that are produced by plants (Marcucci, 1995, Luis-Villaroya et al., 2015). The latter include

flavonoids, phenolic acids and their esters such as polyphenolic esters, as well as terpenoids, steroids, amino acids, aromatic aldehydes, ketones, alcohols, caffeic acids and their esters (Marcucci, 1995, Sforcin, 2007). **Figures 1-1** to **1-4** show the chemical structures of some compounds commonly identified in propolis from different African origins and covered in literature reviews (Blicharska and Seidel, 2019).There are various types of propolis dispersed all over the world which are distinct in their chemical, physical, and textural characteristics. Such differences are related to their geographic origin and composition differs significantly between various geographical zones and depends on prevailing climatic conditions and environmental factors (Freires et al., 2016, Alencar et al., 2007, Toreti et al., 2013).

Cinnamic acid   Caftaric acid

Coumaric acid   Prenyl caffeate

Caffeic acid   Isoferulic acid
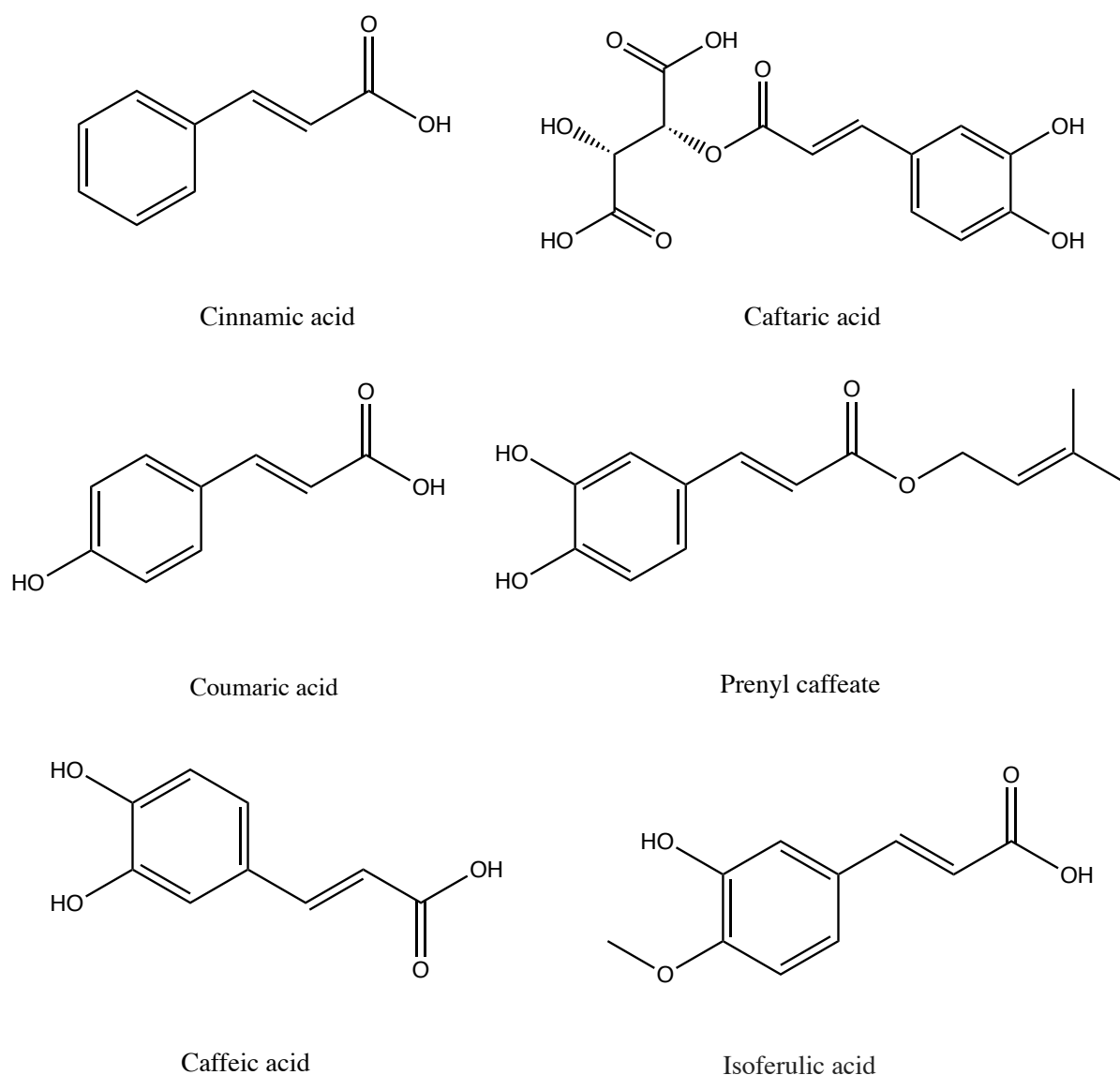
Figure 1-1: Chemical structures of the phenylpropanoids isolated from African propolis

Acacetin

Quercetin

Chrysin

Tectochrysin

Galangin

Pinocembrin

Ladanein

Apigenin

Naringenin

6,8-Diprenyleriodictyol

Pinostrobin

6-Prenylnaringenin
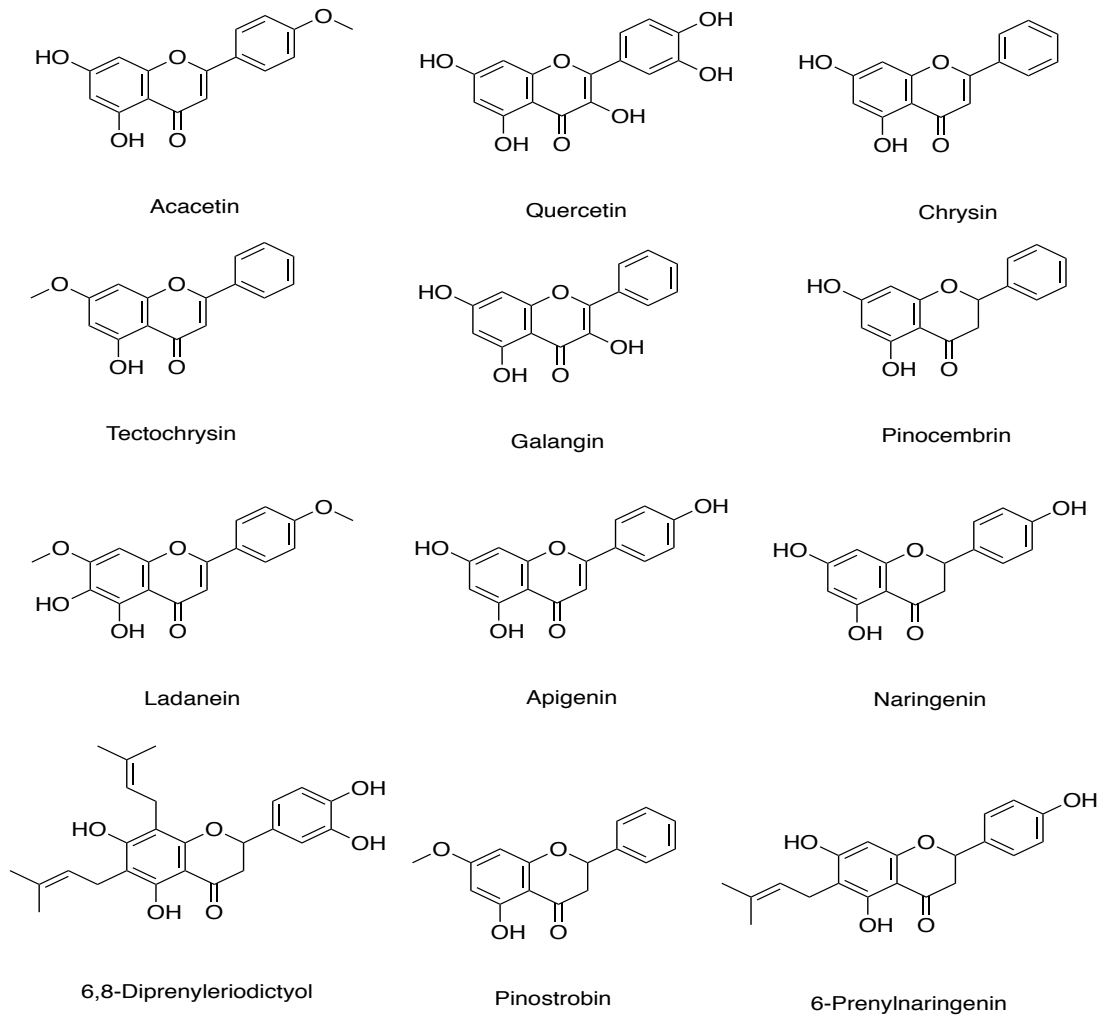
Figure 1-2: Chemical structures of the flavones and flavanones isolated from African propolis

Pinobanksin

Vestitol

Calycosin

Genistein

Liquiritigenin

Medicarpin
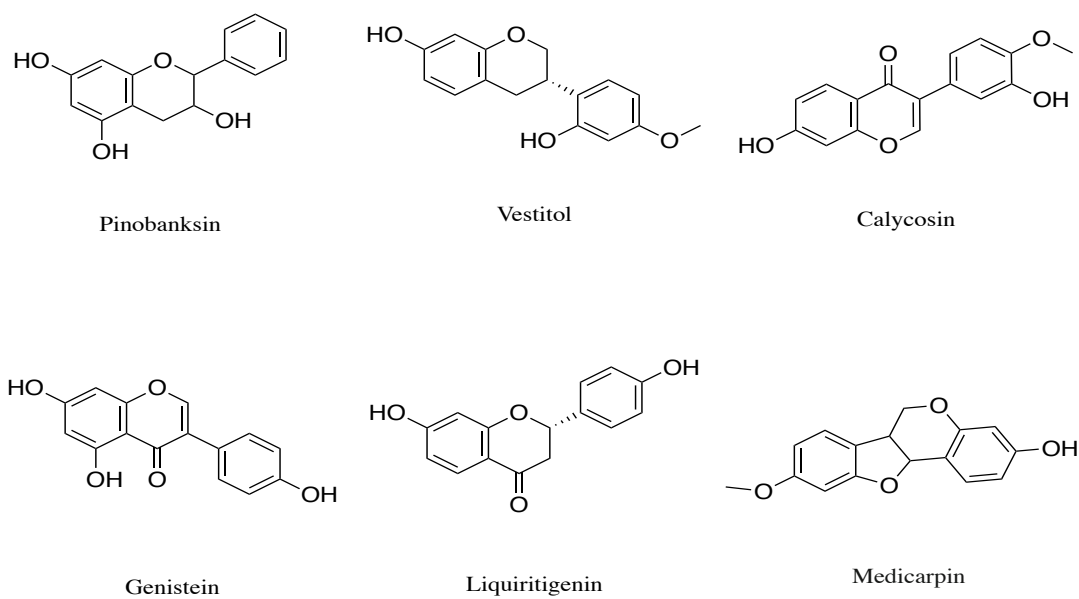
Figure 1-3: Chemical structures of other flavonoids isolated from African propolis
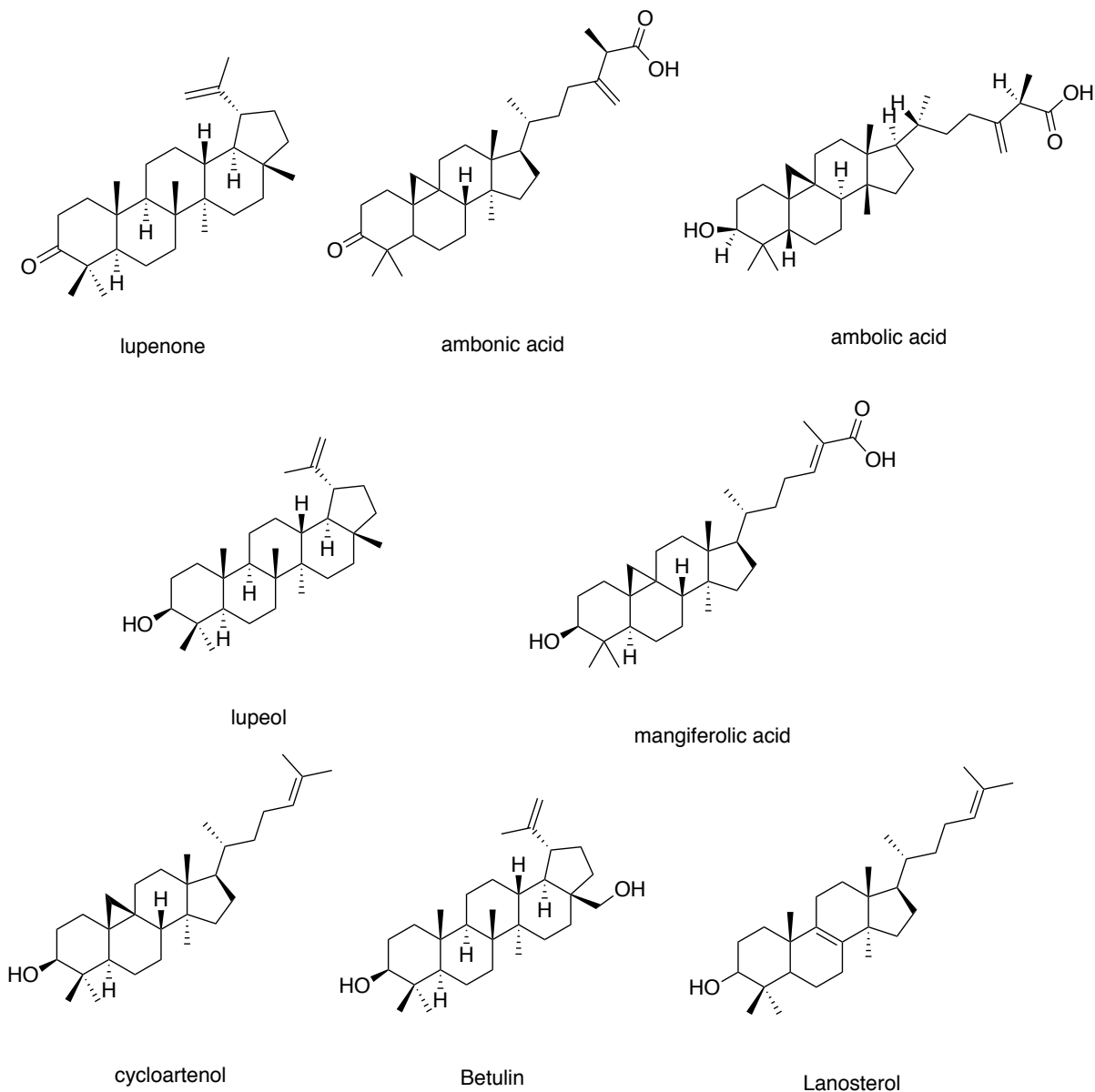
Figure 1-4: chemical structures of some terpenoids isolated from African propolis.

1.4.2 Biological properties of propolis

The bioactivity of propolis mainly depends on its chemical composition. Bankova stated that knowledge of the chemical composition of propolis leads to a prediction of its biological activities (Bankova, 2005). In general, the term biological activity describes the pharmacological activity of a substance in a living organism. However, when the therapeutic product is a complex mixture, the biological activity could be broadly based due to a multiplicity of active ingredients and thus the product could have many therapeutic indications (Jackson et al., 2007). This is the case with propolis, which usually contains many active components, and these lead to numerous pharmacological activities. Propolis has been

demonstrated to be safe and non-toxic for human use. However, some cases of allergic reactions such as contact dermatitis have been reported by beekeepers. There is some variability in the toxic and safe dosages of propolis reported by different studies and this is probably due to the lack of standardized extraction methods (Burdock, 1998a). The effectiveness of propolis preparations is dependent on the method of preparation, including the solvents used during the extraction process (Silva-Carvalho et al., 2015). The following sections will give an overview of some of the biological activity, mainly antimicrobial, studies that have been conducted on propolis samples from different parts of the world.

1.4.2.1 The Antioxidant Properties of Propolis

Many scientific papers have been published on the antioxidant effects of propolis (Piccinelli et al., 2013, Bittencourt et al., 2015,). The relationship between antioxidant activity and the chemical composition of propolis from different origins has been investigated by several authors (Isla et al., 2001, Kalogeropoulos et al., 2009, Mello and Hubinger, 2012, Piccinelli et al., 2013). These studies confirmed that the significant antioxidant activity of propolis is related to the high content of polyphenolic compounds, such as flavonoids, in the sample. Additionally, it has been reported that the essential oil constituents of Thymus vulgaris (thyme) could act as antioxidant agents (Deans et al., 1992). Since one of the main components of propolis has been proven to be essential oils (Marcucci, 1995, Bankova et al., 2014), it might be possible that these components contribute to its antioxidant effects. The study conducted by Kumazawa et al. suggested that propolis could act as an antioxidant agent due to the presence of anti-oxidative compounds such as kaempferol and phenethyl caffeate (Kumazawa et al., 2007). Their conclusion came following the investigation of antioxidant activities of various propolis samples from different geographical origins using the DPPH (2,2-diphenyl-1-picryl-hydrazyl-hydrate) assay.

1.4.2.2 Antimicrobial Properties of Propolis

The most widely investigated property of propolis is its antimicrobial activity, with hundreds of publications on this topic having appeared in the last 50 years (Bogdanov, 2012). Different propolis types contain many chemical constituents responsible for their antimicrobial properties (Bankova, 2005) and it seems that the sum of the propolis antimicrobial components, rather than individual substances, is responsible for the observed antimicrobial effect (Kujumgiev et al., 1999, Bogdanov, 2012). However, according to several papers, there are

many components which are responsible for the biological activity of propolis and these vary with propolis sample type and the solvents used in its extraction (Ugur and Arslan, 2004). Flavonoids and esters of phenolic acids are generally regarded as bioactive compounds which are responsible for antimicrobial activity (Fokt et al., 2010). However, there are many other components with such activity like terpenes, caffeic acid and essential oils (Bogdanov, 2012).

1.4.2.3 Antibacterial properties of propolis

Antibacterial activity is recognised as the most important property of propolis, several studies have been performed to evaluate this property against a large group of Gram-positive and Gram-negative bacteria; both aerobic and anaerobic types. The results of these studies have been recently reviewed (Fokt et al., 2010). Over the last two decades, there have been numerous analytical studies, which describe the antimicrobial properties of propolis, and have identified many active components against various types of microbes. Such a study was conducted by Popova and showed that the antibacterial activities of propolis which have been taken from different regions of Turkey are closely associated with the presence of the following compounds; phenolics, flavones and flavanones (Popova et al., 2005). The flavonoids galangin, pinocembrin and pinostrobin have been most associated with the antibacterial properties of propolis (Bogdanov, 2012). Also, it was also found that propolis showed strong antibacterial activity against 13 different bacterial pathogens (Basim et al., 2006). More recent research has revealed the chemical composition of Brazilian propolis extracts and then, evaluated the extracts on various types of bacteria, the results reported that the propolis sample has effective antimicrobial activities against different bacteria (de Lima et al., 2016).

1.4.2.4 Antifungal properties of propolis

Several studies of the antifungal properties of propolis were conducted based on chemical analysis of propolis linked to bioassay. Polyphenols and flavonoids, terpenes, caffeic acid phenethyl ester (CAPE) and other caffeates are generally regarded as bioactive compounds which are responsible for antifungal activity (Bogdanov, 2012). A study of Brazilian propolis against several strains of Candida yeast was carried out: 20 strains of Candida albicans, 20 strains of *Candida tropicalis*, 20 strains of *Candida krusei*, and 15 strains of *Candida guilliermondii*. The propolis showed clear antifungal activity with the following order of sensitivity: *C. albicans > C. tropicalis > C. krusei > C. guilliermondii*. MICs were in the range 8–12 mg/ml. Patients with full dentures who used a hydroalcoholic propolis extract showed a

decrease in the number of Candida in their saliva (Ota et al., 2001). In a further study patients treated with a commercial ethanol extract of propolis showed lesion regression similar to that observed in patients treated with nystatin (Santos et al., 2005). A study conducted by Freires et al. investigated the chemical composition of Brazilian propolis extract by GC-MS, the chemical analysis found many bioactive fractions including antifungal potential compounds such as quercetin and medicarpin. After which that the bioassay experiment was conducted, the results showed that the Brazilin propolis samples have strong antifungal activities against Candida spp. and yeast growth (Freires et al., 2016). Another study, published bySalas *et al*. demonstrated the antifungal activity of Argentinian propolis against ten Candida strains (Salas et al., 2016).

1.4.2.5 Antiprotozoal properties of propolis

Recently, attention has been focused on the antiparasitic activity of propolis since an improvement from the existing drugs against several tropical diseases caused by different protozoa is required. Numerous assessments have been performed using different *in vivo* and *in vitro* experiments to investigate the activity of propolis and active compounds isolated from propolis. Accordingly, the literature has reported significant effects of propolis against a range parasitic species including: *Cholomonas paramecium, Eimeria magna, Eimeria perforans*, *Giardia lambia, Giardia duodenalis, Trypanosoma cruzi* and *Trypanosoma brucei, Trypanosoma congolense, Crithidia fasciculata* (De Castro and Higashi, 1995, Marcucci, 1995, Freitas et al., 2006, Parreira et al., 2010, Salomão et al., 2010, Almutairi et al., 2014, Falcão et al., 2014, Siheri et al., 2014, Siheri et al., 2016a,). For a recent comprehensive review of the promising anti-protozoan activities of propolis see (Asfaram et al., 2020).

1.4.2.6   Kinetoplastid and Ttrypanosomiasis

Kinetoplastid protozoan parasites cause some of the world's most neglected infectious diseases, trypanosomiasis and leishmaniasis. Trypanosomatids comprise of a group of unicellular flagellated protozoans that are characterized by the presence of large massed DNA structures, known as kinetoplasts. Which are characterized by the presence of a single mitochondrion possessing a large amount of DNA (Stuart et al., 2008). Different species of *Trypanosoma* are responsible for debilitating diseases of humans, the most common genus of the *Trypanosomatidae* class is *Trypanosomes*, which infect a diversity of different vertebrates, including humans, causing Human African Trypanosomiasis (HAT) also known as African

sleeping sickness (Human African trypanosomiasis, HAT), which is transmitted an insect vectors known as the tsetse fly. Other species of Trypanosomes cause Animal African Trypanosomiasis (AAT), including *T. congolense* and *T. vivax*. *T. equiperdum*, and the insect parasites such as all species of Crithidia (insect-to-insect transmission), which are transmitted by direct contact of the host with the pathogen itself without an intermediate host or vector. All other pathogenic trypanosomatids are heteroxenous (they need more than one obligatory host to complete their life cycle) or are transmitted by animal (insect) vectors. They are generally found in the midgut of an invertebrate host, but usually occupy the bloodstream when they invade the mammalian host (Barrett et al., 2003, Stuart et al., 2008, Sternberg, 2004). Tsetse-borne trypanosomiases are endemic in 37 out of 54 African countries, with serious economic and public health consequences (Yaro et al., 2016, Büscher et al., 2017). Although significant progress is being made towards the elimination of HAT as a major public health problem in Western Africa (Franco et al., 2017), tens of millions of cattle, sheep, and goats as well as millions of donkeys, camels and horses are at risk of AAT (Giordani et al., 2016).

1.4.2.6.1 Trypanosoma b. brucei, Trypanosoma congolense and Crithidia fasciculata, as different model organisms to study the Trypanosomid biology

Trypanosoma b. brucei, Trypanosoma congolense and *Crithidia fasciculata* represent interesting models and are unique members of the family Trypanosomatidae to study biological cellular and drug against members of the family Trypanosomatidae. These kinetoplastids have a very similar cellular machinery and are phylogenetically related to the human pathogenic trypanosomatids and non-mammalian infective lower trypanosomatids, which can be handled in a standard laboratory without specific biosafety issues. Also, they have relatively fast growth kinetics and can be easily and inexpensively grown to high cell densities in liquid media. Moreover, they are easily amenable to molecular, genetic and biochemical analyses. Over the past few decades, these organisms have been utilized as a model's system to study the biochemical, cellular, and genetic processes unique to members of the family Trypanosomatidae. This has allowed researchers to uncover the cellular and/or biochemical processes that ultimately could be exploited for the development of novel therapies for the related pathogenic trypanosomatids (Barrett et al., 2010, Achcar et al., 2014, Giordani et al., 2016, Kipandula et al., 2018).

1.4.2.6.1.1 *Trypanosoma brucei*

Trypanosoma brucei, which has different subspecies causes a distinct pathalogy including *T. b. gambiense*, *T. b. rhodesiense* and *T b. brucei*. T.*b gambiense* parasites are found in west and central Africa, where they cause chronic trypanosomiasis disease in humans. While, *T. b rhodesiense* is spread in East Africa and causes acute trypanosomiasis in humans. *T. b. brucei* which is infects domestic and wild animals and is not transferable due to trypanosome lytic factor-1 (TLF-1) which is found in human serum. By contrast *T. b. gambiense* and *T.b. rhodesiense* are resistant to TLF-1 and as a result are infectious to humans (Stuart et al., 2008, Capewell et al., 2011, Kennedy, 2013). The life cycle of a trypanosome has two stages, specific forms in the mammalian host and the other stage in the tsetse fly vector. The life cycles of *T. brucei* and *T. congolense* were described and reviewed recently (Langousis and Hill, 2014).

1.4.2.6.1.2 *Trypanosoma congolense*

T. congolense is another species of trypanosome probably the most prevalent and widespread pathogenic trypanosome in tropical Africa. It is transmitted by the tsetse fly causing AAT that affects the mammals including ruminants, pigs, dogs and other domestic animals. The life cycle of *T. congolense* is quite similar to that of *T. brucei*. In both species bloodstream forms differentiate to procyclics in the midgut of the tsetse fly and lose their variant surface glycoprotein (VSG) coat and the major surface molecules of *T. congolense* are carbohydrates rather than glycoproteins as in *T. brucei* (Giordani et al., 2016)

1.4.2.6.1.3 *Crithidia fasciculata*

The genus *Crithidia* contains a number of species with a wide host specificity. The *Crithidia* is a species that have a single host life cycle in insects thus, they do not infect mammals. Transmission of *C fasciculata* occurs when infected mosquitoes contaminate the aquatic environment as well as flowers when they feed on nectar. Thus, providing chances for transmission of amastigotes which are found in the mosquito gut excreted through the faeces (Wallace, 1966, Kipandula et al., 2018). *C. fasciculata* has been widely used as a model organism in research of trypanosomatid biology that may then be applied to understanding the biology of the human infective species (Kipandula et al., 2018). However, since *Crithidia* attacks several species of insects including bees and has been reported as a possible cause of

winter colony collapse in Europe (Ravoet et al., 2013). Therefore, the role of using the *C. fasciculata* here in this study is to test the effect of propolis as a new therapeutic approach against this parasitic infection to discover the marvelous effect of this exceptional substance in the protection of bee health from the insect infective species.

1.4.2.6.2 New Drugs for protozoa and the Current treatment for disease caused by kinetoplastids

Chemotherapy is still important for the control of most parasitic diseases, such as trypanosomiasis and leishmaniasis. The current HAT treatment is based on old drugs including pentamidine, suramin, melarsoprol, eflornithine, and nifurtimox (**Figure 1-5**). They are associated with a myriad of challenges such as drug toxicity, chemoresistance and a lack of guaranteed supply (Field et al., 2017, de Koning et al., 2000). Resistance to current drugs by trypanosomes is another threat to chemotherapy. The lack of paediatric formulation for some of the drugs together with contraindication for pregnant women and those of childbearing age further limits the use of existing treatments (La Greca and Magez, 2011, Field et al., 2017). Vaccine development for HAT faces the challenge of the parasite's antigenic variation whereby the parasites make several antigenic variants by alternate expression and recombination of a repertoire of variant surface glycoprotein encoding genes, allowing them to escape the host immune response (La Greca and Magez, 2011). Meanwhile three key drugs are used to treat AAT: diminazene aceturate (DA), homidium salts (chloride or bromide), and isometamidium chloride (ISM). However, none of these drugs are absolutely safe as all of them have certain degree of toxicity (Yaro et al., 2016). Only two drugs, nifurtimox, and benznidazole are currently available for treating Chagas disease. These drugs have side effects, a long treatment period (60 days) and variation in effectiveness against the parasites (Moraes et al., 2014).
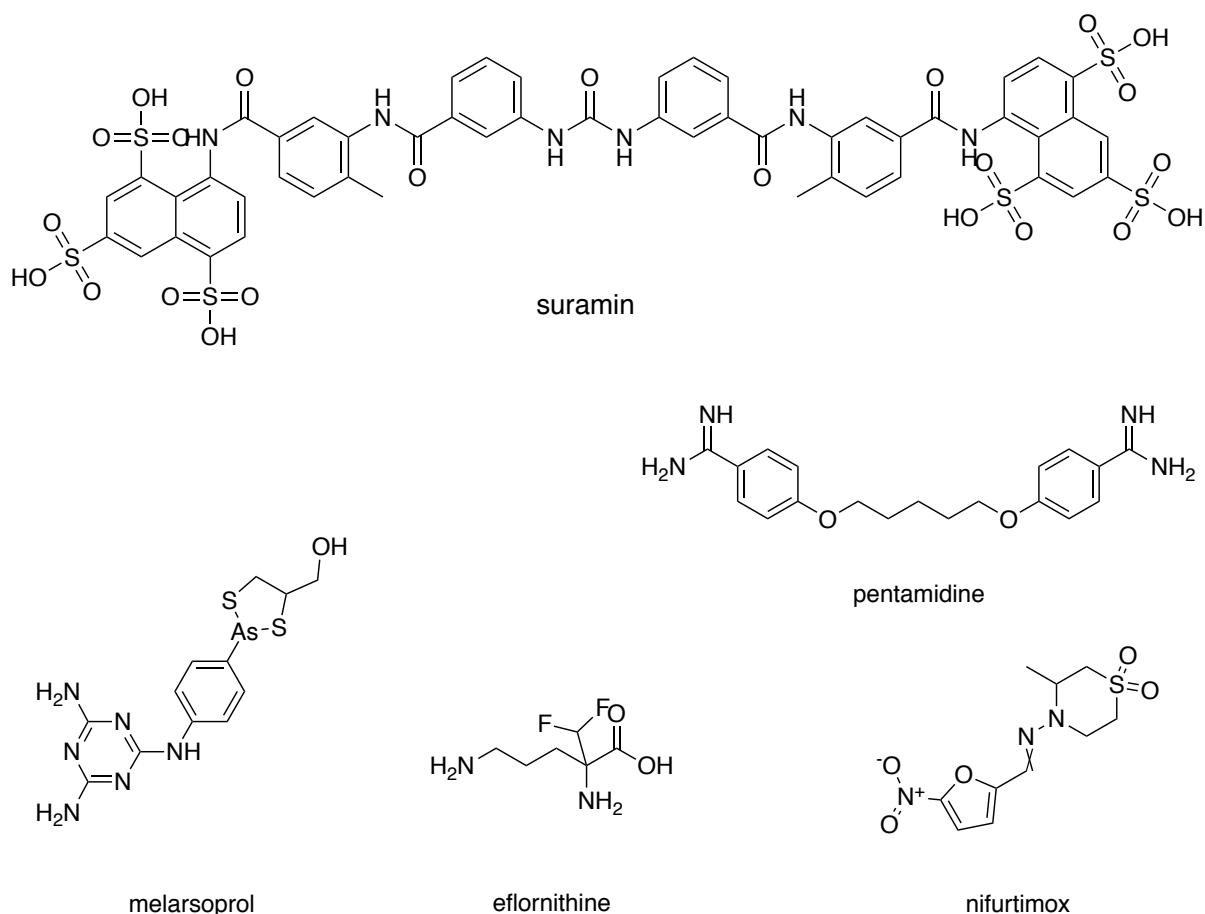
Figure 1-5: The structure of the current HAT treatment pentamidine, suramin, melarsoprol, eflornithine, and nifurtimox

Therefore, there is an urgent need for new treatment approaches. Nevertheless, the progress in discovering new and effective antiparasitic drugs has been very poor. Possible reasons for this include an over confidence in the validation of single molecular targets such as enzymes or receptors and a lack of fundamental knowledge of the biology and metabolism of kinetoplastids (Field et al., 2017). An alternative approach that may accelerate the discovery of novel leads is to use high throughput phenotypic screening assays (Nagle et al., 2014, Pena et al., 2015). Phenotypic screening is considered a robust and inexpensive assay, and has the significant advantage of identifying the activity of unknown compounds with significant antiparasitic activity that could act on either a single or multiple cellular targets that might not be identified in a screen with a defined single target such as an enzyme (Field et al., 2017). Moreover, the key reason for this slow progression is the lack of cooperation among different areas such as parasitology, drug discovery, medical chemistry and safety evaluation. Which are important in finding a good lead clinical candidates as starting points for future clinical aspects of drug discovery and for bringing them to a tangible outcome in delivering a useful drug to market.

Apparently one of the main reasons is the lack of readily available curated collections for lead identification in drug discovery for drug screening and subsequent evaluation. Nature has been a rich source of biologically active compounds for the development of new pharmacological agents themselves or from which active compounds have been derived using their novel structures as a template, over the past decades (Cragg and Newman, 2005, Newman and Cragg, 2020) . Several compounds isolated from natural sources have been shown to inhibit the growth of trypanosomes *in vitro* and *in vivo*, e.g. cordycepin and its chemical analogues (Vodnala et al., 2013, Hulpia et al., 2019) isolated from the fungus *Cordyceps militaris*, and quercetin, polyphenolic flavonoid commonly found in plants, and its derivatives, a (Mamani-Matsuda et al., 2004). Other examples include the trypanocidal activity of two dipeptide compounds isolated from the roots of *Zapoteca portoricensis* (Nwodo et al., 2014), steroid alkaloids from *Holarrhena africana* (Nnadi et al., 2019) and the anti-kinetoplastid properties of propolis (Alotaibi et al., 2019, Siheri et al., 2019). Propolis seems to be a good lead candidate as starting point for future aspects of drug discovery and for bringing a good outcome in delivering a useful drug for HAT. The WHO reported around 1000 new cases of African trypanosomiasis in 2018 (Organization, 2019). In this project propolis was screened against *T. brucei* in order to investigate the potential effect to treat HAT. Also, propolis been screening against *T. Congolense* in order to determine their prospects of being developed to used as veterinary drugs to treat AAT (or nagana), a condition that causes billions of dollars in economic losses in sub-Sharan Africa (Giordani et al., 2016). Besides, *C. fasciculata* was used in this assay to discover the effects of propolis in the protection of bee health from the insect infective species.

1.5 Propolis analysis

Due to the complexity of propolis any successful method of differential analysis should ideally attempt to separate the main components. Generally, it must undergo many processes, in order to isolate individual compounds. The first step in the analysis of propolis is sample extraction, to get rid of insoluble impurities, inert materials, dust and wax. Where the raw propolis sample is extract in organic solvent by soaking the raw propolis in organic solvent (e.g. ethanol) and applying sound energy to agitate the particles in samples to accelerate the extraction then filtration process drying it to form propolis crude extract. Other extraction techniques include hydro distillation and soxhlet extraction. They were not used in the current study due to involvement of high temperature and moisture to avoid any degradation or instability issues. There is a possibility thermal degradation of propolis and a study on green propolis from Brazil

showed that the phenolic content decreased by 30% during exposure to heat during a spray-drying process (Da Silva *et al*., 2011).

After extraction separation processes are carried out to get different fractions for particular chemical and bioactivity evaluations. Then further purification, identification, and structure elucidation processes for the purified compounds. Various of analytical techniques have been involved in propolis analysis ranging from traditional phytochemical methods such as column chromatography to advanced and modern methods including high performance liquid chromatography (HPLC) coupled to different detectors such as evaporative light scattering detector (ELSD), ultraviolet (UV), and high-resolution mass spectrometry (HRMS) detectors. In addition to use of gas chromatography- mass spectrometry (GC-MS), and nuclear magnetic resonance spectroscopy (NMR). There are a number of other techniques which have been also used in propolis analysis include, Solid-phase extraction (SPE), Infrared Spectroscopy (IR) and Melting Point (MP).

1.5.1 Chromatography

Chromatography is a physical method that commonly used in chemical analysis to separate the components in a mixture between two phases, stationary phase and the mobile phase. This is based on the affinity towards the mobile phase and stationary phase. The mobile phase could be either a liquid or a gas, and accordingly we can subdivide chromatography into liquid chromatography (LC) or gas chromatography (GC). In case of LC the mobile phase is miscible solvent mixtures of varying degrees of polarity, whereas in (GC) the mobile phase is a neutral gas that commonly nitrogen or helium. Moreover, chromatography can be classified based on stationary phase type such as thin layer chromatography (TLC), Paper chromatography and column chromatography (CC), or based on the way in which the analyte interacting on stationary phase such as ion-exchange chromatography (IEC), and size-exclusion chromatography (SEC). It also categorized based on the mechanism of separation like Medium pressure liquid chromatography (MPLC) and high-performance liquid chromatography (HPLC) (Hage, 2018). HPLC itself can further be classified according to the type of the interactions of the analyte with the stationary phase surface and according to their relative polarity of the stationary and mobile phases. Firstly, reversed phase (RP-HPLC) where the stationary phases nonpolar (e.g. C18 and C8 hydrocarbons) with polar mobile phase mixtures (e.g. water and acetonitrile). Secondly, normal phase (NP-HPLC) or hydrophilic interaction

liquid chromatography (HILIC) where a stationary phase is more polar (e.g. silica or a polar bonded phase) than the mobile phase and typical mobile phase constituents include water-miscible polar organic solvents (e.g. acetonitrile with a small amount of water and tetrahydrofuran). The third mode is based on ionic interactions of the analyte with the stationary phase, is called ion-exchange (IEX). The separation in this mode is based on the different affinity of the ionic analytes for the counterions on the stationary phase surface (Watson, 2012).

1.5.2 Size Exclusion Chromatography (SEC)

Size Exclusion Chromatography (SEC) also known as gel filtration, is a chromatography technique where molecules are separated based on their physical dimensions (size) and does not require interaction of the solute with the stationary phase. The larger the analyte molecules, the lower the possibility for them to penetrate into the porous space of the column packing material and elute first. Consequently, the smaller molecules the more diffusing into the pores to a greater extent and therefore be eluted later. Particles of the column could be polymeric or dextran gel such as Sephadex which are often have a hydrophilic coating in order to inhibit any solute-particle surface interactions which can be highly detrimental to an SEC separation. Mobile phases are always isocratic and are and relatively polar in nature (e.g. Methanol) to minimize interactions between the solute and the particle surface (Barth et al., 1994)

1.5.3 Medium pressure liquid chromatography (MPLC)

Currently, the Reveleris® or Grace® is considered as the latest reliable automated flash chromatography system. This instrument used for fractionation of complex mixtures to obtain pure components. The pressure required is within the range of 5-20 bars which is generated through a piston pump with an adjustable flow rate. The main components of a medium pressure liquid chromatography system are shown in **Figure 1-6** It involves a solvent system that is capable of running up to four separate solvents through two pumps. The sample is dry loaded onto around 2 g of celite and a cartridge containing up 50 g of silica or modified silica is used. The instrument has a dual detection system of UV-Vis and ELSD detectors to detect both non-chromophoric compounds such as terpenoids and chromophoric compounds such as flavonoids in a given sample during a single run (Claeson et al., 1993, Cheng et al., 2010).
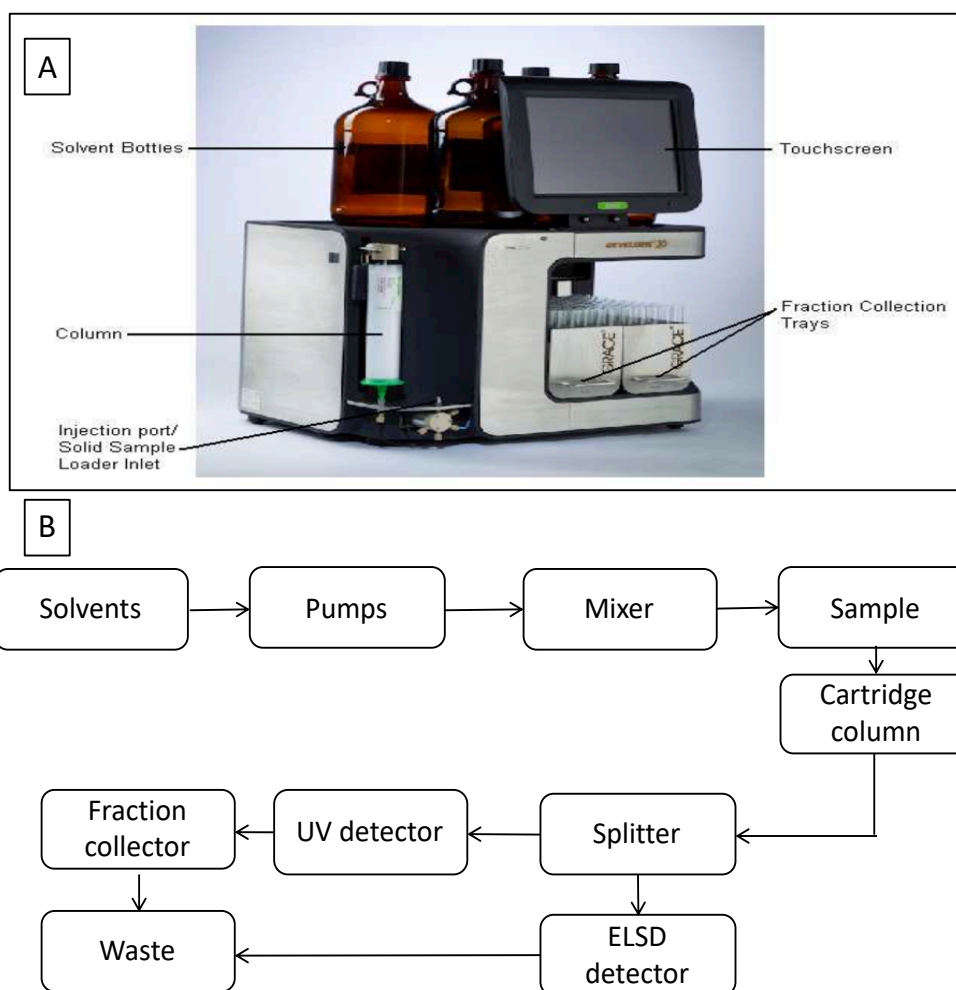
Figure 1-6: (A)The main components of Flash chromatography Grace instruments and (B) a schematic diagram to show the flow of solvent through the main parts on the system (adapted from REVELERIS® X2 Flash Chromatography System Product Manual)

1.5.4 High performance liquid chromatography (HPLC)

High Performance Liquid Chromatography (HPLC) is the most popular analytical technique used in the modern analytical chemistry and the pharmaceutical industry. A typical HPLC system consists of the following main components; solvent reservoirs capable of storing sufficient amount of HPLC solvents for continuous operation, a pump with a proportioning valve for mixing of different solvents from different reservoirs, an injector (most modern injectors are autosamplers), a column which produces a separation of the analytes in the mixture, a detector and a computer-based system for controlling the system parameters and to also act as a recorder (**Figure 1-7**). In HPLC the mobile phase is continuously pumped at a fixed flow rate through the high-pressure pump to transport the analytes (sample) onto the top of the column, which is packed with a stationary phase material. However, the analyte must be

soluble in the mobile phase. The injector is used to introduce a plug of the sample into the mobile phase without having to stop the mobile phase flow, and without introducing air into the system. Mobile phase flow can be programmed to run isocratically, stepwise, or in gradient and thus separated components are detected as they emerge from the column by the detector system. The detector is then used to respond to a physico chemical property of the analyte and sent to a data system where it is recorded as the 'chromatogram'. The most commonly used detectors are ultraviolet (UV) where the chromophore consists of a set of conjugated double bonds or an aromatic group and the evaporative light scattering detector (ELSD) which is the ideal choice for nonvolatile solutes of unknown natural products compounds or compounds that have poor UV absorption due to lack of chromophores in their structures, and the mass spectrometer detector (MS) (Swartz, 2010).
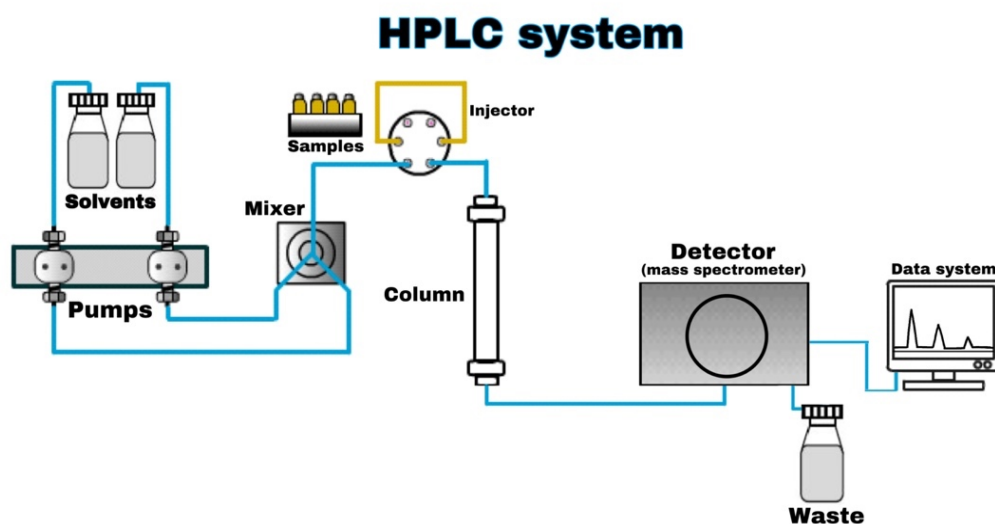
Figure 1-7: HPLC with mass spectrometer detector

1.5.4.1 HPLC with evaporative light scattering (ELSD) and ultraviolet UV-visible (UV-Vis) detectors

The ELSD operates in three stages including nebulization, mobile phase evaporation, and then measurement of scattered light by eluting peaks (**Figure 1-8**). The nebulization process occurs by nebulizing the analyte in a nebulizing chamber and mixing with a nebulizer gas, that is converted by the nebulizer into a fine spray of uniform droplets suspended within a nitrogen gas carrier. Then the atomized spray is moved to a drift tube where heating is applied to

evaporate the mobile phase and leaving behind solid particles of the analyte. A fine cloud of non-volatile solute particles is carried through the detection unit, a light bean source is directed at the solid particles causing light scattering which is detected by a photomultiplier (Mourey, T.H. and Oppenheimer, L.E., 1984). On the other hand, UV-visible detection in HPLC is only useful for compounds that possess UV-Vis absorbing moieties, such as conjugated double bonds or aromatic rings. It operates by passing UV light through the individual components of an analyte mixture as they elute causing radiation to interact which leads to absorption of a photon and transition of electrons between molecular orbitals. The amount of UV-Vis light absorbed for each component is determined by and comparing it with the intensity of light reaching the photodiode after passing through the sample. There are several types of UV detectors including single wavelength that measure the absorption of a single wavelength, multiple wavelength or diode array configurations that measure absorption of multiple wavelengths and are therefore more selective (Swartz, 2010).
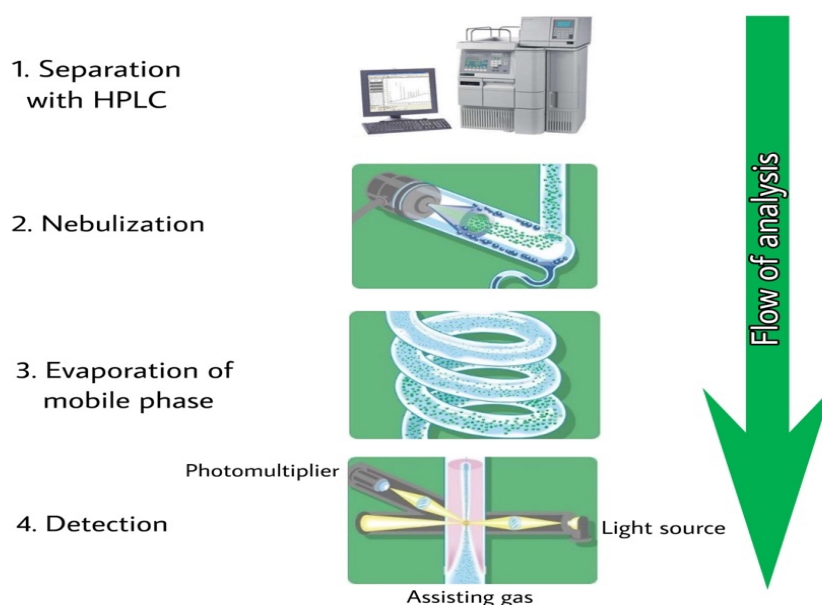
Figure 1-8: Principle of HPLC-ELSD detection of compounds during analysis (SHIMADZU, 2007)

1.5.4.2 HPLC with mass spectrometry (MS)
1.5.4.2.1   Principles of mass spectrometry

Mass spectrometry is a wide-ranging analytical technique, that measures the mass-to-charge ratio of ions. It is used to identify the molecular weights of compounds and is used as a detector that is coupled predominantly with GC or HPLC. Generally, it involves the production of ions

and subsequent separation within the mass analyser based on their mass to charge (m/z) ratios and identification of charged species. The separation of the gas phase ions is achieved within the mass spectrometer using electrical and/or magnetic fields to differentiate ions. All filtration of analyte ions or fragments of analyte ions carried out under high vacuum. The two main modes of ionisation used in are Electrospray Ionisation (ESI) and Atmospheric Pressure Chemical Ionisation (APCI). Both ESI and APCI are termed "soft" ionisation process of producing ions. In contrast, Electron impact (EI) ionization named a hard ionisation technique in which ions are formed as a result of collisions between analyte molecules in the gas phase and high energy electrons. Various types of mass analysers are currently available commercially and including magnetic sector instruments, single and triple quadrupoles, time-of-flight (ToF) instruments, ion traps, Fourier transform ion cyclotron resonance (FT-ICR) spectrometers and Orbitraps (Watson, 2012).

1.5.4.2.2 Ionisation systems

1.5.4.2.2.1 *Electrospray Ionisation (ESI)*

In Electrospray Ionisation (ESI) a high voltage capillary needle is applied to a liquid sample to create an aerosol that becomes ionised. It is ionised by the high voltage of 2-6kV in the inner surface of the spray needle to acquire positive or negative charges. Molecules with charges the same as that on the spray needle are repelled into the centre while those oppositely charged remain stuck on the needle. In the process of evaporation, charged droplets of the analyte to become smaller in size which leads to the formation of gaseous ions which are then sampled and directed to the mass analyser via a heated capillary and a high vacuum analyser region for mass measurement. The process of evaporation the solvent is enhanced by the flow of nitrogen gas and heating. Furthermore, the mobile phase additives such as formic acid, increase the efficiency of the ESI process (Ho et al., 2003).

1.5.4.2.2.2 *Electron impact (EI)*

In the electron impact (EI) process, electrons are emitted from a heated filament by using an appropriate potential energy (5-100V). The analyte molecule *M* is introduced into the EI ion source, where it is bombarded by this beam of ionizing electrons, leading to the formation of an energetic electron analyte radical cation $M^{+\cdot}$. The process can be described as follows: $M + e^- \rightarrow M^{+\cdot} + 2e^-$

The analyte molecule often breaks apart producing a variety of fragments because the collision energy used is higher than the bond strength (typically 4-7 eV). Fragmentation of the *M+*. radical cation can occur via loss of a single radial and several neutral species (Watson, 2012).

1.5.4.2.3 Mass analysers

1.5.4.2.3.1 Quadrupole Mass Analyser

In quadruple mass analyzing devices, electric fields are used to separate ions according to their mass-to-charge ratio (*m/z*) as they pass along the central axis of four parallel equidistant rods). Ion separation is performed by using controlled direct voltages applied to the mass analyser rods which impart an electrostatic field inside the analysing device. Voltage of the same polarity is applied to diagonally opposite poles and opposite voltage polarity is applied to adjacent poles. Only ions with specific m/z values can achieve stable oscillations inside the quadrupole thus being able to reach the detector. The rest of the ions either collide with the poles or fly out of the system (**Figure 1-9**). Quadrupole MS systems are low cost, give reproducible results, easy to operate and maintain. Thus, they are widely used as general-purpose MS instrument for both qualitative and quantitative analysis (Watson, 2012).
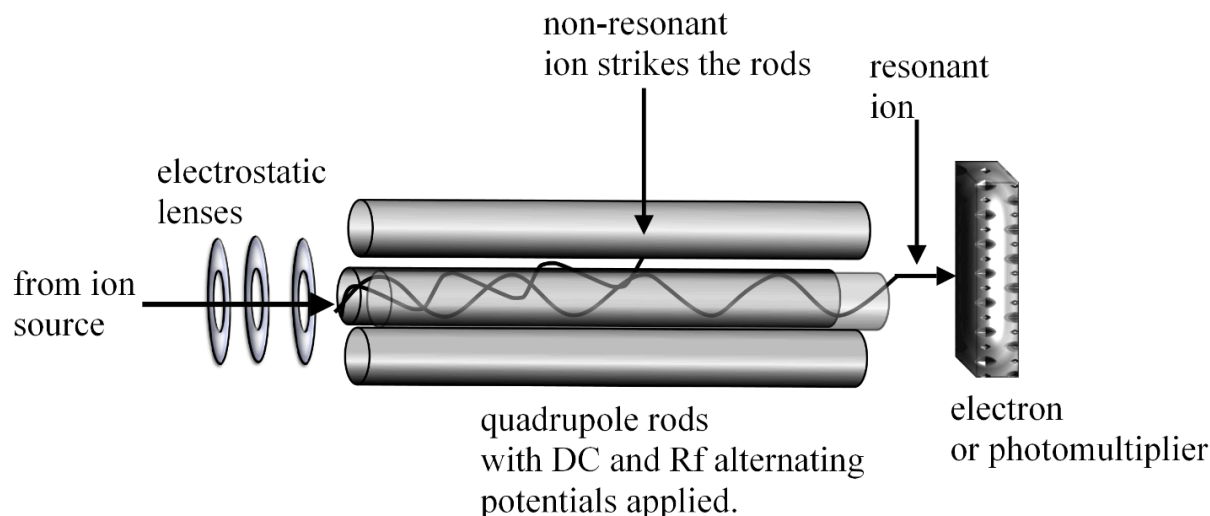
Figure 1-9: Operation of a quadrupole mass analyser. Only ions with specific m/z values can achieve stable oscillations inside the quadrupole thus being able to reach the detector. The rest of the ions either collide with the poles or fly out of the system. Different ions can be detected by varying the rf-voltage applied (Watson, 2012).

1.5.4.2.3.2 Time of Flight Mass Analyser

The principles of mass analysis using time-of-flight mass analysers are relatively straightforward in comparison to many of the other typical mass analysing devices. After ions extracted from the ion source and subjected to an accelerating voltage. The time taken for ions to travel down the flight tube (0.5 to several meters) is dependent upon their mass and charge m/z. The range of m/z values can be measured with good sensitivity and give moderate to high resolving powers (Watson, 2012).

1.5.4.2.4 Tandem mass spectrometry (MS/MS)

The tandem mass spectrometer uses triple quadrupoles (Q1, Q2, and Q3) as its mass analyser (**Figure 1-10**). It has ability to form, and then select, ions in Q1, perform collision induced dissociation (CID) with gas (e.g. argon or nitrogen) molecules in Q2, and scan specific selected mass ranges in Q3 (Watson, 2012). Tandem MS (or MS/MS) is the combination of two or more MS experiments to get structural information by fragmentation of molecular ion through breaking down selected ions into fragments. Commonly MS/MS uses a conjunction of quadrupoles with a collision cell between the analyzing devices in which the ions analyze with one analyzer can be fragmented prior to further mass filtering analysis. Other combinations of mass analysing devices could be quadrupoles and time of flight, or quadrupoles with magnetic sector instruments. Once the fragments have passed the mass analysers then detected and been transformed into a usable signal. These fragments are act as a unique fingerprint of the molecule which aid in the structural elucidation of the compounds (Cutillas and Timms, 2010).
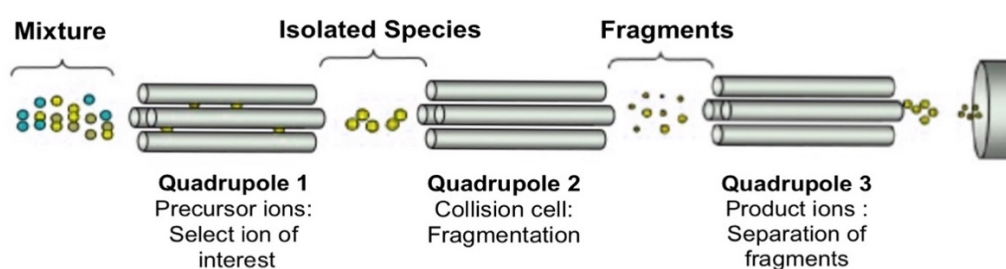
Figure 1-10: Schematic digram of tandem mass spectrometry (Watson, 2012).

1.5.5 Nuclear magnetic resonance (NMR) techniques

NMR is a technique to observe electromagnetic radiation around atomic nuclei. It is considered

the most effective technique for structure elucidation and it is largely used in phytochemical analysis for identification of pure organic compounds. The concept of NMR spectroscopy is based on applying a magnetic field to a sample followed by excitation a nucleus. This is followed by measurement of the reemitted electromagnetic radiation following nuclear relaxation. The effective magnetic field is also affected by the orientation of neighboring nuclei causing spin coupling which is splitting of the signal. The main components of the NMR instrument are shown in (**Figure 1-11**).

NMR spectrometer
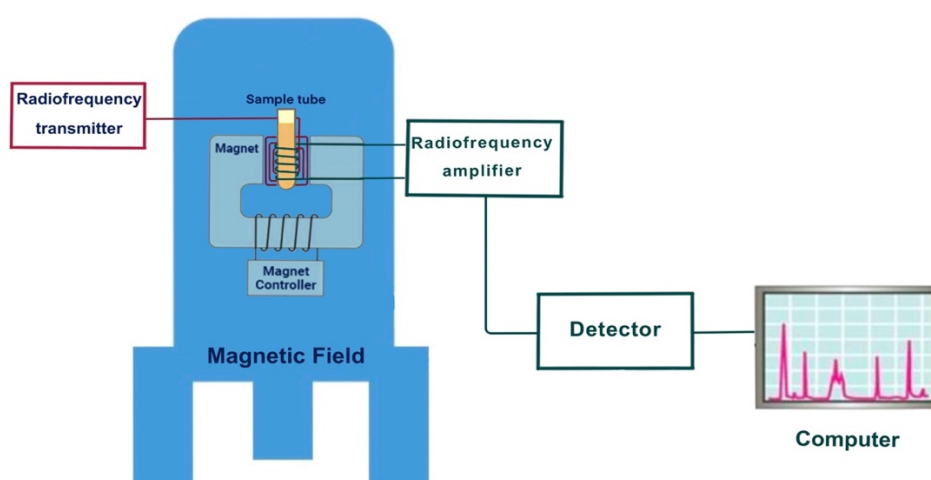
Figure 1-11: Schematic digram of basic elements of classical NMR spectrometer.

The studies of NMR including proton ^{1}H-NMR and carbon-13 NMR spectroscopy that called one-dimensional (1D) experiments and two-dimensional (2D) experiments. ^{1}H NMR gives information about the protons in a compound, their chemical shifts, multiplicity (coupling information) and integration which enables the determination of the number of protons in a molecule and their distribution. The chemical shift of protons is normally influenced by electronegative groups such as C=O and aromatic rings. While, ^{13}C NMR gives information on the number and type of carbons present in a compound. A sequence of pulses with various delay times is the most widely used method of ^{13}C signals to create Distortionless Enhancement by Polarization Transfer (DEPT) spectra where -CH_3 and CH peaks appear as normal position and -CH_2- and quaternary carbon peaks appear inverted. In 2D experiments both the x and the y axes have chemical shift scales and information is obtained from the spectra by looking at the peaks in the grid and matching them to other axes. Correlation spectroscopy (COSY) is a 2D experiment where the proton shifts plotted on both axes that gave ^{1}H-^{1}H coupling in the

molecule and also revealed all coupling relationships in one experiment using a suitable pulse sequence. The information on how the Hs & Cs are matched is obtained by also looking at the peaks inside the grid where the ^{1}H NMR spectrum on one axis and the ^{13}C NMR spectrum on the other are compared this is called Heteronuclear Correlation Spectroscopy (HETCOR). The Heteronuclear Single Quantum Correlation (HSQC) is a 2D ^{1}H-^{13}C experiment which was carried out to shows one-bond (1J) direct correlations. Heteronuclear Multiple Bond Correlation (HMBC) reveals heteronuclear correlations via long-range coupling where a proton couples to the carbons one or two bonds removed where J is a value similar to that of the one-bond ^{1}H-^{13}C coupling. Nuclear Overhauser effect spectroscopy (NOESY) is a stereochemistry experiment that is used to determine all correlations between protons arising from dipolar coupling of the structure through space (Breitmaier, 2002, Sarker and Nahar, 2012).

1.5.6 Infrared Spectroscopy (IR)

Infrared spectroscopy uses electromagnetic radiation in the infrared region for the determination a molecular. It is considered as a very powerful technique, to identify function groups of unknown compounds and study chemicals. In terms of wavenumbers the infrared including near, middle and far region spans from 33 to 12820 cm^{-1}. However, for most organic molecules, infrared analyses are carried out in the mid-infrared region (400 to 4,000 cm^{-1}). Most IR spectrometers can be categorized into two classes: dispersive and Fourier Transform (FT) Infrared instruments. FT-IR spectrometers consist of an IR source, interferometer, sample cell or chamber, detector and a laser as illustration in **Figure 1-12** (Stuart, 2000).
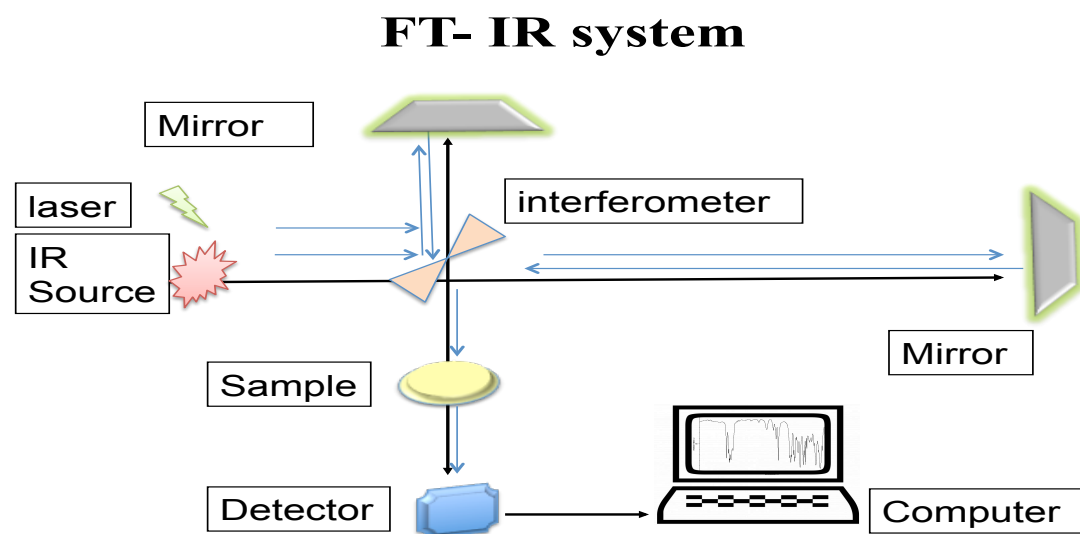
Figure 1-12: Operational Schematic of a FTIR Instrument.

In this project, the IR was conducted using FT-IR spectrometers for the analysis of the fingerprint regions and detection of functional groups. It is well known that an IR spectrum alone does not provide enough information to derive the complete structure of the compound, but it is very useful in combined with other spectroscope techniques such as NMR and mass spectrometry.

1.5.7 Solid-phase extraction (SPE)

Solid-phase extraction (SPE) is a widely applied technique used for isolation of one or more type of analytes from a liquid matrix and purified extracts to obtain a cleaner extract containing the analytes of interest. The principle of SPE involves partitioning between a liquid (sample matrix or solvent with analytes) and a solid stationary phase based on retention mechanism due to interaction between non-polar groups of molecules and non-polar groups of the SPE cartridge. There are different retention mechanisms in SPE, the most common are based on Van der Waals forces also known as nonpolar interactions using reversed-phase, hydrogen bonding using normal phase, and cation-anion interactions using ion exchange. The general procedure is to load a solution onto the SPE phase, wash away undesired components, and then wash off the desired analytes with another solvent system into a collection tube (Ötles and Kartal, 2016). Using a solid phase extraction vacuum to gently pull a solution through the SPE tube using apparatus such as the SPE manifold Biotage® (VacMaster-10) ™ as shown in
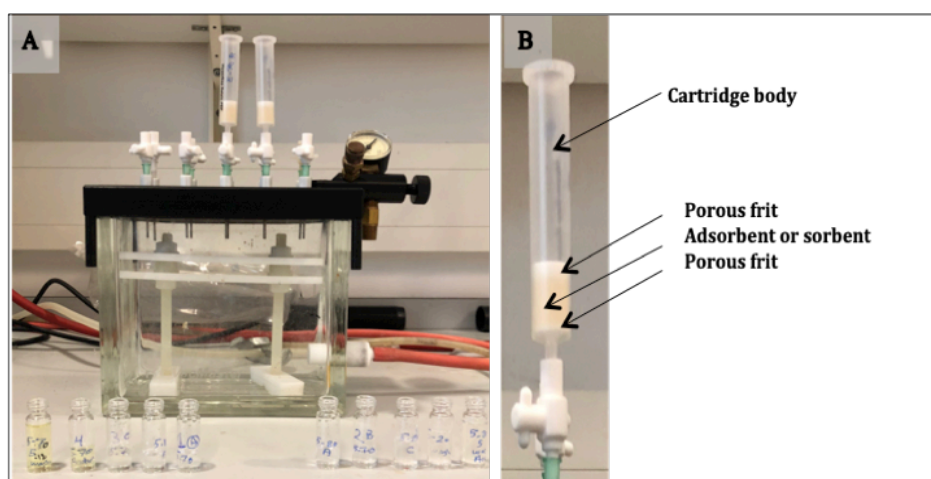
Figure 1-13: (A) Basic apparatus of SPE vacuum manifold (B) Parts of SPE cartridges

1.5.8 UV-visible spectroscopy

UV-visible spectroscopy is one of the commonly used methods for quantifying analytes in the area of analytical chemistry. This is due to the fact that majority of drug molecules absorb radiation in the UV region while others, which have chromophores, absorb radiation in the visible range of the spectrum. A UV-visible spectrophotometer is used to measure the transmittance or absorbance of a sample as a function of the wavelength of the electromagnetic spectrum. The main components of a typical UV-Vis spectrophotometer are light source i.e. deuterium lamp for UV region from 190-350 nm of the spectrum and tungsten lamp for visible region from 350-900 nm, monochromator, sample holder, optics and a detector. As illustrated in **Figure 1-14**. This beam is split by the optics in order to pass through the sample as well as the control. The emitted light passes through the monochromator and leaves with an intensity of I_0. A proportion of this light is absorbed by the analyte. Finally, the detector analyses the light that leaves the sample with an intensity of I_1 and a spectrum is produced. There are several possible configurations for spectrophotometers such as Single, Dual, or Split Beam. UV can help in structural elucidation; hence it gives some information on chromophores in molecules. Also, UV detector is themost common detection system for HPLC, thus it is important to determine the chromatographic data for mixtures of novel compounds (Watson, 2012).
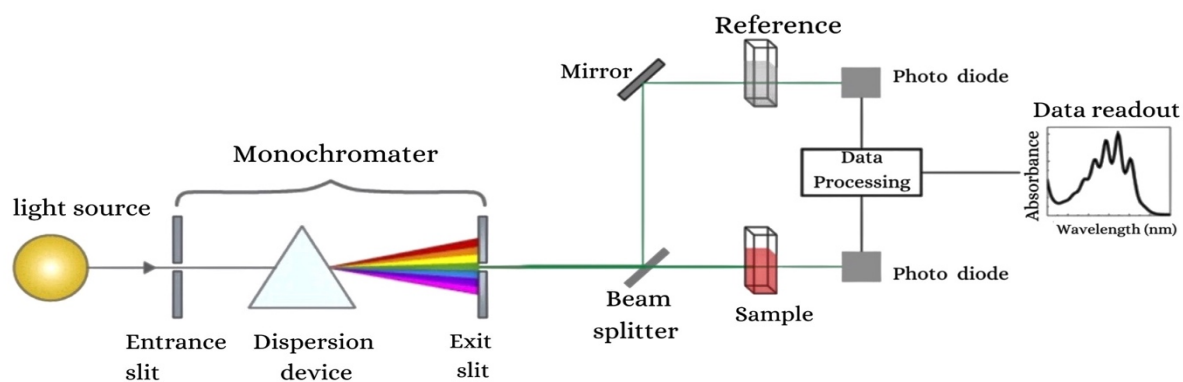
Figure 1-14: Schematic digram of basic of split beam spectrophotometer

1.5.9   Melting Point (MP)

Melting point is one of the important physical property of a compound, hence it can provide useful information which can help in the identification of a sample and determination od its purity. The melting point of an organic solid can be determined by introducing a tiny amount into a small capillary tube, attaching this to the stem of a thermometer centered in a heating

bath, heating the bath slowly, and observing the temperatures at which melting begins and is complete (Jain et al., 2004).

1.6 Aims and Objectives
1.6.1 The aims of this study are:

1. To investigate the constituents and profile 25 propolis samples from different African countries and Pacific Ocean islands by applying the tools of mass spectrometry-based metabolomics.
2. Biological screening of all crude extracts *in vitro* by evaluating their antiparasitic activity against different species of Trypanosoma to determine any potential anti-trypanosomal activities.
3. Purification of crude extracts based on the bioassay results to isolate pure active compounds.
4. To investigation of the toxicity of the extracts and isolated compounds against human cell line (U937 cells) and murine cell line (Raw 246.7) using Alamar blue assay.

1.6.2 The objectives are:

- The extraction of different propolis samples using organic solvents (ethanol).

- The development of a reproducible LC -MS method for the analysis of the main components of the different propolis samples.

- The application of MzMine (data extraction), SIMCA-P (data modelling) and PCA analysis based on the LC-MS data of the propolis samples to classify them according to their chemical profile.

- Testing of the anti-trypanosomal activity of the propolis extracts on *Trypanosoma b. brucei*, *T. congolense* and *C. fasciculata* and determination of their EC_{50} values.

- Determination of the minimum inhibitory concentrations (IC_{50}) of the propolis extracts, fractions and purified compounds against human cell line (U937 cells) and murine cell line (Raw 246.7) and also the selectivity index of the samples to evaluate any potential therapeutic uses.

- Isolation of the active compounds by bioassay-led fractionation using different chromatographic and analytical techniques and purification of the major constituents prior to biological and spectroscopic analysis.

- Chemical characterization of purified compounds by using different analysis techniques including HPLC connected to MS, UV and ELSD detectors, GC-MS, IR, UV, melting point and 1D and 2D NMR.

Chapter Two

2 Material and Methods

2.1 Materials
2.1.1 Chemicals and reagents

HPLC grade solvents included ethanol, acetonitrile. hexane, ethyl acetate, methanol, formic acid, dichloromethane, isopropanol, acetone and water (Sigma Aldrich, UK). Chloroform-d ($CDCl_3$), dimethyl sulfoxide-d6 (DMSO-d6), acetone-d6, β-mercaptoethanol, dimethyl sulfoxide (DMSO), p-Anisaldehyde, sulphuric acid (Sigma Aldrich, UK). Column chromatography separations were carried out in glass columns (2.5×50 cm), using silica-amorphous, precipitated particle size 60 Å x 200-425 mesh (Sigma- Aldrich, UK). cotton wool (Fisher Scientific, UK), filter paper 240 mm, 5-13 μm (VWR International, France), TLC silica gel 60 $F_{254,}$ pre-coated aluminium sheet 10 x 20 cm (Merck, Germany). Silica gel 60 of particle size 0.063-0.200 mm (Merck, Germany), silica gel-amorphous, precipitated filter agent Celite® (Sigma- Aldrich, UK) and Sephadex® LH-20 (Sigma- Aldrich, UK).

2.1.2 Apparatus

The IR spectra were acquired on a Perkin Elmer FTIR model 1725X spectrophotometer with ATR probe (model 1725X spectrophotometer). The ^{1}H and ^{13}C NMR spectra were run on a Bruker AV3HD500 spectrophotometer and the Bruker Avance 600 MHz with a 14.1 T Ultrashield superconducting magnet operating system. The LC-MS was as performed using Exactive Orbitrap mass spectrometer from (ThermoFisher, Hemel Hempstead, UK), using an ACE-C18 column 150 mm × 3 .0 mm, pore size: (3 μm (HiChrom, Reading, UK). MS^n fragmentation experiments were carried out on an LTQ Orbitrap (ThermoFisher, Hemel Hempstead, UK). SPE was carried out using a vacuum manifold Biotage® (VacMaster-10) ™. UV-Vis absorption spectra were recorded on an UNICAM UV 300 spectrophotometer.

2.1.3 General equipment

Balance capable of weighing to 0.0001 mg (METTLER TOLEDO, model AG204. Max= 210 d= 0.1 mg), balance capable of weighing to 0.00001 mg (METTLER TOLEDO, model AT20 Max= 22 g d= 2 μg). Ultrasonic water bath (BRANSON model number 1510, EDP: CPN-952-137). Sample concentrator- nitrogen gas (Techne, UK), vortex -Whirlimixer (Fisons Scientific, England, UK), rotary evaporator (Buchi, Switzerland). microcentrifuge (Centaur, Sanyo, Japan) and microscope (Olympus, Japan). Automatic pipettes, (1000, 200, 50. 10) (Gilson,

UK), multi-channel pipette (Gilson, UK). TLC glass chamber with lid, qualitative filter paper 413, Particle-retention 5-13 micrometer (VWR France), acrodisc filters (Fisher Scientific, UK), and sterile syringe filters (25 mm w/ 0.45 µm Nylon membrane obtained from VWR International)

2.1.4 Materials and cells used in the biological assays

Human monocyte U937 cells (European Collection of Cell Cultures Cat. No. 85011440, supplied by Sigma-Aldrich, UK) and RAW 264.7 murine macrophages (ATCC TIB-71, USA). Wild type *T. b. brucei*, strain Lister 427 (s427; MiTat 1.2/BS221), *C. fasciculata* (ATCC50083) and *T. congolense* BSF IL3000WT. ATCC-formulated Dulbecco's Modified Eagle's Medium (DMEM) (Catalog No. 30-2002), penicillin & streptomycin (Life Tech, Paisley, UK), Foetal bovine serum (FBS) (Sigma-Aldrich, UK), Hirumi's Modified Iscove's medium 9 (HMI-9). Fetal Bovine Serum (FBS), 96 well plate, flat bottom, polystyrene, 0.34cm2, sterile, (TPP, Switzerland), RPMI 1640 cell media (Bio-whittaker, USA) and resazurin powder (Sigma Aldrich, UK) and a plate reader (Perkin Elmer-Wallac).

2.1.5 Propolis Samples

Table 2-1: propolis samples collected from African countries

Sample code	Propolis sample origin	Photo	Sample provider	Weight of raw propolis (g)
1- LM1	Lilongwe Malawi		Goods for good ORG.	0.76
2- KM2	Konowani Kadumbo Malawi		-	10.00
3-BM3	Blantire Malawi		-	
4- PT1	Tanzania		PEMBA Clove Honey Co.	6.00
5- ZP	Zambia North West Zambia		Forest Trust Co.	8.20
6- PT2	Tanzania		-	6.00
7- PT3	Tanzania		-	
8- TP	Tanzania The city of Moshi in Northern		Stingless bee propolis	7.65
9- ZT5	Tanzania		-	

10- SN1	Niger State		-	14.00
11- LN2	Nassarawa State			7.50
12- BN3	Benve State		-	10.00
13- NN4	Nassarawa State		-	4.50
14- GN5	GG/ BB		-	10.00
15- ON6	Ondo State		-	4.00
16- KN7	Kogi State - Nigeria		-	5.00
17- JN8	Josh Plateau State - Nigeria		FIR/ EULALYPTUS	10.00
18- AN9	Adamawa State - Nigeria		-	9.50
19- CN10	Cross Reiver State - Nigeria		-	6.10
20- RN	Nigeria	N/A	-	18.00
21- Cg	Congo			

Table 2-2: propolis samples from islands in the Pacific Ocean

Sample code	sample origin	Photo	Sample provider	Weight of raw propolis (g)
PNG	Eastern Highlands Papua New Guinea		-	38.5
NZ	New Zealand			40.0
Indo-1	Indonesia	N/A		-
Indo-2	Indonesia	N/A		-

2.2 Methods
2.2.1 Extraction

Approximately 5 g of the different propolis samples were extracted by sonication with 100 mL of absolute ethanol (Sigma Aldrich, UK), at room temperature for 60 minutes without applying any heat to avoid thermal degradation. (Clifton ultrasonic bath, Fisher Scientific, Loughborough, UK), after which the extract was filtered and re-extracted twice more with 100 mL of ethanol, filtering each time This step was repeated three times to make sure to fully extract the raw propolis and remove some impurities. The extracts were combined, and the solvent was evaporated using a rotary evaporator (Buchi, VWR, Leicestershire, UK), and the residue weighed.

2.2.2 Column chromatography (CC)

Approximately 3 g of the propolis extract was dissolved in 5 mL of ethyl acetate, 6 g of silica gel was added to the extracts in a beaker and allowed to dry under a fume hood. Amorphous silica (pore size 60 Å) was weighed and mixed with 200 mL hexane to form a homogenous slurry that used to pack a glass column. Next, the hexane was allowed to drain through the column to prevent overflowing and to remove any air bubbles. Also, the external column wall was gently tapped to encourage any bubbles to rise and to keep the silica settle. The dry adsorbed extracts were placed directly onto the column and eluted using 200 mL of hexane, ethyl acetate and methanol mixtures as follows: F1 hexane 100%, F2 hexane /ethyl acetate (80:20), F3 hexane / ethyl acetate (60:40), F4 hexane / ethyl acetate (40:60), F5 hexane / ethyl acetate (20:80), F6 ethyl acetate 100% and then F7 ethyl acetate/ methanol (80:20), F8 ethyl acetate/ methanol (50:50), F9 ethyl acetate/ methanol (20:80), F10 methanol 100% yielding fractions F1-F10 respectively.

2.2.3 Buchi rotary evaporator

All fractions obtained from CC were evaporated and concentrated as a resinous residue, by using the rotary evaporator manufactured by Buchi (switzerland). This is used for solvent distillation under a vacuum at low pressure, the temperature was less than 40°C and the rotation speed of evaporation was 100 rpm. Subsequently, the residue fraction was transferred back to its flask and left in the fume hood to be completely dried and the weight of flasks plus the sample were recorded. Approximately 20 mg from each fraction was weighed and transferred into small clean-weighed vials for a bioassay.

2.2.4 Size-Exclusion Chromatography (SEC)

Preparation of a slurry of Sephadex ® LH-20 (Sigma- Aldrich) involved overnight suspension of the stationary phase in 50:50 dichloromethane/methanol for non-polar fractions and in 100% methanol for polar fractions. This slurry was then used to pack a glass column (2 x 100 cm) plugged with cotton wool. After the settling of the packed bed and the solvent level exceeded the top of the bed, a pasteur pipette was used for cautious application of the sample intended for fractionation following dissolution in the minimal quantity possible of the solvent employed for column packing. Elution was commenced and completed with 100 % MeOH in an isocratic manner and small vials were used for collection of the fractions (Sarker and Nahar, 2012).

2.2.5 The Medium Pressure Liquid Chromatography (MPLC)

The target fractions obtained from CC that showed activity against trypanosomes were further purified using MPLC. About (0.5- 1.5 g) of the sample was weighed and dissolved in 5 mL of ethyl acetate. Then, loaded with a quantity of Celite® powder equivalent to the double weight of the sample and packed into a dry loading cartridge of a Grace Reveleris flash chromatography system (Alltech Ltd., UK). The MPLC system was set up with a 12g silica column and eluted using a stepwise gradient at a 25 mL/min flow rate. The stepwise gradient was set up as follows: 100% hexane 5 min, hexane: ethyl acetate (60:40) 10 min, hexane: ethyl acetate (40:60) 10 min, 100% ethyl acetate for 10 min, ethyl acetate: methanol (90:10) 10 min, ethyl acetate: methanol (80:20) 20 min, ethyl acetate: methanol (60:40) 20 min, ethyl acetate: methanol (50:50) 10 min, ethyl acetate: methanol (40:60) 10 min and washing with 100% methanol. Fractions associated with the same compounds according to TLC were combined.

2.2.6 Solid phase extraction (SPE)

Solid phase extraction (SPE) was carried out to clean up the purified compound (ZP-5-20) from impurities using a SPE vacuum manifold Biotage® (VacMaster-10)™ and CHROMABOND® C18 polypropylene columns as a reverse phase C-18 cartridge (**Figure 1-13**). This is done in five steps illustrated in scheme diagram (**Figure 2-1**). The sample was transferred into a separate vial and dissolve in methanol. The sample was loaded onto the SPE column and washed with 1 mL of methanol followed by 1-2 mL of water, sample loaded slowly and then eluted with 2 mL of methanol, then 2mL 50:50 (water: methanol), and 80:20 (water: methanol). The NMR was performed to detect the pure fractions, then final eluted solutions were run on the LC-MS according to the method described earlier.

Purification of the **novel** organic compound isolated from **Zambia propolis**
Using SPE-C-18 , by the Following these Five Steps:

1. Sample pre-treatment: Dissolve the sample in appropriate organic solvent (MeOH was used in this experiment).

2. Cartridge conditioning
2 ml MeOH follow by
2 ml H_2O

3. Sample loading
For 100 mg silica cartilage a few ml per minute (slowly! 1-2 drops per second).

4. Sample washing
2 ml of methanol: to wash off impurities but retain the compound

5. Sample elution
1-2 ml H_2O / MeOH mix (50:50) then (80:20) to remove the compound but keep the non-polar impurities

Fast!

^ - impurity
*- impurity
x-compound of interest

Fast!

Slow

Figure 2-1: Scheme diagram illustrates the SPE process technique for organic compound ZP-5-20 isolated from Tanzania propolis.

2.2.7 Liquid Chromatography–Mass Spectrometry (LC-MS) analysis

All profiled samples and fractions were dissolved in methanol to give a concentration of 1 mg/mL. LC-MS analysis was carried out on an Accela 600 HPLC system combined with an Exactive (Orbitrap) mass spectrometer from (ThermoFisher, Hemel Hempstead, UK). MS detection range was from 100 - 1200 m/z and the scanning was performed under electrospray ionization polarity switching mode. The needle voltages were set at -4.0 kV (negative) and 4.5 kV (positive); and sheath and auxiliary gases were at 50 and 17 arbitrary units respectively. Separation was performed on an ACE C18 column (Hichrom Reading UK, 150 × 3 mm, 3 μm) with 0.1% v/v formic acid in water as mobile phase A and 0.1% v/v formic acid in acetonitrile as B at a flow rate of 0.3 mL/min, using the following gradient: 25% B for 30 min, 5 min 100% B, and 5 min 25% B, injecting 10 μL of sample solution. The MS^2 spectra were obtained on an LTQ Orbitrap Fourier Transform Mass Spectrometer (FTMS) under the same conditions described for the Exactive instrument, with a collision energy of 35 V, and data were processed using Xcalibur software.

2.2.8 Data Extraction and Database Searching

Since the high resolution MS works in dual polarity mode, the peak lists needed to be split into negative and positive file before transfer to MZ-mine 2.14 to be processed, this was carried out using a MassConvert file (Pluskal et al., 2010). The generated peak lists from both ESI positive and negative modes were imported separately into SIMCA-P 14 (Umetrics, Sweden) for Principal Component Analysis (PCA) for chemical characterization The settings used in m/z Mine were as follows: Mass detection with centroid peaks, noise level set to $1x10^4$, *m/z,* and the MS level to 1. The chromatogram builder was set to minimum time span 0.2 min, minimum peak height $1x10^4$ and tolerance 0.001 *m/z* or 5.0 ppm. The peak detection from peak list methods, for the chromatogram deconvolution, where the algorithm was set as local minimum search. The chromatographic threshold was set to 5%, search minimum in RT range at 0.4 min, minimum relative height at 5%, minimum absolute height at 30000, Min ratio of peak top/edge as 2 and peak duration range within 0.3 – 5 min, while for deisotoping with retention time (RT) is 0.2 min, m/z tolerance is 0.001 *m/z* or 5.0 ppm and a maximum charge of 2, and most intense isotope is filtered out . For alignment join aligner was used with weight function in relation to *m/z* and retention time (20:20); this means RT and *m/z* both have the same importance, RT tolerance of 5%. After that gap filling was used to detect missing peaks at an intensity tolerance of 1%, *m/z* tolerance 0.001 *m/z* or 5 ppm and RT tolerance of 0.2 min, after gap filling all solvent peaks were removed from the data then adducts and complexes peaks were identified. The adduct search was performed with a RT tolerance at 0.2 min absolute, adducts for positive mode was set as Na, K, NH₄, formate for negative mode and ACN + H for both modes, *m/z* tolerance at 0.001 *m/z* or 5 ppm and maximum relative adduct peak height at 30%. The complex search was also done by following parameters; ionization was set as M+H for positive mode and M-H for negative mode, RT tolerance at 0.2 min absolute, *m/z* tolerance at 0.001 *m/z* or 5 ppm and maximum complex peak height at 50%. The formula prediction function was performed within the setting for only C, H, O containing compounds since no compounds containing other elemental compositions were isolated before from propolis. The data were exported as CSV files included MZ-Mine ID, *m/z*, retention time, name (if available) and peak area. The first 2000 LC-HRMS features from each sample were selected based on the mean peak area and putatively identified by searching for the accurate masses against the Dictionary of Natural Products (DNP 2013 version). Moreover, these negative ion data were univariate scaled, and log transformed prior to PCA modeling.

2.2.9 High Pressure Liquid Chromatography HPLC- Evaporative Light Scattering Detection (ELSD)

The samples that were obtained from the MPLC separation were dissolved in methanol to give concentration of 1 mg/mL. They were analysed by using an Agilent 1100 HPLC linked to a Shodex ELSD and an Agilent PDA detector:

Detector 1: ELSD (Bipolar) Range1: 1250 mV, 12.5 Samp. /Sec.,

Detector 2: DAD signal A Range 2: (Bipolar) 100000 mAU, 10 Samp. /sec.

Detector 3: DAD signal B (Bipolar) 100000 mAU, 10 Samp. /sec.

Detection was with ELSD and UV helped to profile the sample component and identifies the pure compounds. An ACE C18 3 mm x 15 mm, 3 μm particle was used with a mobile phase of water (A) and acetonitrile (B) with a flow rate of 0.3 mL/min and the gradient described method for HPLC–MS was used.

2.2.10 Gas chromatography–mass spectrometry (GC-MS)

GC-MS Analysis. A portion of extract (2 mg) was dissolved in 1 mL of ethyl acetate and 1 μL of each prepared sample was injected in splitless mode at 280 °C into the GC–MS (Focus GC-DSQ2, Thermo Fisher Scientific, Hemel Hempstead, UK) system equipped with a Rtx-1 MS column (30 m Å~0.25 μm film Å~0.2mm i.d., Thames Restek UK). The temperature gradient was programmed as follows: 100 °C for 2 min, linearly increasing to 280 °C at the rate of 5 °C/min, holding at 280 °C for 15 mins and linearly increasing to 320 °C at the rate of 10 °C/min and holding for 10 mins. The temperature was 250 °C and the ionisation voltage was 70 eV for EI–MS. The mass axes of MS instrument were externally calibrated according to the manufacturer`s instructions just before commencing the experiment.

2.2.11 Nuclear magnetic resonance spectroscopy analysis

The NMR samples were carried out by using a Bruker AV3HD500 spectrophotometer and the Bruker Avance 600 MHz with a 14.1 T Ultrashield superconducting magnet operating system. Samples to be tested were dissolved in about 0.6 mL of a suitable deuterated solvent either Chloroform-d (CDCl3), dimethyl sulfoxide-d6 (DMSO-d6), acetone-d6 according to their solubility, in NMR tubes. After collecting data of the proton NMR using Mnova Software, the data was evaluated; the integration number of the proton, the chemical shifts, coupling constants and indicated the type of each hydrogen present in the molecule. Then ^{13}C NMR, Distortionless Enhancement by Polarization Transfer (DEPT) experiments were obtained in

order to distinguish the carbons according to the extent of their proton attachments. COSY, HSQC, HMBC, and NOESY experiments were carried out to elucidate the structure of each pure compound. NMR spectra were processed using Mnova (Mestrelab Research, Santiago de Compostela, Spain).

2.2.12 Ultraviolet-Vis Spectroscopy

One milligram of the compound was dissolved in 10 mL of ethanol and the electronic absorption spectra were recorded at room temperature. An UNICAM UV 300 spectrophotometer was used to determine the UV-Vis absorption spectra of the compound in the range from 190-750 nm by using 1 cm^3 path length quartz cell, and the baselines were measured using a blank. The solution was diluted to the correct range of measurement (1mg/mL) then the peak area and the wavelengths were determined.

2.2.13 Infrared (IR) spectroscopy

The IR spectra of some isolated compounds were recorded on the Perkin Elmer FTIR model 1725X spectrophotometer with ATR probe, using potassium bromide (KBr) disc. The measurement mode was setting on transmittance and the resolution was on 4. A very small amount of the dry sample was loaded on top the ATR crystal in a way that it is fully covered and the spectrum was generated as a plot of absorbance against wave numbers were carried out in the mid-infrared region (400 to 4,000 cm^{-1}), using the Lab solution IR computer software. The acquired spectra were reported as the average of sixty-four co-added scans of the sample material at a 4 cm^{-1} resolution and were referenced against an air background.

2.2.14 Melting point

The melting points (uncorrected) were measured for the novel compound isolated from the Zambian propolis using a Stuart Scientific melting point apparatus (Bibby, UK). Thin capillary melting point tubes that are sealed at one end were used to hold melting point samples. Some crystals were transferred from the open end to the bottom of the tube by tapping the bottom gently on the benchtop. Then, it was inserted into the channels located beside the front of the thermometer tube and the heating control was turned on using a slow heating rate. After that, the sample was observed through the lens on the front of the apparatus. the thermometer reading was recorded when the sample started to melt and again when all of the sample had

melted (this gave the melting point range). This process was repeated three times for the same sample, and the average value was reported.

2.2.15 Thin Layer Chromatography (TLC)

TLC was carried out by using Merck KGaA 60 F_{254} TLC plates (Sigma Aldrich UK). First, a pencil line was drawn near the bottom of a thin plate, a small drop of each sample was spotted on TLC plate using a clean capillary. When the spot of mixture was dry, another drop was placed on the same point. The plate was then introduced into a chamber containing a mobile phase, which is combination of varying proportions of hexane and ethyl acetate beginning with 90:10, 70:30 then 50:50, respectively. Then all fractions, in each tube were separated according to their polarity. The plate was left to dry at room temperature for 5 minutes. Following this, spots on the TLC plate were observed, using fluorescence, by exposing to ultraviolet light UV detection with short wavelength (254 nm) and long wavelength (366 nm). Also, the plate was visualized by spraying with anisaldehyde sulphuric acid reagent and then heating to display compounds as purple and brownish spots. Next, the results of all spots on the TLC plates were evaluated and the retention factor (R_f) value was determined by measuring the distance of spot travelled and dividing by the distance of solvent movement from the starting point. The R_f values were used in detection of the similar compounds (**Figure 2-2**).
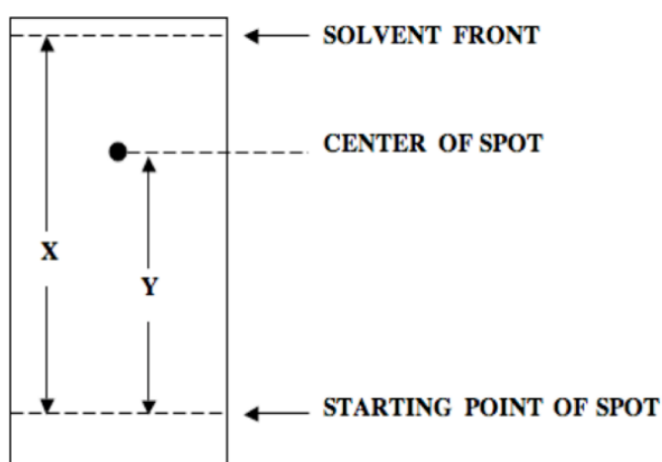
$$R_f = Y/X \text{ (always} \leq 1)$$

Figure 2-2: TLC schematic diagram and its parameters. R_f is defined as the ratio of Y the distance traveled by a compound spot (measured from the center of the spot) to X the distance traveled by the solvent.

2.2.16 Samples preparation for biological assay

Stock solutions for each compound or extract concentration were prepared as 20 mg in 1 mL of DMSO, ensuring that there was a constant percentage of 1% (v/v) DMSO per well.

2.2.17 Parasites cell lines culture

The kinetoplastid parasites used in this study included the bloodstream form (BSF) of *Trypanosoma brucei brucei* we used *Lister s427WT* (de Koning et al., 2000) and the derived drug resistant clone *B48* (Bridges et al., 2007), which was generated by knockout of the TbAT1 drug transporter (Matovu et al., 2003) followed by adaptation to high concentrations of pentamidine which resulted in loss of the *TbAQP2* gene and high levels of resistance to the diamidine and melaminophenyl arsenical drugs (Munday et al., 2014). Culturing of *T. brucei* bloodstream forms was performed in complete HMI-9 medium with 10% fetal bovine serum at 37 °C in a 5% CO_2 atmosphere, in HMI-9 medium (Invitrogen, UK) supplemented with 10% (v/v) heat inactivated fetal bovine serum (FBS), 14 µL/L β-mercaptoethanol, and 3.0 g/L $NaHCO_3$ adjusted to pH 7.4 as described previously (de Koning et al., 2000). The *T. congolense* bloodstream forms of strain IL3000, and the derived diminazene-resistant clone 6C3, were cultured in Minimal Essential Medium (MEM) base with 10% goat serum, supplemented with 14 µL/L β-mercaptoethanol, glutamine and antibiotics at at 34 °C in a 5% CO_2 atmosphere as described (Cerone et al., 2019, Coustou et al., 2010) in basal medium prepared with MEM medium (Sigma-Aldrich), 26 mM $NaHCO_3$, 25 mM HEPES, 5.6 mM D-glucose, 1 mM sodium pyruvate, 100 µM hypoxanthine, 40 µM adenosine, 16.5 µM thymidine and 25 µM bathocuproine disulfonic acid disodium salt, and supplemented with 1.6 mM glutamine, 100 units/mL penicillin, 0.1 mg/mL streptomycin, β-mercaptoethanol (0.0014%, v/v), 15% (v/v) goat serum (Gibco, UK), and 5% (v/v) Serum Plus II (Sigma-Aldrich, UK).

2.2.18 Mammalian cell lines culture

Human U937 cells (European Collection of Cell Cultures Cat. No. 85011440, supplied by Sigma-Aldrich, UK), were cultured in RPMI 1640 medium (Lonza, UK) supplemented with 5% (v/v) FBS, 1% (v/v) L-glutamine and 1% (v/v) penicillin/streptomycin at 37 °C in a humidified atmosphere of 5% CO_2 as previously described (Passmore et al., 2001). RAW 264.7 (ATCC TIB-71, USA) murine macrophages were cultured using ATCC-formulated Dulbecco's Modified Eagle's Medium (DMEM) (Catalog No. 30-2002) supplemented with 10% (v/v) FBS,

1% (v/v) glutamine, and 1% (v/v) penicillin-streptomycin at 37 °C in a humidified atmosphere of 5% CO_2 (Han et al., 2002, Ayupova et al., 2019)

2.2.19 Trypanosoma brucei and Trypanosoma congolense bloodstream forms (BSF)

Crude extracts, fractions, and isolated compounds were tested *in-vitro* against BSF *T. b. brucei* s427 WT and *T. b. brucei* B48; BSF *T. congolense Tc*-IL3000 WT and *T. congolense* 6C3 in order to assess the potential for cross-resistance with existing drugs exactly as described previously (Omar et al., 2017, Alotaibi et al., 2019). This assay is based on viable cells metabolizing the blue resazurin dye to resorufin, which is pink and fluorescent (Gould et al., 2008). 11 double dilutions of the compound (in the appropriate culture medium for the species) were prepared from 20 mg/mL stock solution in 96-well plates (Greiner Bio-one GmbH, Germany), starting from 200 µg/mL down to 0.19 µg/mL with the 12th well containing no drug. Dilutions of pentamidine or diminazene were prepared in parallel to serve as positive controls. This involves adjusting cell density of T.b. brucei S427 to the desired concentration of 2×10^4 cells/well, while *T. congolense* at the seeding density of 5×10^4 cells/well and the cells were exposed for 48 h to the test compounds, at 37°C/5% CO_2, before the addition of the resazurin dye at a final concentration of 10% of well volume and a further incubation of 24 h under the same conditions was applied. Pentamidine and Diminazene were used in this assay as positive controls. Fluorescence was determined in a FLUOstar Optima (BMG Labtech, Durham, NC, USA) at wavelengths of 544 nm for excitation, 590 for emission, and a gain of 1250. The results were expressed as half maximal effective concentration (EC_{50}) values were calculated by non-linear regression using an equation for a sigmoidal dose-response curve with variable slope (GraphPad Prism).

2.2.20 Anti-Crithidia fasciculata assays

C. fasciculata (ATCC50083) were grown at 27 °C with gentle agitation in serum-free defined media as described by (Kipandula et al., 2017). These cells were then used to inoculate wells of a 96 well plate with 1×10^5 cells per well in 100µl of medium. Stock samples were prepared with a concentration of 20 mg/mL in DMSO, the assays were performed using a1:1 serial dilution (i.e. 12 double dilutions starting from 200 ug/ml as the top concentration until 0.19 ug/mL and a no-drug control well) in each raw of the white opaque plastic 96-well plates (F Cell Star, Greiner Bio-one GmbH, Frickenhausen, Germany). The plate was incubated for 48

h at 27°C in an atmosphere of 5% CO2, before the addition of the resazurin dye and a further incubation of 24 h under the same conditions. Fluorescence measurements in this study were performed with a FLUOstar Optima with wavelengths of 530 nm for excitation, 560 nm for emission. Pentamidine was included as a control drug in all assays but it shows variable activity against *C. fasciculata* and thus Phenylarsine oxide (PAO) was used as an additional control drug.

2.2.21 Drug sensitivity using Cell count

Effect of different concentrations of the purified compound PNG-F5 was tested on BSF *T. b. brucei* s427 WT were tested for monitoring *in vitro* cell growth using cell count following long exposures. The cells were taken from cultures at the late logarithmic phase of growth and cell density was determined using a haemocytometer. Cell density was adjusted to the desired concentration of 2×10^5 cells/mL with fresh complete HMI-9 medium containing PNG-F5 at $0.5 \times$, $1 \times$, $2 \times$ and $4 \times$ EC_{50} (determined by the resazurin-based assay, above) in 25-mL culture flasks. The flasks were incubated at 37 ºC and 5% CO_2 and the cells of each culture were counted in a Neubauer counting chamber under a phase-contrast microscope in triplicate at several time points (0, 6, 12, 18, 24, 30, 36, 42 and 48 h) for different concentration of the compound and pentamidine, as well as free drug cells to serve as a positive control, as well as the no drug control. The experiment was repeated two more times and the counts of the three independent determinations were averaged and used for plotting the growth curve.

2.2.22 Cell Toxicity Assay by Using U937 and RAW 246.7 cell lines

The cytotoxic effect of crude extracts, fractions, and isolated compounds on RAW246.7 were carried out as previously described (Ayupova et al., 2019). Cells were grown to log phase and adjusted to a density of 1×10^5 cells/mL. 100 µL/well of the cells were added to a 96 well plate (TPP, Switzerland) and the plate incubated for 24 hours at 37°C, 5% CO_2, 100% humidity. The stock solution was prepared in another 96 well plate in 8 different concentrations in the full, supplemented DMEM medium (section 2.2.1) using 1:1 serial dilution (i.e. starting from 200 µg/mL as the top concentration until 1.56 µg/mL). The samples were then transferred (100 µL) to the cultured cells using a multichannel pipette and left in the incubator for 24 h. After incubation, 5 mM resazurin sodium salt (Sigma Aldrich, UK) was added (20 µL per well) and the plate incubated for a further 24 hours. Fluorescence readings of the plate were taken using a Perkin Elmer Wallac Victor2 1420 Multilabel Counter (λex 570 and λ em 600 nm). While,

U937 cells were grown to log phase, counted and adjusted to a density of 1×10^5 cells/mL. A volume of 100 μL of cells was then added to each well of a 96-well plate (TPP, Switzerland) and incubated for 24 h at 37 °C, 5% CO_2 and 100% humidity. From a 200 μg/mL stock solution, a 2-fold serial dilution of the test compound was carried out in the full, supplemented RPMI medium, (section 2.2.18) to determine the IC_{50} value for the samples. In another 96-well plate, 100 μL of each dilution was transferred to the cultured cells using a multichannel pipette, followed by incubation for 24 h. Controls consisted of 10% (v/v) DMSO (positive, cell death control), cells and medium (negative control) and 0.5% (v/v) DMSO (solvent control). This was followed by addition of 20μL of 5 mM resazurin sodium salt (Sigma Aldrich, UK) and the plates incubated for a further 24 h after which fluorescence was measured using a Spectramax plate reader (Molecular Devices, USA) or a Wallac Victor 2 (Perkin Elmer, UK) microplate reader (λ exc = 560 nm, λem = 590 nm). The compounds or extracts was tested in triplicate and cell viability was expressed as a percentage of the drug-free control. The resulting data were analyzed using GraphPad Prism 8.0 (GraphPad Software Inc., San Diego) to obtain a dose-response curve and the mean 50% inhibitory concentration (IC_{50}) value. The viability of the cells was determined from fluorescence measurements representing the extent of reduction of resazurin to resorufin by cell respiration. The percentage of viable cells was calculated for each concentration (n = 3) to obtain IC_{50} values using the formula shown below:

$$\text{Cell viability test\%} = \frac{(\text{Fluorescence of treated cells})}{(\text{Fluorescence of blank})} \times 100$$

Chapter Three

3 Chemical and Biological Profiling of Propolis from Some African Countries and Pacific Ocean Island Countries

3.1 Propolis in different geographic regions

Every geographic region has a unique propolis composition which depending on the bee species as well as the variety of the plant species that are foraged by bees in that particular zone. Therefore, a wide range of compounds are present in propolis from different sources and this leads to disparities in its biological activity (Bankova, 2005, Miguel and Antunes, 2011, Toreti et al., 2013). In the last few decades, several studies have proved the diversity of propolis in terms of its chemical composition and how this is dependent on geographic origin. For example, a study of 40 propolis samples collected from different geographic locations, found that the samples taken from similar regions, possessed similarity in their chemical composition. Particularly, samples from the temperate regions that were collected from Europe, New Zealand, Western Asia, and North America, which were shown to be rich in phenolic compounds such as flavonoids, aromatic acids, and esters, while samples from tropical regions such as Ghana and Nigeria contained only traces of phenolic compounds. This is probably due to the fact that the phenolic compounds originate from exudates of the poplar tree, which is located in temperate areas but not tropical regions (Seidel et al., 2008, Isla et al., 2005, Orsi et al., 2005). Subsequently more comprehensive profiling of African propolis revealed several different types some of which contained complex mixtures of phenolics while others were dominated by triterpenes indicating that there was no clear geographic delineation for the classification of these African propolis samples (Zhang et al., 2014).It has been shown that propolis from different geographic locations has significant biological activity, regardless of the great variation in its chemical composition (Kujumgiev et al., 1999). Many other studies have confirmed this fact by testing different propolis samples from all around the world. For comprehensive review of the variations in propolis composition, see (Silva-Carvalho et al., 2015).

3.2   Metabolomics tools

Metabolomics is a comprehensive study of metabolites and biomarkers among experimental groups to understand the function of living organisms (Kaddurah-Daouk et al., 2008). The application of metabolomics in natural products research provides a useful tool in drug discovery studies. Metabolites defined as small molecular weight molecules (<1500 Da) present in the living organism. Primary metabolites include sugars, amino acids, proteins and nucleic acids that play an important role in cell growth. While, secondary metabolites include alkaloids, phenolics, steroids, essential oils, lignins, resins and tannins that are produced biochemically from primary metabolites and play an important role for cell functions (Emara et al., 2017). Propolis consists of bioactive organic compounds which are derived from secondary metabolites produced by plants. Analysis by using metabolomics is important for identifying, quantifying, and classifying the secondary metabolites. As a result of complexity and variability of chemical components in secondary metabolites that are present in a certain natural product, it is challenging to identify and quantify them, therefore, the application of certain analytical techniques is required. various analytical techniques and many softwares have all been applied for metabolite analysis. The most popular analytical techniques are mass spectrometry (MS) and nuclear magnetic resonance (NMR) in conjunction with MNOVA software, while the most commonly used MS software includes MZmine and MZmatch. The software can be coupled with an online or commercially available database such as Dictionary of Natural Product (DNP), ChemSpider, or in-house metabolomics databases to dereplicate the secondary metabolites (Harvey et al., 2015). Then, the data processing is exposed to statistical modelling to provide information about the diversity of chemical components either by unsupervised clusterings such as principle component analysis (PCA) or supervised clusterings such as orthogonal partial least squares discriminant analysis (OPLS-DA) by using software such as SIMCA P. Recently, bioassay-guided fractionation in natural products research was carried out using a metabolomics approach for searching for biologically active or novel compounds (Tawfike et al., 2013).The current study applied metabolomic tools that to provide a powerful method to distinguish the putative bioactive metabolites prior to the chromatographic separation which can save experimental time. To investigate the constituents and profile of 25 propolis samples from different geographic regions including some African countries and Pacific Ocean islands **(Figure 3-1)**.
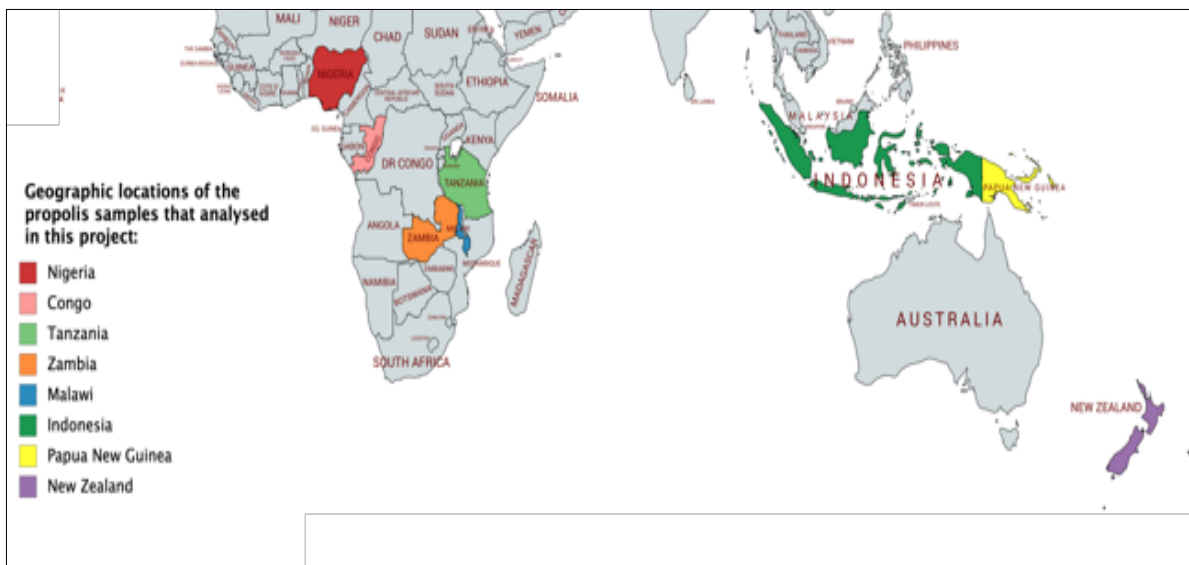
Figure 3-1: Geographic map showing the localities of the analysed propolis samples used in this project

3.3 Chemical profiling by Principle components analysis (PCA)

Chemical profiling was conducted by using negative ion spray ESI (LC-MS). Principle components analysis (PCA) of the processed LC-MS data collected gave the chemical composition of the crude extracts from different samples (**Figure 3-2**) that also showed some activity against the parasites.
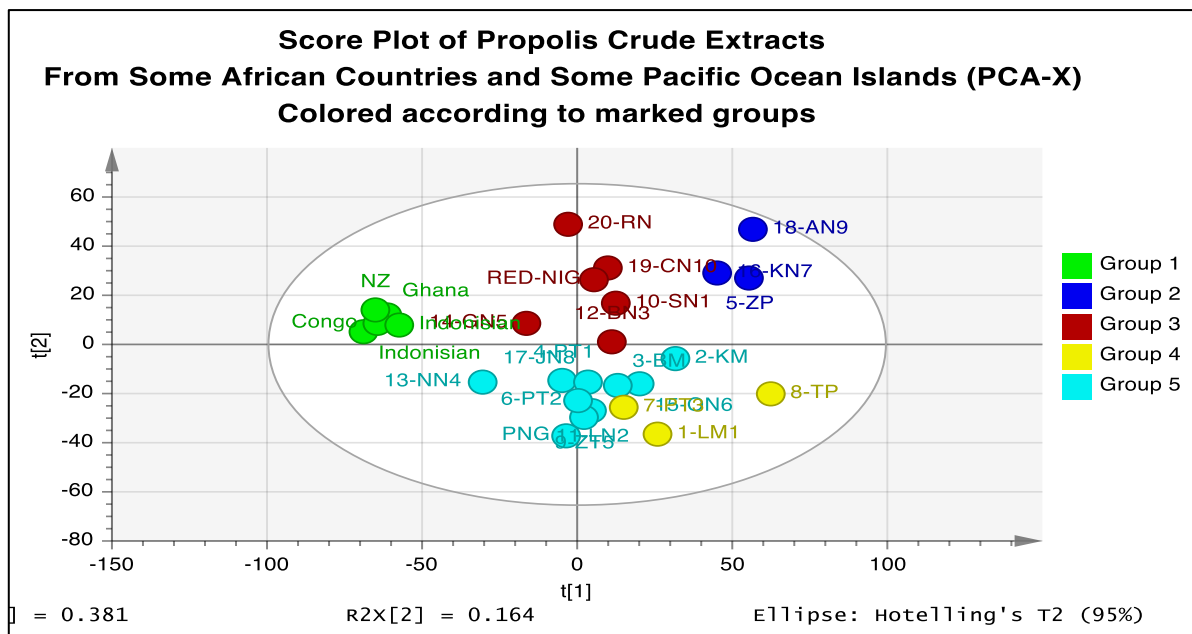
Figure 3-2: Score plot of PCA-X for duplicate analyses of propolis crude extracts of samples collected from some African countries and Pacific Ocean islands countries The figures based on 25 propolis samples in negative ion mode showed a separation between the samples into five groups, coloured according to the similarity of chemical profiling. The modelled represented the samples as dots and codes are based on the initial letter of the origin of the propolis samples.
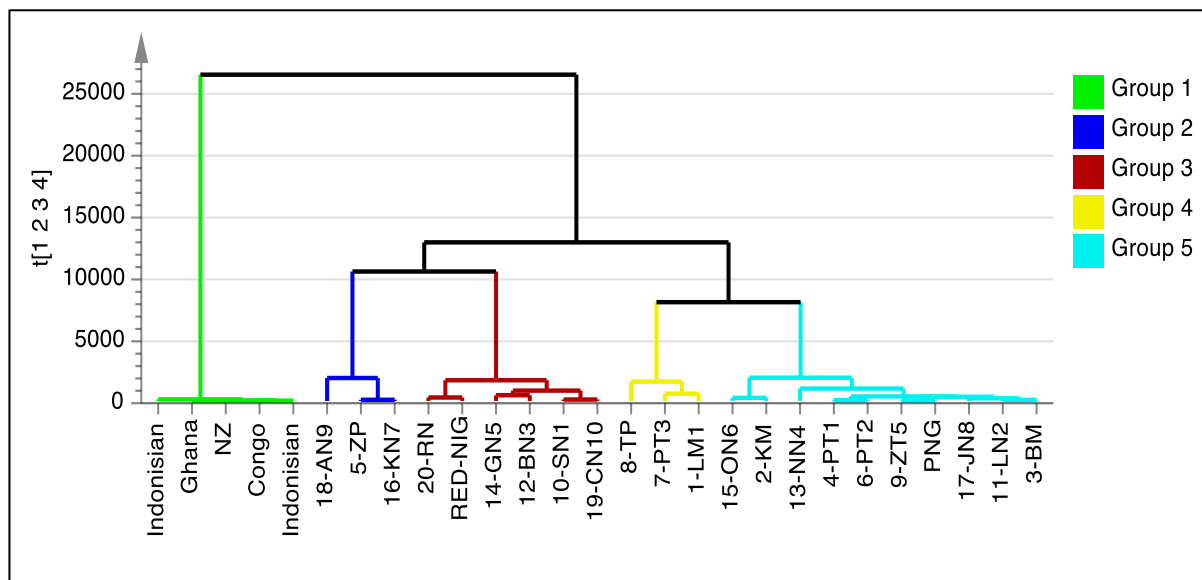
Figure 3-3: Hierarchical clustering generated from the PCA for the crude propolis African and Pacific Ocean islands countries extracts grouping them into five groups (coloured according to marked groups).

Hierarchical cluster analysis (HCA) was used to divide the samples into five groups (**Figure 3-3**), according to similarity in chemical composition. Each elemental compositions generally corresponded to many isomers within the dictionary of natural products (DNP) database. It is noteworthy that three of Pacific Ocean islands extracts which are two samples from Indonesia and New Zealand were clustered together with Congo and Ghana samples. In contrast, the Papua New Guinea (PNG) sample looks different since it was clustered with the African samples. Samples from the Zambia code 5-ZP and two of samples from Nigeria were clustered together to some extent. It was clearly observed that the Tanzania sample code 8-TP was clustered with another Tanzania sample code 7-PT3 and the Malawi sample code 1-LM1.

3.4 Antitrypanosomal activity *in vitro*

23 crude propolis extracts were tested in vitro against *T. brucei* BSF, the multidrug-resistant *B48*, *Trypanosoma congolense* and its resistant strain, and *C. fasciculata* alongside the drugs currently used for the treatment of African trypanosomiases (pentamidine and diminazene), using Alamar blue assays. Most of the crude propolis extracts tested showed EC$_{50}$ values in the low microgram range.

3.4.1 *In vitro* antitrypanosomal activity and cross-resistance studies of propolis extracts

The anti-trypanosomal activity of the primary extracts was tested at a starting concentration of 200 μg/mL down to 0.19 ug/mL along with a no-drug (control well. **Table 3-1** shows the results obtained in testing the 23 samples of some African countries and Pacific Ocean islands propolis against *T. brucei (s427)* strain and the multidrug resistant strain of *T. brucei (B48) in vitro*. Of these, 8 samples displayed high activity, i.e. EC_{50} values < 10 μg/mL on wild type *T.brucei S427* and nine of the crude extracts exhibited activity < 10 μg/mL for the standard drug-sensitive strain *T. brucei B48*. The propolis samples from Tanzania (8-TP) is exhibited the highest activity, followed by the Malawi (1-LM), Nigeria (20-RN), Papua New Guiana (PNG), Zambia (5-ZP) and New Zealand (NZ) propolis samples. The other crude extracts showed intermediate activity with average EC_{50} values <29 (μg/mL) against *T. brucei (s427)* strain and the drug resistant strain of brucei BSF *B48*. The Resistance Index (RI) of *T. brucei (s427)* strain and its resistant strain *B48* for most of the propolis samples were ≤ 1, except for two crude samples 4-PT1 and 5-ZP which were less active against B48, RI= 1.3322, P<0.05) and 5-ZP which was also significantly less active against B48 (RI= 1.7834, P<0.05). However, the RI for pentamidine was 68.46 and the P value was < 0.001.

Table 3-1: The activity (μg/mL) of 23 African propolis samples and some Pacific Ocean islands propolis against the standard drug-sensitive *T. brucei* 427WT and multi-drug resistant strain *T. brucei B48*

Samples	*T. brucei S427*WT			*T. brucei B48* (Pentamidine Resistance)				
	Mean of EC_{50} (μg/mL)	SD	%RSD	Mean of EC_{50} (μg/mL)	SD	RI	t-test	%RSD
propolis samples from some African countries								
1- LM	2.16	0.1326	6.12	2.30	0.36	1.0633	0.5694	15.63
2-KM	16.85	1.2291	7.30	14.28	2.73	0.8476	0.2121	19.14
3-BM	18.65	2.3756	12.74	16.97	2.45	0.9097	0.4411	14.44
4-PT1	8.02	0.0973	1.21	10.68	1.14	1.3322	0.0157	10.66
5-ZP	4.14	0.2012	4.86	7.39	0.86	1.7834	0.0032	11.70
6-PT2	18.43	1.9248	10.45	12.48	1.61	0.6771	0.0148	12.89
7-PT3	16.86	1.6618	9.85	16.58	0.87	0.9834	0.8086	5.22
8-TP	1.20	0.0706	5.88	1.02	0.12	0.8457	0.0843	11.95
9-ZT5	11.87	2.8684	24.17	7.12	1.19	0.5997	0.0569	16.68
10- SN1	13.83	1.7916	12.95	13.58	1.72	0.9819	0.8702	12.70
11- LN2	20.13	0.8072	4.01	14.29	0.49	0.7099	0.0004	3.46
12-BN3	13.11	3.4397	26.24	13.01	2.12	0.9924	0.9681	16.26

13-NN4	16.29	0.6229	3.82	13.35	1.00	0.8196	0.0125	7.52
14-GN5	28.43	3.8965	13.70	18.40	1.96	0.6472	0.0163	10.63
15-ON6	16.68	2.2744	13.63	14.29	1.05	0.8563	0.1730	7.37
16- KN7	15.91	1.4476	9.10	13.22	1.79	0.8311	0.1136	13.56
17-JN8	21.97	1.8832	8.57	18.37	2.45	0.8364	0.1144	13.34
18-AN9	21.40	2.6182	12.23	12.53	1.99	0.5853	0.0095	15.91
19-CN10	15.16	3.0413	20.06	6.06	1.14	0.3995	0.0083	18.79
20 RN	3.97	0.6779	17.10	4.45	0.53	1.12	0.3849	11.90
Hugo sample	5.61	0.7647	13.63	5.39	0.87	0.9599	0.7537	16.19
propolis samples from some Pacific Ocean islands countries								
PNG	4.01	0.0953	2.38	3.85	0.37	0.9599	0.5028	9.52
NZ	5.03	0.3406	6.77	4.29	0.94	0.8520	0.2672	21.97
Control								
Pentamidine	0.0026	0.0005	21.30	0.1760	0.0230	68.456	0.0002	13.05

The Effective Concentration 50% (EC_{50}) results are given in (µg/mL) as averages of 3 independent experiments P value is based on a Student's unpaired t-test, comparing *T. brucei* WT and *B48*. R. I. is the resistance index, being the ratio of the EC_{50} values for *T. brucei* WT and *B48*.

3.4.2 *In vitro* Antitrypanosomal activity and cross-resistance studies of propolis extracts using *T. congolense (1L300)* and a derived diminazene-resistant *T. congolense* strain (6C3)

The same propolis samples were also tested against the veterinary trypanosome species *T. congolense* (1L300) and a derived diminazene-resistant *T. congolense* strain (6C3). The results found no significant differences in the activity of the propolis extracts against the two strains (P > 0.05), showing that these propolis samples were not cross-resistant with first-line trypanosomiasis drugs such as diminazene aceturate. The most active samples against *T. congolense* (1L300) and the diminazene resistance strain were Tanzania (8-TP), followed by the Malawi (1-LM), Papua New Guiana (PNG) and Nigerian red propolis sample (20-RN). The rest of samples showed intermediate activity with average EC_{50} values <27 (µg/mL) against T. congolense1L300 (**Table 3-2)**. Most of the samples showed slightly higher activity against *T. congolense* than *T. brucei*, as the EC_{50} (*Tbb427*WT)/ EC_{50} (*T. congolense* 1L300) of most of the samples were >1 and the average of the ratio was 1.17 **Table 3-4**. Nevertheless, the Zambian sample (5-ZP) obviously was less active against *T. congolense*1L300 than the *WT T. brucei*.

Table 3-2: The activity (µg/mL) of 23 African propolis samples and some Pacific Ocean islands propolis against the *T. congolense* (IL300) and its drug resistant strain (6C3)

Samples	*T. congolense* (IL300)			Diminazen resistance *T.congolense* (6C3)				
	Mean of EC$_{50}$ (µg/mL)	SD	RSD%	Mean of EC$_{50}$ (µg/mL)	RF	t-test	SD	%RSD
propolis samples from some African countries								
1- LM	1.97	0.16	8.27	2.82	1.44	0.1295	0.76	26.98
2-KM	15.18	1.36	8.94	14.16	0.93	0.6795	3.71	26.17
3-BM	13.57	2.27	16.70	13.38	0.99	0.9367	3.20	23.93
4-PT1	5.48	1.27	23.27	5.40	0.99	0.9521	1.55	28.60
5-ZP	14.39	0.64	4.45	9.59	0.67	0.0041	1.24	12.97
6-PT2	12.35	2.63	21.33	11.30	0.92	0.6640	2.85	25.25
7-PT3	9.41	1.43	15.24	11.97	1.27	0.2284	2.78	23.25
8-TP	1.80	0.46	25.32	2.20	1.22	0.3441	0.45	20.46
9-ZT5	7.05	0.66	9.39	8.24	1.17	0.2121	1.23	14.95
10- SN1	26.09	4.78	18.31	22.99	0.88	0.4558	4.41	19.18
11- LN2	11.51	2.56	22.23	10.92	0.95	0.7689	1.99	18.27
12-BN3	14.71	2.57	17.48	15.65	1.06	0.7501	4.00	25.56
13-NN4	13.75	2.34	17.00	10.43	0.76	0.1721	2.55	24.49
14-GN5	24.49	0.61	2.48	18.31	0.75	0.0218	2.86	15.64
15-ON6	13.05	0.79	6.03	15.75	1.21	0.0799	1.84	11.68
16- KN7	7.89	1.75	22.21	4.77	0.60	0.0613	1.14	24.01
17-JN8	22.25	4.33	19.48	14.57	0.65	0.0441	1.51	10.35
18-AN9	16.09	3.17	19.68	16.63	1.03	0.8025	1.44	8.66
19-CN10	21.89	1.59	7.27	34.47	1.57	0.0123	4.76	13.82
20 RN	4.28	0.63	14.75	4.47	1.04	0.7537	0.75	16.82
Congo	6.52	1.19	18.24	7.14	1.09	0.5110	0.89	12.49
propolis samples from some Pacific Ocean islands countries								
PNG	3.35	0.47	14.15	3.51	1.05	0.7776	0.78	22.24
NZ	4.55	0.73	15.97	4.15	0.91	0.4598	0.42	10.00
Control								
Diminazen	0.0865	0.0164	18.92	3.1327	36.2074	0.00005	0.28	9.00

The Effective Concentration 50% (EC50) results are given in (µg/mL) as averages of 3 independent experiments P value is based on a Student's unpaired t-test, comparing *T. congolense* IL300 and its diminazen resistant strain 6C3 R. I. is the resistance index, being the ratio of the EC50 values for T. congolense and its drug resistant strain.

3.5   Effect of propolis extracts on *in vitro* growth of *C. fasciculata*

Table 3-3 displays the data obtained from testing some propolis samples against *C. fasciculata* which is a closer relative to the trypanosomatids that infect bees. A wide range of intermediate activities were obtained, the highest activities against *C. fasciculata* in this study were for Tanzania (8-TP) EC_{50} = 13.79 µg/mL and Malawi (1- LM) EC_{50} = 14.13 µg/mL. While the rest of the samples showed average EC_{50} values range between 20 and 50 µg/mL. All the samples showed significantly less activity against *C. fasciculata* compared with *T. brucei*, as the EC_{50} (*TbbS427*WT)/ EC_{50} (*C. fasciculata*) of all the samples were <1 **Table 3-4**.

Table 3-3: The activity EC_{50} (µg/mL) of 23 African propolis samples and some Pacific Ocean islands propolis against *C. fasciculata*

Propolis Origin	Samples	Mean of EC_{50} (µg/mL)	SD	RSD%
Malawi	1- LM	14.13	2.92	20.65
Malawi	2-KM	21.95	3.58	16.32
Malawi	3-BM	26.80	3.86	14.38
Tanzania	4-PT1	44.17	4.69	10.61
Zambia	5-ZP	19.87	3.29	16.55
Tanzania	6-PT2	19.99	4.55	22.76
Tanzania	7-PT3	42.06	4.74	11.26
Tanzania	8-TP	13.79	1.39	10.08
Tanzania	9-ZT5	45.96	5.43	11.82
Nigeria	10- SN1	48.65	8.97	18.43
Nigeria	11- LN2	26.72	4.35	16.29
Nigeria	12-BN3	27.35	3.95	14.44
Nigeria	13-NN4	38.13	8.57	22.47
Nigeria	14-GN5	50.99	5.36	10.51
Nigeria	15-ON6	30.50	6.76	22.16
Nigeria	16- KN7	50.81	2.34	4.61
Nigeria	17-JN8	26.34	6.36	24.14
Nigeria	18-AN9	31.83	6.09	19.12
Nigeria	19-CN10	33.81	4.95	14.63
Papua New Guiana	PNG	30.21	6.99	23.15
Control				
Phenylarsine oxide	PAO(µM)	4.17	0.66	15.78

Table 3-4: Comparison of the average of the ratio of EC_{50} of crude propolis extracts against Trypanosoma spp. And Selectivity Index (SI) on U937 and RAW 246.7

Samples	$EC_{50}(Tbb)/$ $EC_{50}(T.c)$	P Value	$EC_{50}(Tbb)/$ $EC_{50}(C.f)$	P Value	$IC_{50}(U937)/$ $IC_{50}(RAW$ 246.7)	P Value	SI on U937 IC_{50} value / $EC_{50}(Tbb$	SI on RAW246.7 IC_{50} value / $EC_{50}(T.C$
1- LM	1.1014	0.1751	0.1532	0.0021	0.8283	0.07255	23.4376	31.15
2-KM	1.1100	0.1892	0.7676	0.0800	0.7158	0.00557	7.1765	11.13
3-BM	1.3740	0.0554	0.6958	0.0356	0.8974	0.01624	7.0509	10.80
4-PT1	1.4634	0.0263	0.1815	0.0002	1.2076	0.01563	17.7327	21.49
5-ZP	0.2879	0.00001	0.2085	0.0012	0.8328	0.00081	40.1240	13.87
6-PT2	1.4916	0.0322	0.9218	0.6128	1.2902	0.00378	8.1386	9.41
7-PT3	1.7930	0.0042	0.4010	0.0010	0.6061	0.00008	8.7171	25.79
8-TP	0.6653	0.0864	0.0870	0.0001	1.6211	0.00015	123.3269	50.73
9-ZT5	1.6846	0.0470	0.2582	0.0007	0.7080	0.00083	11.1139	26.44
10- SN1	0.5301	0.0141	0.2843	0.0027	0.6318	0.00152	7.8178	6.56
11- LN2	1.7492	0.0051	0.7534	0.0614	0.5978	0.00222	4.9442	14.47
12-BN3	0.8912	0.5537	0.4793	0.0092	0.4857	0.00007	7.2846	13.37
13-NN4	1.1847	0.1431	0.4273	0.0432	0.3644	0.00006	3.8861	12.50
14-GN5	1.1612	0.1580	0.5576	0.0041	0.3392	0.00007	2.1019	7.19
15-ON6	1.2781	0.0593	0.5471	0.0284	0.5002	0.00033	5.7077	14.58
16- KN7	2.0174	0.0036	0.3131	0.0000	0.5866	0.00046	5.2208	17.95
17-JN8	0.9871	0.9214	0.8340	0.3170	0.6045	0.00058	5.3869	8.80
18-AN9	1.3302	0.0886	0.6724	0.0526	0.5413	0.00012	4.9992	12.29
19-CN10	6.9197	0.0018	0.4485	0.0051	0.3919	0.00003	5.1565	91.04
20-RN	0.9273	0.5919	N/D	-	0.8514	0.08038	30.2396	32.90
Congo	0.8500	0.3034	-	-	1.3238	0.00226	34.2543	22.26
PNG	1.1961	0.0782	0.1326	0.0029	0.9662	0.47195	29.0025	35.93
NZ	1.1068	0.3532	-	-	0.8974	0.01972	31.6567	39.00

The Effective Concentration 50% (EC_{50}) results are given in (µg/mL) as averages of 3 independent experiments. The Inhibition Concentration 50% (IC_{50}) results are given in (µg/mL) as averages of 3 independent experiments. P value is based on a Student's unpaired t-test, SI is the selectivity index, being the ratio of the average IC_{50} value and the average of EC_{50} values.

3.6 *In vitro* cytotoxicity of propolis extracts on mammalian cells

Table 3-5: IC$_{50}$ of Cytotoxicity of 23 African propolis samples and some Pacific Ocean islands propolis against U937 cell line and RAW 246.7 cell line.

Propolis Sample Origin	Samples code	U937			RAW 246.7		
		Mean of IC$_{50}$ (µg/mL)	SD	RSD%	Mean of IC$_{50}$ (µg/mL)	SD	RSD%
propolis samples from some African countries							
Malawi	1- LM	50.70	7.14	14.09	61.22	2.34	3.82
Malawi	2-KM	120.90	10.83	8.96	168.90	10.81	6.40
Malawi	3-BM	131.50	5.57	4.23	146.53	3.40	2.32
Tanzania	4-PT1	142.13	4.80	3.37	117.70	9.32	7.92
Zambia	5-ZP	166.17	5.68	3.42	199.53	2.85	1.43
Tanzania	6-PT2	149.97	7.98	5.32	116.23	5.45	4.69
Tanzania	7-PT3	147.00	6.72	4.57	242.53	7.32	3.02
Tanzania	8-TP	148.03	4.16	2.81	91.32	5.62	6.16
Tanzania	9-ZT5	131.90	5.73	4.34	186.30	8.70	4.67
Nigeria	10- SN1	108.12	13.68	12.66	171.13	3.63	2.12
Nigeria	11- LN2	99.53	11.82	11.88	166.50	11.70	7.03
Nigeria	12-BN3	95.50	6.89	7.22	196.63	7.70	3.92
Nigeria	13-NN4	62.66	8.82	14.08	171.97	5.81	3.38
Nigeria	14-GN5	59.76	3.41	5.70	176.17	11.17	6.34
Nigeria	15-ON6	95.22	12.80	13.44	190.37	6.57	3.45
Nigeria	16- KN7	83.06	6.27	7.55	141.60	7.33	5.18
Nigeria	17-JN8	118.33	6.02	5.08	195.77	12.14	6.20
Nigeria	18-AN9	107.00	6.02	5.63	197.67	8.71	4.41
Nigeria	19-CN10	78.19	4.42	5.65	199.50	9.01	4.51
Nigeria	20-RN	119.90	14.32	11.94	140.83	6.12	4.35
Ghana	GN	47.83	7.6	15.89	199.50	9.40	4.71
Congo	Hugo	192.17	6.31	3.28	145.17	9.88	6.80
propolis samples from some Pacific Ocean islands countries							
Papua New Guiana	PNG	116.30	5.70	4.90	120.37	6.80	5.65
Indonesian	INDO-1	83.27	5.67	6.81	157.73	6.48	4.11
Indonesian	INDO-2	215.63	4.75	2.20	274.57	20.94	7.63
New Zealand	NZ	159.23	2.97	1.87	177.43	7.83	4.41

AVG of IC50 =average of half maximal The Inhibition Concentration of at least 3 independent determinations. SD= Standard deviation of all determinations. RSD%= Relative Standard Deviation= (SD/ Avg.) x100.

In order to determine whether the activity of propolis extracts are specifically antiprotozoal or the result of general toxicity. The cytotoxicity activities of all the crude extracts were tested on human U937 cell line and murine RAW 246.7 cell line using a resazurin assay, involving a total incubation period of 72 hours. The results showed low levels of toxicity, with variable IC_{50} against the two cell lines. The toxicity results showed that the highest mean cytotoxicity was for sample 1-LM IC_{50} which had cytoxicities of 61.22µg/mL against the Raw 246.7 cell line and 50.7 µg/mL against U937. Interestingly, we observed, that most of the crudes had greater cytotoxicity against the human U937 cell line in comparison to the murine cell line RAW246.7, as the average of the ratio of IC_{50} U937/IC_{50} RAW 246.7 was <1 as shown in **Table 3-5**. An assay precision of <15% RSD was achieved for all samples tested on U937 and RAW 246.7.

Bioactivity-guided isolation of some of the active constituents from extracts was carried out on four samples from among these 23 samples in this which were PNG, TP, ZP and RN; these samples were from each group clusters in the PCA analysis, with sufficient weight, an EC_{50} value below 15 µg/mL and exhibiting a highly selective index.

Chapter Four

4 Triterpenes from Papua New Guinea Propolis Show Anti-Trypanosomal, Anti-Crithidia Fasciculata Activity and Cytotoxic Activity

Abstract

Chemical profiling and phytochemical screening of a propolis sample from the Eastern highlands of Papua New Guinea was conducted by using negative ion spray ESI (LC-MS) and indicated that the ethanolic extract of PNG contained a series of triterpenes in which were probably derivatives of amyrin and lupeol. Principle components analysis (PCA) of the processed LC-MS data collected was demonstrated the uniqueness in chemical composition of the fractions prepared from the sample that were also active against the parasites. Cytotoxicity guided fractionation in addition to metabolomics tools were used towards the identification of new lead compounds from propolis and evaluation of their potency. Active principles were isolated by using medium pressure chromatographic (MPLC). Spectroscopic and spectrometric means of purified compounds elucidated the structures of 12 triterpenoid compounds identified as mangiferonic acid, ambonic acid, isomangiferolic acid, ambolic acid, 27-hydroxyisomangiferolic acid, cycloartenol, cycloeucalenol, 24-methylenecycloartenol, 20-hydroxybetulin, betulin, betulinic acid and madecassic acid. The extracts and compounds were assayed against *Crithidia fasciculata*, *Trypansoma congolense*, drug resistant *Trypansoma congolense*, *Trypanosoma b. brucei* and drug resistant *Trypanosoma brucei* (B48). They were also assayed for their toxicity against U947 human cells and RAW 246.7 murine cells. A growth curve for *T. brucei* at concentrations $\geq EC_{50}$ for the most active compound in these assays was conducted and it was found that 20 hydroxy betuline was trypanostatic. Overall, the PNG propolis and its fractions showed low toxicity to both U937 cell growth and RAW 246.7 cell lines and conversely were efficacious against kinetoplastid parasites.

4.1 Method of extraction

About 38.5 of Papua New Guinea Propolis sample was extracted by sonication with 600 mL of absolute ethanol (Sigma Aldrich, UK), at room temperature for 60 minutes without applying any heat to avoid thermal degradation. (Clifton ultrasonic bath, Fisher Scientific, Loughborough, UK), after which the extract was filtered and re-extracted twice more with 100 mL of ethanol, filtering each time This step was repeated three times to make sure to fully extract the raw propolis and remove some impurities. The extracts were combined, and the solvent was evaporated using a rotary evaporator (Buchi, VWR, Leicestershire, UK), and the residue weighed. **Figure 4-1** and **4-2** show the protocol used for fractionation of the extract of PNG propolis. General details of the apparatus used, methods and the materials are given in chapter 2.
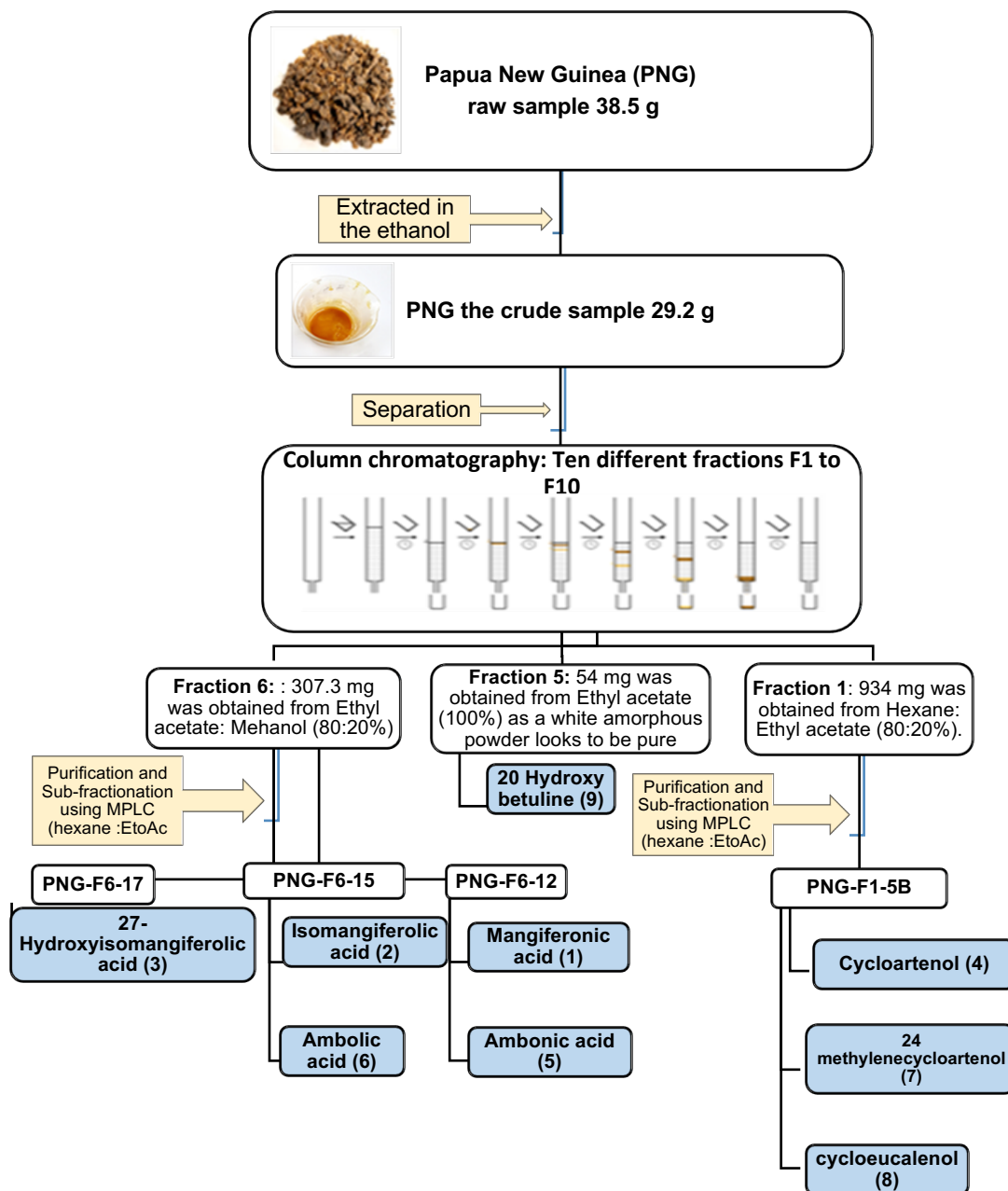
Figure 4-1: Workflow of PNG extract analysis and subfractionation of PNG-F1 and PNG-F6
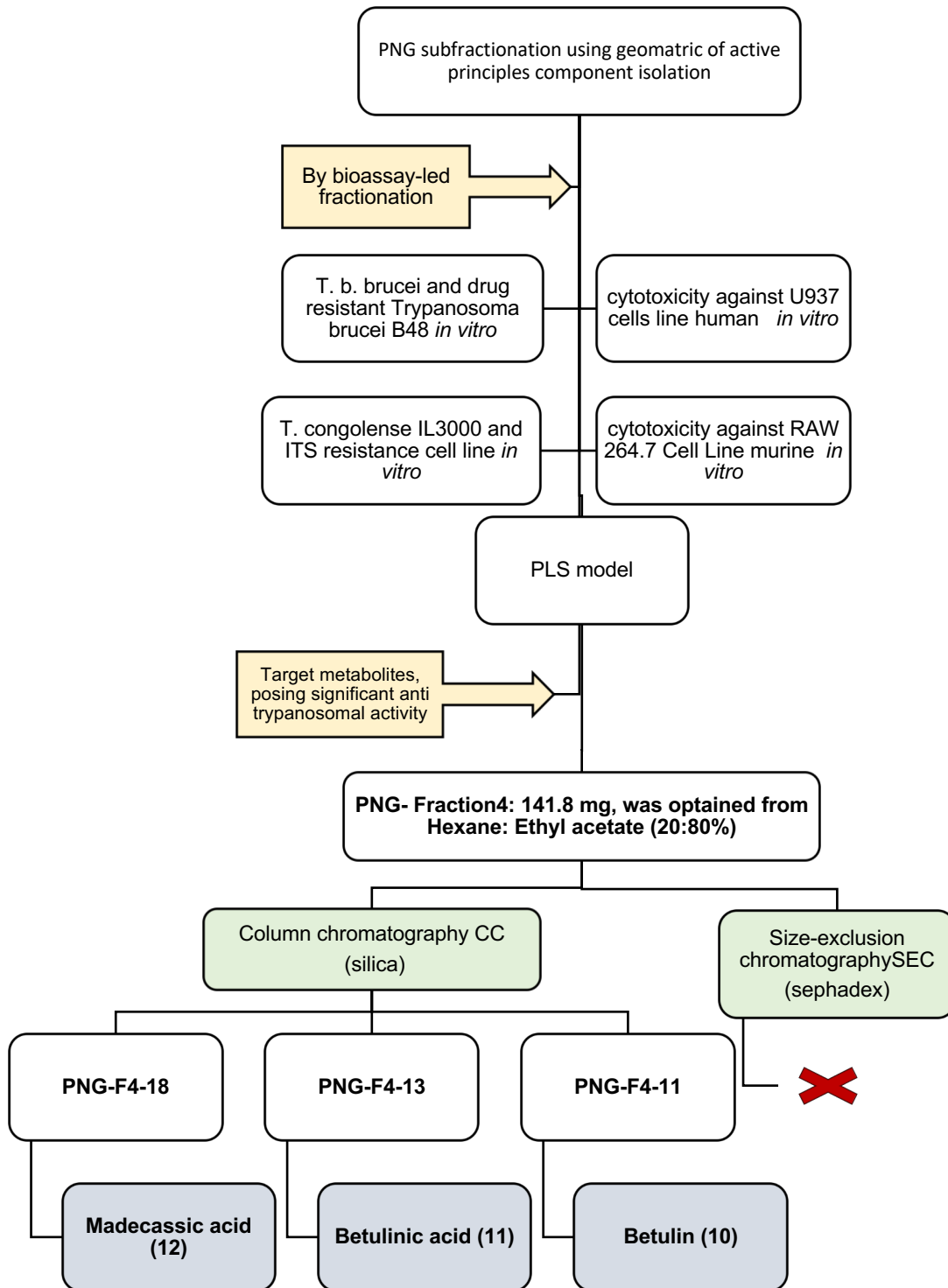
Figure 4-2: Workflow of PNG extract analysis and subfractionation of PNG-F4

4.2 Results and Discussion

4.2.1 Extraction and Fractionation of the PNG sample

Figure 4-3: Raw Papua New Guinea propolis sample before extraction (1), and after extraction (2)

About 38.4 g of the raw PNG propolis went through extraction with ethanol to obtain a crude sample weighing 29.2 g (Figure 4-3). The sample was fractionated using CC to obtain the fractions PNG F1 to PNG F10.The masses of the different fractions collected is presented in Table 4-1. The sufficient weight would give the opportunity for further analysis, separation, and biological assay.

Table 4-1: Summary of preliminary PNG propolis fractions yield from collected CC

Fraction's code	Mass of fraction (mg)
F1	934
F2	301.4
F3	227.2
F4	141.8
F5	54
F6	307.3
F7	172.6
F8	98.3
E9	52.2
E10	32.8

From the above data in **Table 4-1**, the greatest weight was in the fractions F1 (934 mg, which collected from the solvent system of Hexane: Ethyl acetate (80:20%). Fraction F2 was 301.4 which also collected from non-polar solvent system Hexane: Ethyl acetate (60:40%). Also, Fraction F6 collected from the solvent system of Methanol: Ethyl acetate (80:20%) had a sufficient weight of (307.3 mg). While lower weights were collected from Methanol (100%). These results indicate that the components of propolis sample are slightly non-polar because, most of it eluted in slightly non-polar mobile phase while a negligible amount eluted in the polar mobile phase. The two fractions with the greatest weights (PNG-F1 and PNG-F6), have

been chosen for further separation process. **Figures 4-1** and **4.2** show workflows for the extraction and fractionation of the PNG propolis sample.

4.2.2 Chemical Profiling of Papua New Guinea PNG propolis sample
4.2.2.1 Characterization of the PNG crude using ^{1}HNMR

The proton NMR spectrum of the PNG crude extract revealed a mixture of triterpenes (**Figure 4-4**) as judged by the absence of aromatic signals and the abundance of signals due to methyl groups. The major constituents of crude were putatively identified to be lupeol, beta and alpha amyrin and possibly their esters (due to the chemical shift of their H-3 protons to δ_H 4.45 ppm) or methyl esters, possibly the acetates and the non-esterified compounds (due to the chemical shift of their H-3 protons at δ_H 3.19 ppm (Tsichritzis and Jakupovic, 1990).
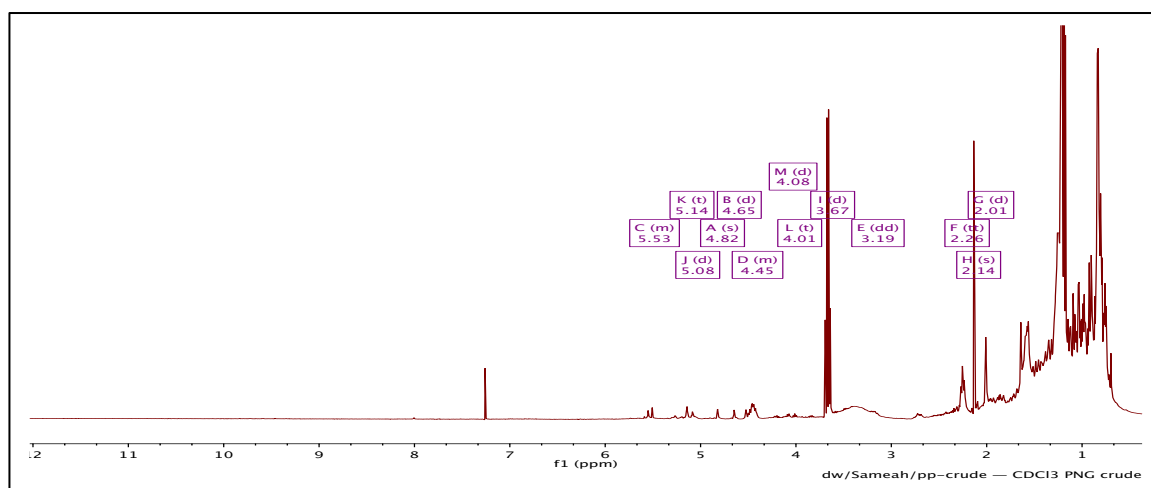
Figure 4-4:: ^{1}**H NMR (500 MHz) spectrum of the crude PNG propolis sample in CDCl₃**

4.2.2.2 Chemical profiling of the PNG crude sample using LC-MS

The chemical profiling of the Papua New Guinea propolis sample was carried out by using ESI MS (negative ion masses) as shown in **Table 4-2** and **Figure 4-5** and indicated a clear series of triterpenes with varying degrees of oxygenation such as $C_{29}H_{47}O_8$ and $C_{30}H_{48}O_8$ and some with a high degree of unsaturation such as $C_{30}H_{46}O_4$. The most abundant compounds were $C_{30}H_{48}O_4$ and $C_{30}H_{50}O_3$. Up to now, in the literature, there is no scientific published data on Papua New Guinea propolis to make a comparison with this sample. Generally, these triterpenes look different from the ones that were isolated from some Papua New Guinea plant species for example Terminalia species. The latter were found to have tri-hydroxylated triterpene acids arjunolic acid and asiatic acid. These differences in the organic compounds in the propolis may

be due to the plants from which the propolis is collected, secreted substances from honeybee metabolism, and materials that are introduced during propolis formation (Marcucci, 1995)
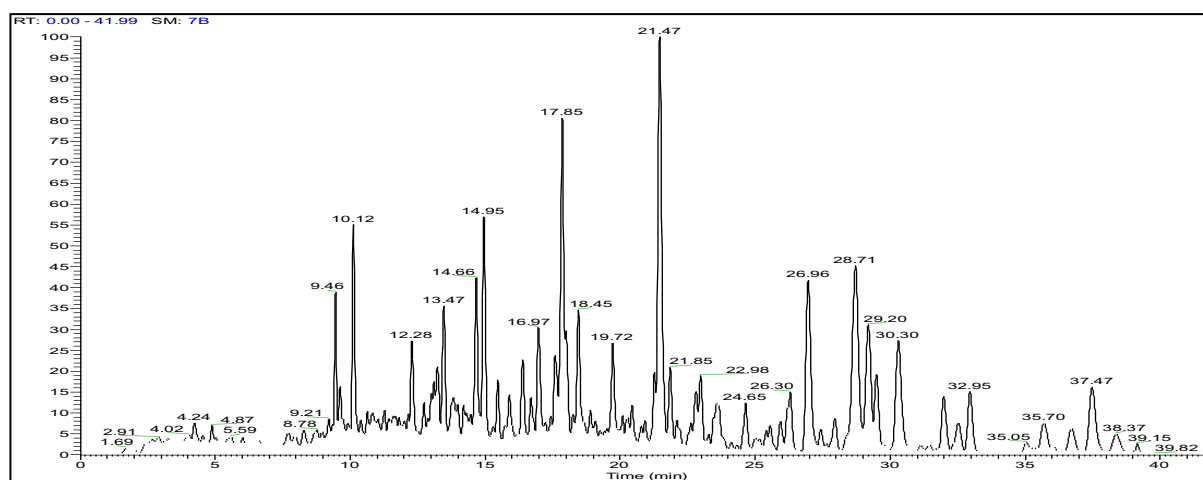
Figure 4-5: LC-MS spectral analysis of PNG crude extract using (ESI) Orbitrap Exactive Mass Spectrometer (negative ion masses)

Table 4-2: Profiling of crude from Papua New Guinea propolis sample using the negative ion masses in the LCMS

Peak no	RT (min)	M-1	Formula	RDB	Delta (ppm)	Intensity
1	9.45	431.33743	$C_{24}H_{47}O_8$	1.5	0.887	4.30E6
2	10.10	405.26456	$C_{24}H_{37}O_5$	6.5	-0.216	6.58E6
3	14.6	503.33759	$C_{30}H_{47}O_8$	13	-0.432	4.86E6
4	14.97	487.34253	$C_{30}H_{47}O_5$	13	-0.744	6.31E6
5	15.85	489.32184	$C_{29}H_{46}O_8$	7.5	-0.659	1.03E6
6	21.47	485.32657	$C_{30}H_{45}O_5$	8.5	-1.396	1.12E7
7	21.86	471.34738	$C_{30}H_{47}O_4$	7.5	-1.280	2.18E6
8	23.00	473.36307	$C_{30}H_{49}O_4$	7.0	1.182	2.02E6
		453.33731	$C_{30}H_{45}O_3$	8.5	-0.237	1.10E6
9	25.58	469.33185	$C_{30}H_{45}O_4$	8.5	-1.029	6.8E5
		453.33740	$C_{30}H_{45}O_3$	8.5	0.4355	7.3E5
10	26.29	469.33173	$C_{30}H_{45}O_4$	8.5	-1.285	1.60E6
		455.35272	$C_{30}H_{47}O_3$	7.5	-0.760	
11	26.95	471.34735	$C_{30}H_{47}O_4$	7.5	-1.343	4.55E6
12	27.96	455.35257	$C_{30}H_{47}O_3$	7.5	-1.095	9.49E5
13	28.71	471.34711	$C_{30}H_{47}O_4$	7.5	-1.653	4.83E6
14	29.19	471.34738	$C_{30}H_{47}O_4$	7.5	-1.280	3.41E6
		453.33713	$C_{30}H_{45}O_3$	8.5	-0.641	
15	30.31	471.34738	$C_{30}H_{47}O_4$	7.5	-1.343	2.99E6
16	32.98	457.36826	$C_{30}H_{49}O_3$	6.5	-1.003	1.52E6
17	35.68	457.36829	$C_{30}H_{49}O_3$	6.5	-0.937	8.50E5
18	36.71	457.36847	$C_{30}H_{49}O_3$	6.5	-0.544	6.63E6
19	38.36	457.36838	$C_{30}H_{49}O_3$	6.5	-0.740	5.33E6

4.2.2.3 The Chemical Profiling of PNG Fraction1:

The general chemical profiling of fraction (F1) by using the negative ESI LC-MS is presented in **Table 4-3** and shown in **Figure 4-6.**

Table 4-3: Profiling of the PNG Fraction 1 (F1) from Papua New Guinea propolis sample by using the negative ion masses in the LCMS

Peak no,	RT (min)	M-1	Formula	RDB	Delta (ppm)	Intensity
1	10.60	266.15137	$C_{15}H_{22}O_4$	5	-3.710	6.77E4
2	11.62	431.31638	$C_{27}H_{43}O_4$	6.5	-0.703	7.52E4
5	13.91	255.23282	$C_{16}H_{31}O_2$	1.5	-0.523	3.48E5
		353.30560	$C_{22}H_{41}O_3$	2.5	-1.467	
		427.28497	$C_{27}H_{39}O_4$	8.5	-0.966	
6	14.94	503.33737	$C_{30}H_{47}O_6$	7.5	0.879	2.86E5
7	16.51	255.23308	$C_{16}H_{31}O_2$	1.5	0.496	1.41E5
		487.34354	$C_{30}H_{47}O_5$	7.5	1.318	
8	16.90	473.32751	$C_{29}H_{45}O_5$	7.5	-0.207	2.75E5
9	17.80	473.36340	$C_{30}H_{49}O_4$	6.5	0.493	6.4E5
		273.15584	$C_{15}H_{25}O_2$	3.5	-0.689	
10	21.46	485.32684	$C_{30}H_{45}O_5$	8.5	-0.840	9.33E5
11	26.96	471.34747	$C_{30}H_{47}O_4$	7.5	-1.089	7.02E5
12	28.65	471.34753	$C_{30}H_{47}O_4$	7.5	-0.9652	7.94E5
13	29.14	471.34756	$C_{30}H_{47}O_4$	7.5	-0.898	4.47E5
14	30.41	471.34827	$C_{30}H_{47}O_4$	7.5	0.608	6.89E5
15	33.32	383.35278	$C_{24}H_{47}O_3$	1.5	-0.753	4.32E5
		337.34766	$C_{23}H_{45}O$	1.5	0.209	
		255.23277	$C_{16}H_{31}O_2$	1.5	-0.719	
		427.38055	$C_{26}H_{51}O_4$	1.5	2.964	
16	34.65	255.23285	$C_{16}H_{31}O_2$	1.5	-0.406	1.03E6
17	36.27	255.23279	$C_{16}H_{31}O_2$	1.5	0.933	2.73E
		411.38409	$C_{28}H_{51}O_3$	1.5	0.818	
		481.42466	$C_{30}H_{57}O_4$	2.5	-0.577	
18	37.20	489.37903	$C_{32}H_{51}O_4$	7.5	-0.507	4.22E5
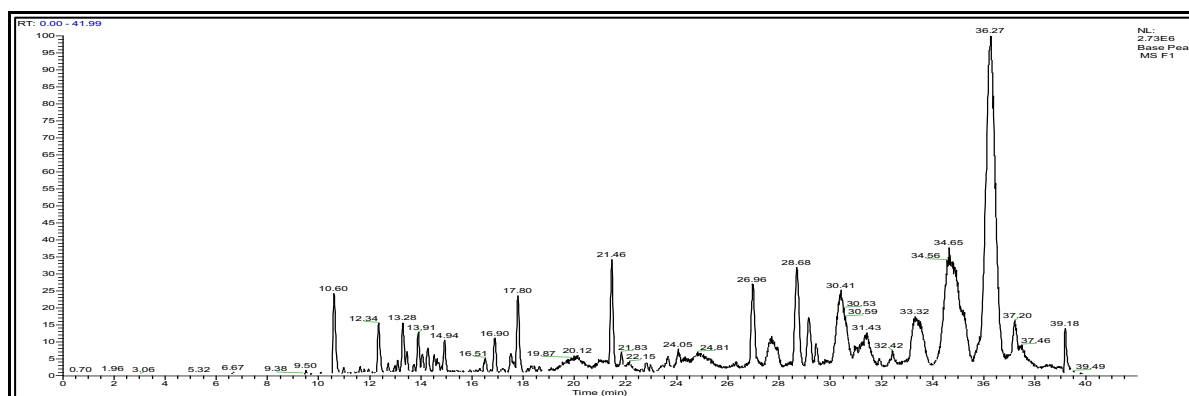
Figure 4-6: LC-MS spectral analysis for F1 PNG propolis sample by using (LTQ) Orbitrap Mass Spectrometry (negative ion masses)

4.2.2.4 The Chemical Profiling of PNG Fraction 6

The general chemical profiling of fraction (F6) by using the negative ESI LC-MS is presented in **Table 4-4** and shown in **Figure 4-7**

Table 4-4: Profiling of Fraction 6 from PNG propolis sample by using the negative ion masses in the LCMS

Peak no,	RT (min)	M-1	Formula	RDB	Delta (ppm)	Intensity
1	4.07	389.37875	$C_{27}H_{49}O$	3.5	0.957	1.71E6
		539.09808	$C_{30}H_{19}O_{10}$			
1	4.88	549.34302	$C_{31}H_{49}O_8$	7.5	-0.495	1.15E6
2	8.93	519.33276	$C_{30}H_{47}O_7$	7.5	0.064	2.39E6
	9.22	517.31708	$C_{30}H_{45}O_7$	8.5	1.1	
3	10.21	405.26462	$C_{24}H_{37}O_5$	6.5	-0.068	2.52E6
		517.31720	$C_{30}H_5O_7$	8.5	0.238	
		343.26450	$C_{26}H_{35}O_2$	6.5	0.718	
4	10.71	503.33801	$C_{30}H_{47}O_6$	7.5	0.393	2.1E6
5	11.53	441.26434	$C_{27}H_{37}O_5$	9.5	-0.697	1.68E6
		501.32199	$C_{30}H_{45}O_6$	8.5	-0.344	
		563.35864	$C_{32}H_{51}O_8$	7.5	-0.536	
6	12.11	501.32214	$C_{30}H_{45}O_6$	8.5	-0.045	2.09E6
		473.32730	$C_{29}H_{45}O_5$	7.5	0.110	
7	12.78	483.31165	$C_{30}H_{43}O_5$	9.5	0.108	1.59E6
		559.32727	$C_{32}H_{47}O_8$	9.5	-0.664	
8	12.83	427.28552	$C_{27}H_{39}O_4$	8.5	0.321	1.51E6
		483.31171	$C_{30}H_{43}O_5$	9.5	0.232	
9	13.37	501.32186	$C_{30}H_{45}O_6$	8.5	-0.643	4.59E6
10	13.55	533.34802	$C_{31}H_{49}O_7$	7.5	-0.669	5.78E6
11	14.43	485.32727	$C_{30}H_{45}O_5$	8.5	0.046	2.24E6
12	15.59	547.36481	$C_{32}H_{51}O_7$	7.5	1.430	1.87E6
13	16.93	471.34790	$C_{30}H_{47}O_4$	7.5	-0.177	1.59E6
14	17.95	473.32733	$C_{24}H_{45}O_5$	7.5	0.174	1.15E6
15	19.25	485.32745	$C_{30}H_{45}O_5$	8.5	0.417	1.15E6
16	21.65	485.32690	$C_{30}H_{45}O_5$	8.5	-0.717	5.61E6
17	22.03	471.34787	$C_{30}H_{47}O_4$	7.5	-0.688	2.49E6
18	22.99	471.34766	$C_{30}H_{47}O_4$	7.5	-0.688	2.31E6
19	23.15	473.36328	$C_{30}H_{49}O_4$	6.5	0.746	9.71E5
20	24.48	485.32697	$C_{30}H_{45}O_5$	8.5	-0.572	4.13E5
21	26.10	515.37390	$C_{32}H_{51}O_5$	7.5	-0.578	8.15E5
22	27.14	471.34753	$C_{30}H_{47}O_4$	7.5	-0.962	2.48E6
23	28.88	471.34760	$C_{30}H_{47}O_4$	7.5	-0.813	2.24E6
24	29.33	471.34750	$C_{30}H_{47}O_4$	7.5	-1.025	1.75E6
25	30.44	471.34756	$C_{30}H_{47}O_4$	7.5	-0.898	1.23E6
26	33.03	457.36853	$C_{30}H_{49}O_3$	6.5	-0.413	5.82E5
27	35.76	457.36847	$C_{30}H_{49}O_3$	6.5	-0.544	1.48E5
28	36.79	457.36859	$C_{30}H_{49}O_3$	6.5	-0.281	1.89E5
29	38.41	457.36850	$C_{30}H_{49}O_3$	6.5	-0.478	2.17E5
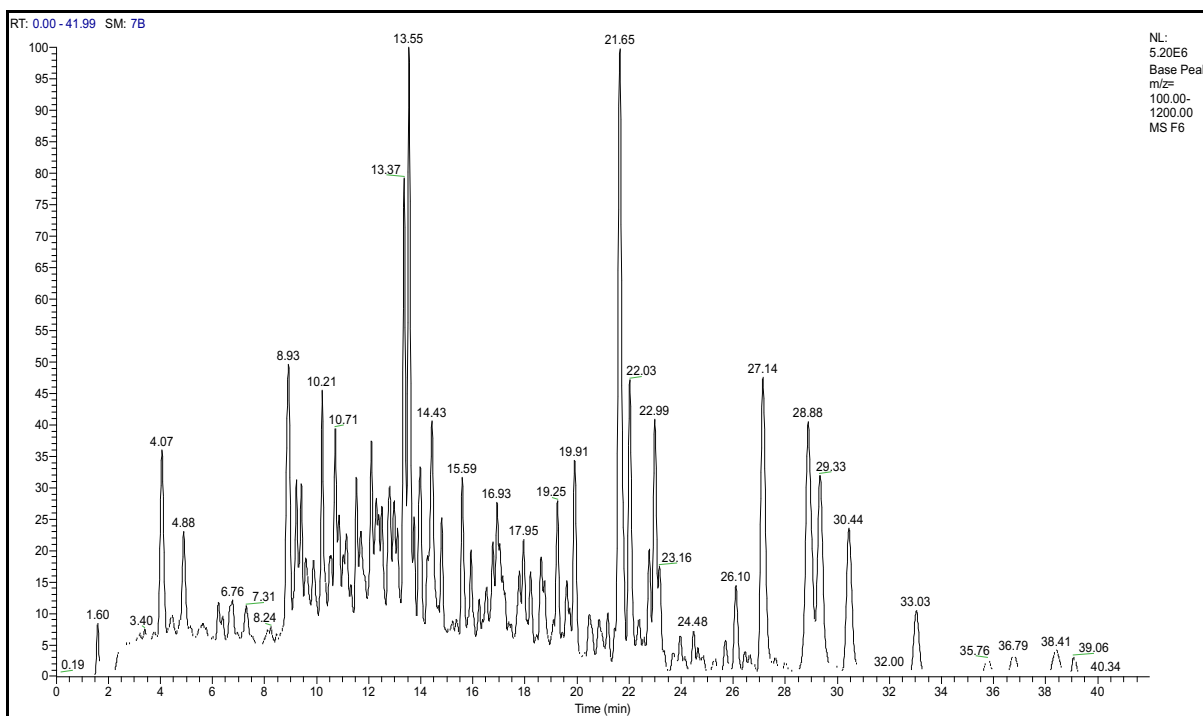
Figure 4-7: **LC-MS spectral analysis for F6 PNG propolis sample by using (LTQ) Orbitrap Mass Spectrometry (negative ion masses)**

4.2.3 *In vitro* studies of the PNG propolis extract and its fractions using wild type *T. b. brucei s427* and the derived, multi-drug resistant clone *B48*

The *in vitro* activity of the PNG extract and fractions on wild-type *T. b. brucei* s427 and the derived, multi-drug resistant clone *B48* was determined in three independent resazurin-based drug sensitivity assays as shown in **Table 4-5**. The PNG crude displayed activity against *T. b. brucei* s427 with an EC_{50} value of 4.01 µg/mL. The most active fractions were F5, F4 and F6 with EC_{50} values of 2.04, 4.05 and 4.83 and µg/mL, respectively. A notable observation was that virtually none of the fractions showed reduced activity against the drug resistant strain B48 (RF<1), therefore they were not cross resistant to pentamidine. Moreover, the drug sensitivity of PNG crude and most of fractions didn't show significant differences between the two strains while some other fractions were significantly more active against *B48* such as F2, F4, F5, F6, F7, F8 (p<0.05). However, the RF for pentamidine was 210.84 and the P value was 0.00001.

66

Table 4-5: EC$_{50}$ values of PNG propolis and its fractions on T. brucei. S427 wild-type, and B48 (n=3).

Samples	T. brucei S427WT			T. brucei B48 (Pentamidine Resistance)				
	AVG of EC$_{50}$ (µg/mL)	SD	RSD%	AVG of EC$_{50}$ (µg/mL)	R. F	t-test	SD	RSD%
20-PNG	4.01	0.0953	2.4	3.85	0.96	0.5028	0.3661	9.52
PNG-F1	10.24	2.4969	24.37	5.90	0.58	0.0553	1.2816	21.71
PNG-F2	14.85	1.2651	8.52	9.82	0.66	0.0400	2.6142	26.62
PNG-F3	8.15	0.7278	8.93	5.82	0.71	0.0544	1.3750	23.61
PNG-F4	4.05	0.2698	6.66	2.15	0.53	0.0047	0.5104	23.69
PNG-F5 (9)	2.04	0.1121	5.49	0.97	0.47	0.0003	0.1115	11.55
PNG-F6	4.83	0.6014	12.44	2.13	0.44	0.0039	0.4992	23.49
PNG-F7	15.46	0.9834	6.36	7.84	0.51	0.0004	0.7070	9.02
PNG-F8	15.79	1.4011	8.87	9.16	0.58	0.0070	1.7595	19.20
PNG-F9	7.85	1.0116	12.89	6.55	0.83	0.2809	1.4980	22.88
PNG-F10	15.82	1.7198	10.87	12.10	0.76	0.1094	2.6328	21.76
Pentamidine (µM)	0.0034	0.0008	22.16	0.7214	210.84	0.00001	0.0487	6.75

AVG of EC$_{50}$ =average of half maximal effective concentration, average of at least 3 independent determinations. [a]EC$_{50}$ in µg/mL; [b]EC$_{50}$ in µM. SD= Standard deviation of all determinations. RSD%= Relative Standard Deviation= (SD/ Avg.) x100. RF= Resistance factor. Statistical significance was determined using an unpaired two-tailed Student's t-test comparing EC$_{50}$ value of the resistant strain with that of the same sample for the control strain s427. Pentamidine and Diminazen, both are known trypanocides.

4.2.4 Activity of PNG propolis and its fraction against Trypanosoma congolense and C. fasciculata (*In vitro).*

The PNG crude and the primary fractions from the PNG propolis were screened against T. congolense and diminazene resistant strains of T. congolense strain 6C3. The PNG crude, PNG-F5, PNG-F4 and PNG-6, were the most active among the PNG fractions. Tables 4-6 display the EC50 values against all two pathogens T. congolense -IL3000 WT and T. congolense 6C3 side-by-side. The level of anti-parasite activity for PNG-F5 makes this a promising lead compound against kinetoplastid pathogens. PNG extract and its fractions were also tested in vitro against a C. fasciculata cell line. It clear from Table 4-7 that all the fractions exhibited moderate activity against C. fasciculata with EC50 values (54<EC50 >20). Most of the fractions were somewhat more active against T.congolense than against C. fasciculata , as shown in Table 4-20, the EC50 (T.C WT)/ EC50 (C. fasciculata) of all the samples were <1 as well as all the PNG fraction were more active against T.brucie than against C. fasciculata where the EC50 (T.b brucie WT)/ EC50 C. fasciculata of all the samples were <1. Since the PNG crude and its fractions displayed low activity against C. fasciculata cell line, it was decided that the results were not sufficiently encouraging to continue and test the purified compounds.

Table 4-6: EC$_{50}$ values of PNG propolis and its fractions on *T. congolense IL300*, and *T. congolense* resistance to diminazene (n=3).

Samples	Trypanosoma congolense IL300			Trypanosoma congolense Diminazene Resistance				
	Mean of EC$_{50}$ (µg/mL)	SD	RSD%	Mean of EC$_{50}$ (µg/mL)	SD	RF	t-test	%RSD
20-PNG	3.39	0.4174	12.31	4.4	0.3723	1.29	0.0389	8.52
PNG-F1	13.47	3.2694	24.27	13.3	3.3951	0.99	0.9468	25.57
PNG-F2	11.41	2.4912	21.82	12.0	2.3369	1.05	0.7862	19.50
PNG-F3	11.48	2.9354	25.57	12.8	2.6497	1.11	0.5941	20.70
PNG-F4	10.46	2.4102	23.03	9.3	0.7931	0.89	0.4611	8.55
PNG-F5 **(9)**	5.77	1.2826	22.22	2.8	0.3252	0.48	0.017	11.76
PNG-F6	9.30	1.6431	17.67	7.8	0.6935	0.84	0.2215	8.88
PNG-F7	12.64	1.4215	11.24	12.4	2.5468	0.98	0.9038	20.49
PNG-F8	15.62	3.1057	19.88	14.6	2.6461	0.93	0.6873	18.12
PNG-F9	18.12	2.1440	11.83	20.5	3.0497	1.13	0.3393	14.91
PNG-F10	18.16	3.9400	21.70	21.2	4.1686	1.17	0.4045	19.62
Diminazene	0.0865	0.0164	18.92	3.14	0.2819	36.20	0.00005	9.00

Table 4-7: EC$_{50}$ (µg/mL) of PNG propolis and its fractions on *C. fasciculata*

Exp code	AVG of EC$_{50}$ (µg/mL)	SD	%RSD
20-PNG	20.77	1.25	6.02
PNG-F1	22.07	4.44	20.12
PNG-F2	34.31	2.80	8.15
PNG-F3	28.10	1.96	6.96
PNG-F4	20.81	2.73	13.12
PNG-F5 **(9)**	23.44	3.15	13.46
PNG-F6	53.12	4.35	8.20
PNG-F7	38.52	5.67	14.71
PNG- F8	31.25	5.87	18.79
PNG-F9	24.65	1.17	4.74
PNG-F10	32.24	2.29	7.10
PAO (µM)	3.06	0.08	2.47

AVG of EC$_{50}$ =average of half maximal effective concentration, average of at least 3 independent determinations. SD= Standard deviation of all determinations. RSD%= Relative Standard Deviation= (SD/ Avg.) x100. RF= Resistance factor. Statistical significance was determined using an unpaired two-tailed Student's t-test comparing EC$_{50}$ value of the resistant strain with that of the same sample for the control strain s427. Pentamidine and Diminazen aceturate, both are known trypanocides. AVG of EC$_{50}$ =average of half maximal effective concentration, SD = standard deviation, RSD%= Relative Standard Deviation

4.2.5 Prediction of the most active compounds in the PNG propolis by usingPartial Least Squares (PLS) Analysis.

In order to determine what is the most active components in the extracts PLS modeling was carried out using the high-resolution mass spectrometry data for the fractions. The loadings plot for a PLS model (**Figure 4-8**) found that the most active component appears to have the formula $C_{30}H_{46}O_5$ and thus a target for isolation and testing. This compound found in fraction PNG-F4 therefore, this fraction was purified by CC .
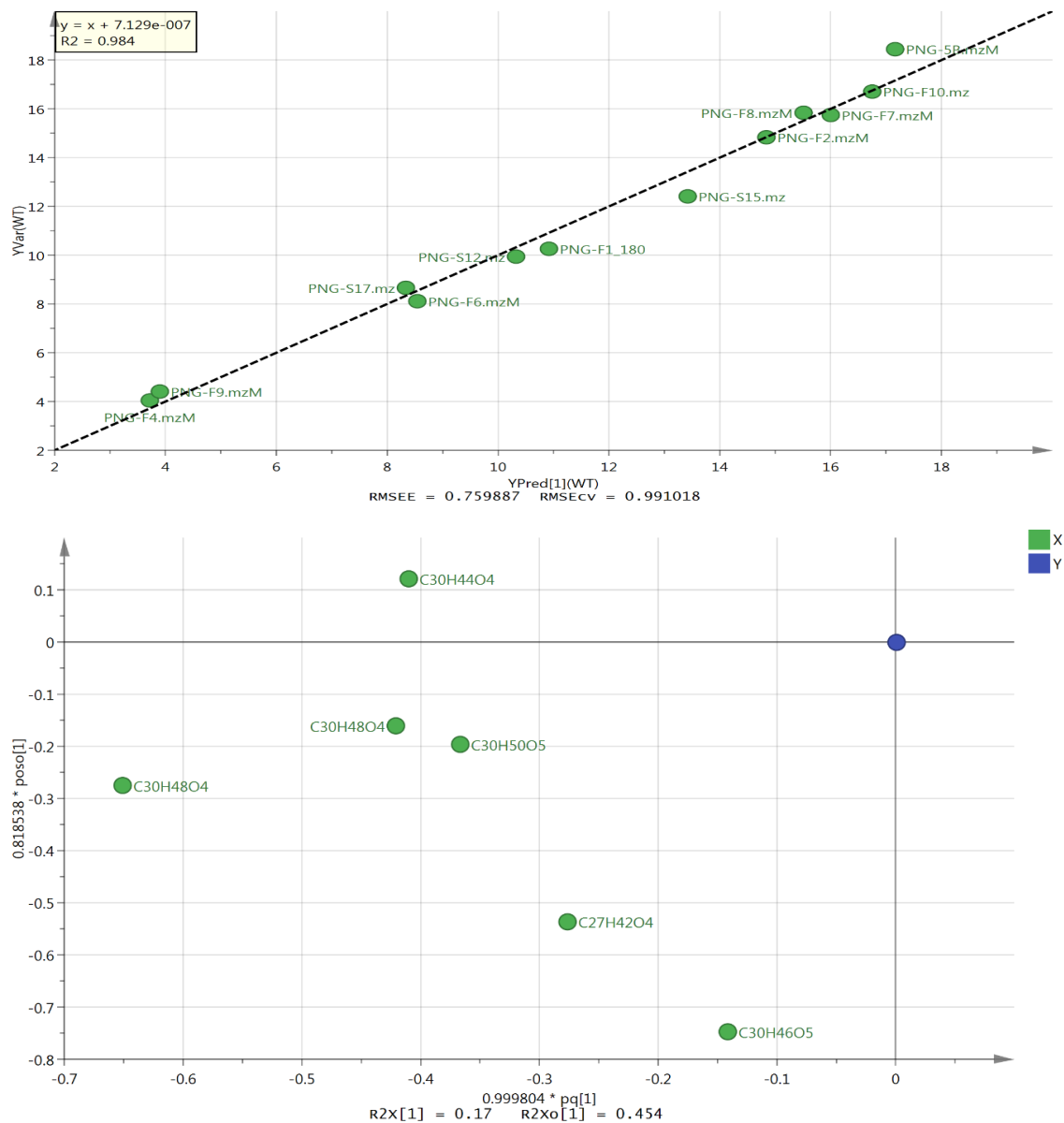
Figure 4-8:: PLS model of predicted against masured anti-trypanosomal activity against *T.b. brucei* S427WT of PNG propolis

4.2.6 Sub-fractionation with MPLC on the Grace® system

Further separation was conducted for two samples with the greatest weights, the fractions PNG-F1 and PNG-F6 which were obtained from CC and were nontoxic to the human cells following preliminary bioassays. It is clear from the chromatogram shown in **Figure 4-9** that all the compounds eluted from PNG-F1 within the first 20 minutes of the run. The third peak eluted between 11 – 25 minutes and was very broad. All the compounds eluted between hexane (100%) and hexane: ethyl acetate (90:10). This means that the eluted compounds were non-polar, since in this chromatography system the column used was normal phase.
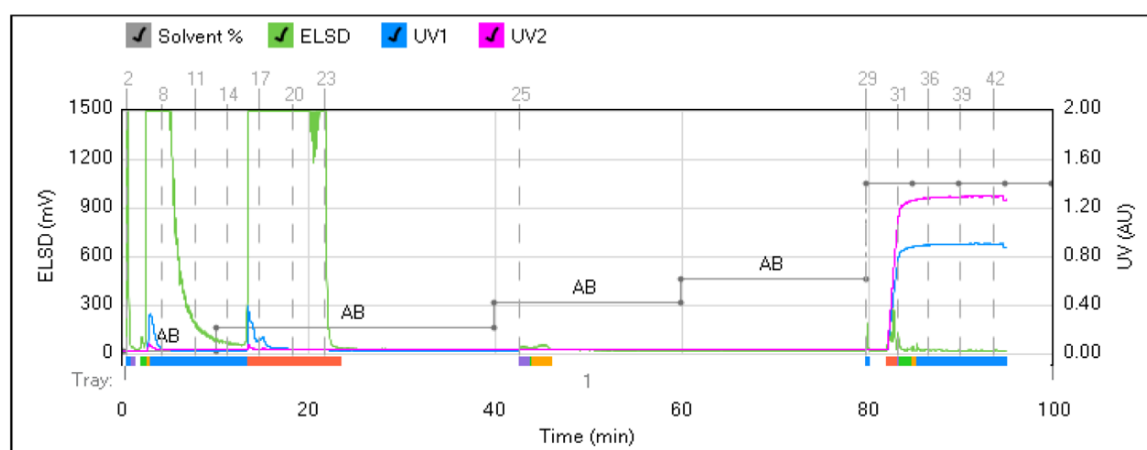
Figure 4-9: Chromatogram of PNG fraction 1 on Grace Reveleris® Flash chromatography
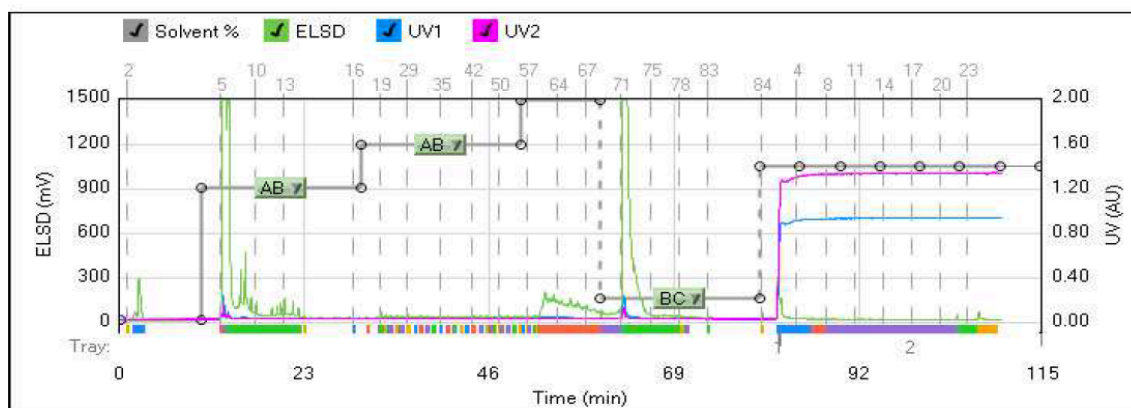
Figure 4-10: Chromatogram of PNG fraction 6 on Grace Reveleris® Flash chromatography

The chromatogram in **Figure 4-10** shows that there were three peaks which are all baseline separated and within ten minutes there was a sharp peak where the solvent system was hexane (100%) and the other peak come out with (40:60) hexane: ethyl acetate. Finally, one single sharp peak comes out at the beginning of the washing time with the ethyl acetate.

Apart from tubes 2 and 3 (**Figure 4-9**) and 70 to 73 (**Figure 4-10**), which were, pooled together, all the rest of the tubes (sub-fractions) from both fractions PNG-F1 and PNG-F6 were analysed

separately by TLC and then HPLC-ELSD. TLC was employed in order to, determine which fractions were similar so that they could be pooled together for further analysis. HPLC-ELSD was used to determine the purity of the sub-fractions (either pooled or not) prior to NMR analysis of the pure samples.

4.2.7 Analysis of subfractionation by HPLC-ELSD

All the sub-fractions were run using the HPLC-ELSD instrument. It is clear from the chromatogram results (**Figures 4-11 to 4-14)** that there were some fractions which gave single peaks, while the other fractions appeared as multiple peaks. That gave an estimation of which fractions were pure compounds, while the final judgment would be obtained according to the NMR results as well as LCMS results.
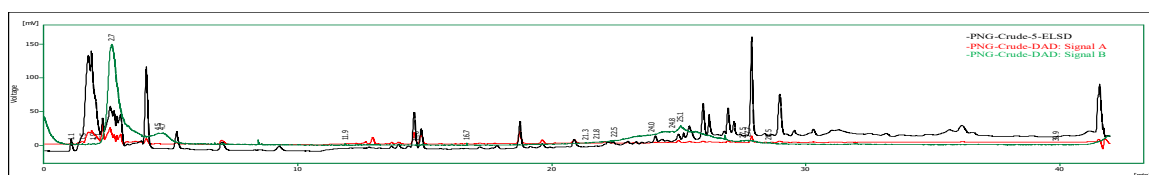
Figure 4-11: HPLC-ELSD Chromatogram result of the filtered crude extract on a C18 column
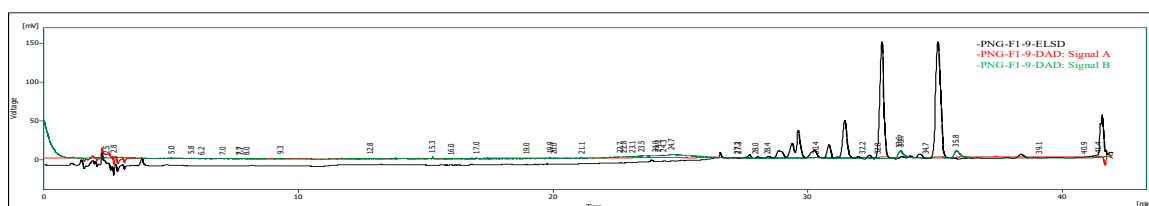
Figure 4-12: HPLC-ELSD Chromatogram result of the sub-fraction PNG-F1-S9 on C18 column, which is a mixture.
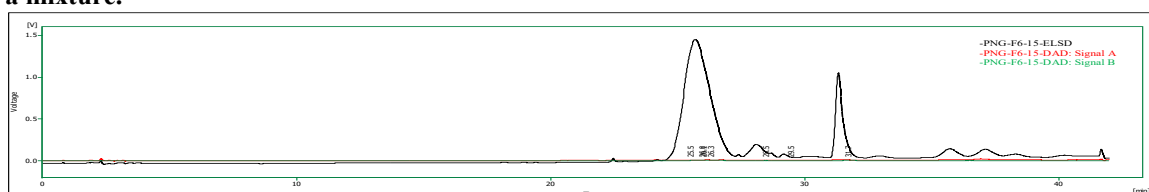
Figure 4-13: HPLC-ELSD Chromatogram result of the sub-fraction PNG-F6-S15 on C18 column, which is a mixture of two components.
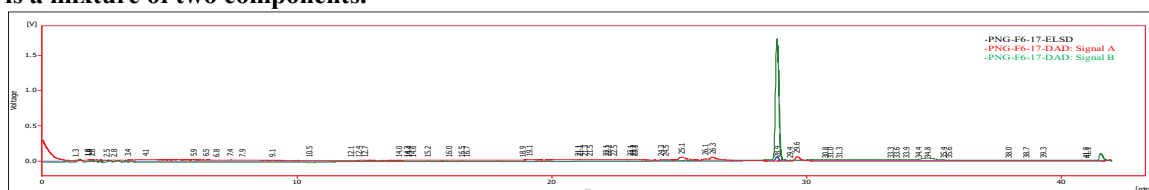
Figure 4-14: HPLC-ELSD Chromatogram of pure compound PNG-F6-S17 on C18 column, which gave single peak at 9.09 min.

4.2.8 Isolation and purification of compounds (1 to 12) from PNG

The anti-trypanosomal activity of the PNG fractions PNG-F1-F10 that shown in **Table 4-5**, was guided the sub-fractionation process. Besides, the highest weights among PNG fractions were in the fractions PNG-F1 and PNG-F6 were the targets of further separation, resulted identification and isolation of 12 compounds. Firstly PNG-F1 which was collected from the nonpolar solvent hexane, purification of fraction (F1) yielded cycloartenol (**4**), 24 (28)-methylenecycloartenol (**7**) and cycloeucalynol (**8**). Secondly, PNG-F6 which was collected from the solvent system of ethyl acetate/methanol (80:20) gave mangiferonic acid (**1**), isomangiferolic acid (**2**), 27-hydroxymangiferolic acid (**3**), ambolic acid (**6**) and ambonic acid (**5**). F5 was identified to be 20-hydroxybetulin (**9**). Further separation of fraction 4 was conducted based on chemo-metric analysis of the MS data. Thus, according to the PLS model (**Figure 4-8)** the most bioactive compounds was found in fraction 4 (PNG-F4). Therefore, this fraction was purified by CC yielded of three compounds botulin (**10**), betulinic acid (**11**) and madecassic acid (**12**). The characterization discussion, MPLC, HPLC-ELSD, LC-MS and NMR results were provided in the following paragraphs. Figures 4-1 and 4.2 show workflows for the extraction, fractionation, puirification and isolation of the PNG propolis sample
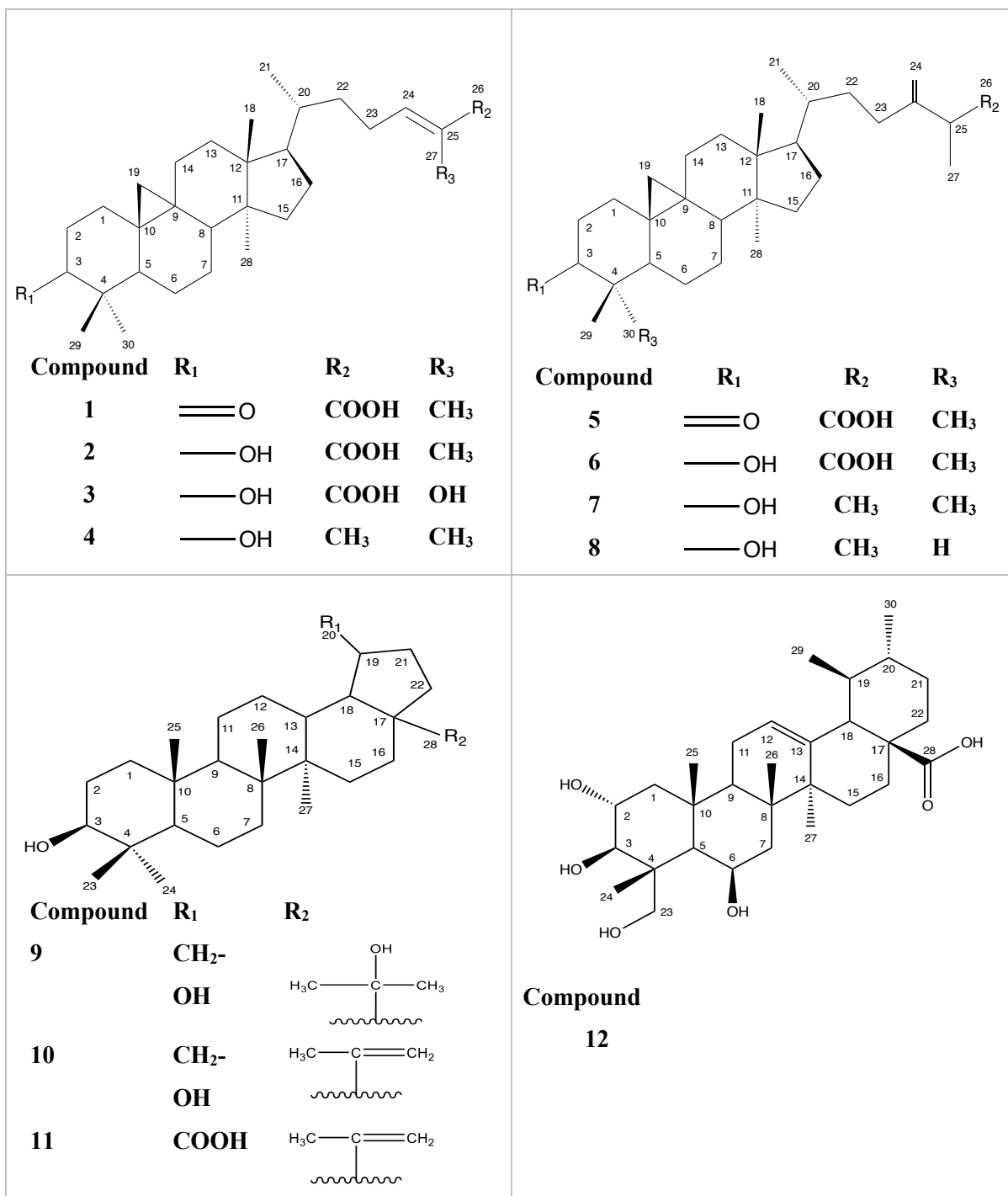
Figure 4-15: Structures of compounds isolated from Papua New Guinea propolis

Compound	R₁	R₂	R₃
1	=O	COOH	CH₃
2	—OH	COOH	CH₃
3	—OH	COOH	OH
4	—OH	CH₃	CH₃

Compound	R₁	R₂	R₃
5	=O	COOH	CH₃
6	—OH	COOH	CH₃
7	—OH	CH₃	CH₃
8	—OH	CH₃	H

Compound	R₁	R₂
9	CH₂-OH	
10	CH₂-OH	
11	COOH	

Compound 12

73

4.2.8.1 Characterization of PNG-F6-12 as Mangiferonic acid (1) and Ambonic acid (5)

The high resolution mass spectral data of PNG-F6-12, the mass associated with the ESI peak at 25.10 min in the positive mode was found at $[M+H]^+$ m/z 455.3508 and had the elemental composition $C_{30}H_{47}O_3$, (Calc. 455.35252) which is consistent with the compound being mangiferonic acid and at for the other peak at 28.58 min the mass was [M+H]+ m/z 469.3666 and the elemental composition $C_{31}H_{48}O_3$, (Calc 468.3603) consistent the elemental composition for ambonic acid (**Figure 4-16**). The proton spectrum of fraction PNG-F6-S12 (**Figure 4-19**) showed the presence of two sets of olefinic protons at δ_H 6.93 and 4.99/4.95 ppm. Other proton signals observed were for six methyl groups and two shielded cyclopropane protons at δ_H 0.81 (1H, d, J = 3.6 Hz) and 0.59 (1H, d, J = 3.7 Hz). These cyclopropane protons were indicative of a cycloartane moiety in the compounds. The carbon signals, including a carbonyl (ring ketone carbon) at δ_C 216.6 ppm were identical. Differences were only observed for the side chain carbons corresponding to C-23, 24, 25, 26, 27 and 28, in addition to a methylene at C-31 for one of the compounds (**Figure 4-20**). Analysis of the 2D spectra (**Figures 4-21** and **4-22**) especially the long-range ($3J$) correlations between the protons and the carbons enabled the identification of the two compounds in the fraction to be Mangiferonic acid (**1**) and Ambonic acid (**5**) (**Figures 4-17** and **4-18**). Ambonic acid has the methylene protons at δ_H 4.95 and 4.99 at position C-31 (δ_C = 110.0 ppm) in addition a carboxylic acid carbon at C-26 (δ_C = 180.1 ppm). While for Mangiferonic acid, the olefinic proton was observed at 6.93 ppm and attached to C-24 at δ_C 145.8 ppm and the carboxylic acid carbon at δ_C 173.2 ppm (**Figure 4-22**). The chemical shift assignments for the two compounds (**Table 4-8**) were in good agreement with literature reports (Escobedo-Martínez et al., 2012, Kardar et al., 2014)
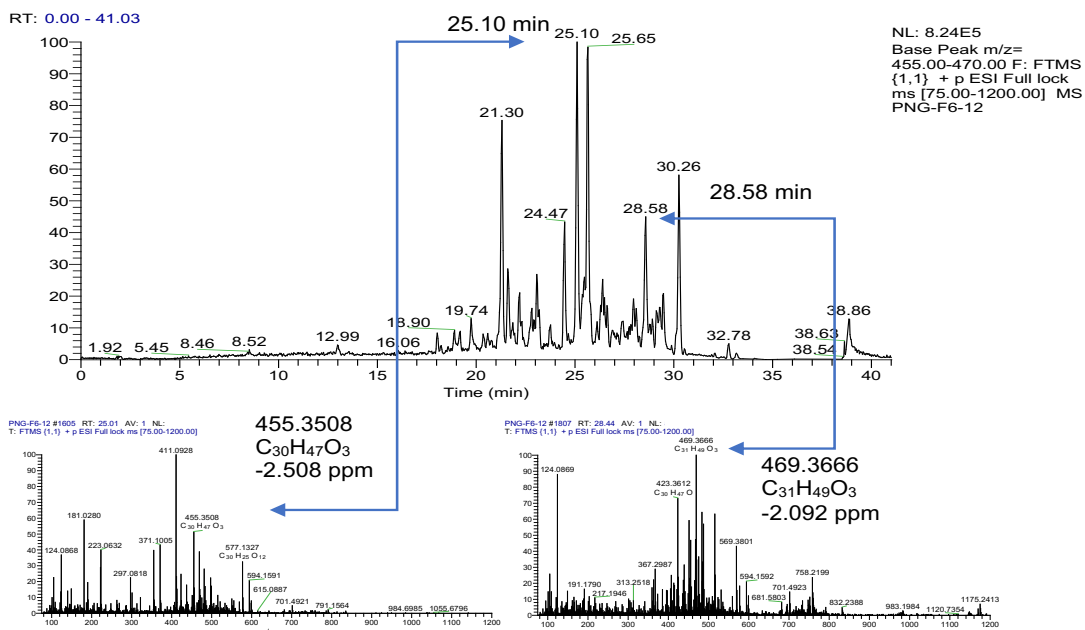
Figure 4-16: LC-MS chromatogram (ESI positive mode) for compound 1 and 5
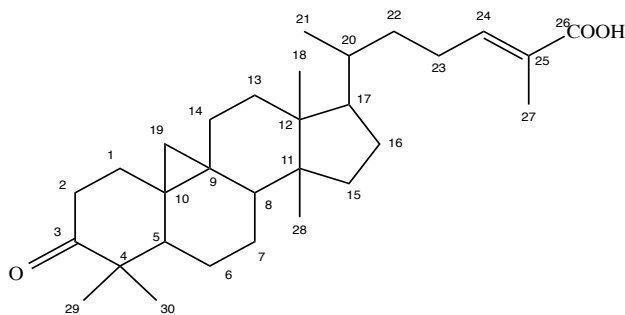
Figure 4-17: structure of mangiferonic acid (1)
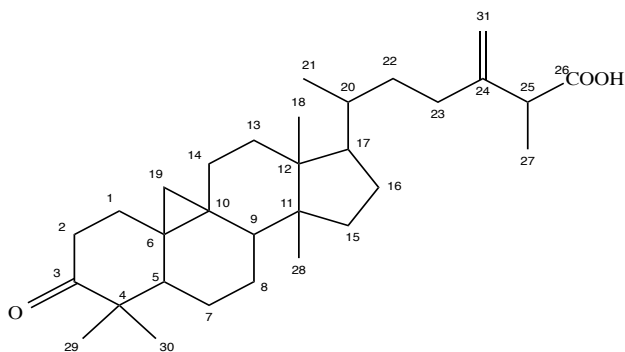
Figure 4-18: structure of ambonic acid (5)

Table 4-8: ^{1}H (500MHz), ^{13}C (100MHz) data of compound (1) and (5) in fraction PNG-F6-12

Position			Compound		
	(1) Mangiferonic acid			(5) Ambonic acid	
	^{1}H δ ppm (mult, *J*)	^{13}C δ ppm	^{1}H δ ppm (mult, *J*)	^{13}C δ ppm
1	1.88 1H (m), 1.57 1H (m)	33.4 (CH$_2$)	1.68 1H (m), 1.40 1H (m)	32.7 (CH$_2$)
2	2.73 1H (td, 13.84, 6.40) 2.33 1H (td, 14.17, 3.49)	37.4 (CH$_2$)	2.73 1H (td, 13.84, 6.40) 2.33 1H (td, 14.17, 3.49)	37.4 (CH$_2$)
3	-	216.6 (C)	-	216.6 (C)
4	-	50.2 (C)	-	50.2 (C)
5	1.73 1H (dd, 12.17, 4.33)	48.4 (CH)	1.73 1H (dd, 12.17, 4.33)	48.4 (CH)
6	1.57 1H (m), 0.97 1H (m)	21.5 (CH$_2$)	1.57 1H (m), 0.97 1H (m)	21.4 (CH$_2$)
7	1.40 1H (m), 1.16 1H (m)	25.9 (CH$_2$)	1.40 1H (m), 1.16, 1H (m)	25.9 (CH$_2$)
8	1.58 1H (m)	47.8 (CH)	1.58 1H (m)	47.8 (CH)
9	-	21.0 (C)	-	21.0 (C)
10	-	25.9 (C)	-	25.9 (C)
11	2.07 1H (m), 1.19 (m)	26.7 (CH$_2$)	2.07 1H (m), 1.19 1H (m)	26.6 (CH$_2$)
12	1.68 1H (m), 1.19 1H (m)	32.7 (CH$_2$)	2.07 1H (m), 1.68 1H (m)	32.7 (CH$_2$)
13	-	45.3 (C)	-	45.3 (C)
14	-	48.7 (C)	-	48.7 (C)
15	1.58 1H (m), 1.40 1H (m)	35.5 (CH$_2$)	1.58 1H (m), 1.40 1H(m)	35.5 (CH$_2$)
16	1.91 1H (m), 1.68 1H (m)	28.0 (CH$_2$)	1.91 1H (m), 1.68 1H (m)	28.0 (CH$_2$)
17	1.68 1H (m)	52.2,1H (CH)	1.68, 1H (m)	52.2 (CH)
18	1.01 3H (s)	18.0 (CH$_3$)	01.02 3H (s)	18.0 (CH$_3$)
19	0.81 1H (d, 3.55) 0.59 1H (d, 3.73)	29.5 (CH$_2$)	0.81 1H (d, 3.55) 0.59 1H (d, 3.73)	29.5 (CH$_2$)
20	1.40 1H (m)	35.9 (CH)	1.40 1H (m)	35.9 (CH)
21	0.94 3H (d, 6.31)	18.2 (CH$_3$)	0.94 3H (d, 6.31)	18.2 (CH$_3$)
22	1.19 1H (m), 1.58 1H (m)	34.7 (CH$_2$)	1.19 1H (m), 1.58 1H (m)	34.5 (CH$_2$)
23	2.28 1H (m), 2.15 1H (m)	25.8 (CH$_2$)	2.21 2H (m)	31.6 (CH$_2$)
24	6.93 1H (t, 7.52)	145.8 (CH)	-	148.0 (C)
25	-	126.6 (C)	3.19 1H (q, 7.08)	45.6 (CH)
26	-	173.2 (C)	-	180.1 (C)
27	1.86 3H (s)	11.9 (CH$_3$)	1.33 3H (d, 7.0)	16.3 (CH$_3$)
28	1.07 3H (s)	22.1 (CH$_3$)	1.07 3H (s)	19.3 (CH$_3$)
29	1.12 3H (s)	21.1 (CH$_3$)	1.12 3H (s)	22.1 (CH$_3$)
30	0.93 3H (s)	19.3 (CH$_3$)	0.913H (s)	20.7 (CH$_3$)
31	-	-	4.99 (1H, s), 4.95 (1H, s)	111.0 (CH$_2$)
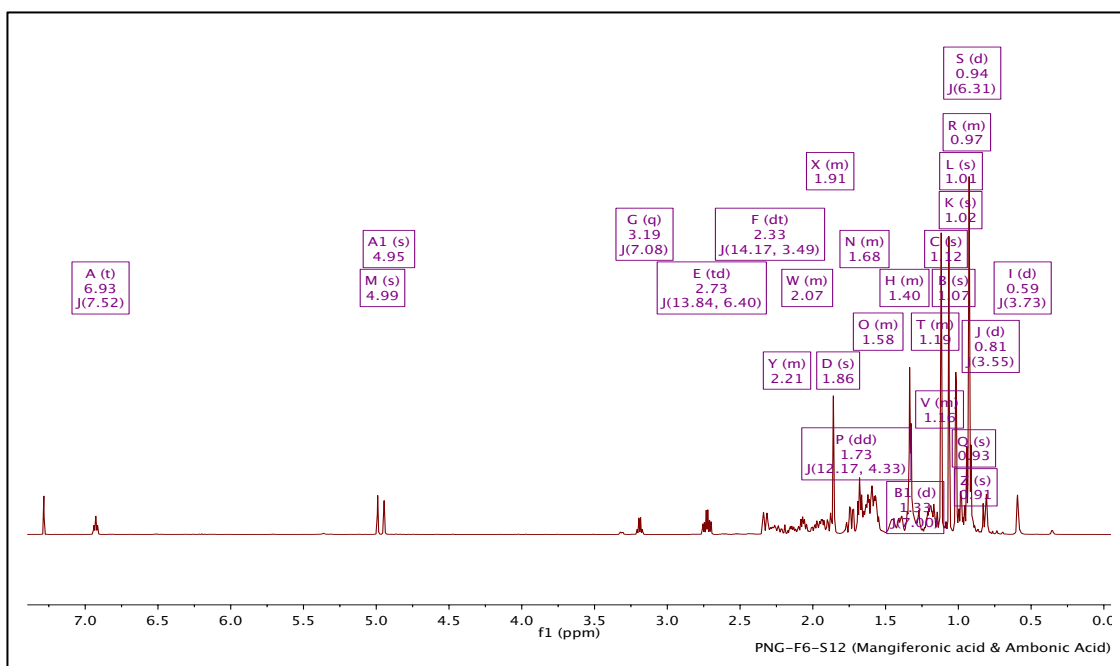
Figure 4-19: ^{1}H NMR (500 MHz) spectrum of compound (1) and (5) in CDCl$_3$.
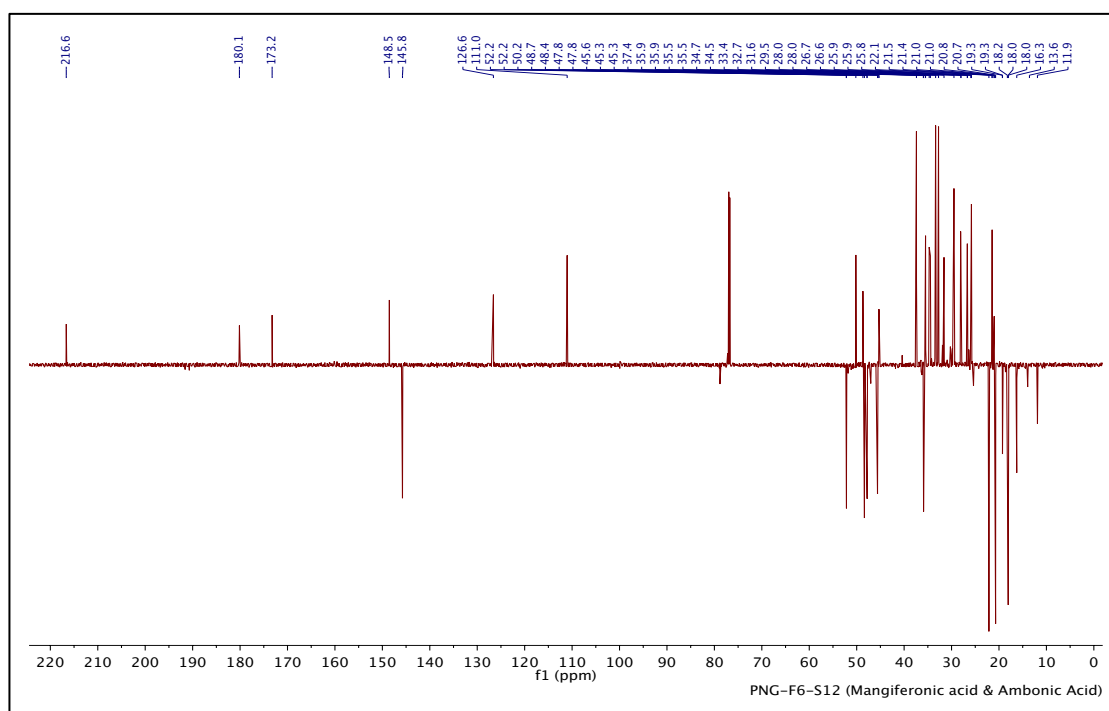
Figure 4-20:^{13}C NMR (100 MHz) spectrum of the compound (1) and compound (5) in CDCl$_3$
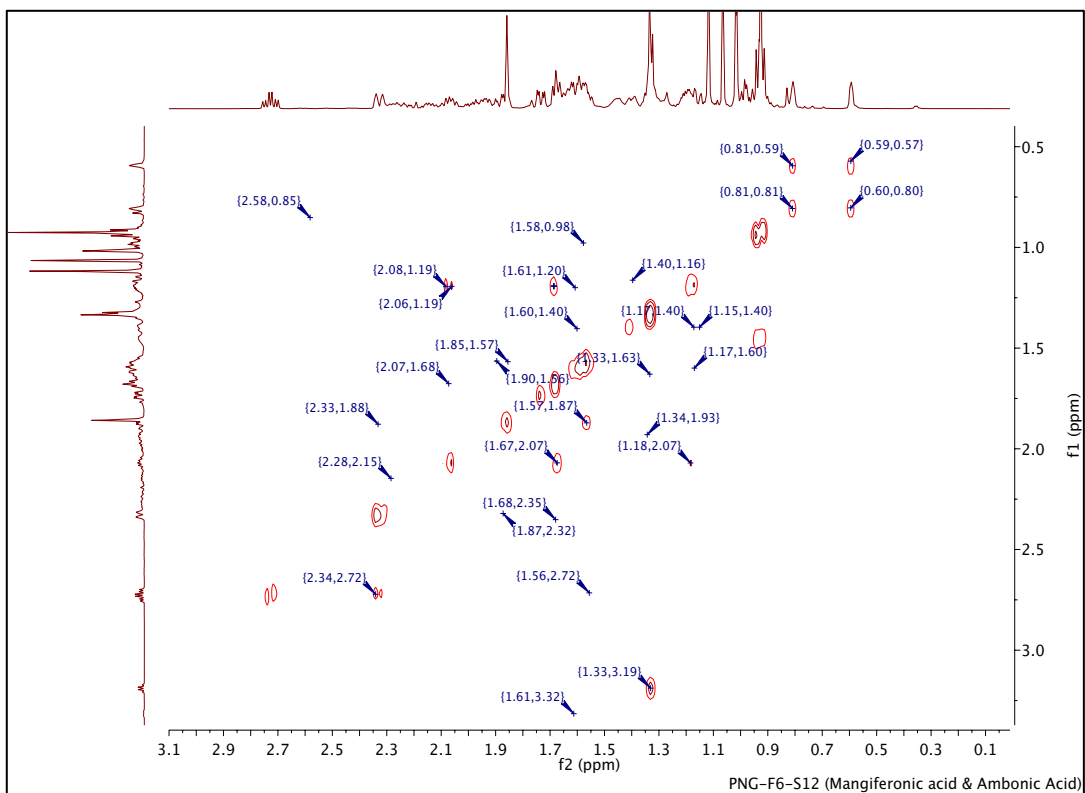
Figure 4-21: COSY (500 MHz) Spectrum of of the compound (1) and compound (5) in CDCl₃
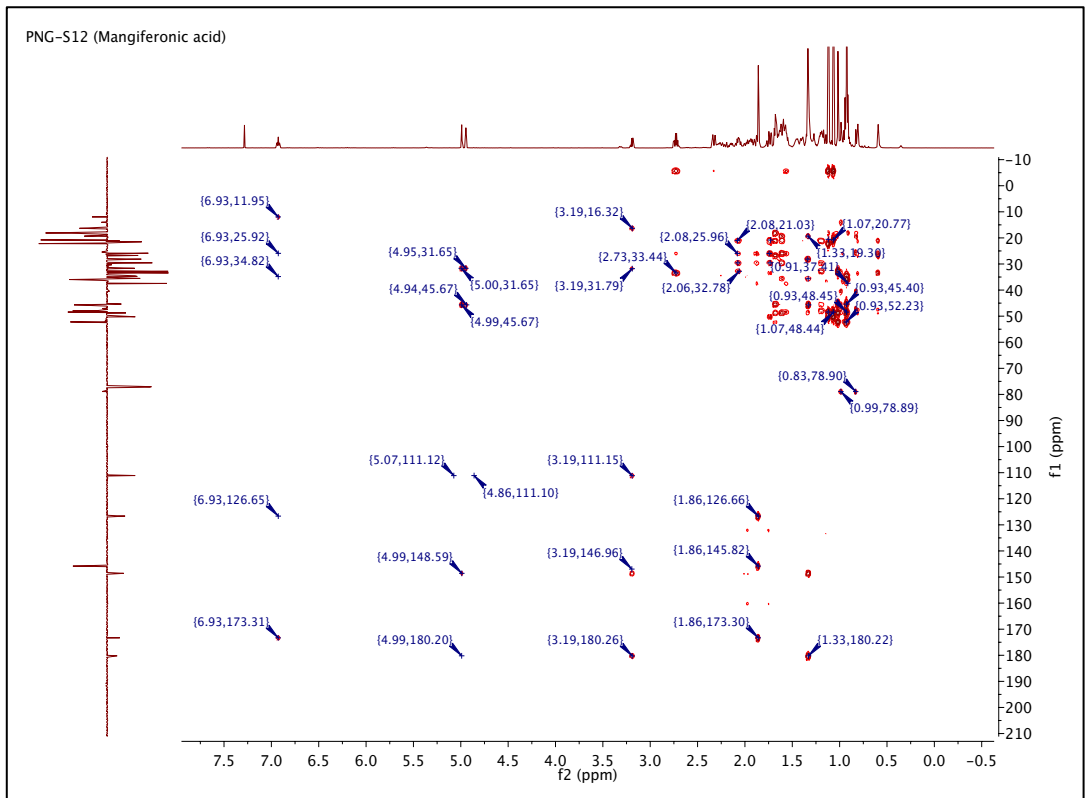
Figure 4-22: HMBC (500 MHz) Spectrum of of the compound (1) and compound (5) in CDCl₃

4.2.8.2 Characterization of PNG-F6-15 as Isomangiferolic acid (2) and Ambolic acid (6)

The proton spectrum of this fraction PNG-F6-15 was characteristic of a 9,19-cyclolanostane derivative and identical to that of fraction PNG-F6-S12 except for the presence of oxymethine protons at δ_H 3.50 (m) attached to C-3 (δ_C = 77.1 ppm) and the corresponding absence of the ketone carbonyl observed for compounds 1 and 5 at 216.7 ppm. For the two compounds in this mixture, the differences in the carbon signals were also those corresponding to C-23, 24, 25, 26, 27 and 28 of the side chain as well as the methylene at C-31. Analysis of the 1D and 2D spectra (**Figures 4-26** to **4-30**) for the compounds identified them to be isomangiferolic acid (**2**) and ambolic acid (**6**) as shown in **Table 4-9** were in good agreement with literature reports (Kardar et al., 2014). Furthermore, the high resolution mass spectral of PNG-F6-S15, the mass associated with the ESI peak at 22.97 min in the negative mode was found at [M-H]⁻ m/z 469.3681 and had the elemental composition $C_{31}H_{49}O_3$, (Calc. 469.3682) which is consistent with the compound being Isomangiferolic acid and at for the other peak at 30.03 min the mass was [M-H]⁻ m/z 455.3528 and the elemental composition $C_{30}H_{47}O_3$, (Calc. 455.3526) consistent the elemental composition for Ambolic acid, as shown in **Figure 4-23.**
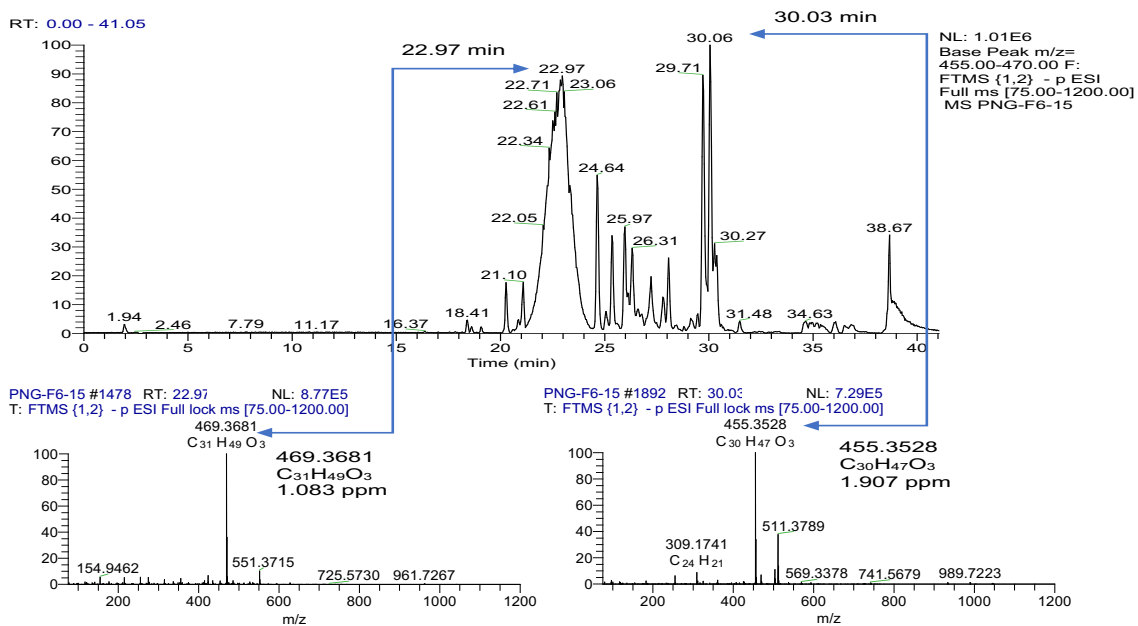
Figure 4-23: LC-MS chromatogram (ESI negative mode) for compound 2 and 6
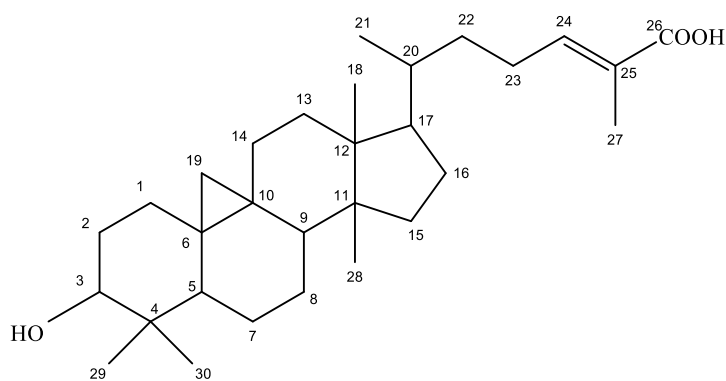
Figure 4-24: structure of Isomangiferolic acid (2)
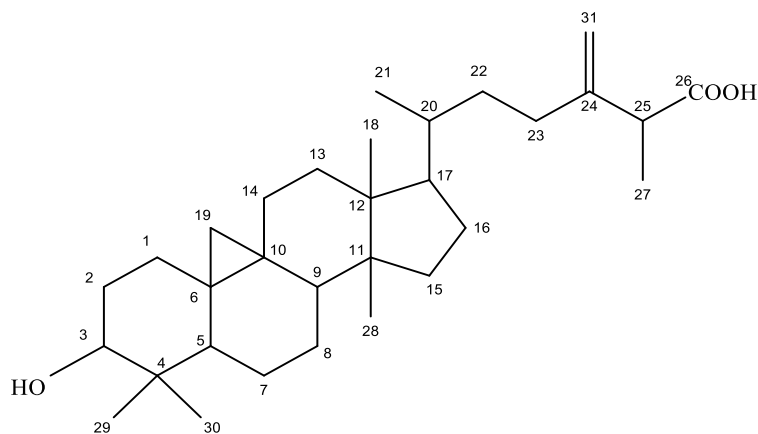
Figure 4-25: Structure of Ambolic acid (6)

Table 4-9: ^{1}H (500MHz), ^{13}C (100MHz) data of compound (2) and (6) in fraction PNG-F6-15

Position	Compound			
	(2) **Isomangiferolic acid**		**(6)** **Ambolic acid**	
	^{1}H δ ppm (mult, *J*)	^{13}C δ ppm	^{1}H δ ppm (mult, *J*)	^{13}C δ ppm
1	1.74 1H (m), 1.04 1H (m)	27.5 (CH$_2$)	1.92 1H (m), 1.27 1H (m)	32.0 (CH$_2$)
2	1.92 1H (m), 1.64 1H (m)	28.5 (CH$_2$)	1.74 1H (m), 1.52 1H (m)	30.3 (CH$_2$)
3	3.5 1H (m)	77.1 (CH)	3.5 1H (m)	77.1 (CH)
4	-	39.5 (C)	-	40.5 (C)
5	1.831H (m)	41.1 (CH)	1.27 1H (m)	47.1 (CH)
6	1.65 1H (m), 0.80 1H (m)	21.1 (CH$_2$)	1.651H (m), 0.80 1H (m)	21.1 (CH$_2$)
7	1.27 1H (m), 1.14 1H (m)	25.7 (CH$_2$)	1.27 1H (m), 1.14 1H (m)	26.0 (CH$_2$)
8	1.52 1H (m)	48.0 (CH)	1521H (m)	48.1 (CH)
9	-	19.8 (C)	-	19.8 (C)
10	-	26.5 (C)	-	26.5 (C)
11	2.03 1H (m), 1.14 (m)	26.3 (CH$_2$)	2.03 1H (m), 1.14 1H (m)	26.3 (CH$_2$)
12	1.65 2H (m)	32.9 (CH$_2$)	1.65 2H (m)	32.9 (CH$_2$)
13	-	45.3 (C)	-	45.3 (C)
14	-	48.9 (C)	-	48.9 (C)
15	1.34 2H (m)	35.5 (CH$_2$)	1.34 2H (m)	35.5 (CH$_2$)
16	1.92 1H (m), 1.30 1H (m)	28.1 (CH$_2$)	1.92 1H (m), 1.30 1H (m)	28.1 (CH$_2$)
17	1.65 1H (m)	52.2 (CH)	1.65 1H (m)	52.2 (CH)
18	0.90 3H (s)	18.0 (CH$_3$)	0.90 3H (s)	18.1 (CH$_3$)
19	0.54 1H (d, 4.09) 0.37 1H (d, 4.03)	29.8 (CH$_2$)	0.54 1H (d, 4.09) 0.37 1H (d, 4.03)	29.8 (CH$_2$)
20	1.44 1H (m)	36.0 (CH)	1.44 1H (m)	36.0 (CH)
21	0.92 3H (d, 6.31)	18.0 (CH$_3$)	0.94 3H (d, 6.31)	18.1 (CH$_3$)
22	1.58 1H (m), 1.19 1H (m)	34.8 (CH$_2$)	1.58 1H (m), 1.19 1H (m)	34.6 (CH$_2$)
23	2.27 1H (m), 2.14 1H (m)	25.9 (CH$_2$)	2.03 1H (m), 1.92 1H (m)	25.9 (CH$_2$)
24	6.92 1H (t d, 7.52, 1.57)	145.7 (CH)	-	148.7 (C)
25	-	126.6 (C)	3.19 1H (q, 7.13)	45.6 (CH)
26	-	173.0 (C)	-	45.7 (C)
27	1.86 3H (s)	12.0 (CH$_3$)	1.32 3H , 7.05)	16.3 (CH$_3$)
28	0.99 3H (s)	25.8 (CH$_3$)	0.99 3H (s)	25.4(CH$_3$)
29	0.97 3H (s)	21.2 (CH$_3$)	0.83 3H (s)	14.0 (CH$_3$)
30	0.92 3H (s)	19.3 (CH$_3$)	0.92 3H (s)	19.3 (CH$_3$)
31	-	-	4.98 (1H, s) 4.94 (1H, s)	111.0 (CH$_2$)
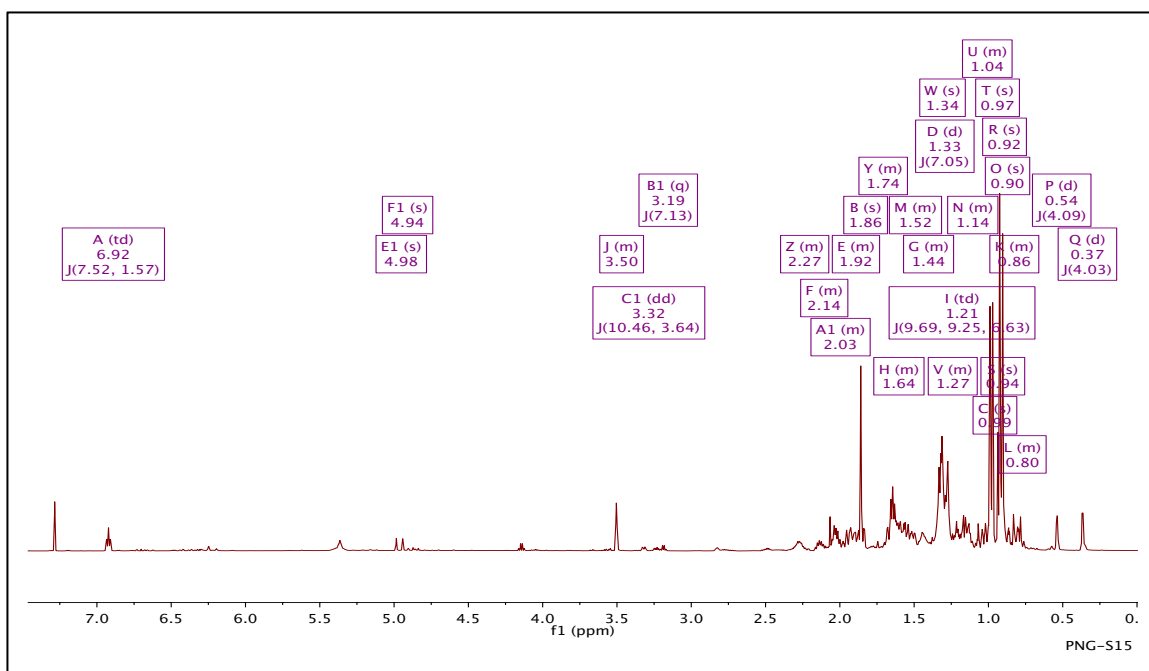
Figure 4-26: ¹H NMR (500 MHz) spectrum of compound (2) and compound (6) in CDCl₃.
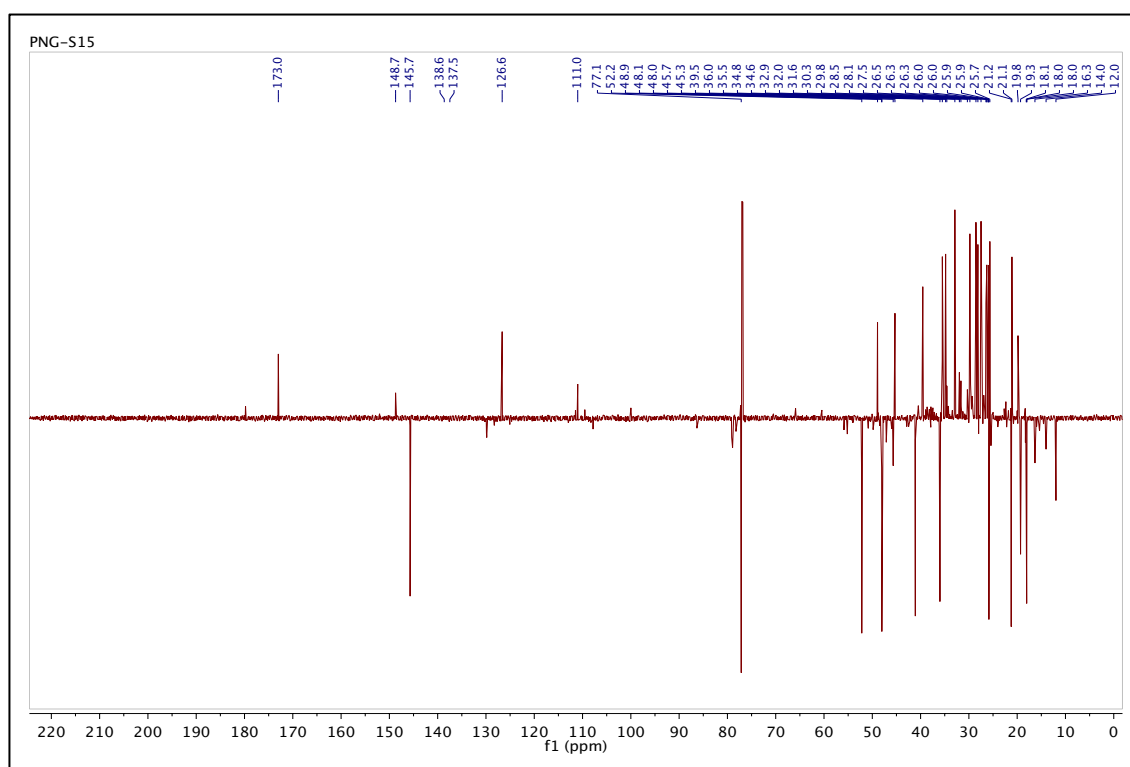
Figure 4-27: ¹³C NMR (100 MHz) spectrum of compound (2) and compound (6) in CDCL₃.
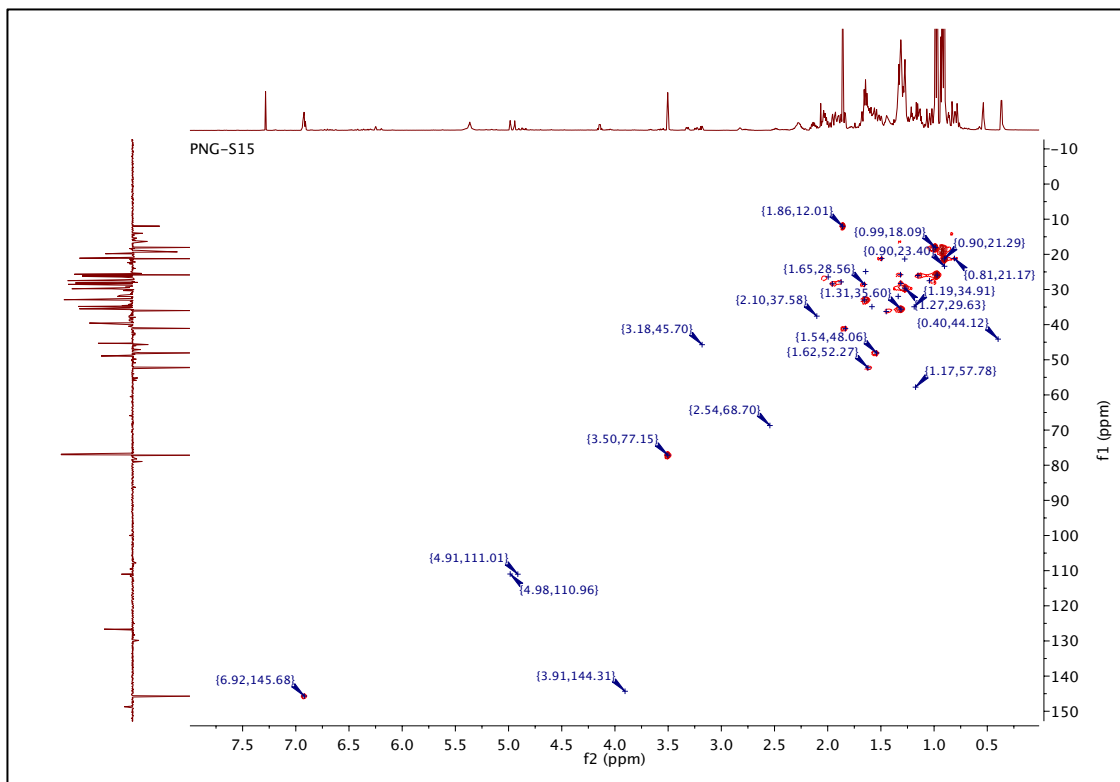
Figure 4-28: HSQC (500 MHz) Spectrum of of the compound (2) and compound (6) in CDCl₃.
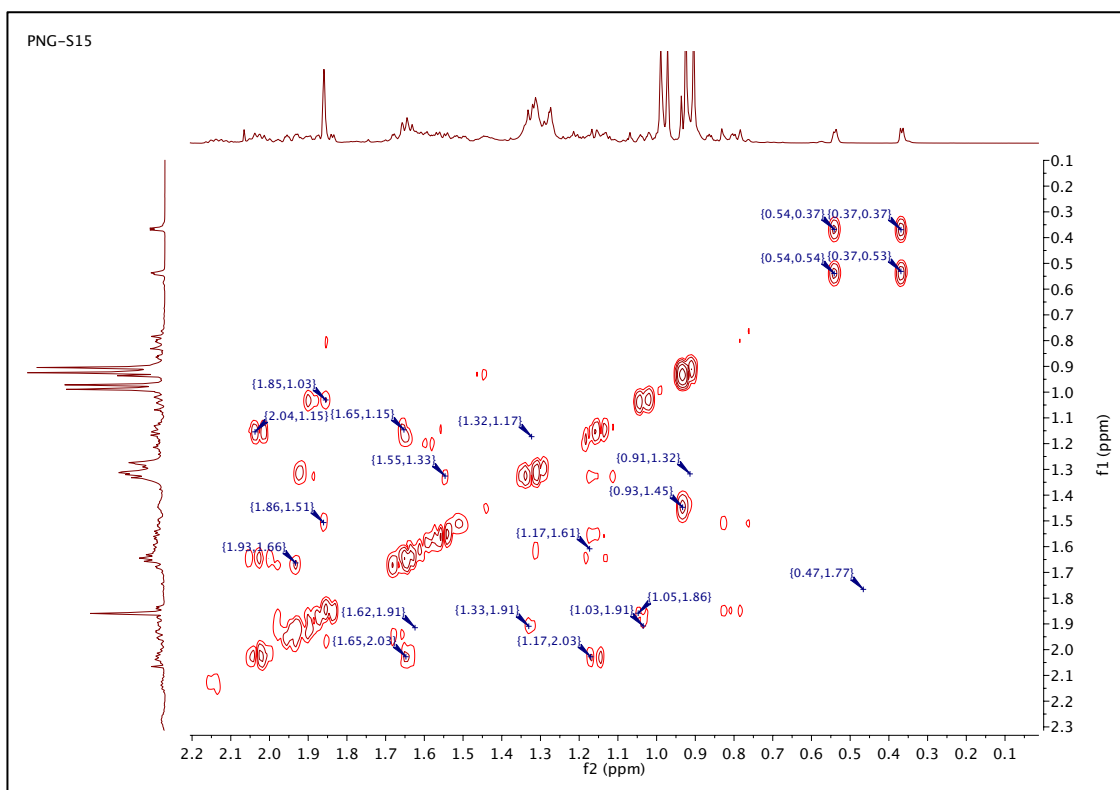
Figure 4-29: COSY (500 MHz) Spectrum of the compound (2) and compound (6) in CDCl₃

Figure 4-30: HMBC (500 MHz) Spectrum of of the compound (2) and compound (6) in CDCl₃

4.2.8.3 Characterization of PNG-6-17 as 27- Hydroxyisomangiferolic acid(3)

The proton and carbon spectra for the compound were similar to compound 3 except for the chemical shift of H-27 observed at δ_H 4.11 indicating a –CH_2OH substituent (**Figure 4-33)**. This was confirmed by the carbon resonance of C-27 observed at δ_C 55.8 ppm (**Figure 4-34**). The ESI peak at 26.57 min in the negative mode was found at [M-H]⁻ m/z 471.3475 corresponding to $C_{30}H_{47}O_4$ (Calc. 471.3474) as shown in **Figure 4-32**. Further analysis of its NMR data (**Figures 4-35** to **4-37**) in comparison to compound 3 enabled the identification of the compound as 27- hydroxyisomangiferolic acid (**Figure 4-31**). The chemical shifts for the protons and carbons were fully assigned as given in **Table 4-10.** The chemical shifts for the compounds were confirmed using literature reports (Kardar et al., 2014, Nguyen et al., 2017).

Figure 4-31: structure of 27- Hydroxyisomangiferolic acid (3)

84

Figure 4-32: LC-MS chromatogram (ESI negative mode) for compound 3.

Table 4-10: ^{1}H (500MHz), ^{13}C (100MHz) data of the compound (3) in fraction PNG-F6-17

Position	Compound	
	(3) **27- Hydroxyisomangiferolic acid**	
	^{1}H δ ppm (mult, *J*)	^{13}C δ ppm
1	1.85 1H (m), 1.26 1H (m)	28.1 (CH_2)
2	1.92 1H (m), 1.55 1H (m)	29.1 (CH_2)
3	3.06 1H (q, 4.75)	77.1 (CH)
4	-	39.6 (C)
5	1.78 1H (m)	40.6 (CH)
6	1.47 1H (m), 0.75 1H (m)	21.1 (CH_2)
7	1.26 1H (m), 1.14 1H (m)	25.0 (CH_2)
8	1.55 1H (m)	47.8 (CH)
9	-	19.5 (C)
10	-	26.7 (C)
11	2.21 1H (s), 1.14 1H (m)	26.3 (CH_2)
12	1.55 2H (m)	33.0 (CH_2)
13	-	45.3 (C)
14	-	48.9 (C)
15	1.26 2H (m)	35.5 (CH_2)
16	1.92 1H (m), 1.26 1H (m)	28.2 (CH_2)
17	1.60 1H (m)	52.1 (CH)
18	0.94 3H (s)	18.3 (CH_3)
19	0.49 1H (d, 3.96), 0.30 1H (d, 3.86)	29.7 (CH_2)
20	1.47 1H (m)	35.9 (CH)
21	0.87 3H (d, 3.55)	18.4 (CH_3)
22	1.55 1H (m), 1.14 1H (m)	35.5 (CH_2)
23	2.29 1H (m), 2.12 1H (m)	26.1 (CH_2)
24	6.62 1H (t, 7.7)	145.8 (CH)
25	-	132.8 (C)
26	-	171.1 (C)
27	4.11 2H (s)	55.8 (CH_2)
28	0.94 3H (s)	26.1 (CH_3)
29	0.88 3H (s)	21.7 (CH_3)
30	0.88 3H (s)	19.8 (CH_3)
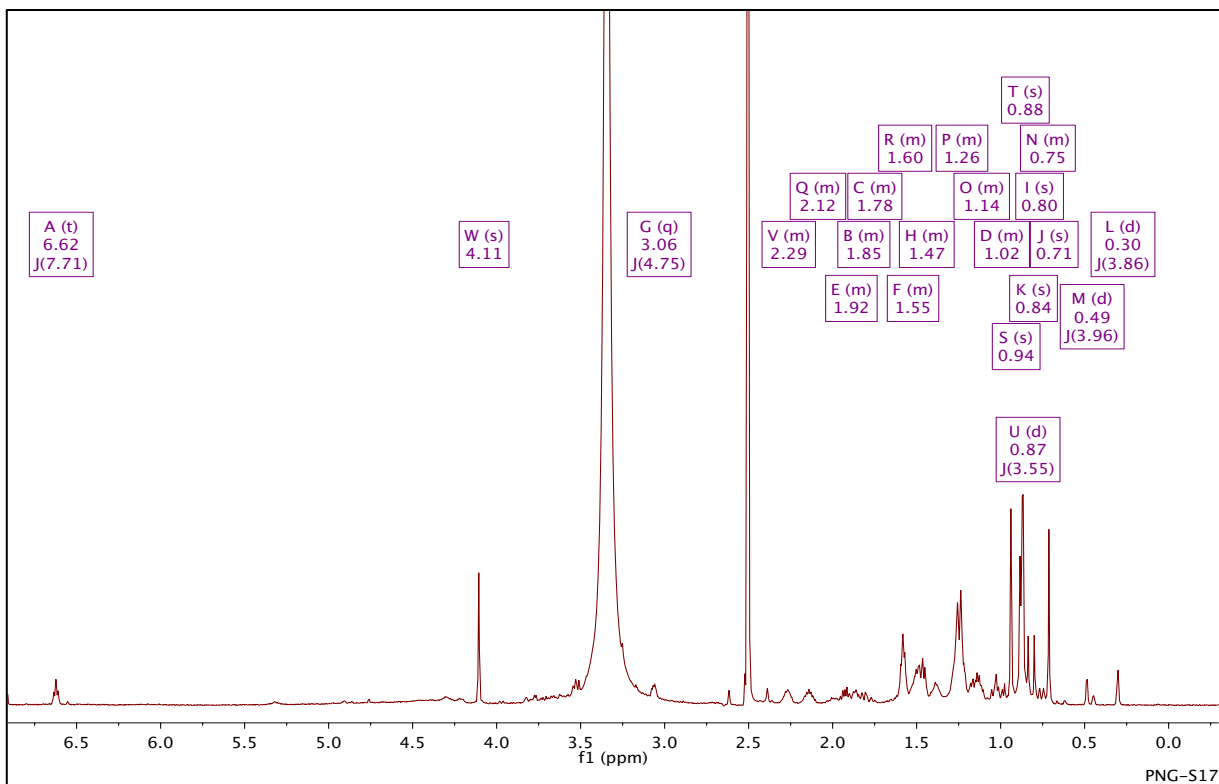
Figure 4-33: 1H NMR (500 MHz) spectrum of the compound (3) in DMSO-d₆

Peak labels:

A (t) 6.62 J(7.71)
W (s) 4.11
G (q) 3.06 J(4.75)
V (m) 2.29
Q (m) 2.12
E (m) 1.92
B (m) 1.85
C (m) 1.78
R (m) 1.60
F (m) 1.55
H (m) 1.47
P (m) 1.26
O (m) 1.14
D (m) 1.02
S (s) 0.94
T (s) 0.88
U (d) 0.87 J(3.55)
K (s) 0.84
I (s) 0.80
N (m) 0.75
J (s) 0.71
M (d) 0.49 J(3.96)
L (d) 0.30 J(3.86)

13C NMR peak labels: 171.9, 156.1, 145.8, 132.8, 109.2, 55.8, 52.1, 48.9, 47.8, 45.3, 40.6, 40.2, 39.8, 39.6, 35.9, 35.5, 35.5, 33.0, 29.9, 29.7, 29.1, 28.2, 28.1, 26.7, 26.7, 26.3, 26.1, 25.0, 21.7, 21.1, 19.8, 19.5, 18.4, 18.3, 13.5
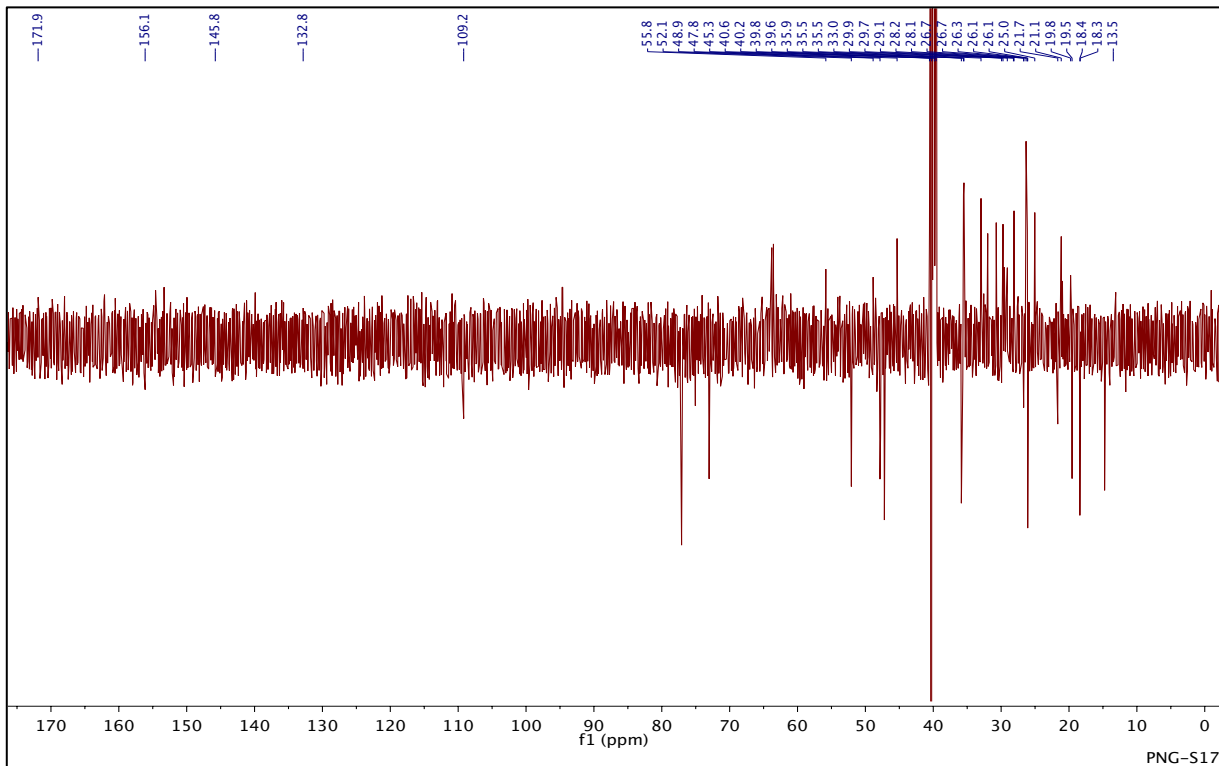
Figure 4-34: ¹³C NMR (100 MHz) spectrum of the compound (3) in DMSO-d₆
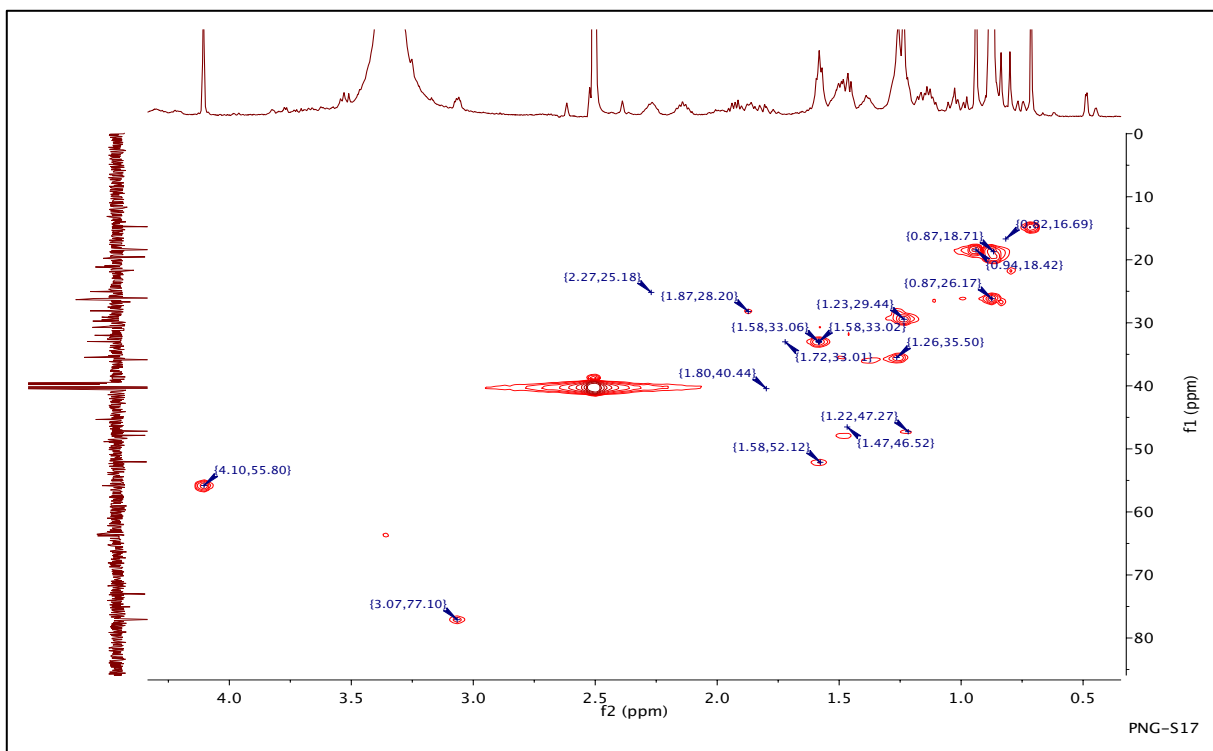
Figure 4-35: HSQC (500 MHz) Spectrum of the compound (3) in DMSO-d$_6$.
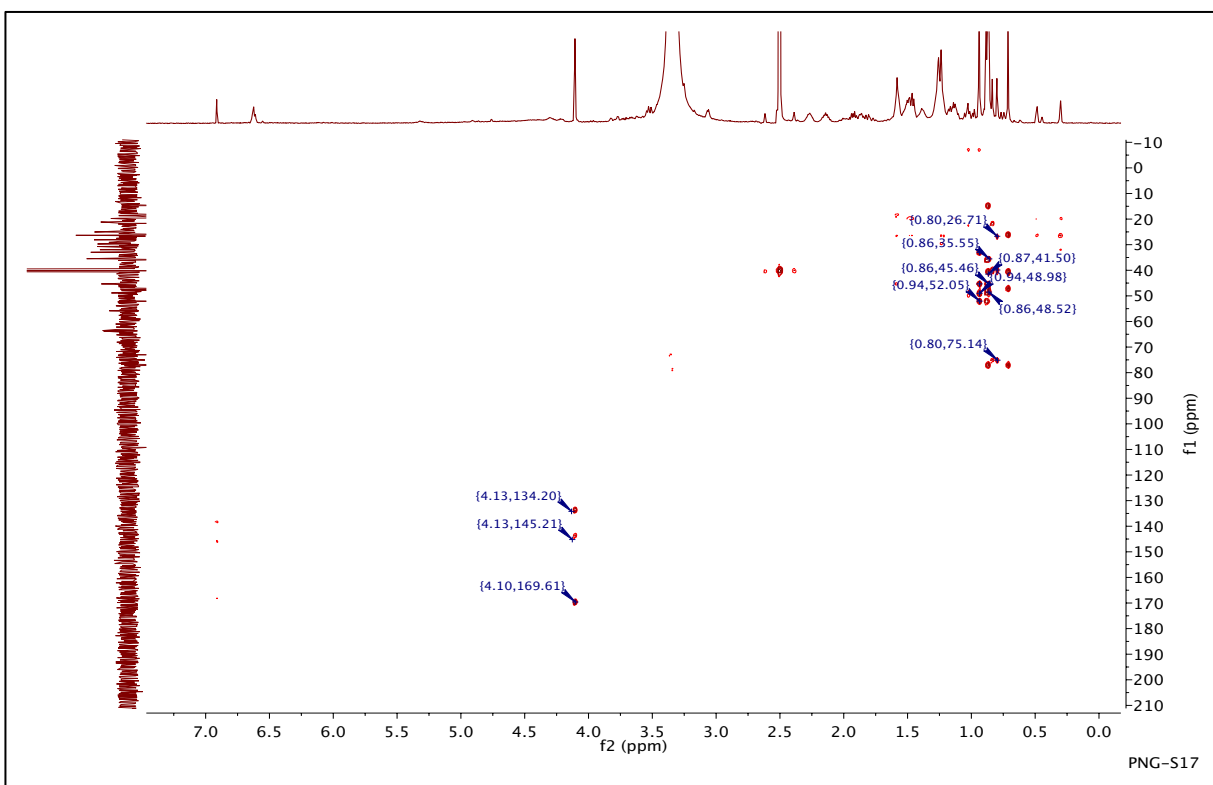
Figure 4-36: HMBC (500 MHz) Spectrum of the compound (3) in DMSO-d$_6$

87
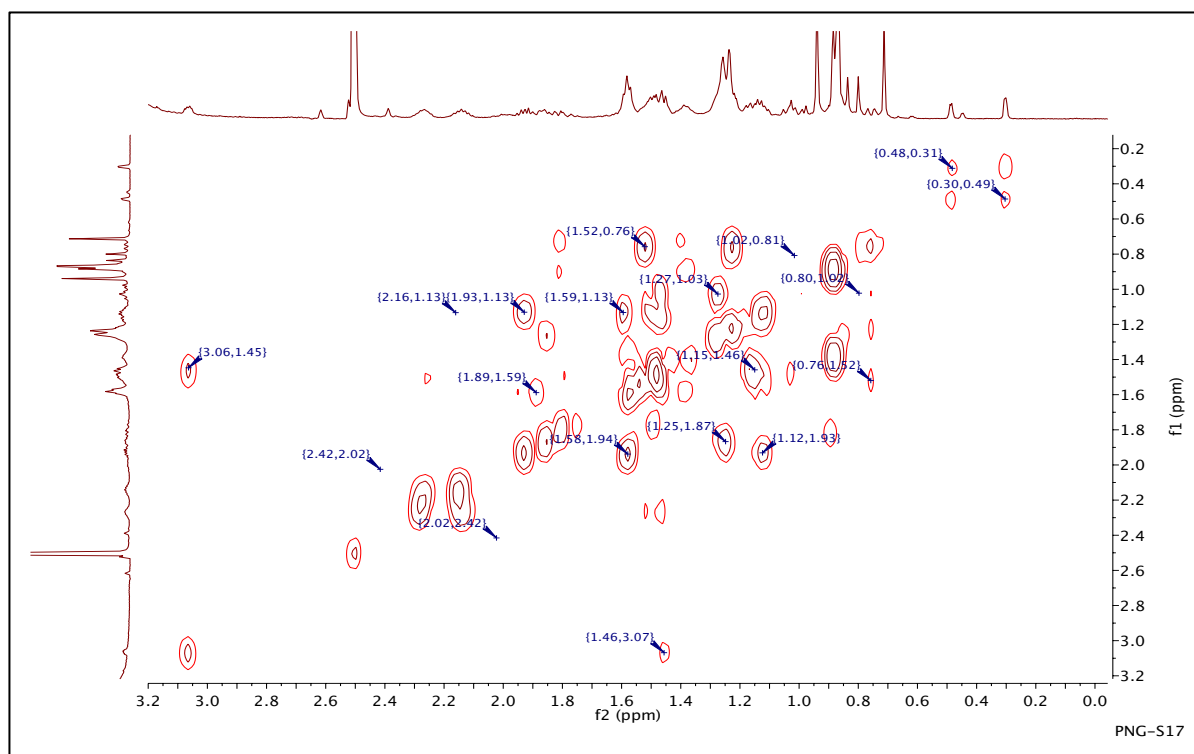
Figure 4-37: COSY (500 MHz) Spectrum of compound (5) in DMSO-d$_6$

4.2.8.4 Characterization of PNG-F1-5B as mixture of Cycloartenol (4), 24 (28)-Methylenecycloartenol (7) and Cycloeucalenol (8)

The proton spectrum for the fraction PNG-F1-5B was also characteristic of cycloartane triterpenes and similar to compounds 2 and 6 except for the absence of the highly deshielded olefinic proton at δ$_H$ 6.93 ppm. This may be due to the absence of a carboxylic acid group in the compounds contained in this fraction. Several olefinic protons were observed between δ$_H$ 4.69 and 5.21 ppm (**Figure 4-44**). Two of these were methylene protons observed at δ$_H$ 4.69 ppm and 4.74 ppm and were attached to a carbon at δ$_C$ 105.9 ppm, while the other two protons δ$_H$ 4.59 ppm and 4.71 ppm were attached to a carbon at δ$_C$ 109.3 ppm. Also, there was a vinyl proton at δ$_H$ 5.13 attached to a carbon at δ$_C$ 121.7 ppm (**Figure 4-40B**). These protons are for H-24 of cycloartenol and cycloeucalenol and H-31 of 24 (28)-methylenecycloartenol. The proton spectrum also had signals for H-3 of –OH bearing triterpenes at C-3 (δ$_C$ =79.1 ppm) between δ$_H$ 3.22 and 3.31 ppm. The cycloeucalenol was also characterized by the presence of a quartet at 1.34 ppm attached a carbon at δ$_C$ 39.0 ppm (C-4) and different from the cycloartenols that had C-4 as a quaternary carbon (δ$_{C = }$40.0). From the 1D and 2D correlations (**Figures 4-44 to 4-47**), the characteristic chemical shifts for the compounds in the mixture are given in **Table 4-11**. Thus, the compounds were identified as cycloartenol (4), 24 (28)-

methylenecycloartenol (7) and cycloeucalenol (8) (**Figures 4-41** to **4-43**). The exact mass was determined by using GC-MS and LC-MS (**Figures 4-38 and 4-39**) and the chemical shifts for the compounds were confirmed using literature reports (De et al., 1987, Hosoe et al., 1990).
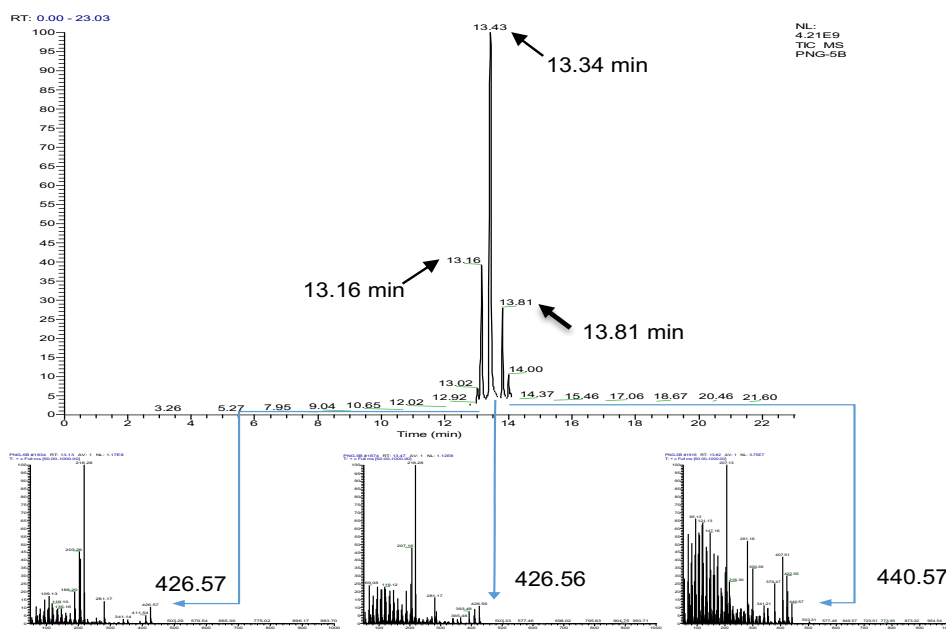
Figure 4-38: GC-MS analysis of the purified compounds 4, 7 and 8 in fraction PNG-F1-5B
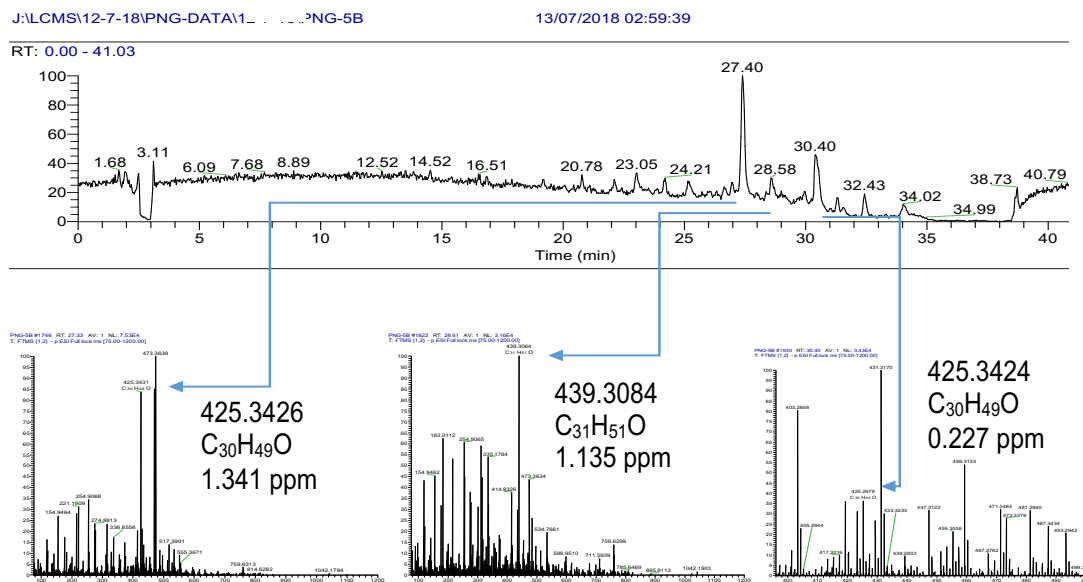
Figure 4-39: LC-MS chromatogram (ESI negative mode) for compounds 4, 7 and 8.
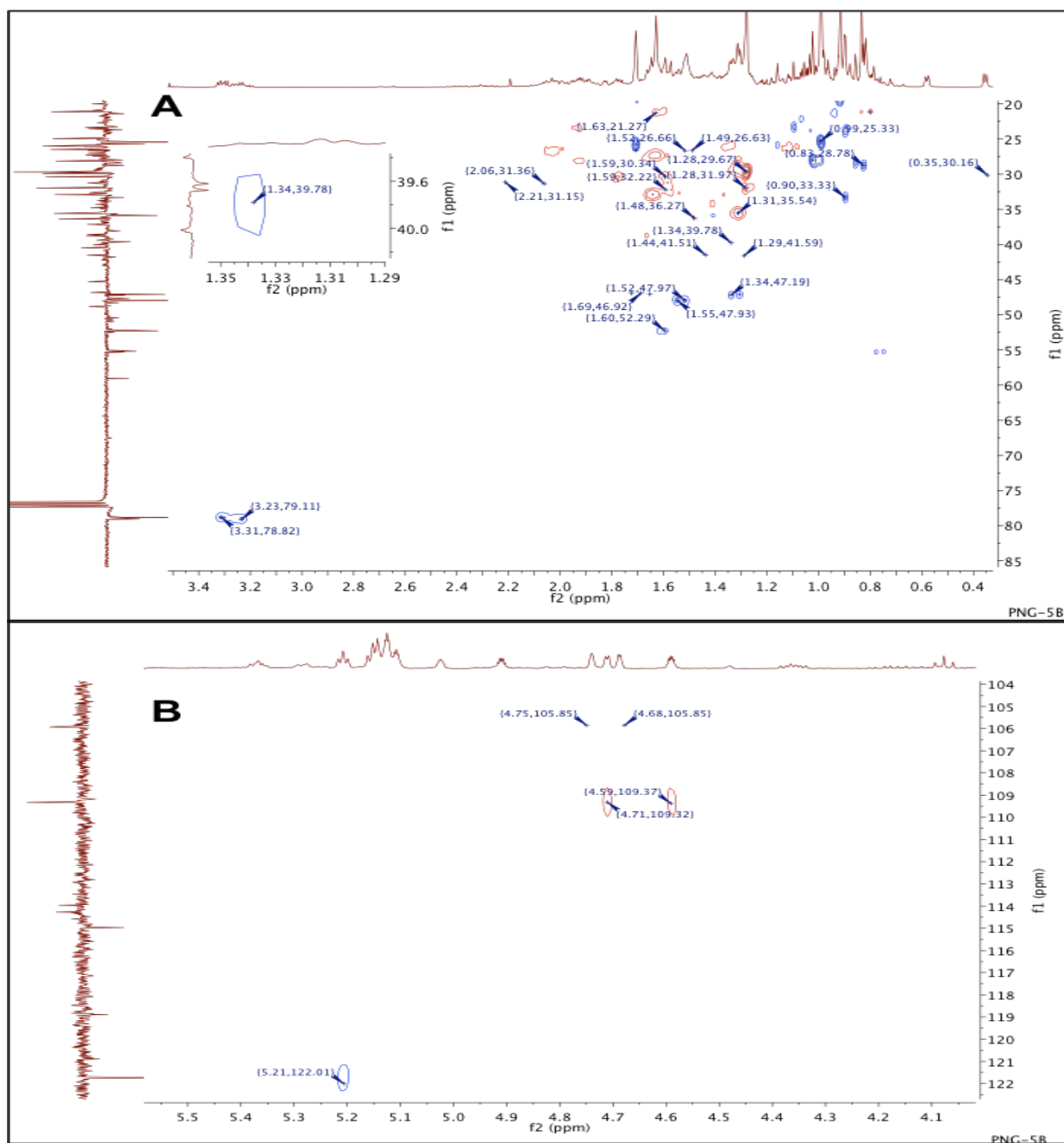
Figure 4-40: HSQC spectra (500 MHz) of the mixture Illustrate direct C-H coupling characterized of the three cycloartenols compounds 4, 7 and 8.
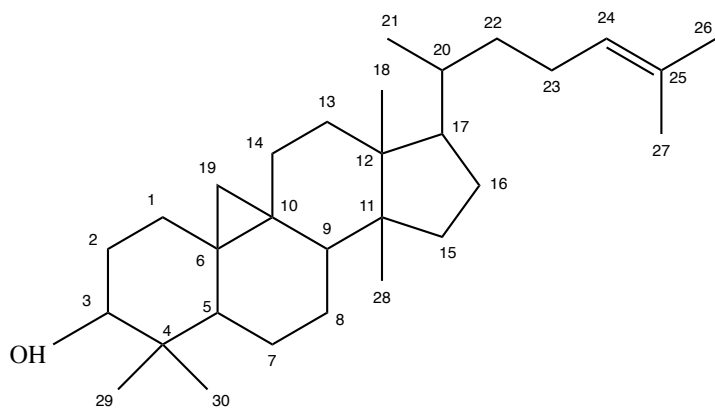
Figure 4-41: structure of cycloartenol (4)
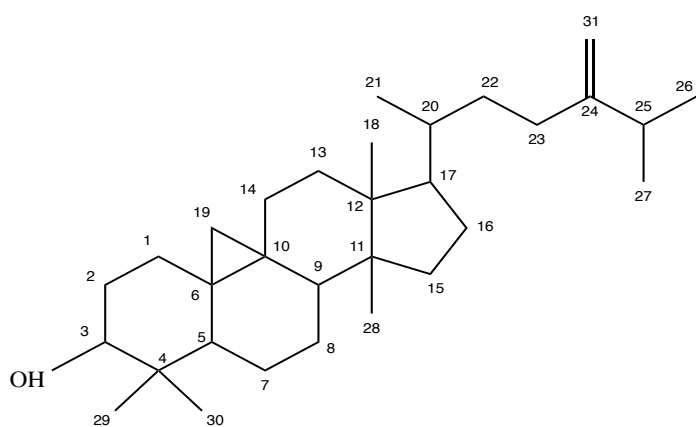
Figure 4-42: structure of Cycloeucalenol (8)
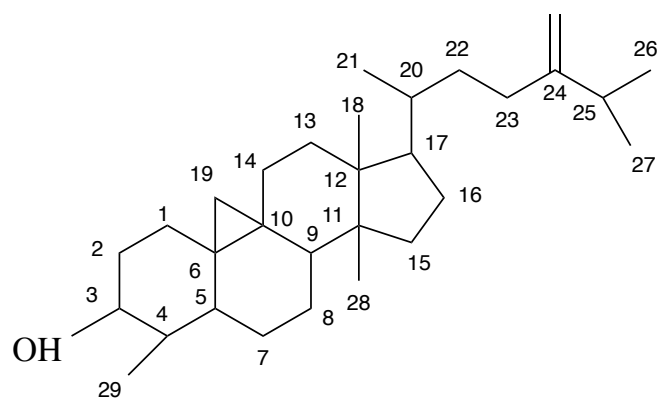
Figure 4-43: structure of 24 (28) Methylenecycloartanol (7)

Table 4-11: ^{1}H (500MHz), ^{13}C (100MHz) data of compounds 4, 7 and 8 in fraction PNG-F1-5B

Position	(4) Cycloartenol		(7) 24 (28)-methylenecycloartenol		(8) Cycloeucalenol	
	^{1}H δ ppm (mult, *J*)	^{13}C δ ppm	^{1}H δ ppm (mult, *J*)	^{13}C δ ppm	^{1}H δ ppm (mult, *J*)	^{13}C δ ppm
1	1.55 1H (m), 1.28 1H (m)	32.0 (CH$_2$)	1.55 1H (m), 1.28 1H (m)	32.0 (CH$_2$)	1.55 1H (m), 1.28 1H (m)	30.4 (CH$_2$)
2	1.92 1H (m), 1.65 1H (m)	26.5 (CH$_2$)	1.92 1H (m), 1.65 1H (m)	26.6 (CH$_2$)	1.83 1H (m) 1.59 1H (m)	27.0 (CH$_2$)
3	3.31 (m)	78.9 (CH)	3.26 (m)	79.1 (CH)	3.22 (m)	79.0 (CH)
4	-	40.5 (C)	–	40.0 (C)	1.32 (m)	41.5 (C)
5	1.32 1H (m)	39.6 (CH)	1.32 1H (m)	39.7 (CH)	1.32 1H (m)	41.8 (CH)
6	1.65 1H (m), 0.81 1H (m)	21.1 (CH$_2$)	1.65 1H (m), 0.81 1H (m)	21.1 (CH$_2$)	1.65 1H (m), 0.81 1H (m)	20.9 (CH$_2$)
7	1.15 1H (m), 1.32 1H (m)	26.0 (CH$_2$)	1.15 1H (m), 1.32 1H (m)	26.0 (CH$_2$)	1.15 1H (m), 1.32 1H (m)	26.5 (CH$_2$)
8	1.52 1H (m)	47.1 (CH)	1.52 1H (m)	47.1 (CH)	1.52 1H (m)	47.2 (CH)
9	-	20.1 (C)	–	19.9 (C)	-	23.6 (C)
10	-	26.0 (C)	–	26.1 (C)	-	26.2 (C)
11	1.07 1H (m), 0.81 (m)	28.1 (CH$_2$)	1.07 1H (m), 0.81 (m)	28.1 (CH$_2$)	1.07 1H (m), 0.81 (m)	28.1 (CH$_2$)
12	1.59 1H (m), 1.28 1H (m)	32.9 (CH$_2$)	1.59 1H (m), 1.28 1H (m)	35.7 (CH$_2$)	1.59 1H (m), 1.28 1H (m)	32.9 (CH$_2$)
13	-	45.2 (C)	–	45.2 (C)	-	45.3 (C)
14	-	48.7 (C)	–	49 (C)	-	49.0 (C)
15	1.33 1H (m), 0.90 1H (m)	32.9 (CH$_2$)	1.33 1H (m), 0.90 1H (m)	32.9 (CH$_2$)	1.33 1H (m), 0.90 1H (m)	32.9 (CH$_2$)
16	2.02 1H (m), 1.32 1H (m)	71.8 (CH$_2$)	2.02 1H (m), 1.32 1H (m)	26.5 (CH$_2$)	2.02 1H (m), 1.32 1H (m)	28.6 (CH$_2$)
17	1.65 1H (m)	52.3 (CH)	1.65 1H (m)	52.5 (CH)	1.65 1H (m)	52.2 (CH)
18	0.99 3H (s)	18.2 (CH$_3$)	0.99 1H (s)	18 (CH$_3$)	0.99 1H (s)	17.8 (CH$_3$)
19	0.58 1H (d, 4.21), 0.35 1H (d, 4.18)	29.7 (CH$_2$)	0.58 1H (d, 4.21), 0.35 1H (d, 4.18)	29.9 (CH$_2$)	0.58 1H (d, 4.21), 0.35 1H (d, 4.18)	29.9 (CH$_2$)
20	1.40 1H (m)	30.3 (CH)	1.40 1H (m)	36 (CH)	1.40 1H (m)	36.0 (CH)
21	0.92 3H (s)	18.0 (CH$_3$)	0.92 3H (s)	18.3 (CH$_3$)	0.92 3H (s)	18.4 (CH$_3$)
22	1.33 2H (m)	35.5 (CH$_2$)	1.33 2H (m)	35.6 (CH$_2$)	1.33 2H (m)	35.6 (CH$_2$)
23	1.77 1H (m), 0.97 1H (m)	24.9 (CH$_2$)	2.02 1H (m), 1.65 1H (m)	31.2 (CH$_2$)	2.23 1H (m), 1.65 1H (m)	31.1 (CH$_2$)
24	5.21 IH (t, 3.68)	121.7 (CH)	-	156.9 (C)	-	156.5 (C)
25	-	130.7 (C)	2.33 (m)	33.8 (CH)	2.33 (m)	33.9 (CH)
26	1.71 3H (s)	26.1 (CH$_3$)	1.28 3H	21.8 (CH$_3$)	1.026 d	22.1 (CH$_3$)
27	1.63 3H (s)	18.2 (CH$_3$)	1.02 3H (s)	23.7 (CH$_3$)	1.03 3H (s)	23.3 (CH$_3$)
28	0.90 3H (s)	19.3 (CH$_3$)	0.90 3H (s)	19.1 (CH$_3$)	0.90 3H (s)	19.1 (CH$_3$)
29	0.83 3H (s)	14.0 (CH$_3$)	0.83 3H (s)	10.1 (CH$_3$)	0.83 3H (s)	14.46 (CH$_3$)
30	0.99 3H (s)	25.5 (CH$_3$)	0.99 3H (s)	25.7 (CH$_3$)	4.59 1H (dd,, 2.74, 1.38) 4.71 1H (d, 2.64)	106.9 (CH$_2$)
31			4.69 IH (d, 1.59) 4.74 1H (s)	109.3 (CH$_2$)		

92
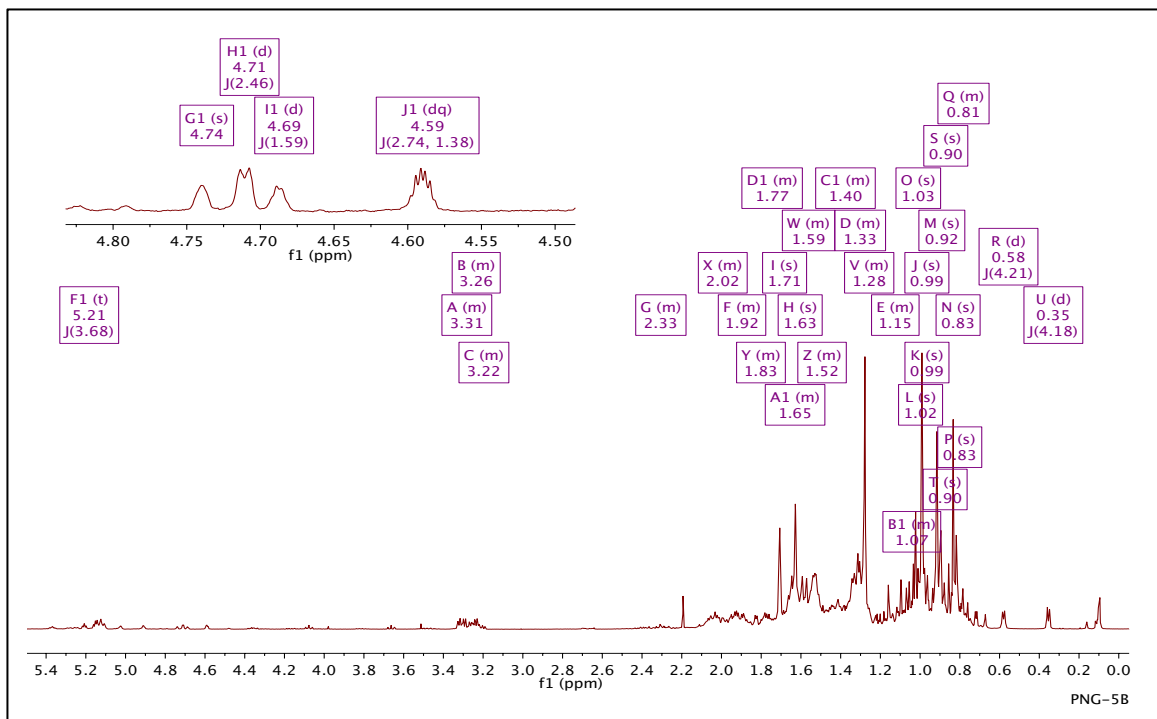
Figure 4-44: ^{1}H NMR (500 MHz) spectra of compounds (4), (7) and (8) in CDCl$_3$
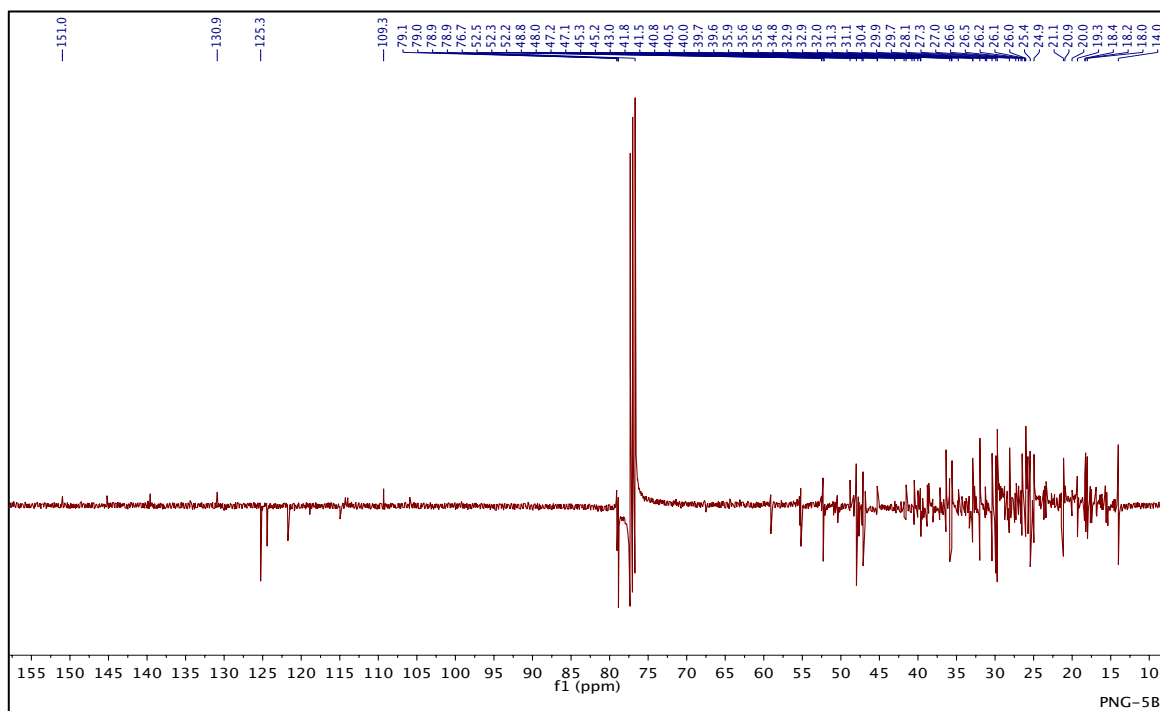
Figure 4-45: ^{13}C NMR (100 MHz) spectra of compounds (4), (7) and (8) in CDCl$_3$
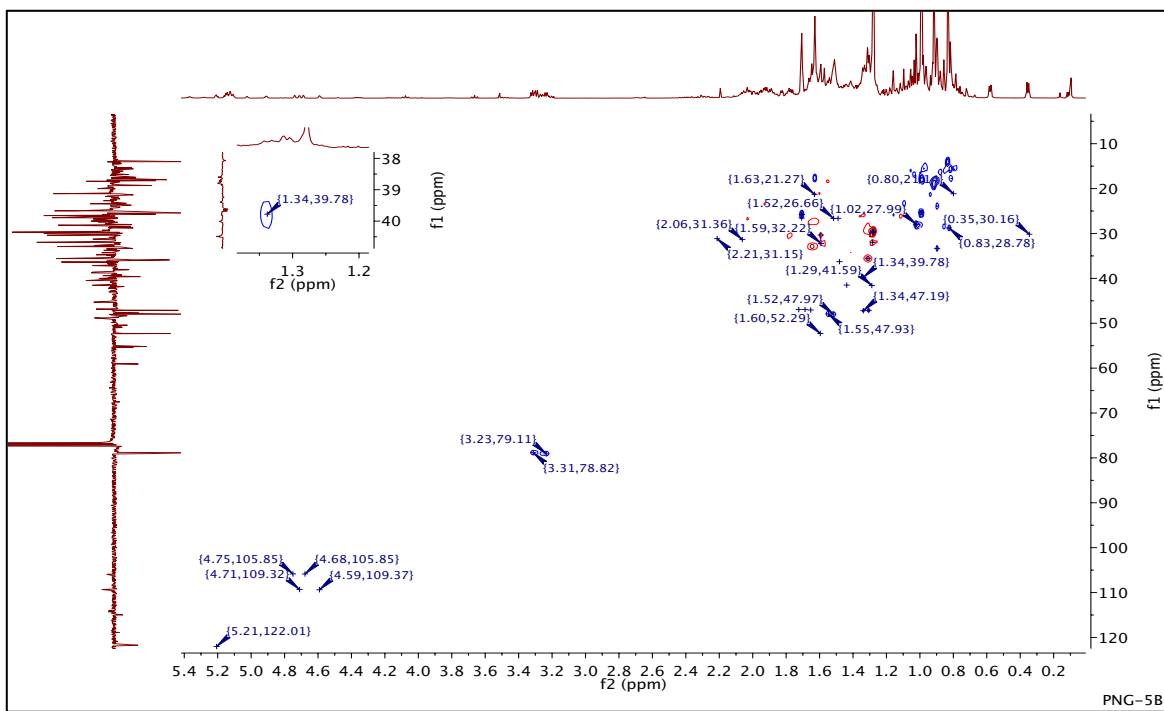
Figure 4-46: HSQC (500 MHz) Spectrum Compound (4), (7), and (8) in CDCl₃
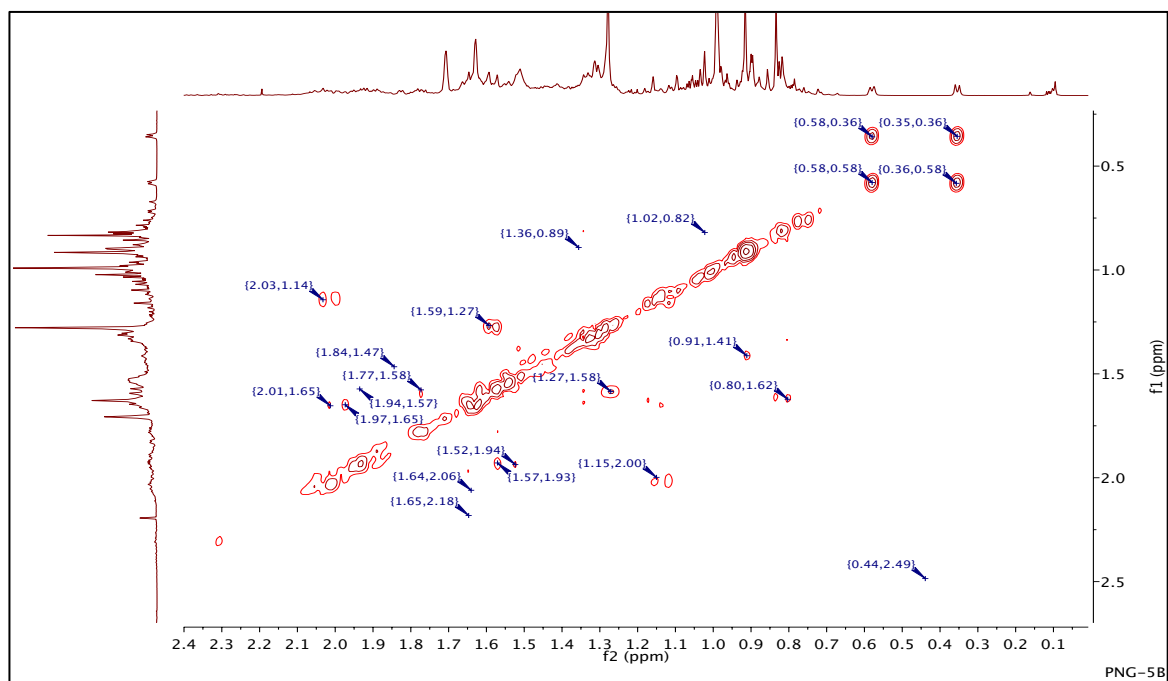
Figure 4-47: COSY (500 MHz) Spectrum of Compound (4), (7), and (8) in CDCl₃

4.2.8.5 Characterization of PNG-F5 as 20-hydroxybetulin (9)

The proton NMR of fraction F5 obtained from the column chromatography of ethanol extract of PNG indicated a single triterpene. The proton spectrum showed signals for two hydroxymethylene protons at δ_H 3.93 (d, J = 12.0 Hz) and 4.02 (d, J = 12.0 Hz) for H-28 and an oxymethine proton at δ_H 3.25 1H (dd, J = 11.10 5.53) for H-3 of the triterpene (**Figure 4-50**). The structure was established by analysis of its 2D (COSY, HSQC and HMBC) spectra (**Figures 4-52** to **4-54**) as follows: HSQC correlations from the methylene protons δ_H 3.93 (d, J = 12.0), 4.02 (d, J = 12.0) indicated they were attached to the same carbon at δ_C 62.9 ppm (C-28) and the proton at δ_H 3.93 was attached to C-3 at δ_C 79.3 (**Figure 4-52**). HMBC correlations showed the methyl groups at 1.17 and 1.26 were germinal and attached to the quaternary oxygenated carbon at δ_C 73.6 (**Figure 4-54**). This carbon must be on a side chain hence the triterpene moiety must be that of a lupane type. Examination of other correlations from COSY and HMBC established the structure as 3, 20, 28-Trihydroxylupane (9) (**Figures 4-49**) and this was confirmed by comparison of the spectral data with literature reports (**Table 4-12**) (Fuchino et al., 1996). The formula $C_{30}H_{52}O_3$, was confirmed from its ESI, LCI-MS spectrum which gave a molecular in ion negative mode at [M-H]- m/z 459.38489, 1.135 ppm (**Figure 4-48**).
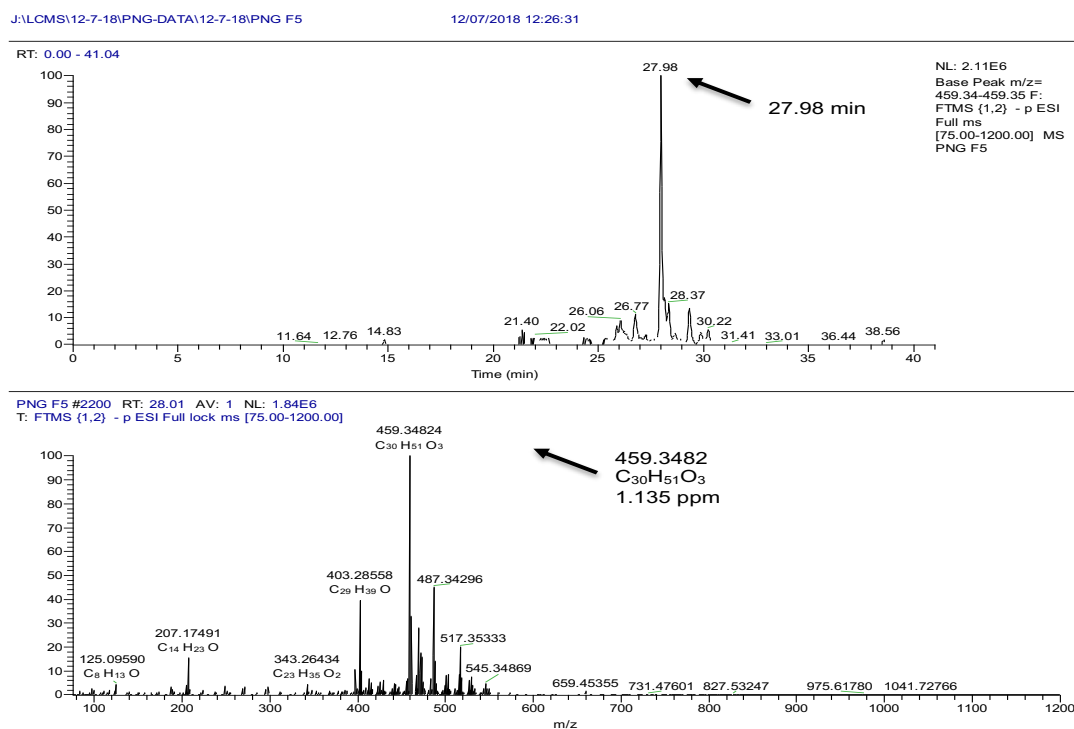
Figure 4-48: LC-MS chromatogram (ESI negative mode) for compound 9
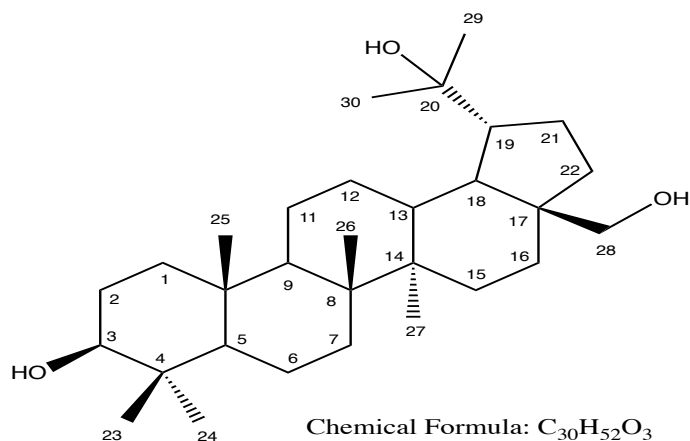
Figure 4-49: structure of 20-hydroxybetulin

Table 4-12: ¹H (500MHz), ¹³C (100MHz) data of compound (9) in fraction PNG-F5

Position	Compound	
	(9) **20-hydroxybetulin**	
	¹H δ ppm (mult, *J*)	**¹³C δ ppm**
1	1.34 1H (m), 1.15 1H (m)	40.6 (CH₂)
2	1.77 1H (m), 1.68 1H (m)	27.8 (CH₂)
3	3.25 1H (dd, *J* = 11.10 5.53)	79.3 (CH)
4	-	38.2 (C)
5	0.87 1H (m)	55.9 (CH)
6	1.71 1H (m), 0.85 1H (m)	19.6 (CH₂)
7	2.34 1H (m), 1.65 1H (m)	35.2 (CH₂)
8	-	41.8 (C)
9	1.38 1H (m)	52.0 (CH)
10	-	39.1 (C)
11	1.81 1H (m), 1.05 1H (m)	29.1 (CH₂)
12	1.40 1H (m), 0.84 1H (m)	28.8 (CH₂)
13	1.40 1H (m)	36.0 (CH)
14	-	42.1 (C)
15	1.69 1H (m), 1.84 1H (m)	28.2 (CH₂)
16	1.91 1H (m), 1.30 1H (m)	30.1 (CH₂)
17	-	48.8 (C)
18	1.85 1H (m)	50.4 (CH)
19	1.37 1H (m)	48.4 (CH)
20	-	73.6 (C)
21	1.69 1H (m), 1.84 1H (m)	28.2 (CH₂)
22	2.30 1H (m), 0.88 1H (m)	33.8 (CH₂)
23	1.17 3H (s)	25.2 (CH₃)
24	0.793H (s)	16.1 (CH₃)
25	0.82 3H (s)	17.0 (CH₃)
26	1.53 3H (s)	18.4 (CH₃)
27	1.01 3H (s)	15.7 (CH₃)
28	3.93(d, *J* = 12.0), 4.02 (d, *J* = 12.0)	62.9 (CH₂)
29	1.77 3H (s)	24.5 (CH₃)
30	1.26 3H (s)	32.0 (CH₃)
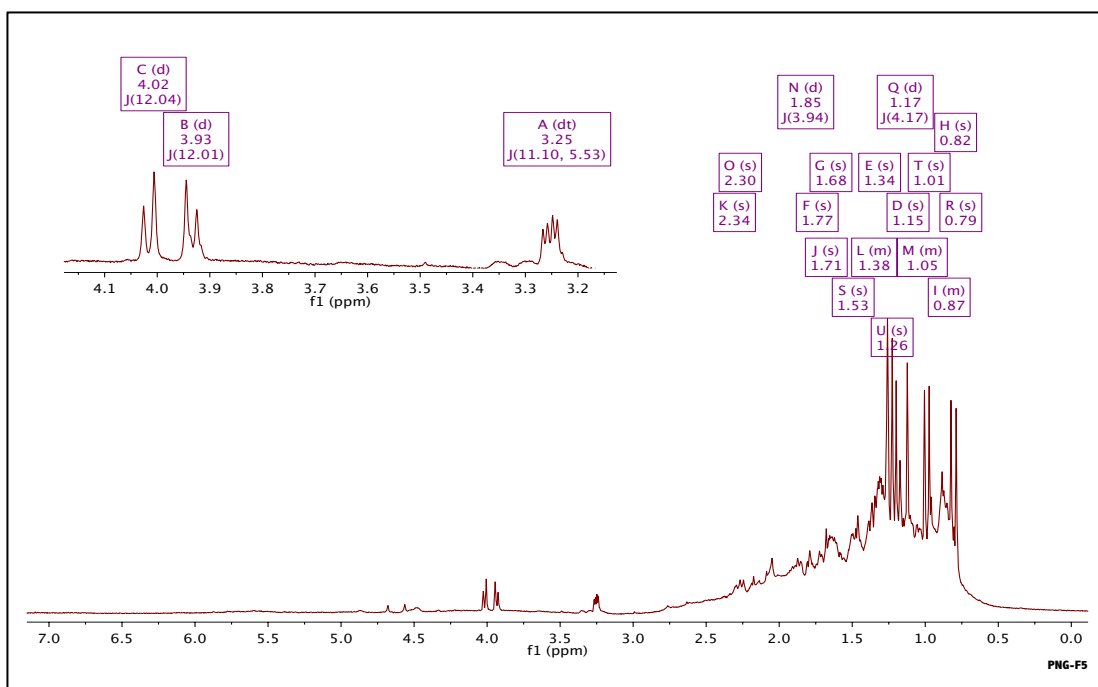
Figure 4-50: ¹H NMR (500 MHz) spectra of the compound (9) in CDCl₃
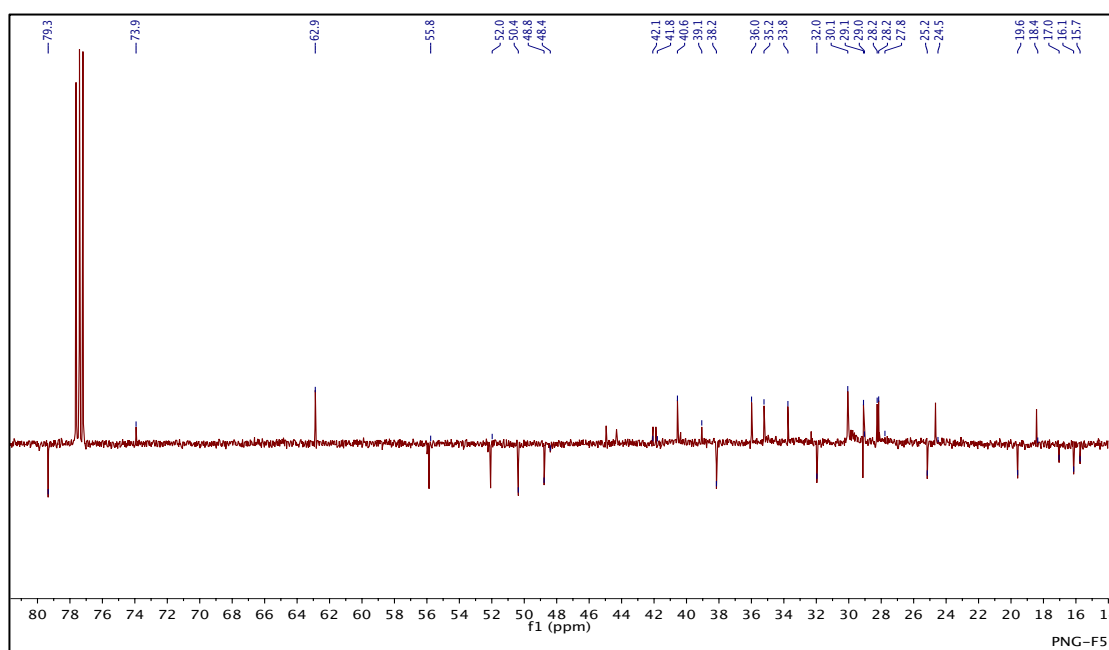
Figure 4-51: ¹³C NMR (100 MHz) spectra of compounds (9) in CDCl₃
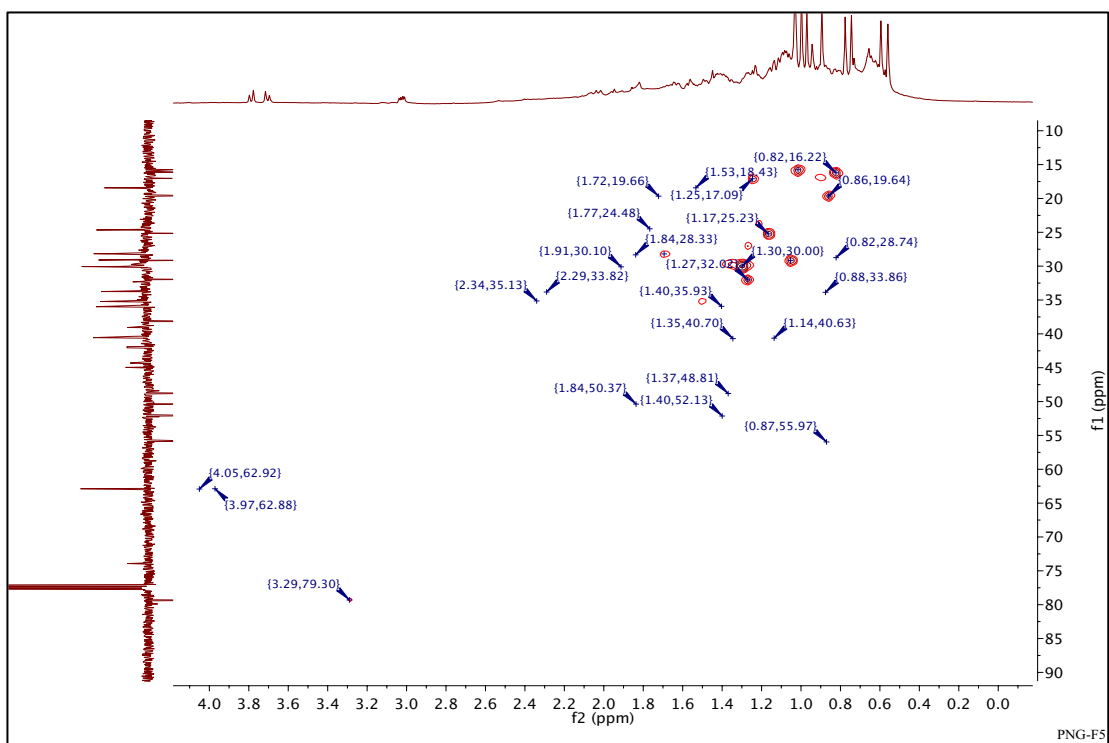
Figure 4-52: HSQC (500 MHz) Spectrum of compound (9) in CDCl₃
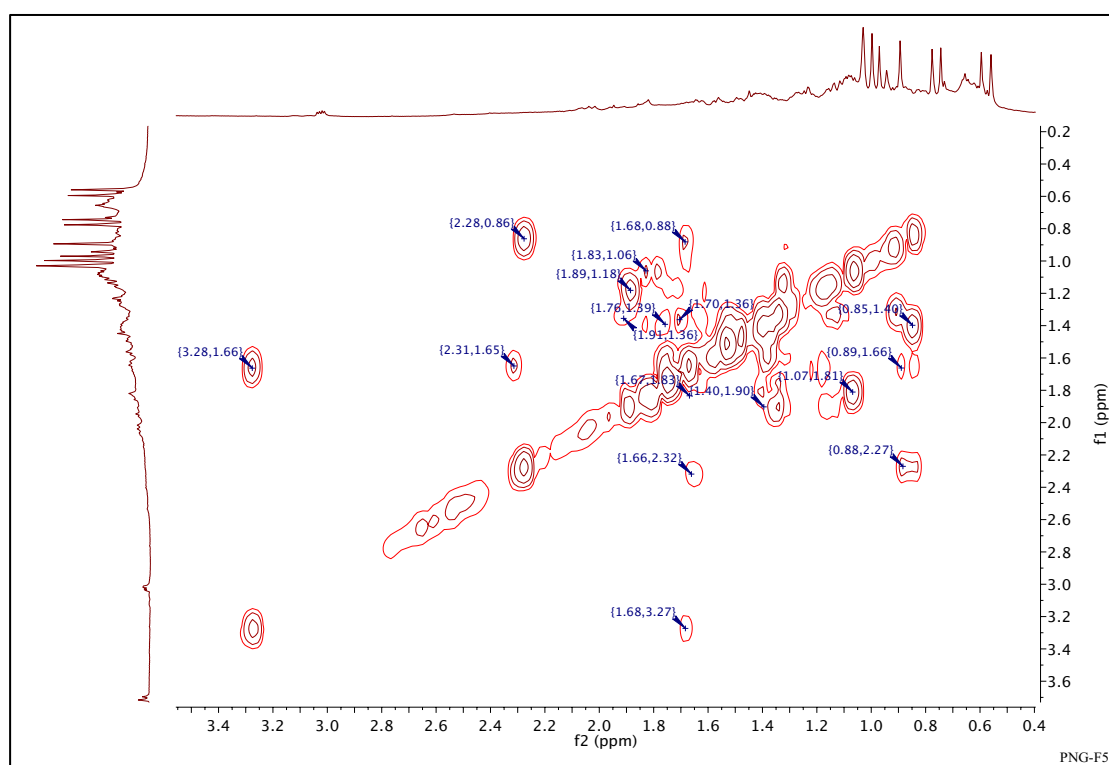
Figure 4-53: COSY (500 MHz) Spectrum of compound (9) in CDCl₃
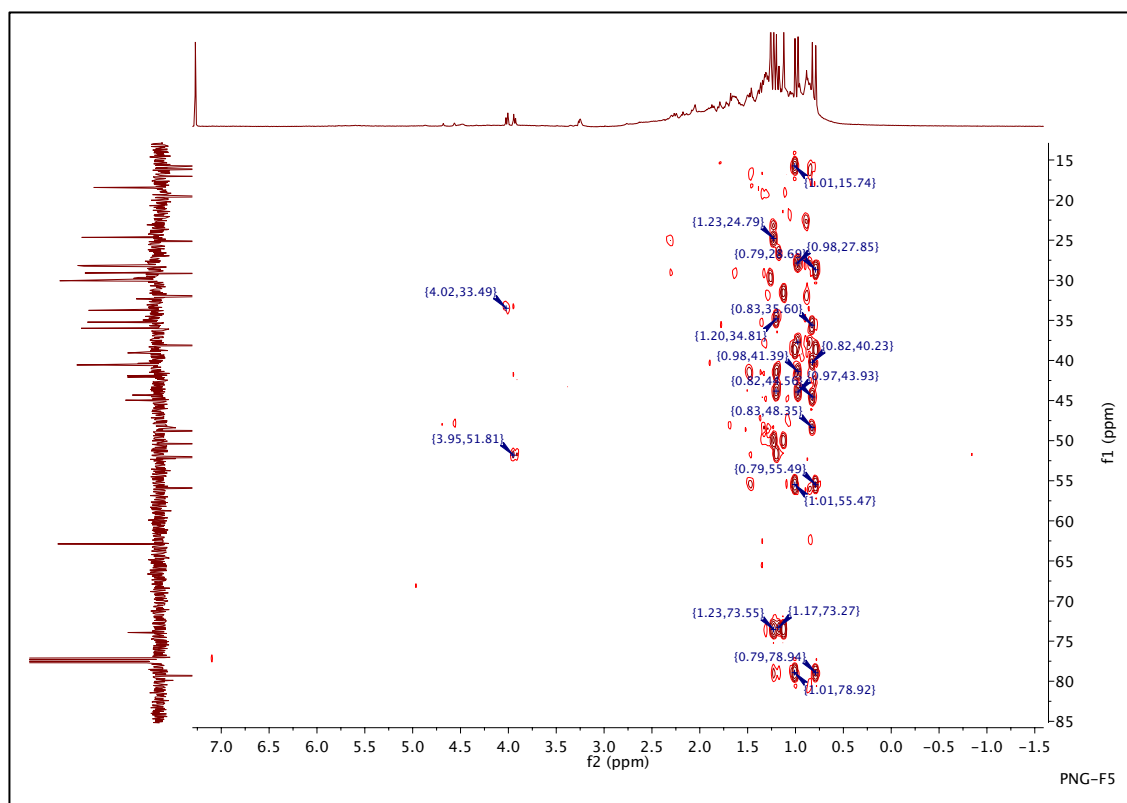
Figure 4-54: HMBC (500 MHz) Spectrum of compound (9) in CDCl₃

4.2.8.6 Characterisation of PNG-F4-11 as Betulin (Compound 10)

The compound had a retention time of 30.787 min in its LC-MS spectrum and an $[M+H]^+$ ion at m/z 443.3884, corresponding to $C_{30}H_{51}O_2$ (calc. 443.3889) and this established the molecular formula to be $C_{30}H_{50}O_2$ (**Figure 5-55**). This formula is typical of a triterpene (**Figure 5-56**). The ¹H NMR spectrum in **Figure 5-57** showed the presence of two vinyl methylene protons at δ_H (ppm) 4.68 (d, $J = 2.2$) and 4.58 (m) for H-29, a vinylic methyl at δ_H 1.68 (s) for H-30 and five tertiary methyl groups between δ_H 0.76-1.03 ppm. The H-3 and H-19 protons were observed at δ_H 3.19 (dd, $J = 11.4, 4.8$) and 2.38 (td, $J = 11.0, 5.8$) respectively. The ¹³C NMR **Figure 5-58** showed a total of 30 carbon atoms including six methyl groups, one hydroxymethylene group, one vinylic methylene, one quaternary olefinic and one hydroxymethyl carbon. No carbonyl carbon was observed. The compound retained all the spectral properties for compound **9** except for the absence of the hydroxyl group at C-20 and the presence of a vinyl group hence the compound must be betulin (**10**) (**Table 4-13**) and this was confirmed by comparison of the spectral data with literature reports (Tijjani et al., 2012).
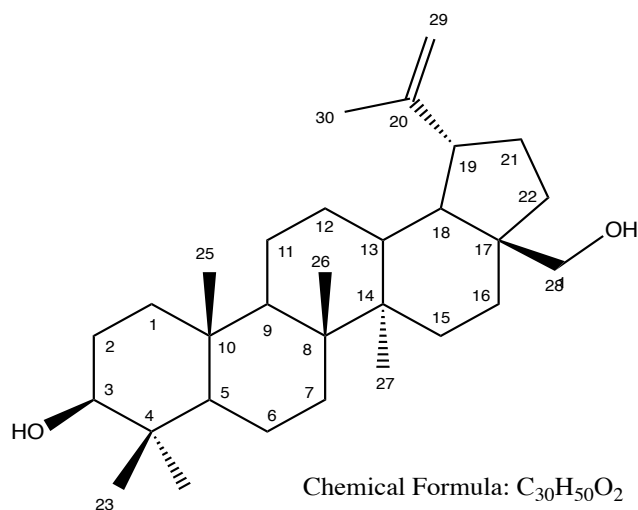
Figure 4-55: structure of betulin (10)
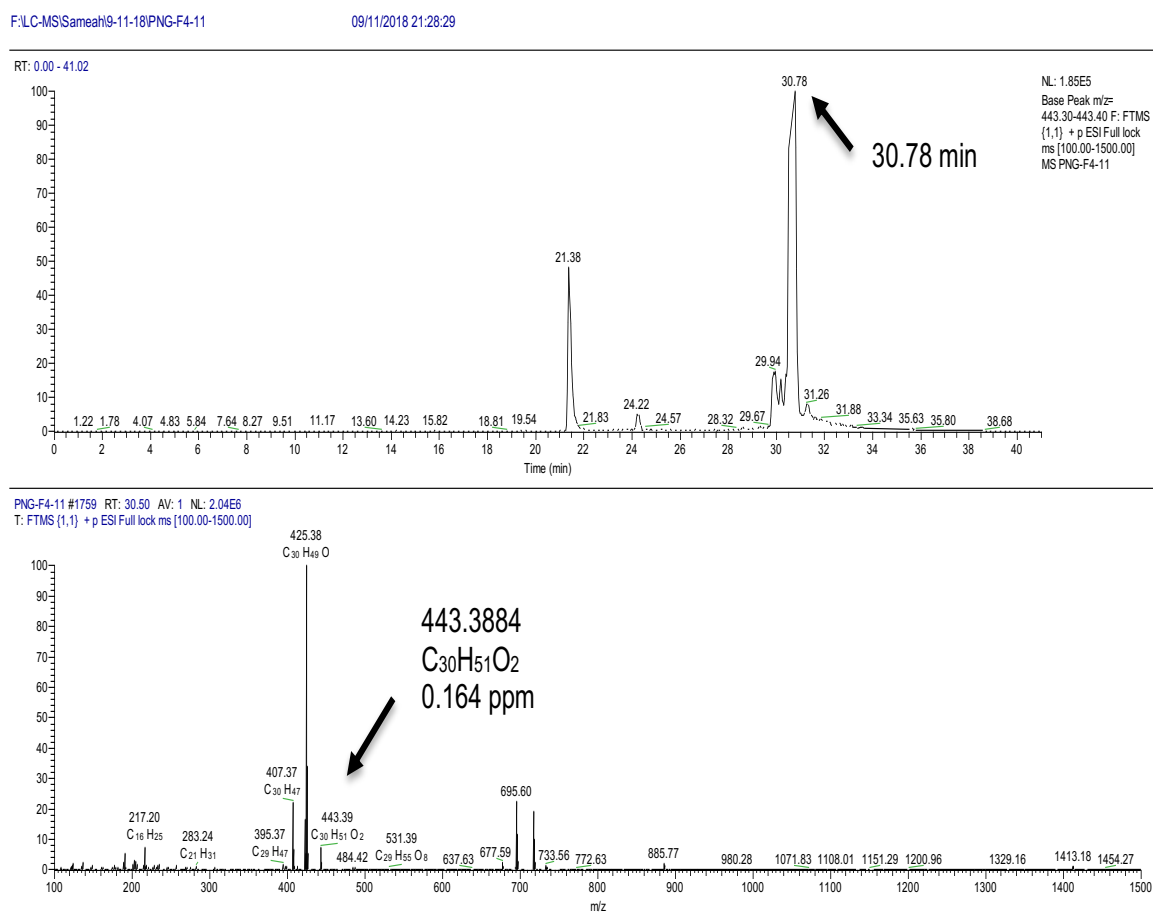
Figure 4-56: LC-MS chromatogram (ESI positive mode) for compound 10.

100

Table 4-13: ^{1}H (500MHz), ^{13}C (100MHz) data of compound (10)

Position	Compound	
	(10) **Betulin**	
	^{1}H δ ppm (mult, J (Hz))	**^{13}C δ ppm (mult)**
1	1.66 1H (m) 0.89 1H (m)	37.3 (CH$_2$)
2	1.57 1H (m) 1.07 1H (m)	28.0 (CH$_2$)
3	3.19 1H (dd, J = 11.4, 4.8)	79.0 (CH)
4	-	38.7 (C)
5	0.68 1H (m)	55.3 (CH)
6	1.52 1H (dt J = 11.1, 4.1) 1.41 1H (m)	18.4 (CH$_2$)
7	1.41 2H (m)	34.2 (CH$_2$)
8	-	38.9 (C)
9	1.27 1H (m)	50.4 (CH)
10	-	37.2 (C)
11	1.41 2H (m)	20.8 (CH$_2$)
12	1.66 1H (m) 1.07 1H (m)	25.2 (CH$_2$)
13	1.66 1H (m), 0.97 1H (m)	28.0 (CH)
14	-	40.9 (C)
15	1.61 1H (m), 1.07 1H (m)	27.1 (CH$_2$)
16	1.95 1H (m), 1.27 1H (m)	29.2 (CH$_2$)
17	-	42.7 (C)
18	1.57 1H (m),	48.8 (CH)
19	2.38 1H (td, J = 11.0, 5.8)	47.8 (CH)
20	-	150.5 (C)
21	1.41 1H (m), 1.20 1H (m)	29.8 (CH$_2$)
22	1.85 1H (ddd, J = 12.3, 8.5. 1.3) 1.07 1H (m)	34.0 (CH$_2$)
23	0.97 3H (s)	28.0 (CH$_3$)
24	0.76 3H (s)	15.4 (CH$_3$)
25	0.82 3H (s)	16.1 (CH$_3$)
26	0.98 3H (s)	16.0 (CH$_3$)
27	1.02 3H (s)	14.8 (CH$_3$)
28	3.80 1H (dd, J = 10.8, 1.9) 3.33 1H (d J = 10.6)	60.6 (CH$_2$)
29	4.68 1H (d J = 2.2) 4.58 1H (m)	109.7 (CH$_2$)
30	1.68 3H (s)	19.1 (CH$_3$)
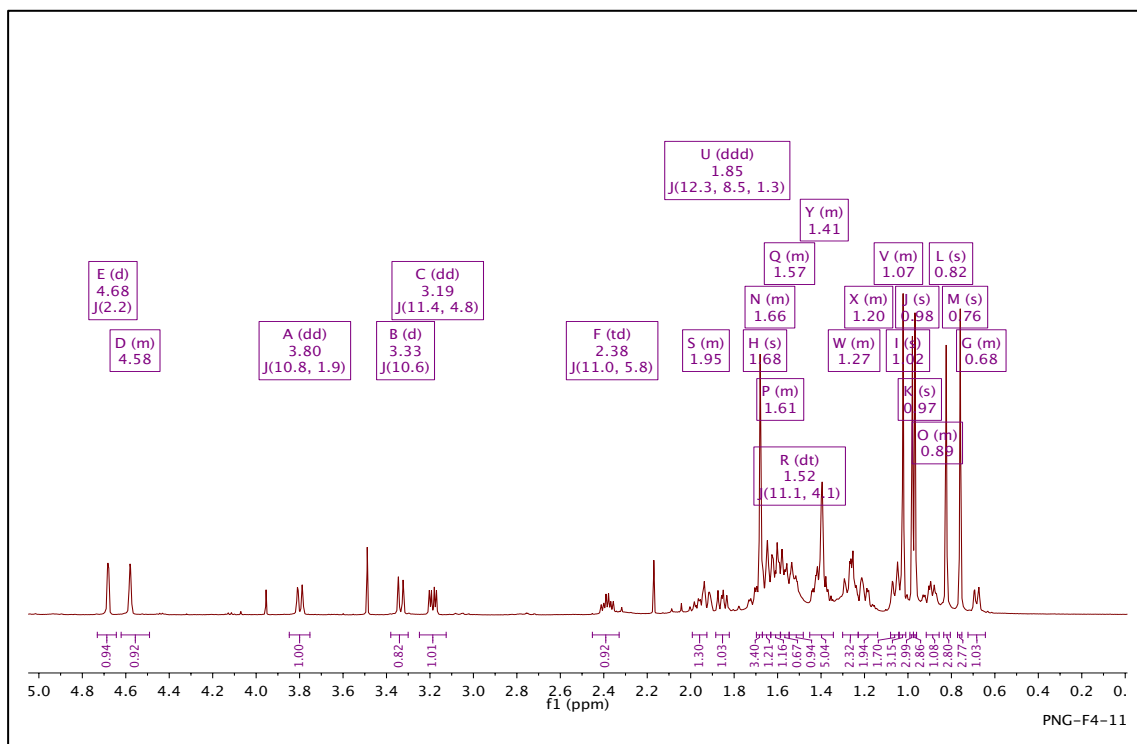
Figure 4-57: ¹H NMR (500 MHz) spectrum of compound 10 in CDCl₃
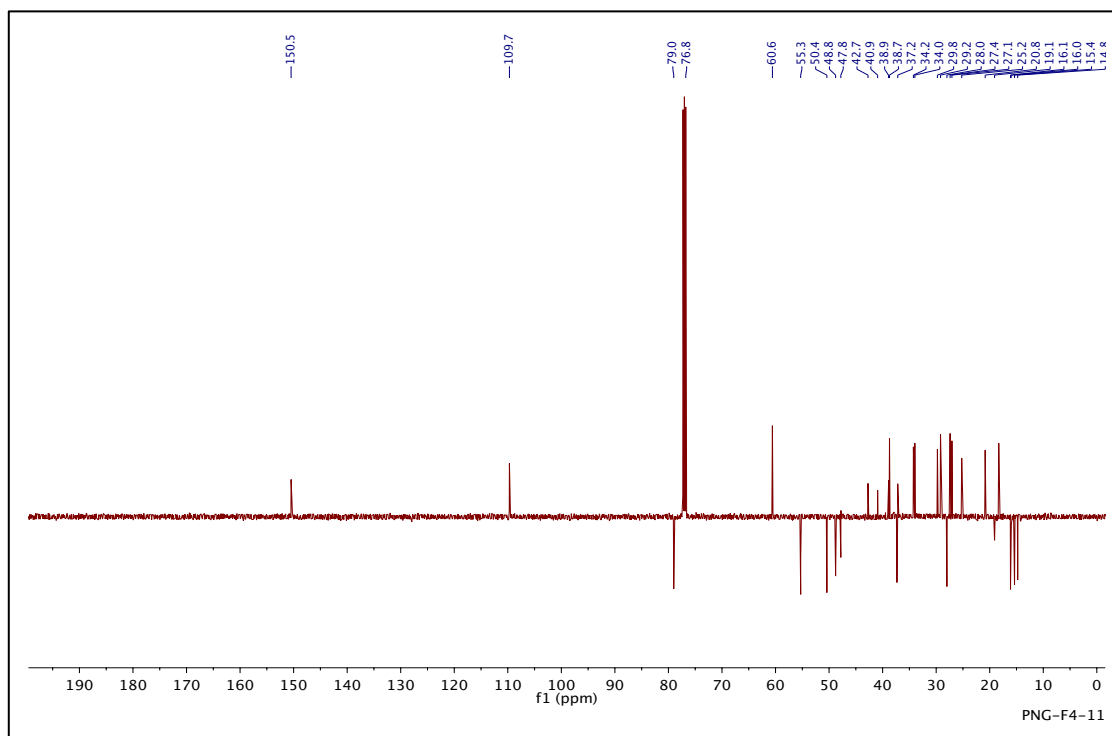
Figure 4-58: ¹³C NMR (100 MHz) spectrum of compound 10 in CDCl₃

4.2.8.7 Characterisation of PNG-F4-13 as Betulinic acid (11)

LC-MS data of fraction PNG-F4-13 gave a peak at Rt = 18.49 min and the ESI gave an $[M+H]^+$ at m/z 457.3675, corresponding to a formula $C_{30}H_{49}O_3$ (calc 457.3681), hence the molecular formula $C_{30}H_{48}O_3$ (**Figure 5-60**). The ^1H NMR spectrum in **Figure 5-61** showed the presence of two methylene protons at δ_H (ppm) 4.68 (d, J = 2.5 Hz) and 4.56 (d, J = 2.3 Hz) for H-29, a vinylic methyl at δ_H 1.64 (s) and five tertiary methyl groups between δ_H 0.65-0.93. Further, the spectrum showed signals for two protons at δ_H 2.95 (ddt, J = 16.5 Hz, 11.2 Hz, 5.6 Hz) attributable to H-3 and H-19. The DEPT ^{13}C NMR in **Figure 5-62** showed a total of 30 carbon atoms including six methyls, one hydroxymethine, one vinylic methylene, one quaternary carbon attached to the vinylic methylene and one carboxylic acid carbon at δ_C 177.2. It also showed a close similarity to compound (**10**) with little variations especially the absence of the oxymethylene carbon and protons at C-28 and the presence of a carboxylic acid carbon. The compound was therefore identified as betulinic acid (**11**) (**Figure 4-59**) by comparison of experimental data (**Figure 4-63**) with literature report (Prakash and Prakash, 2012). The chemical shifts for the protons and carbons were fully assigned as given in **Table 4-14.**
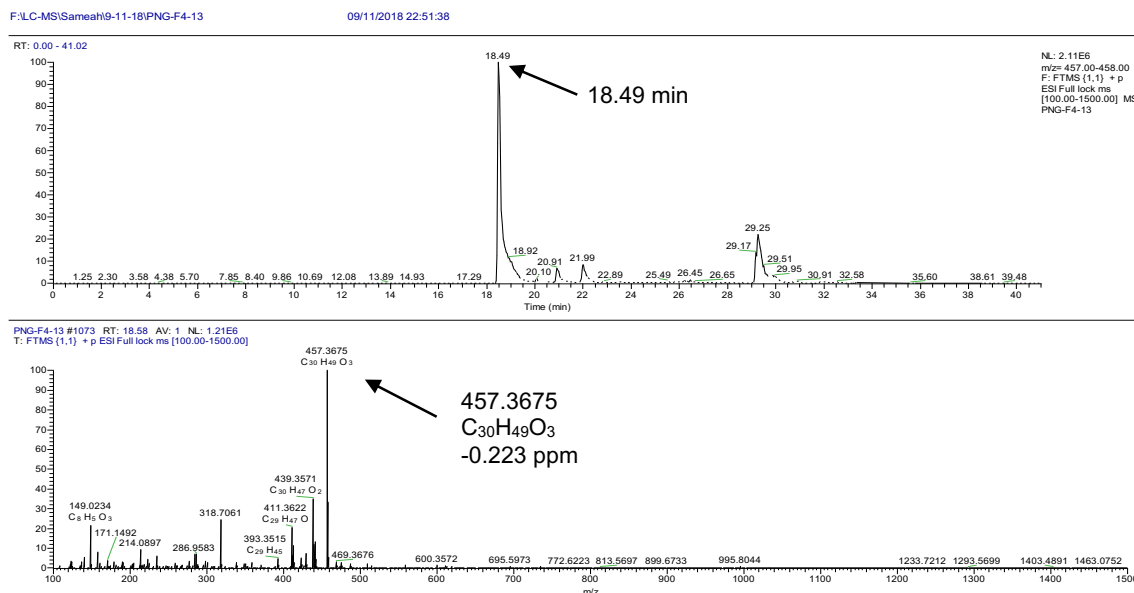
Figure 4-59: LC-MS chromatogram (ESI positive mode) for compound 11.

Chemical Formula: $C_{30}H_{48}O_3$
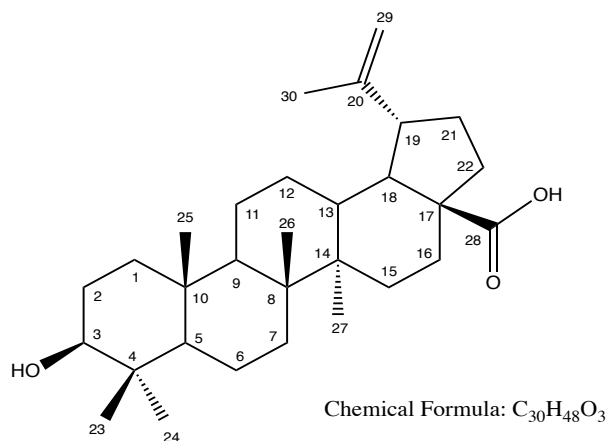
Figure 4-60: structure of betulinic acid (11)

Table 4-14: ^1H (500MHz), ^{13}C (100MHz) data of compound Betulinic acid (11) in fraction PNG-F4-13

Position	Compound	
	(11) **Betulinic acid**	
	^1H **δ ppm (mult, J (Hz))**	^{13}C **δ ppm (mult)**
1	1.57 1H (m) 0.81 1H (m)	38.3 (CH_2)
2	1.43 2H (m)	27.2 (CH_2)
3	2.95 1H (ddt, J = 16.5, 11.2, 5.6)	76.8 (CH)
4	-	38.5 (C)
5	0.62 1H (m)	54.9 (CH)
6	1.43 1H (m) 1.36 1H (m)	18.0 (CH_2)
7	1.36 2H (m)	33.9 (CH_2)
8	-	40.3 (C)
9	1.25 1H (dd, J = 12.7, 2.5)	49.9 (CH)
10	-	36.7 (C)
11	1.36 1H (m) 1.14 1H (m)	20.5 (CH_2)
12	1.57 1H (m) 1.09 1H (m)	25.1 (CH_2)
13	2.21 1H (td, J = 12.3, 3.5)	37.6 (CH)
14	-	42.0 (C)
15	1.79 1H (q, J = 8.2, 6.8), 1.31 1H (m)	30.1 (CH_2)
16	2.101H (m), 1.36 1H (m)	31.7 (CH2)
17	-	55.4 (C)
18	1.50 1H (d, J = 11.3)	46.6 (CH)
19	2.95 1H (ddt, J = 16.5, 11.2, 5.6)	48.6 (CH)
20	-	150.4 (C)
21	1.31 1H (m), 1.08 1H (m)	29.2 (CH_2)
22	1.79 1H (q, J = 8.2, 6.8) 1.43 1H (m)	36.3 (CH_2)
23	0.86 3H (s)	28.1 (CH_3)
24	0.65 3H (s)	15.7 (CH_3)
25	0.76 3H (s)	16.0 (CH_3)
26	0.86 3H (s)	15.8 (CH_3)
27	0.93 3H (s)	14.5 (CH_3)
28	-	177.2 (C)
29	4.68 1H (d, J = 2.5) 4.56 1H (s)	109.6 (CH_2)
30	1.64 3H (s)	19.0 (CH_3)
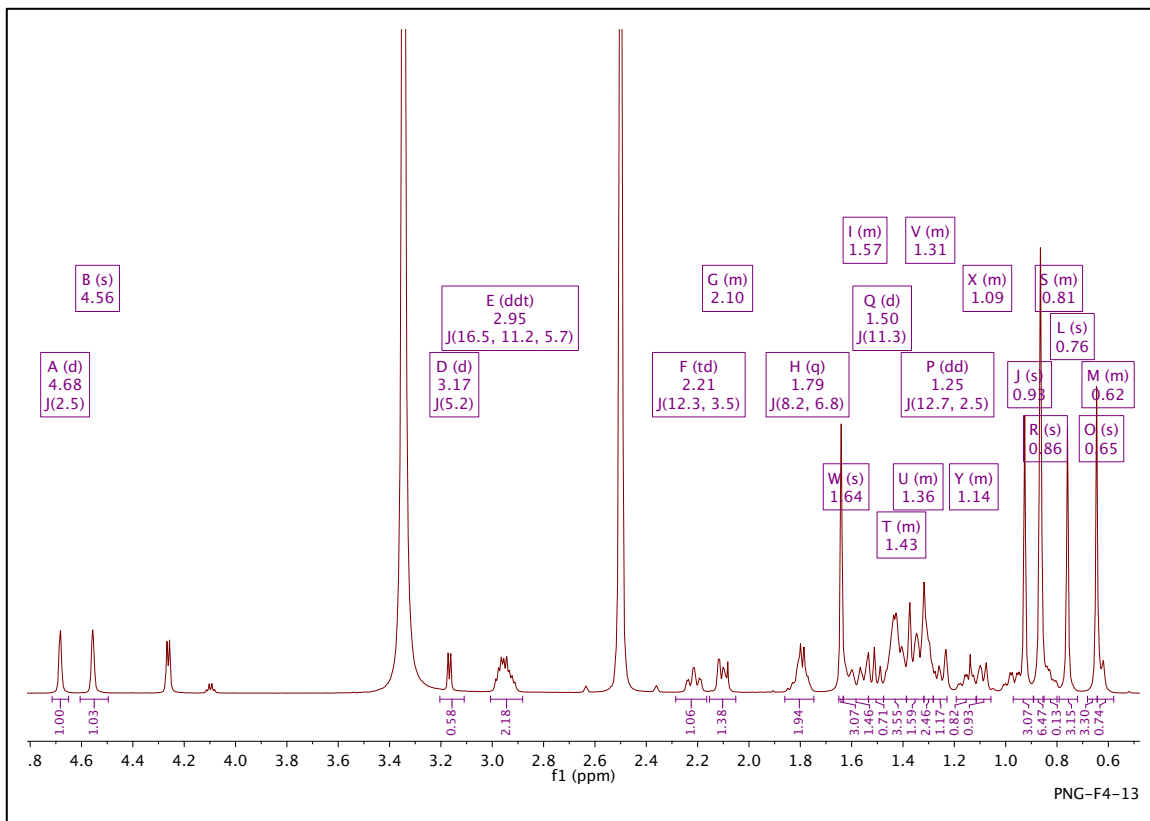
Figure 4-61: ^{1}H NMR (500 MHz) spectrum of compound 11 in DMSO-d_6
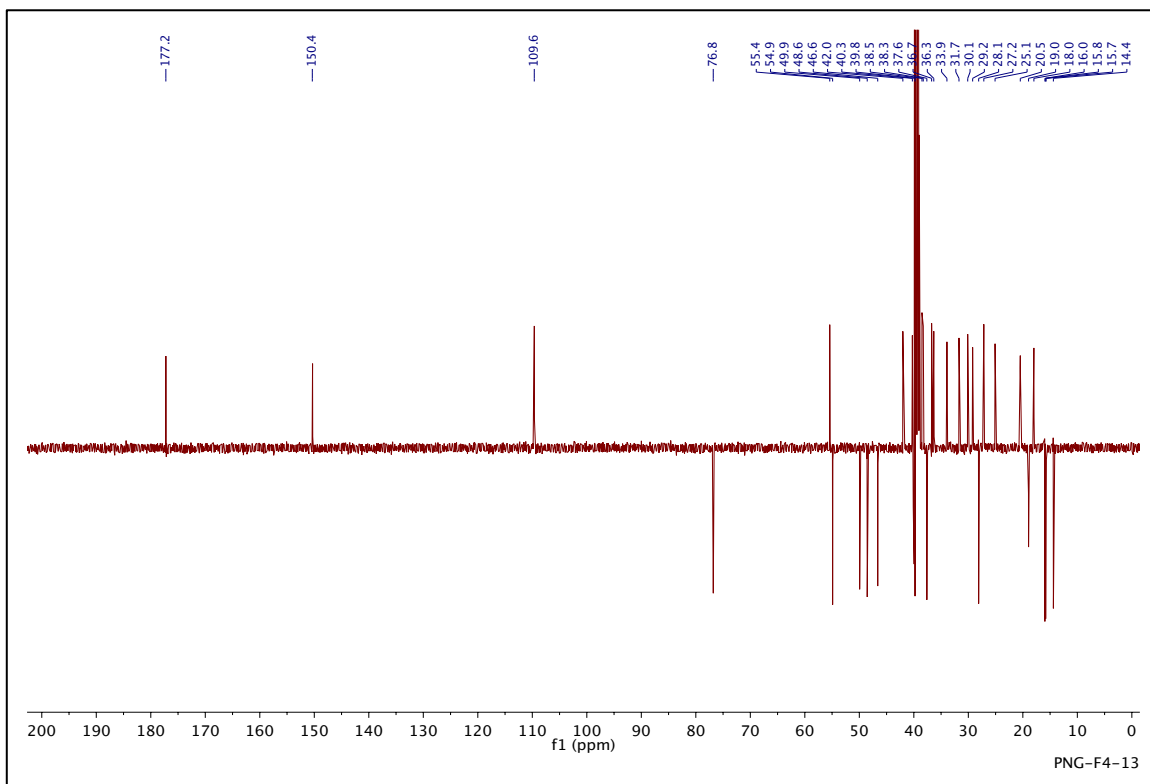
Figure 4-62: ^{13}C NMR (100 MHz) spectrum of compound 11 in DMSO-d_6
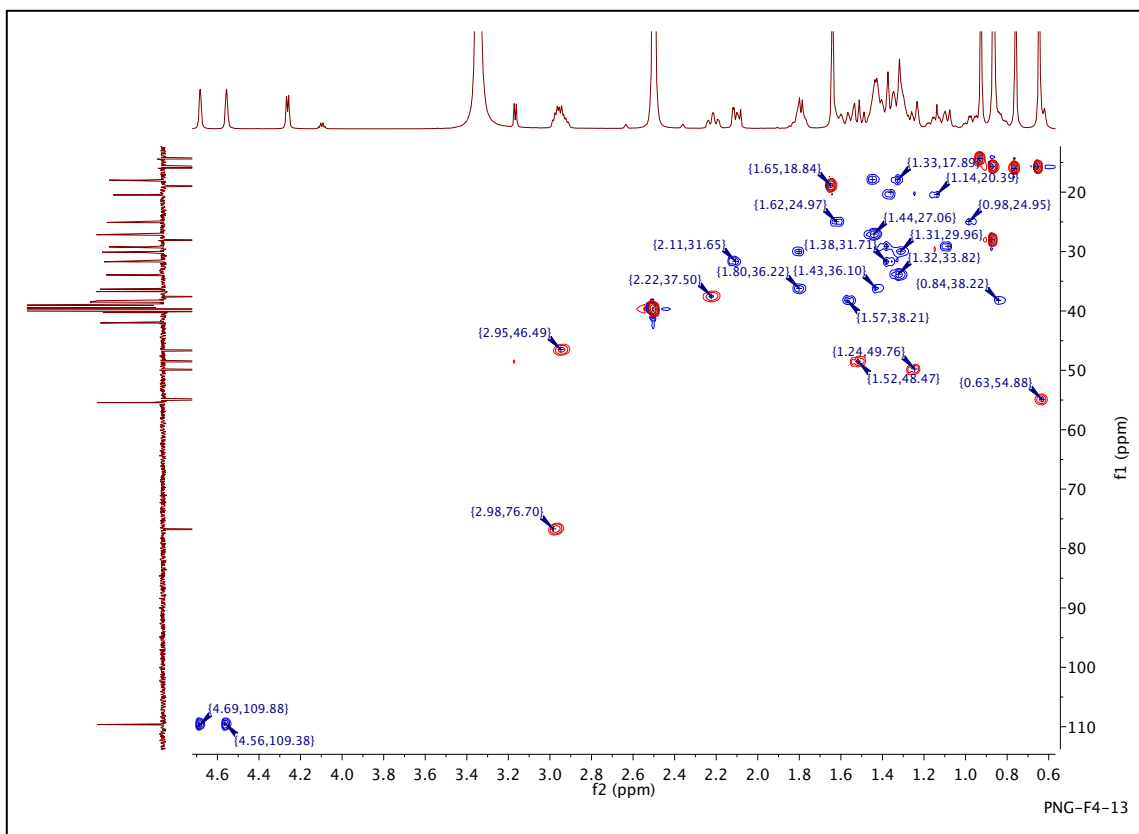
Figure 4-63: HSQC (500 MHz) Spectrum of compound 11 in DMSO-*d₆*

4.2.8.8 Characterization of PNG-F4-18 as Madecassic acid (12)

Based on the high-resolution mass spectral data (**Figure 4-65**), the ESI peak at 14.31 (min) in negative mode was found at m/z 503.3378 [M-H]⁻ $C_{30}H_{47}O_6$., (calcd. 503.3373 g/mol). corresponding to the molecular formula $C_{30}H_{48}O_6$. Its IR spectrum in **Figure 5-66** showed absorption bands at (3560, 3180 cm-1) and (1726, 1646 cm-1), ascribable to hydroxyl and carboxyl functions, respectively. There was also an absorption stretch at 1260-1050 cm⁻¹ that indicating the presence of C–O. The ¹³C- DEPT NMR spectra showed six signals for methyl carbons, ten methylenes, seven methines, and six quaternary carbons, together with a carboxyl group. A total of 30 carbon resonances were observed, which confirmed its triterpenic nature (**Figure 4-68**). The following NMR data suggested the structural features of madecassic acid, contained six methyl signals two of the signals were observed as doublets at δ_H 0.91 (3H, d, J = 5.9 Hz) for H-30 and 0.82 (3H, d, J = 6.4 Hz) for H-29, and four singlets at δ_H 0.91, 0.99, 1.00 and δ_H 1.28. The spectrum also showed signals at δ_H 3.51 (m), and δ 3.11 (d, J = 9.4 Hz) ascribable to the H-2- and H-3 protons on carbons bearing a hydroxyl function, respectively.

Another doublet at δ_H 3.20 (d, J = 10.5) on another carbon bearing a hydroxyl function, indicated the presence of a –CH₂OH function (**Figure 4-67**). The carbonyl carbon resonance was at δ_C 180.1 ppm (C-28). The chemical shifts of C-4 and Me-24 led to placement of the -CH₂OH at the C-23 position. **Figure 4-70** shows the HMBC correlations between H-30 with C-19 and C-21, H-29 and C-18, C-19, C-20, H-18 with C-13, C-12, C-20, C-21 and C-28, H-3 and C-2, C-4, C-23, C-24. Thus 1H- and 13C-NMR spectra were completely assigned by detailed 2D-NMR experiments (**Figures 4-67** to **4-70**), which confirmed that compound **12** was madecassic acid (**Figure 4-64**). The chemical shifts for the compounds were confirmed using literature reports (Matsuda et al., 2001). This compound was first reported in 1967 and was isolated and identified from *Centella asiatica* (Boiteau and Chanez, 1967). The chemical shifts for the protons and carbons were fully assigned as given in **Table 4-15.**

Chemical Formula: $C_{30}H_{48}O_6$

madecassic acid

Figure 4-64: structure of medecassic acid

Figure 4-65: LC-MS chromatogram (ESI negative mode) for compound 12.

Figure 4-66: Infrared Spectrum of PNG-F4-18 was consitent with compound 12 being madecassic acid

Table 4-15: ^{1}H (500MHz), ^{13}C (100MHz) data of madecassic acid (12)

Position	Compound	
	(12) **Madecassic acid**	
	^{1}H δ ppm (mult, *J*, (Hz))	**^{13}C δ ppm (mult)**
1	0.71 1H, (t, *J* = 11.9) 1.72 1H (dd, *J* = 12.5, 4.6)	49.2 (t)
2	3.51 (1H, m)	67.5 (d)
3	3.11 (1H, d, *J* = 9.4 Hz)	76.2 (d)
4	-	43.4 (s)
5	1.15 1H (d, *J* = 1.8 Hz)	47.0 (d)
6	4.25 (1H, m)	65.9 (CH)
7	1.58 (1H, m), 1.37 (1H, m)	40.0 (CH$_2$)
8	-	42.2 (C)
9	1.52 (1H, m)	47.3 (CH)
10	-	38.3 (C)
11	1.95 1H (m), 1.52 1H (m)	23.4 (CH$_2$)
12	5.17 (q, 4.2)	124.9 (CH)
13	-	137.7 (C)
14	-	42.6 (C)
15	1.87 1H, (m) 0.95 1H, (t, *J* = 11.9)	28.1 (CH$_2$)
16	1.95 1H (m), 1.02 1H (m)	23.8 (CH$_2$)
17	-	49.2 (C)
18	2.12 (m)	52.6 (CH)
19	1.31 1H (m)	38.5 (CH)
20	1.31 1H (m)	38.5 (CH)
21	1.43 1H (m) 1.31 1H (m)	30.2 (CH$_2$)
22	1.37 (1H, m), 0.91 (1H, m)	38.8(CH2)
23	3.51 1H (m), 3.20 1H (d, *J* = 10.5)	63.7 (t)
24	0.91 (3H, s)	15.0 (CH$_3$)
25	1.00 (3H, s)	18.3 (CH$_3$)
26	1.28 (3H, s)	18.2 (CH$_3$)
27	0.99 (3H, s)	18.3 (CH$_3$)
28	-	178.3 (C)
29	0.82 (3H, d, *J* = 6.4 Hz)	17.1 (CH$_3$)
30	0.91 (3H, d, J = 5.9 Hz)	21.1 (CH$_3$)
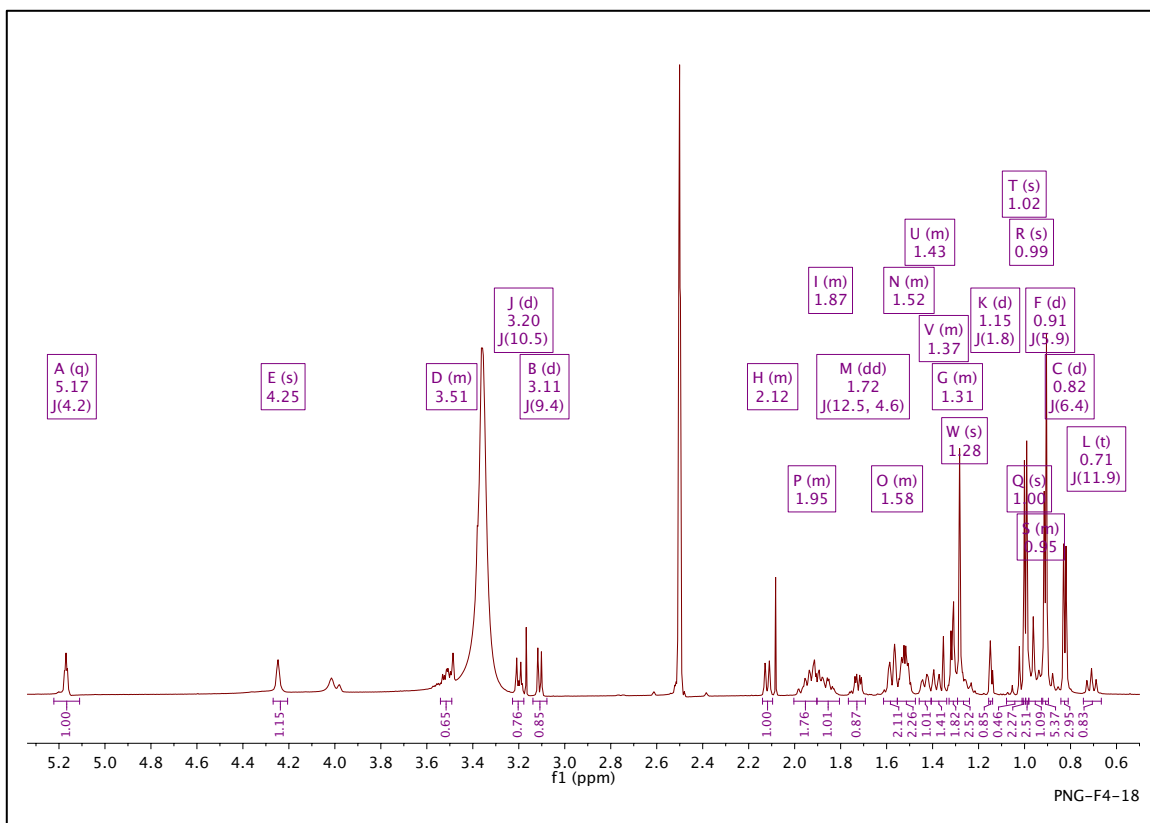
Figure 4-67: ^{1}H NMR (500 MHz) spectrum of compound 12 in DMSO-d_6.
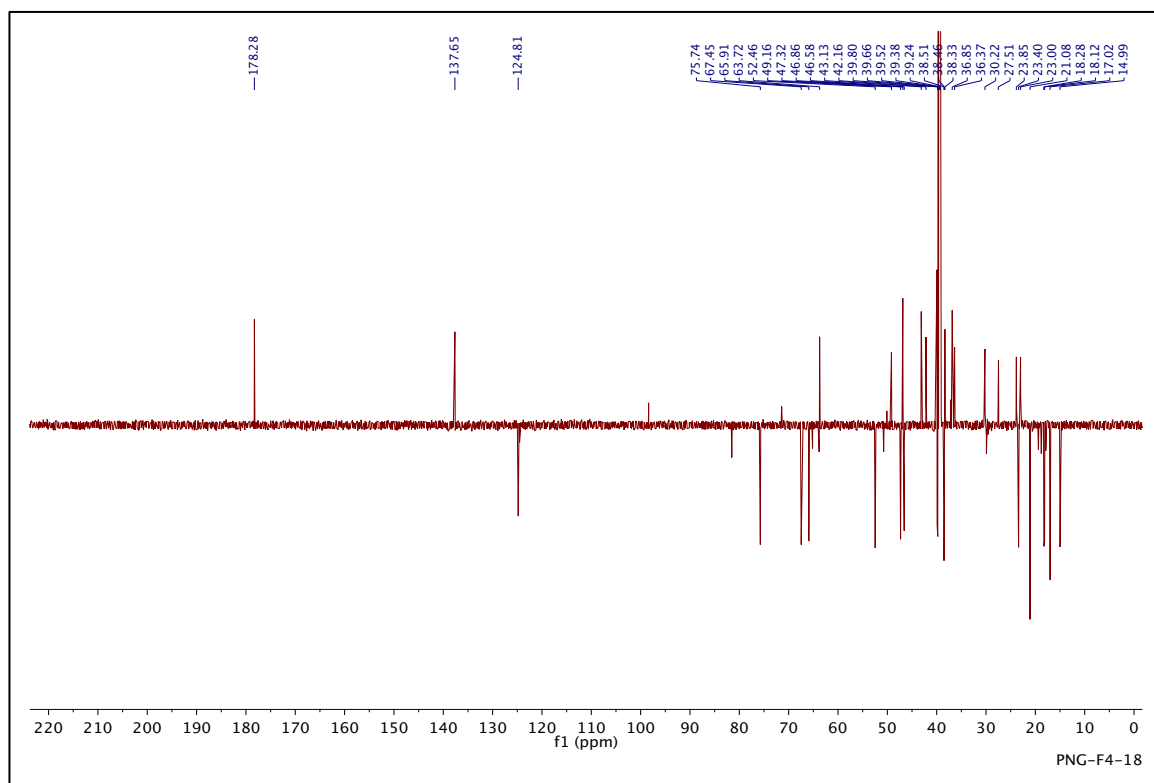
Figure 4-68: ^{13}C NMR (100 MHz) spectrum of compound 12 in DMSO-d6.
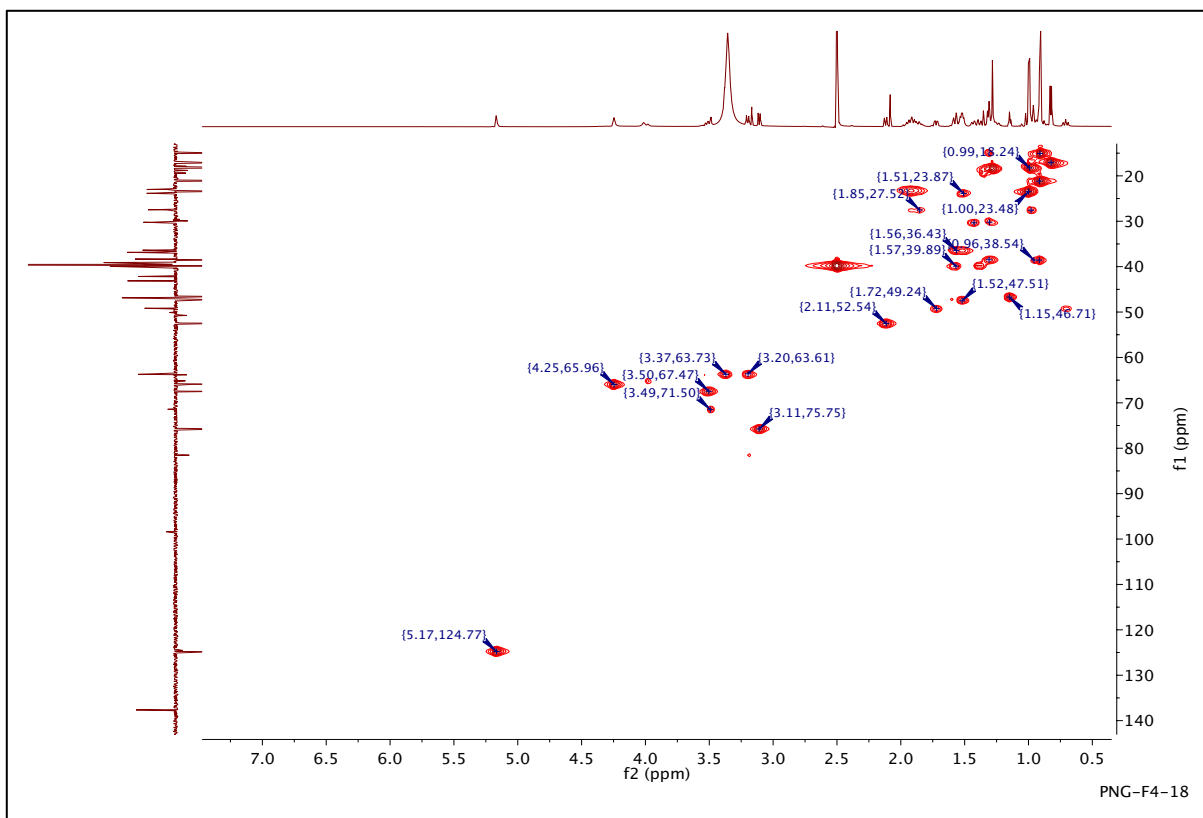
Figure 4-69: HSQC (500 MHz) Spectrum of compound 12 in DMSO-*d₆*
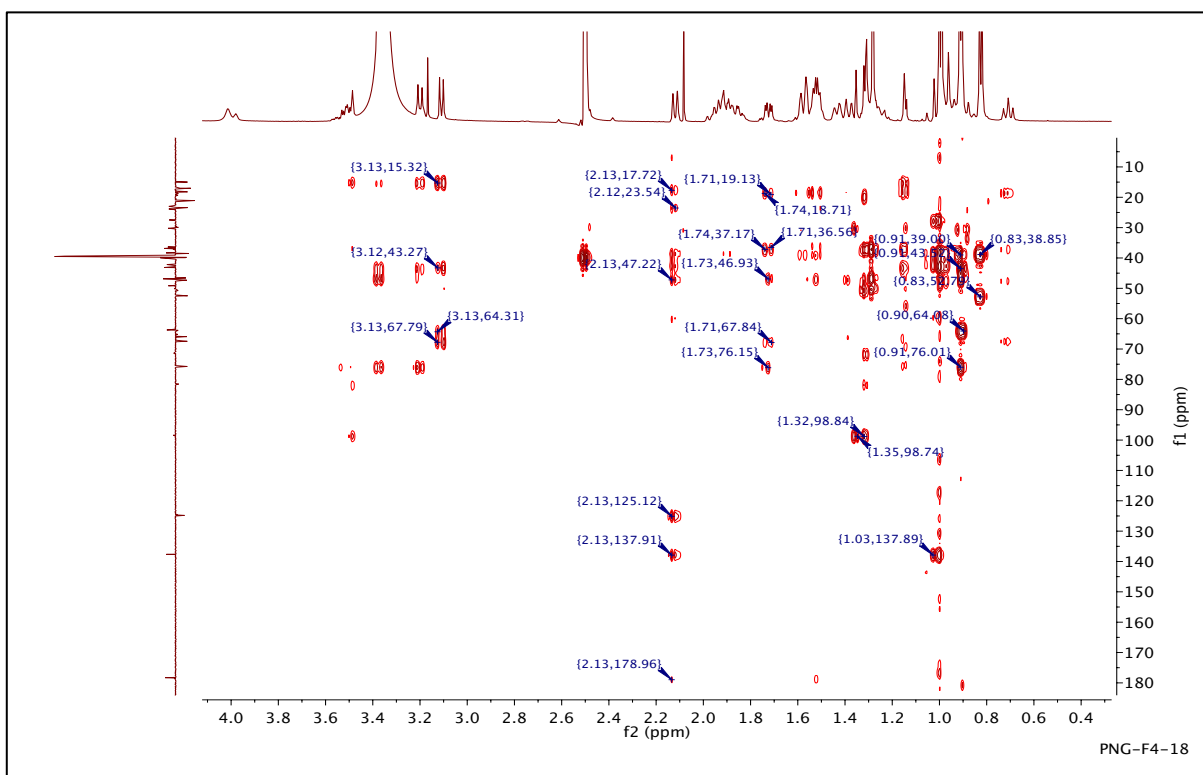
Figure 4-70: . HMBC (500 MHz) Spectrum of compound 12 in DMSO-*d₆*

4.2.9 *In vitro* studies of the PNG propolis fractions using wild type *T. b. brucei s427* and the derived, multi-drug resistant clone *B48*

The *in vitro* activity of the PNG purified compounds on wild-type *T. b. brucei* s427 and the derived, multi-drug resistant clone *B48* was determined in three independent resazurin-based drug sensitivity assays as shown in **Table 4-16**. Like the extract fractions tested above (**section 4.3**), none of the purified compounds showed reduced activity against the drug resistant strain B48 (RF<1), therefore they were not cross resistant to pentamidine. The drug sensitivity of PNG purified compounds didn't show significant differences between the two strains apart from PNG-F5 which was significantly more active against *B48* with RF= 0.47 and p = 0.0003 (p<0.05). However, the RF for pentamidine was 145.34 and the P value was 0.00001.

The fractions such as PNG-F6-S12, PNG-F6-S15 and PNG-F1-5B that were composed of two or more known compounds and showed moderate activity, so there was no point in further separation. It was previously reported that both compounds 1 and 5 had been isolated as single compounds from Nigerian propolis and tested against WT *T. b brucei* showed EC_{50} of 11.6 and 18.5 µg/mL, respectively (Omar et al., 2017). Besides, we also reported the isolation of compound 1 and 4 from Libyan propolis and performed preliminary tests against WT *T. b. brucie.* showed EC_{50} of 14.6 and 3.7 µg/mL, respectively (Siheri et al., 2019).

Table 4-16: EC_{50} values of purified compounds isolated from PNG propolis on *T. brucei. S427* wild-type, and B48 (n=3).

Purified compounds	T. brucei S427WT				T. brucei B48 (Pentamidine Resistance)					
	AVG of EC_{50} (µg/mL)	AVG of EC_{50} (µM)	SD	%RSD	AVG of EC_{50} (µg/mL)	AVG of EC_{50} (µM)	R. F	t-test	SD	RSD %
PNG-F5 (**9**)	2.04	4.44	0.1121	5.49	0.97	2.09	0.47	0.0003	0.1115	11.55
PNG-F6-S12 (**1** and **5**)	15.97	-	1.4706	9.21	11.29	-	0.71	0.0508	2.5420	22.52
PNG-F6-S15 (**2** and **6**)	13.52	-	0.8418	6.22	12.35	-	0.91	0.1247	0.6207	5.02
PNG-F6-S17 (**3**)	13.63	28.84	1.4533	10.66	11.82	25.00	0.87	0.3330	2.4607	20.82
PNG-F1-5B (**4,7** and **8**)	18.45	-	0.7193	3.90	17.60	-	0.95	0.2114	0.6755	3.84
PNG-F4-11 (**10**)	26.61	60.12	2.6934	10.12	22.34	50.47	0.84	0.1337	2.8750	12.87
PNG-F4-13 (**11**)	24.23	53.05	2.6417	10.90	19.57	42.85	0.81	0.0610	1.6632	8.50
PNG-F4-18 (**3**)	18.16	35.98	1.8086	9.96	16.02	31.74	0.88	0.2327	1.9150	11.95
Pentamidine	-	0.0043	0.0020	47.3	-	0.62	145.34	0.0005	0.1027	16.48

AVG of EC_{50} =average of half maximal effective concentration, average of at least 3 independent determinations. SD= Standard deviation of all determinations. RSD%= Relative Standard Deviation= (SD/ Avg.) x100. RF= Resistance factor. Statistical significance was determined using an unpaired two-tailed Student's t-test comparing E_{C50} value of the resistant strain with that of the same sample for the control strain s427. Pentamidine and Diminazen aceturate, both are known trypanocides.

4.2.10 Activity of PNG propolis and its fraction against Trypanosoma congolense and diminazene resistant strains of *T. congolense* strain 6C3 (*In vitro*).

The PNG purified fractions were also tested on *T. congolense* and diminazene resistant strains of *T. congolense* strain *6C3*. the results are presented in the **Table 4-17**. The PNG purified fractions displayed moderate against *T. congolense.* The EC_{50} values for diminazene resistant strains of *T. congolense* strain *6C3* were within 1~fold ($P > 0.05$), thus the compounds were not cross-resistant with first-line AAT treatments diminazene. The RF for diminazene, included as control, was 74.38 ($P = 0.0006$; **Table 4-17**). Like the fractions tested above **(section 4.4)**, the purified compounds displayed less potent activity against *T. congolense* than against *T. brucei* under the assay conditions

Table 4-17: EC$_{50}$ values of purified compounds isolated PNG propolis on T. congolense IL300, and *T. congolense* resistance to diminazene (n=3).

Samples	Trypanosoma congolense IL300				Trypanosoma congolense Diminazene Resistance					
	AVG of EC_{50} (µg/mL)	AVG of EC_{50} (µM)	SD	%RSD	AVG of EC_{50} (µg/mL)	AVG of EC_{50} (µM)	R. F	t-test	SD	RSD %
PNG-F5 **(9)**	5.77	14.38	1.2826	22.22	2.8	6.087	0.48	0.017	0.3252	11.76
PNG-F6-S12 **(1** and **5)**	14.23	-	2.7534	19.35	16.86	-	1.18	0.3989	3.9673	23.54
PNG-F6-S15 **(2** and **6)**	13.74	-	2.7575	20.07	13.21	-	0.96	0.8297	2.8250	21.38
PNG-F6-S17 **(3)**	16.67	35.25	3.4860	20.92	15.69	33.20	0.94	0.7542	3.6231	23.09
PNG-F1-5B **(4,7** and **8)**	18.93		2.8966	15.30	19.51		1.03	0.8488	4.0011	20.51
PNG-F4-11 **(10)**	21.52	70.11	3.1522	14.65	22.10	49.92	1.03	0.8397	3.4607	15.66
PNG-F4-13 **(11)**	17.21	44.47	2.9270	17.01	18.12	28.53	1.05	0.7547	3.7336	20.60
PNG-F4-18 **(3)**	22.62	67.62	3.2455	14.35	19.82	59.06	0.88	0.4831	5.3691	27.09
Diminazene	-	0.0534	0.0106	19.86	-	4.68	74.38	0.0006	0.81	17.29

4.2.11 *In vitro* cells viability studies of PNG extract and its fractions on U937 human cells and RAW 246.7 murine cells

Table 4-18: IC$_{50}$ of Cytotoxicity of PNG propolis sample and its fractions against U937 cell line and RAW 246.7 cell line.

Samples	U937			RAW 246.7		
	Mean of IC$_{50}$ (µg/mL)	SD	RSD%	Mean of IC$_{50}$ (µg/mL)	SD	RSD%
20-PNG	116.30	5.70	4.90	126.27	8.91	7.06
PNG-F1	83.26	11.08	13.31	70.31	3.30	4.69
PNG-F2	135.10	20.08	14.86	110.27	12.15	11.02
PNG-F3	84.87	4.95	5.83	88.40	5.85	6.62
PNG-F4	40.08	1.50	3.74	68.37	3.28	4.79
PNG-F6	84.35	9.51	11.28	81.11	2.42	2.99
PNG-F7	57.96	6.84	11.81	93.05	5.25	5.64
PNG-F8	95.63	2.31	2.42	104.40	13.48	12.91
PNG-F9	45.89	2.01	4.38	65.62	5.31	8.09
PNG-F10	53.43	5.21	9.75	81.05	8.14	10.04

Table 4-19: IC$_{50}$ of cytotoxicity of isolated purified compounds from PNG propolis against U937 cell line and RAW 246.7 cell line.

Samples	U937				RAW 246.7			
	Mean of IC$_{50}$ (µg/mL)	Mean of IC$_{50}$ (µM)	SD	RSD%	Mean of IC$_{50}$ (µg/mL)	Mean of IC$_{50}$ (µM)	SD	RSD%
PNG-F5 **(9)**	46.97	102.0	9.63	20.50	112.84	244.9	15.54	13.77
PNG-F6-S12 **(1** and **5)**	107.05	N/A	9.55	8.92	150.80	N/A	5.99	3.97
PNG-F6-S15 **(2** and **6)**	145.80	N/A	12.30	8.44	110.33	N/A	11.51	10.44
PNG-F6-S17 **(3)**	122.95	260.1	7.42	6.04	118.70	251.1	5.31	4.47
PNG-F1-5B **(4,7** and **8)**	92.70	N/A	6.24	6.73	109.03	N/A	10.21	9.36
PNG-F4-11 **(10)**	55.80	126.0	4.34	7.78	115.40	260.7	21.09	18.27
PNG-F4-13 **(11)**	51.65	113.1	4.85	9.38	94.79	207.6	6.43	6.79
PNG-F4-18 **(3)**	90.73	179.8	5.50	6.06	103.48	205.0	7.69	7.43

The PNG crude extract, fraction and purified compounds were tested for their effects on human cell line U937 and murine RAW 246.7 cell line to determine whether the antiprotozoal activity is the result of general toxicity or is more specifically antiprotozoal. The toxicity assays showed that the PNG showed low toxicity to these cell lines. In this experiment the IC$_{50}$ value of PNG-crude on U937and Raw246.7 was found to be 116.30 and 126.27 (µg/mL), respectively. Thus,

PNG-crude appears to be non-toxic at a concentration of 100 μg/ mL and below, although higher doses are partially toxic. The IC_{50} of compound 9, which was the most active against trypanosomes, was 47 μg/mL. All the samples expressed an acceptable RSD% value in the bioassay validation ≤ 25% (Little, 2016). From the results and **Table 4-17**, we conclude that the crude sample had more activity than most the purified compounds, apart from compound 9, and also had a higher selectivity index.

Table 4-20: Comparison of the average ratio of EC_{50} of PNG propolis extracts against Trypanosoma spp. and Selectivity Index (SI) on U937 and RAW 246.7

Samples	Ratio EC_{50}(Tbb)/ EC_{50}(T.c)	P Value	Ratio EC_{50}(Tbb)/ EC_{50}(C.f)	P Value	Ratio IC_{50}(U937)/ IC50(RAW 246.7)	P Value	SI on U937 IC_{50} value / EC_{50}(Tbb	SI on RAW246.7 IC_{50} value / EC_{50}(T.C
20-PNG	1.13	0.0670	0.1930	$2.0 X10^{-5}$	0.9211	0.1782	29.00	37.25
PNG-F1	0.44	0.2456	0.4642	$1.6 X10^{-2}$	1.1842	0.1336	8.13	5.22
PNG-F2	0.86	0.1005	0.4327	$3.9 X10^{-4}$	1.2251	0.1727	9.10	9.66
PNG-F3	0.51	0.1295	0.2902	$7.61X10^{-5}$	0.9601	0.5375	10.41	7.70
PNG-F4	0.21	0.0102	0.1947	$4.5 X10^{-4}$	0.5862	0.0016	9.90	6.54
PNG-F5 **(9)**	0.17	0.0074	0.0872	$3.0 X10^{-4}$	0.4163	0.0138	22.98	19.56
PNG-F6	0.23	0.0115	0.0910	$4.5 X10^{-5}$	1.0399	0.5862	17.46	8.72
PNG-F7	0.62	0.0475	0.4014	$2.3 X10^{-3}$	0.6229	0.0071	3.75	7.36
PNG-F8	0.59	0.9353	0.5052	$1.1 X10^{-2}$	0.9160	0.4498	6.06	6.68
PNG-F9	0.36	0.0017	0.3184	$4.7 X10^{-5}$	0.6993	0.0170	5.85	3.62
PNG-F10	0.67	0.3998	0.4907	$5.8 X10^{-4}$	0.6592	0.0254	3.38	4.46
PNG-F6-S12 **(1** and **5)**	0.79	0.3882	-	-	0.7099	0.0074	6.70	10.60
PNG-F6-S15 **(2** and **6)**	0.90	0.9042	-	-	1.3215	0.0458	10.78	8.03
PNG-F6-S17 **(3)**	0.71	0.2366	-	-	1.0358	0.5007	9.02	7.12
PNG-F1-5B **(4,7** and **8)**	0.93	0.7944	-	-	0.8502	0.0773	5.02	5.76
PNG-F4-11 **(10)**	1.04	0.1003	-	-	0.4835	0.0087	2.10	5.36
PNG-F4-13 **(11)**	1.14	0.0367	-	-	0.5448	0.0008	2.13	5.51
PNG-F4-18 **(3)**	0.71	0.1061	-	-	0.8768	0.0797	5.00	4.57

4.2.12 Effect of the purified compound 9 (20-hydroxybetulin) on the growth of *T.b. brucei* bloodstream forms

In order to verify whether 20-hydroxybetulin, the most active compound in this assay which is compound 9 acted as a trypanocide or a trypanostatic, we tested its effect over time on log phase culture of T. *b. brucei* $2x10^5$ cells/mL in HMI-9 with 10% (v/v) FBS, incubated at 37∘C and 5% CO_2 were exposed to 1x, 2x, and 4x EC_{50}, separately. As a control, cells were grown in absence of drug (drug-free control). The cell density was determined by counting using a hemocytometer at several time points in triplicate and the average values obtained were plotted against time. The growth curves of the parasite following a continuous exposure to 20-hydroxybetulin is shown in Figure 4-71. We verified that 20-hydroxybetulin had a trypanostatic effect on as cultures incubated with it at 4x EC_{50} were still able to grow, although the growth rate was found to be reduced. 20-hydroxybetulin is by some way the most active compound isolated and it would appear that the presence of a carboxyl group in most of the other compounds reduces their activity. In addition, very slight structural change between botulin and hydroxy botulin produces large increase in activity.
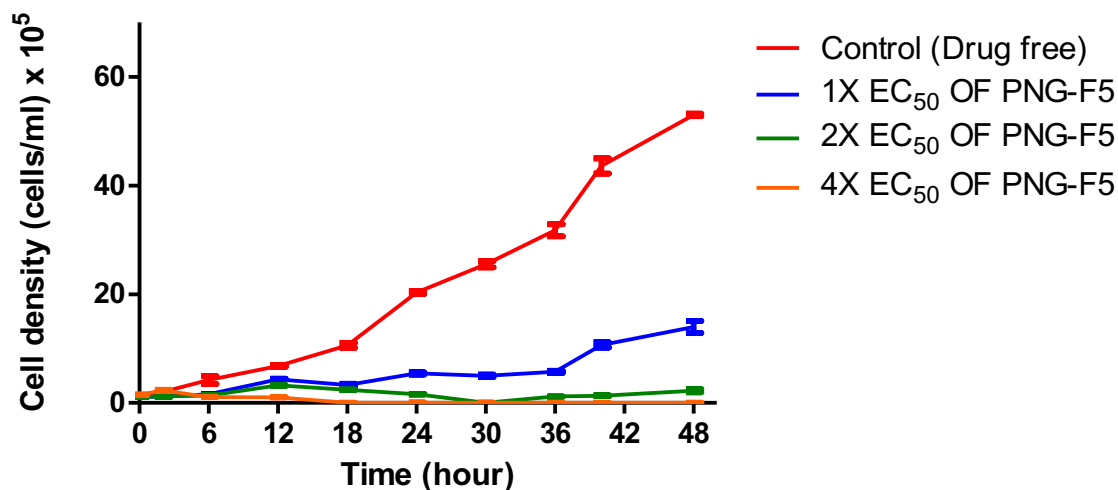
Figure 4-71: Growth of *T. brucei* s427WT in drug free culture (control) or in the presence of 1×, 2× or 4× the EC_{50} concentration of 20-hydroxybetulin. Cell seeding density was 2×10^5 cells/mL in HMI-9 with 10% (v/v) FBS, incubated at 37°C and 5% CO_2 (drug free) and counted at 0, 2, 6, 12, 18, 24, 30, 36, 42, and 48 h. Growth curves show the effect of test compounds on trypanosome growth after a continuous exposure to the drug. Cell counts are averages of three independent experiments, each counted in triplicate.

Chapter Five

5 Isolation of Two Novel Compounds From Zambia and Tanzania Propolis

Abstract

A bioassay-guided phytochemical investigation of propolis samples from Tanzania and Zambia that were screened for activity against *Trypanosoma brucei* led to the isolation of two novel flavanones with promising antitrypanosomal activity. The compounds were characterized based on their spectral and physical data and were identified as 6-(1,1-dimethylallyl) pinocembrin and 5-hydroxy-4″,4″-dimethyl-5″-methyl-5″-*H*-dihydrofuranol [2″,3″,6,7] flavanone. The two compounds, together with the propolis extracts and fractions, were assayed against a standard drug-sensitive strain of *T. b. brucei (*s427 wild-type), multi-drug resistant-resistant *T. b. brucei* (B48), drug-sensitive *T. congolense* (1L300) and a derived diminazene-resistant *T. congolense* strain (6C3), and for toxicity against U947 human cells and RAW 246.7 murine cells. Activity against *T. b. brucei* was higher than against *T. congolense*. Interestingly, the Tanzanian propolis extract was found to be more active than its fractions and purified compounds in these assays, with an EC_{50} of 1.20 μg/mL against *T. b. brucei*. The results of the cytotoxicity assay showed that the propolis extracts were less toxic than the purified compounds with mean IC_{50} values >165.0 μg/mL.

5.1 Introduction:

The biological activities of propolis have been well-studied and reported in the literature. Previously, 22 propolis samples from nine sub-Saharan African countries including Zambia and Tanzania, were profiled using high resolution LC-MS, GC-MS and HPLC and they were observed to have a high degree of diversity in chemical composition. However, there was no clear geographic discrimination between the samples (Zhang et al., 2014). It has also been reported that Tanzanian propolis showed greater antibacterial activity against a range of gram positive bacteria than Zambian propolis (Seidel et al., 2008). However, there is still a lack of information on propolis from Zambia and Tanzania, particularly the bioactivity of isolated compounds from these samples. In the current study, a bioassay guided isolation technique was used to identify some active metabolites from these samples using *in vitro* assays against *Trypanosoma b. brucei*, drug-resistant *T. b. brucei*, *T. congolense*, and drug-resistant *T. Congolense*. The *in vitro* cytotoxicity of the samples was also evaluated against human U937 cells and murine RAW 246.7 cells. We have shown in chapter three (see **section 3.6**) that none of the crude extracts were toxic to human cells U937 or on the murine RAW246.7 cell line. However, promising activity was found against wild type strain of *T.b. brucei* (s427-WT) and a multi-drug resistant strain, B48. Therefore, this chapter reports the chemical analysis including the isolation process of the compounds from the two of the most promising extracts (Tanzania and Zambia) found in this work.

5.2 Method of extraction

Approximately 8 g of the Zambian propolis was extracted with 150 mL of ethanol, three times under sonication (Clifton ultrasonic bath, Fisher Scientific, Loughborough, UK) for 1 h at room temperature. The extracts were combined, filtered and the solvent removed using a rotary evaporator (Buchi, VWR, Leicestershire, UK) to obtain a crude ethanol extract weighing 6.48 g. CC was performed for primary fractionation and yielded of 9 fractions.. **Figure 5-2** shows the protocol used for fractionation of the extract of Zambian propolis. While, 7.7 g of the Tanzanian propolis, was extracted consecutively with solvents of increasing polarity starting with n-hexane, followed by ethyl acetate and methanol. Recovery of residues and re-extraction with the solvent was carried out using sonication. The extracts were filtered and concentrated under vacuum using a Buchi rotary evaporator. to yield the Tanzanian propolis hexane extract (TP-Hx), ethyl acetate extract (TP-EtOA) and the methanol extract (TP-MeOH). Recovery of residues and re-extraction with the solvent was carried out using sonication. The extracts were filtered and concentrated under vacuum using a Buchi rotary evaporator. Fractionation of the extracts was carried out as described in **Figure 5-5**. General details of the apparatus used, methods and the materials are given in chapter 2.

5.3 Results and Discussion

5.3.1 Isolation and purification of compounds (13, 14, and 15) from Zambian and Tanzanian propolis

5.3.1.1 Zambian propolis

The isolation of active compounds which were guided by the activity of each fraction and the purification was monitored with NMR and mass spectrometry. Fractions 3 and 4 from the Zambian sample were combined because they showed activity against trypanosomes, as shown in **Table 5-3**, and because they have identical proton spectra as shown in **Figure 5-1.** The combined fractions were further purified using CC, followed by solid phase extraction (SPE). The resulting sub-fractions were examined by LC-MS and 1D NMR, while 2D NMR were used for the structure elucidation of the pure compounds. As a result, one known and one new compound were obtained from the Zambian propolis sample. The structures of the isolated compounds were elucidated on the basis of NMR, UV, IR and LC-MS/MS data. The workflow for the fractionation and analysis of Zambian propolis is illustrated in **Figure 5-2**.
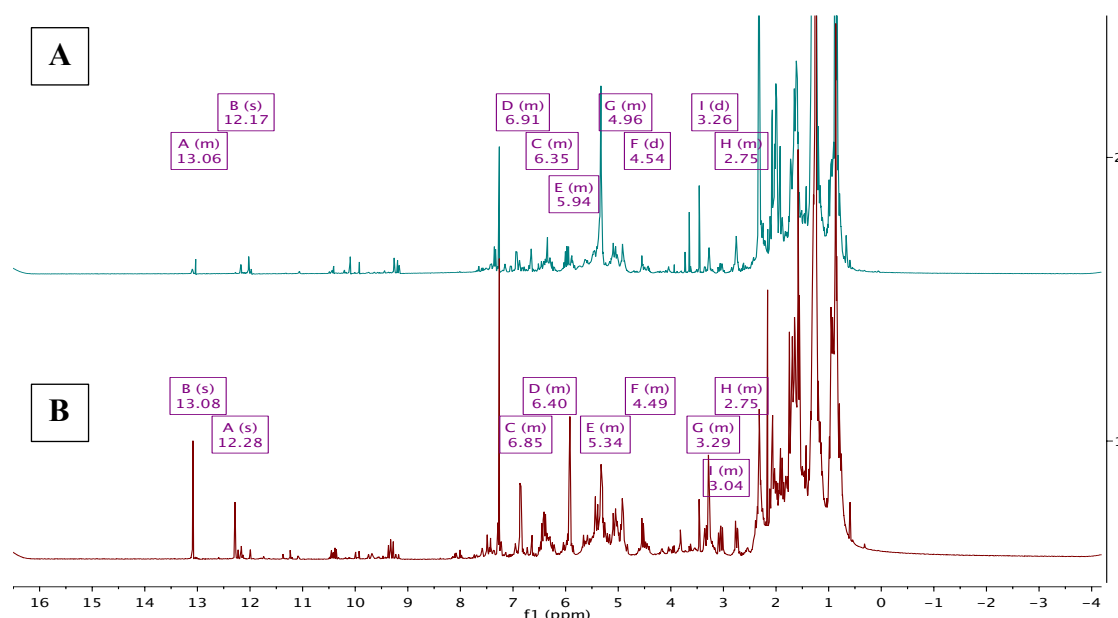
Figure 5-1: A) HNMR spectra of ZP-fraction 3 in CDCl₃ and B) HNMR spectra of ZP-fraction 4 in CDCl₃
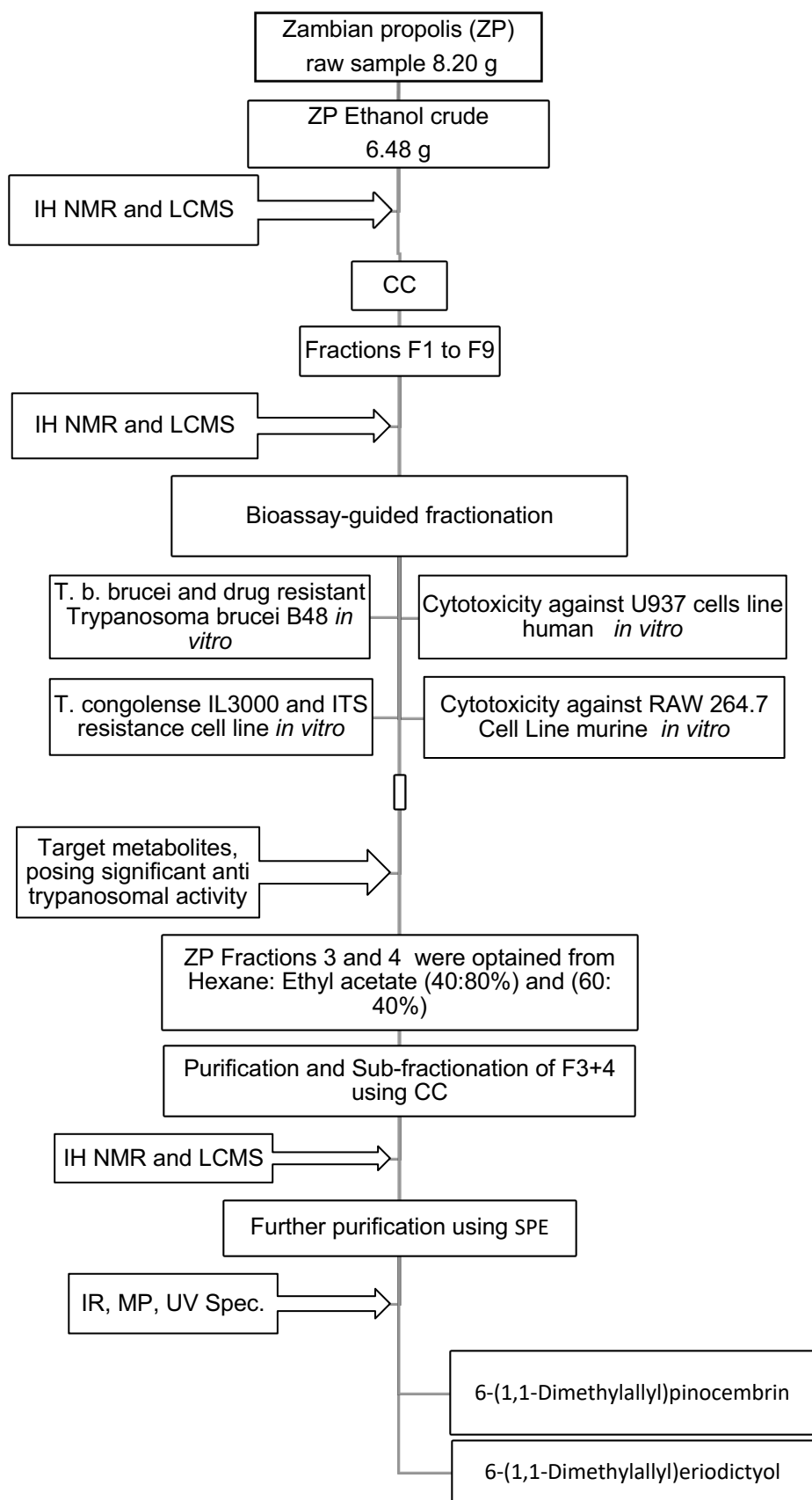
Figure 5-2: Workflow of analysis and fractionation of Zambian propolis

5.3.1.2 Tanzania Samples

The three TP extracts; hexane extract (TP-Hx), ethyl acetate extract (TP-EtOA) and the methanol extract (TP-MeOH) were monitored and profiled using ^{1}H NMR (**Figure 5-3**). It was hoped that the consecutive solvent extraction method might give better recovery but this was apparently not the case. TP-Hx and TP-EtOAc were found to be identical based on their proton NMR but TP-MeOH was different (**Figure 5-3**). Therefore, TP-Hx and TP-EtOA were combined to yield approximately 3 g and fractionated using CC to obtain fractions F1-F9. The isolation of active compounds which were guided by the activity of each fraction and the purification was monitored with NMR and mass spectrometry. Fraction 4 from the Tanzanian sample, which was obtained from CC, showed the highest activity against trypanosomes as shown in **Table 5-3**. Therefore, it was further purified using several chromatographic methods, including, MPLC, TLC and SEC. MPLC was applied in the fractionation of TP-F4 resulting in 95 fractions (**Figure 5-4**) and similar fractions (examined by TLC) were pooled yielding nine fractions. These sub-fractions were further examined by proton NMR and three sub-fractions, which showed identical spectra, were combined and purified using SEC. ^{1}H NMR and LCMS were performed on the resulting subfractions and then 2D NMR was run for structure elucidation to identify the two pure compounds. Meanwhile, fractionation of TP-MeOH using SEC did not yield any pure compounds. The workflow for the fractionation and analysis of Tanzanian propolis is illustrated in **Figure 5-5**.
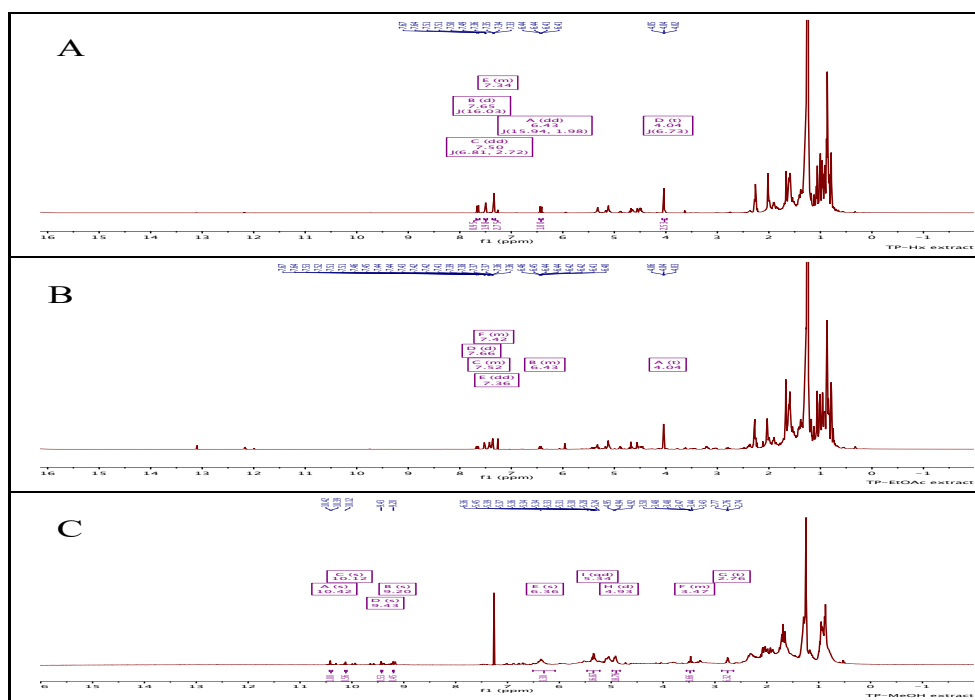
Figure 5-3: ¹H NMR of TP extracts A)TP-Hex B) TP- EtOAc C) TP-MeOH in CDCl₃
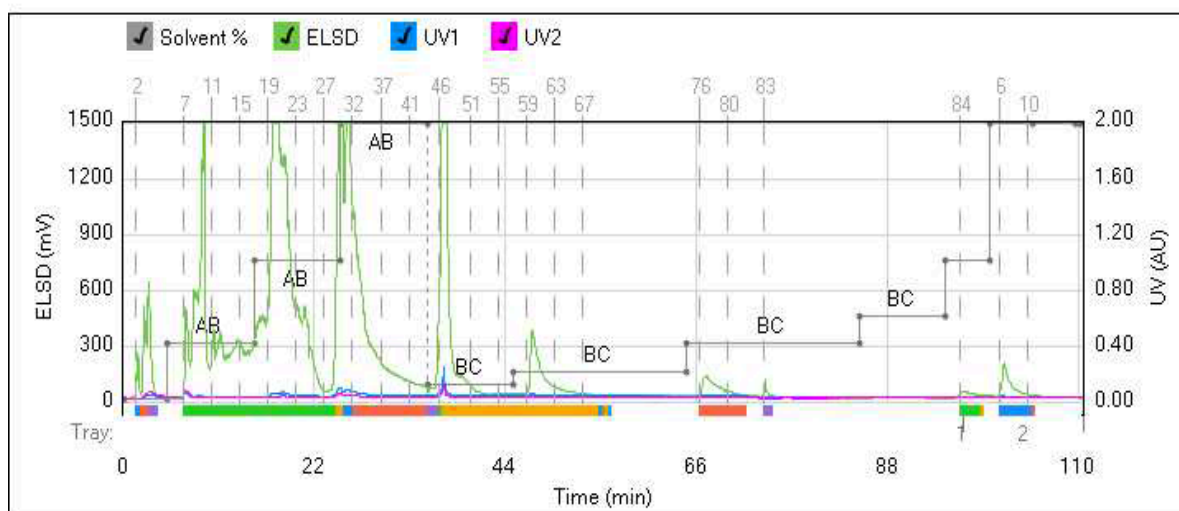
Figure 5-4: Chromatogram of Tanzania propolis fraction 8TP-F4 on Grace Reveleris® Flash chromatography
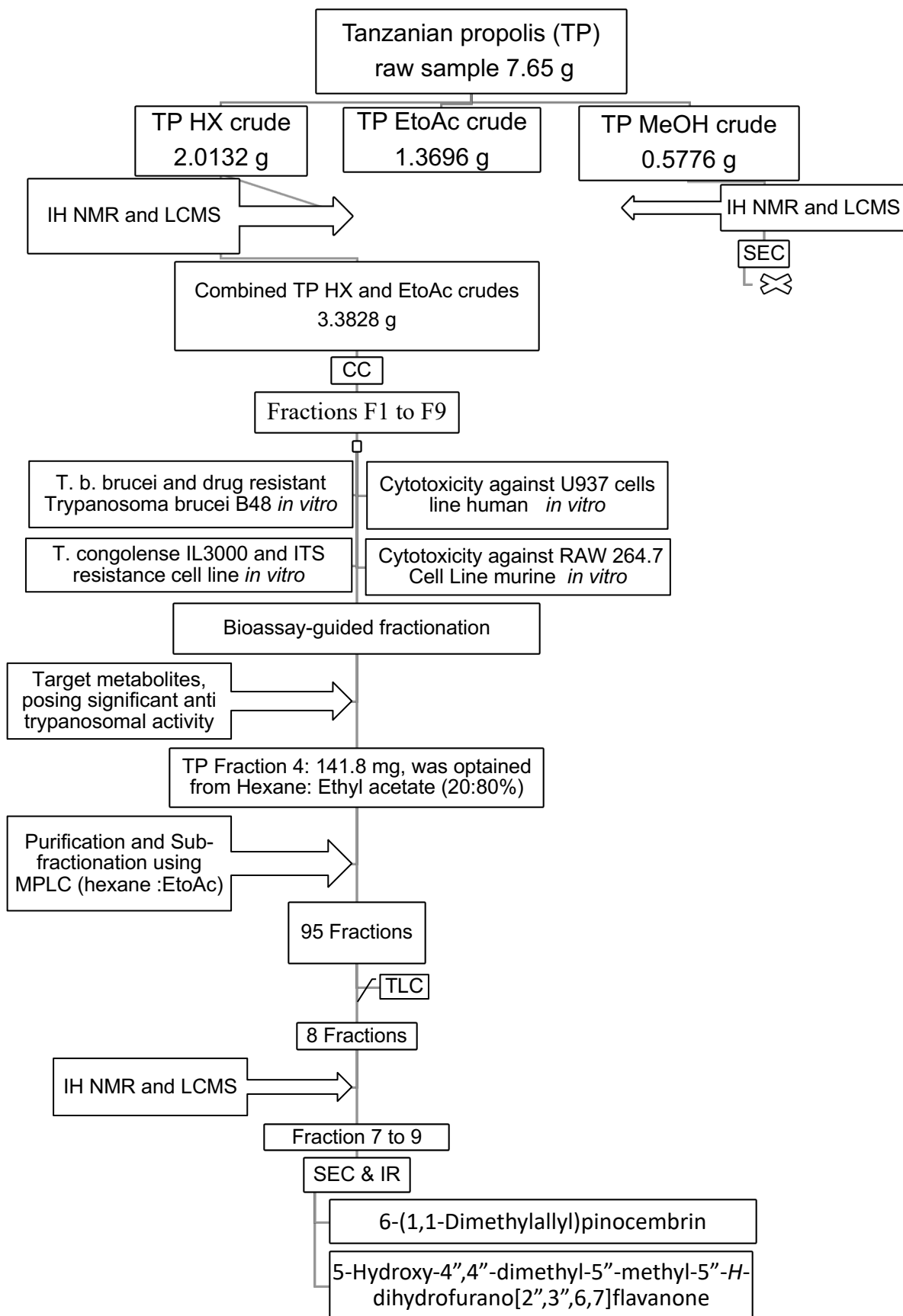
Figure 5-5: Workflow of analysis and fractionation of Tanzanian propolis

5.3.2 Chemical profiling of the crude Zambian propolis (ZP)
5.3.2.1 Characterization of Zambia propolis crude extract using ^{1}HNMR

The proton NMR spectrum of the Zambian crude sample (**Figure 5-6**) showed the presence of triterpenoids with methyl group signals between δ_H 0.52 and 1.71 ppm. The triterpenoids must be of the lupane and amyrin types as there were olefinic protons between 4.60 and 5.16 ppm which could imply lupeol, α- or β-amyrins. There was also the presence of some exo-methylene protons which could be substituents on the moieties present or diterpenoids in the sample. The presence of flavonoids with a 5-OH chelated to a 4-C=O was confirmed by the proton signal at 13.16 ppm. The sample also showed signals for oxygenated methine or methylene protons at 4.14 ppm indicating the presence a lignan or flavan/isoflavan. The presence of aromatic and olefinic protons between 6.12 and 7.14 also confirmed the presence of aromatic moieties in the flavonoids, lignan, flavan and isoflavan. There were no methoxy protons therefore the aromatic moieties were not substituted with methoxy groups.
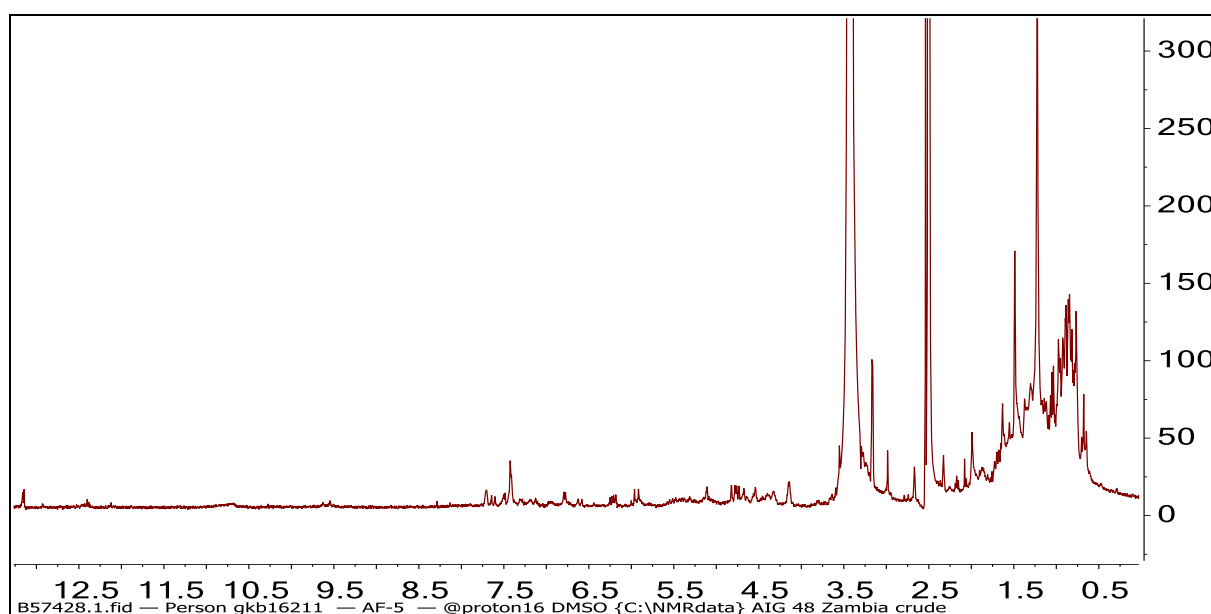
Figure 5-6: [1]**H NMR (500 MHz) spectrum of the crude ZP propolis sample in DMSO-*d_6***

5.3.2.2 Characterization of Zambia propolis crude extract using LC-MS

Profiling of the Zambia crude sample by LC-MS in **Table 5-1** and **Figure 5-7** suggested a wide diversity in the chemical composition of Zambian crude of phenolic compounds with different degrees of oxygenation such as flavonoids and lignans, the most abundant components in the sample had the formulae $C_{20}H_{19}O_4$, $C_{20}H_{19}O_5$, $C_{25}H_{27}O_6$ and $C_{25}H_{21}O_6$.

Table 5-1: Profiling of Zambian propolis crude extract using the negative ion masses in the LCMS

Peak no	RT (min)	M-1	Formula	RDB	Delta (ppm)	Intensity
1	6.72	287.0562	$C_{15}H_{11}O_6$	10.5	0.45	7.93E6
		329.1607	$C_{16}H_{25}O_7$	4.5	0.41	
2	15.29	323.1291	$C_{20}H_{19}O_4$	11.5	0.55	2.37E7
3	15.84	439.1763	$C_{25}H_{27}O_7$	12.5	0.24	1.36E7
4	16.53	455.1715	$C_{25}H_{27}O_8$	12.5	0.88	1.88E7
5	17.52	339.1240	$C_{20}H_{19}O_5$	12.5	0.48	2.76E7
6	17.91	383.1141	$C_{21}H_{19}O_7$	12.5	1.16	9.84E7
7	18.56	395.1138	$C_{22}H_{19}O_7$	13.5	0.36	2.32E7
		339.1240	$C_{20}H_{19}O_5$	11.5	0.66	
8	19.29	381.1346	$C_{25}H_{21}O_6$	12.5	0.57	5.77E7
		319.2280	$C_{20}H_{31}O_3$	5.5	0.41	
9	19.82	417.2288	$C_{24}H_{33}O_6$	8.5	1.33	1.72E7
		485.3277	$C_{30}H_{45}O_5$	8.5	0.87	
10	20.78	339.1240	$C_{20}H_{19}O_5$	11.5	0.57	2.36E7
		483.2025	$C_{27}H_{31}O_8$	12.5	0.54	
11	21.44	367.1190	$C_{21}H_{19}O_6$	12.5	0.76	7.76E7
		339.1241	$C_{20}H_{19}O_5$	11.5	1.04	
12	23.20	423.1818	$C_{25}H_{27}O_6$	12.5	1.20	3.62E7
13	23.52	423.1815	$C_{25}H_{27}O_6$	12.5	0.49	1.46E7
		323.1291	$C_{20}H_{19}O_4$	11.5	0.64	
14	24.92	407.1865	$C_{25}H_{27}O_5$	12.5	0.30	6.65E7

Figure 5-7: LC-MS spectral analysis of ZP crude extract using Orbitrap Exactive Mass Spectrometer (negative ion masses)

5.3.3   Chemical profiling of the crude Tanzanian sample (TP)
5.3.3.1 Characterization of Tanzanian propolis crude extract using ^{1}HNMR

The proton NMR of the Tanzanian propolis crude sample also showed the presence of triterpenoids between 0.59 and 1.43 ppm (**Figure 5-8**). The triterpenes may also be of the lupane and amyrin type as there were olefinic protons between 4.60 and 5.16 ppm which could imply lupeol, betulinic acid, α- or β-amyrin. There was also the presence of exo-methylene protons which could either be substituents on certain moieties present or diterpenes in the sample. The Tanzanian sample also showed the presence of flavonoids containing the 5-OH chelated to a 4-C=O and possibly some xanthones or anthraquinones with similar H-bonded – OH protons at 14.05, 13.65 and 13.11 ppm. The sample showed the presence of oxygenated methine or methylene protons between 3.55 and 4.00 ppm indicating the presence of lignans or flavans or isoflavans. The presence of aromatic and olefinic protons was confirmed by aromatic proton signals between 6.80 and 7.46 ppm. There was also the presence of phenolic hydroxyl protons at 9.28 and 9.20 and a methoxy proton at 3.86 ppm confirming the presence of hydroxyl and methoxy groups on aromatic rings in the compounds.

E42105.1.fid — Person gkb16211 — AF-8 Tanzania crude
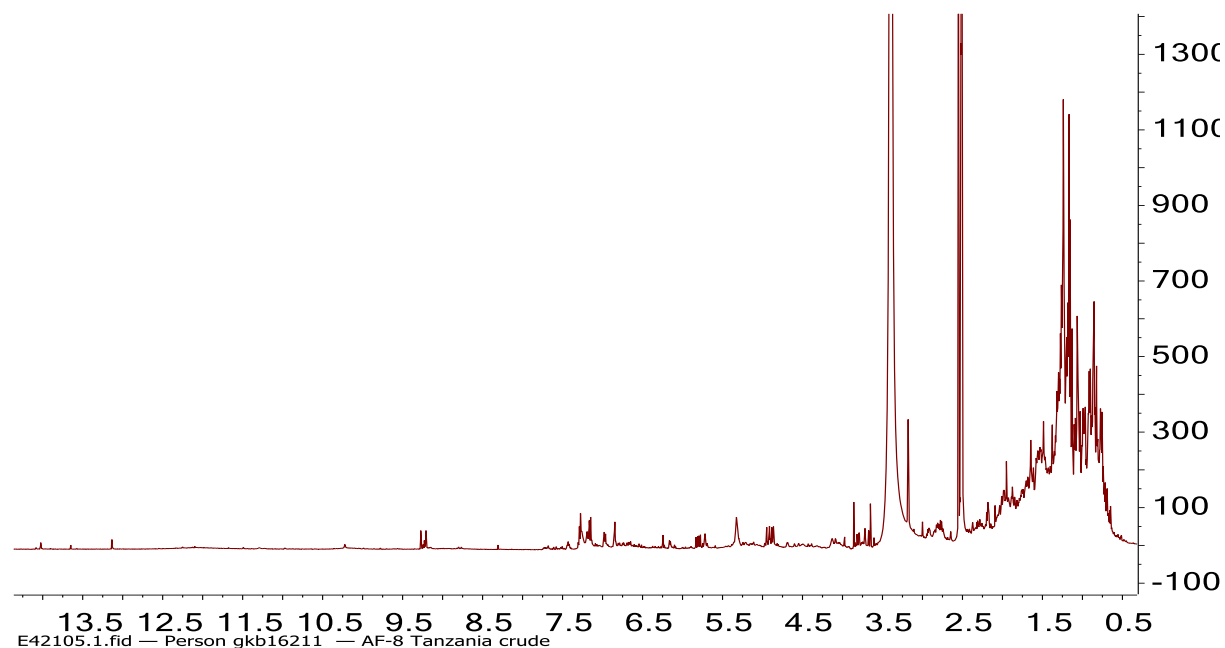
Figure 5-8: ^{1}H NMR (500 MHz) spectrum of the ethanol TP extract propolis sample in DMSO-*d6*

5.3.3.2 Characterization of Tanzanian propolis crude extract using LC-MS

Profiling of the Tanzanian crude sample by LC-MS shown in **Table 5-2** and **Figure 5-9** demonstrated relatively similar components to those showing in the chemical composition of

127

the Zambian crude sample including range of phenolic compounds with different degrees of oxygenation such as flavonoids, lignans, the most abundant components in the sample had the formulae $C_{19}H_{23}O_5$, $C_{20}H_{19}O_5$, $C_{20}H_{19}O_4$ and $C_{20}H_{25}O_4$

Table 5-2: Profiling of the crude Tanzanian propolis sample using the negative ion masses in the LCMS

Peak no	RT (min)	M-1	Formula	RDB	Delta (ppm)	Intensity
1	9.26	285.1506	$C_{18}H_{21}O_3$	8.5	3.55	8.65E5
		347.1511	$C_{19}H_{23}O_6$	8.5	3.10	
		379.1775	$C_{20}H_{27}O_7$	7.5	3.41	
2	10.61	319.1927	$C_{19}H_{27}O_4$	6.5	3.78	9.45E5
3	11.95	331.1562	$C_{19}H_{23}O_5$	8.5	3.39	1.05E6
		361.1670	$C_{19}H_{25}O_6$	8.5	3.76	
4	14.68	331.1560	$C_{19}H_{23}O_5$	8.5	2.85	4.65E6
5	15.81	301.1818	$C_{19}H_{25}O_3$	7.5	2.99	4.27E6
		345.1718	$C_{20}H_{25}O_5$	8.5	3.17	
6	16.18	287.1664	$C_{18}H_{23}O_3$	7.5	3.66	2.87E6
		331.1563	$C_{19}H_{23}O_5$	8.5	3.75	
7	17.54	285.1870	$C_{19}H_{25}O_2$	7.5	3.64	2.92E6
		329.1769	$C_{20}H_{25}O_4$	8.5	3.27	
8	18.79	281.2494	$C_{18}H_{33}O_2$	2.5	2.90	7.88E6
		439.1776	$C_{20}H_{31}O_3$	12.5	3.01	
9	20.41	339.1250	$C_{20}H_{19}O_5$	11.5	3.55	1.24E6
	20.63	329.1767	$C_{20}H_{25}O_4$	8.5	2.54	8.04E6
	22.11	329.1768	$C_{20}H_{25}O_4$	8.5	3.09	4.18E6
10	22.56	351.1251	$C_{21}H_{19}O_5$	12.5	3.68	5.88E6
		423.1830	$C_{25}H_{27}O_6$	12.5	4.01	
11	24.31	323.1299	$C_{20}H_{19}O_4$	11.5	3.09	2.35E6
12	25.70	331.1565	$C_{19}H_{23}O_5$	8.5	4.21	4.38E5
13	27.56	405.1724	$C_{25}H_{25}O_5$	13.5	4.05	6.49E5
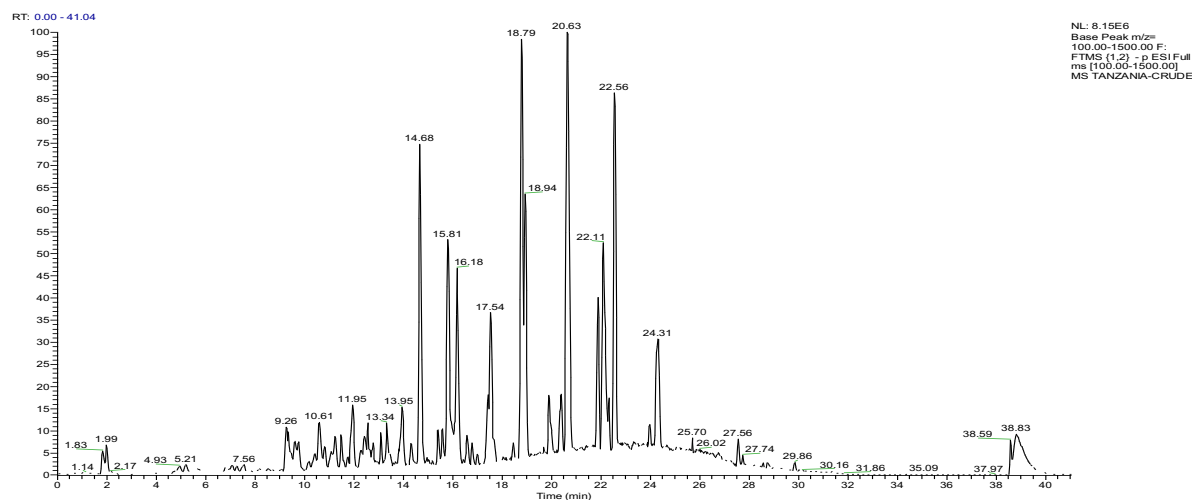
Figure 5-9: LC-MS spectral analysis of TP crude extract using (ESI) Orbitrap Mass Spectrometer (negative ion masses)

5.3.4 *In-vitro* antitrypanosomal activity and cross-resistance studies of Zambian and Tanzanian propolis extracts

In order to determine the *in vitro* anti-Trypanosomal activity of Zambian and Tanzanian propolis samples, the crude extracts and fractions were tested against *T. brucei S427WT* and the multi-drug resistant strain *B48* (**Table 5-3**). The results revealed that fraction ZP-F3 and ZP-F4 from the Zambian propolis sample gave the best activity against *T. brucei s427WT in vitro* (EC_{50} values of 0.94 and 1.10 µg/mL) respectively, while the most active fraction from the Tanzanian sample was TP-F4 (EC_{50} = 2.36 µg/mL). There were no significant differences in the EC_{50} values for the standard drug-sensitive strain Lister *T. brucei 427WT* and its derived resistant cell line *B48* apart from ZP-F3, which showed a just-significant increase in its EC_{50} value with a resistance factor (RF) of 1.59, compared to an RF of 158 for pentamidine (*P* <0.0001; Student's unpaired t-test).

The same fractions were also tested against the main AAT pathogen, *T. congolense*, and its resistant strain, finding no significant differences between the two strains (P > 0.05), showing that these propolis fractions were not cross-resistant with first-line trypanosomiasis drugs such as diminazene aceturate (**Table 5-4**). Interestingly, the same order of potency for these fractions applied for *T. brucei* and *T. congolense*, with ZP-F3 and ZP-F4 being the most active fractions from the Zambian propolis sample against *T. congolense* IL3000 as well (EC_{50} values of 5.85 and 3.92 µg/mL, respectively), and TP-F4 exhibiting the most activity among Tanzanian fractions (EC_{50} = 6.34 µg/mL). **Figure 5-10** shows strong correlation between the effects against *T. brucei* and *T. congolense*, for both Zambian and Tanzanian fractions, but while the Zambian fractions were much more potent against *T. brucei* than against *T. congolense* (slope of 4.74 in the correlation plot; AVG of 3.85-fold), the Tanzanian propolis differentiated much less between the two *Trypanosoma* species, indicating broader trypanocidal activity (slope of 4.74 in the correlation plot; AVG of 1.92-fold).

Table 5-3: EC$_{50}$ values of ZP and TP propolis samples and its fractions on *T. brucei* s427 wild-type and B48 (n=3)

Samples	*T. brucei* S427WT	*T. brucei* B48		
	AVG of EC$_{50}$ ± SEM	AVG of EC$_{50}$	R. F	t-test
Zambian propolis (ZP) and its fractions				
ZP Crude [a]	4.14 ± 0.12	7.39 ± 0.50	1.78	0.0032
ZP-F1[a]	17.05 ± 0.75	16.66 ± 1.90	0.98	0.8557
ZP-F2 [a]	1.76 ± 0.06	1.95 ± 0.15	1.11	0.2976
ZP-F3[a]	0.94 ± 0.06	1.50 ± 0.13	1.59	0.0165
ZP-F4 [a]	1.10 ± 0.03	0.97 ± 0.05	0.89	0.0821
ZP-F5 [a]	1.23 ± 0.03	1.07 ± 0.07	0.87	0.0986
ZP-F6 [a]	2.26 ± 0.03	2.30 ± 0.20	1.02	0.8813
ZP-F7 [a]	4.31 ± 0.17	4.36 ± 0.28	1.01	0.8733
ZP-F8 [a]	5.41 ± 0.15	6.10 ± 0.27	1.13	0.1761
ZP-F9 [a]	7.75 ± 0.35	7.46 ± 0.48	0.96	0.6509
Tanzanian propolis (ZP) and its fraction				
TP crude [a]	1.20 ± 0.04	1.02 ± 0.07	0.85	0.0843
TP-F1 [a]	5.78 ± 0.44	6.07 ± 0.67	1.05	0.7392
TP-F2 [a]	8.76 ± 0.44	8.54 ± 0.65	0.98	0.8001
TP-F3 [a]	4.87 ± 0.21	5.78 ± 0.61	1.19	0.2272
TP-F4 [a]	2.36 ± 0.18	2.58 ± 0.33	1.10	0.5751
TP-F5 [a]	4.23 ± 0.21	5.45 ± 0.41	1.29	0.0565
TP-F6 [a]	15.78 ± 0.74	16.84 ± 1.26	1.07	0.5110
TP-F7 [a]	4.45 ± 0.36	6.04 ± 0.66	1.36	0.1021
TP-F8 [a]	8.23 ± 0.48	7.82 ± 1.38	0.95	0.7936
TP-F9 [a]	138.73 ± 8.18	152.80 ± 12.07	1.10	0.3893
Control				
Pentamidine [b]	0.0031 ± 0.0003	0.4816 ± 0.02	157.84	<0.0001

The EC$_{50}$ values are the average ± SEM of at least 3 independent determinations. [a] EC$_{50}$ in µg/mL; [b] EC$_{50}$ in µM. RF= Resistance factor, being EC$_{50}$(*T. brucei* S427WT)/EC$_{50}$(B48). Statistical significance was determined using an unpaired two-tailed Student's t-test comparing the EC$_{50}$ values of the resistant strain with those obtained for the control strain s427. Pentamidine is a known trypanocide and used as positive control and strain control for B48.

Table 5-4: EC$_{50}$ values of ZP and TP propolis fractions on *T. congolense* IL3000 and the diminazene-resistant *T. congolense* clone 6C3 (n=3)

Samples	*Trypanosoma congolense* IL3000	*Trypanosoma congolense* 6C3		
	EC$_{50}$ ± SEM (μg/mL)	EC$_{50}$± SEM (μg/mL)	R. F	t-test
Zambian propolis (ZP) and its fractions				
ZP Crude [a]	14.39 ± 0.37	13.48 ± 1.12	0.94	0.4821
ZP-F1[a]	84.65 ± 4.98	76.45 ± 2.68	0.90	0.2205
ZP-F2 [a]	10.89 ± 0.72	14.22 ± 1.47	1.31	0.1117
ZP-F3[a]	5.85 ± 0.54	5.50 ± 0.29	0.94	0.5943
ZP-F4[a]	3.92 ± 0.39	4.25 ± 0.23	1.08	0.5081
ZP-F5 [a]	5.97 ± 0.74	8.92 ± 0.82	1.50	0.0557
ZP-F6 [a]	6.30 ± 0.74	6.70 ± 1.01	1.06	0.7715
ZP-F7 [a]	7.28 ± 0.78	8.84 ± 0.67	1.21	0.1656
ZP-F8 [a]	9.57 ± 0.64	9.35 ± 0.36	0.98	0.7578
ZP-F9 [a]	23.00 ± 1.90	23.15 ± 1.97	1.01	0.9607
Tanzanian propolis (ZP) and its fraction				
TP crude [a]	1.46 ± 0.29	1.62 ± 0.27	1.11	0.7031
TP-F1 [a]	16.09 ± 2.32	17.55 ± 1.16	1.09	0.6045
TP-F2 [a]	16.32 ± 1.16	19.17 ± 0.88	1.18	0.1214
TP-F3 [a]	11.83 ± 1.00	12.40 ± 1.49	1.05	0.7652
TP-F4 [a]	6.34 ± 0.67	5.91 ± 0.60	0.93	0.6596
TP-F5 [a]	9.34 ± 0.58	9.63 ± 0.67	1.03	0.7613
TP-F6 [a]	21.34 ± 1.58	21.69 ± 0.86	1.02	0.8540
TP-F7 [a]	12.49 ± 1.02	15.48 ± 1.31	1.24	0.1464
TP-F8 [a]	8.29 ± 0.61	9.66 ± 0.89	1.17	0.2734
TP-F9 [a]	113.97 ± 5.55	103.03 ± 2.84	0.90	0.1544
Control				
Diminazene [b]	0.20 ± 0.03	1.51± 0.09	7.75	0.0002

The EC$_{50}$ values are the average ± SEM of at least 3 independent determinations. [a] EC$_{50}$ in μg/mL; [b] EC$_{50}$ in μM. RF= Resistance factor, being EC$_{50}$(*T. brucei* S427WT)/EC$_{50}$(B48). Statistical significance was determined using an unpaired two-tailed Student's t-test comparing the EC$_{50}$ values of the resistant strain with those obtained for the control strain IL3000. Diminazene is the most used trypanocide against AAT and used as positive control and strain control for 6C3.
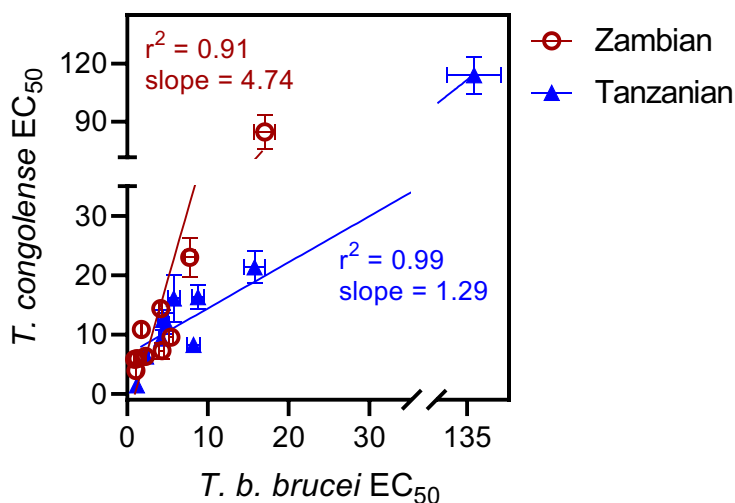
Figure 5-10: Correlation plot for EC$_{50}$ values of *T. b. brucei* and *T. congolense* for extracts of Zambian and Tanzanian propolis. The trend lines were generated by linear regression using Prism 8.4. Values were abstracted from Tables 1 and 2. Error bars are SD; when not shown, fall within the symbol.

Having successfully identified the most active fractions from each propolis sample we proceeded to purify and identify the active compounds from the selected fractions. Three new trypanocides were isolated. The fractionation methods are described in **section 5.3.1**. General profiling of the composition of the most active fractions from the two propolis samples was carried out by high resolution mass spectrometry and the results are presented in the following paragraphs **section 5.3.5**. The elemental compositions of the peaks in both active fractions were consistent with most of the components being modified flavonoids.

5.3.5 Chemical profiling of the biologically active fractions from Zambian and Tanzanian propolis

The most abundant components in the Zambia crude such as [M-H]$^-$ ion C$_{20}$H$_{19}$O$_4$ at m/z = 323.129 and [M-H]$^-$ ion C$_{20}$H$_{19}$O$_5$ at m/z =339.1240 had the elemental compositions found in fractions 3, while, other abundant components in the Zambia crude such as [M-H]$^-$ ion C$_{25}$H$_{27}$O$_6$ at m/z =423.1818 and [M-H]$^-$ ion C$_{25}$H$_{21}$O$_6$ at m/z = 417.1354, had the elemental compositions found in fractions 3-4 as shown in **Table 5-5, Figure 5-11** and **Table 5-6, Figure 5-12** . Therefore, ZP-F3 and ZP-F4 were selected for further fractionation by repeated CC. Thus, the isolation was not completely based on bioassay guided isolation but partly on targeted isolation of specific components.

Table 5-5: High resolution MS profiling of fraction 3 from CC of Zambian propolis sample using the negative ion masses in the LCMS

Peak no	RT (min)	M-1	Formula	RDB	Delta (ppm)	Intensity
1	16.21	439.1775	$C_{25}H_{27}O_7$	12.5	2.95	1.50E6
		413.1257	$C_{22}H_{21}O_8$	12.5	3.65	
2	16.72	439.1776	$C_{25}H_{27}O_7$	12.5	3.21	1.77E6
3	17.95	397.1304	$C_{22}H_{21}O_7$	12.5	2.75	5.62E6
4	18.48	355.1200	$C_{20}H_{19}O_6$	11.5	3.52	2.99E6
5	16.83	455.1729	$C_{25}H_{27}O_8$	12.5	3.43	2.93E7
6	18.46	439.1776	$C_{25}H_{27}O_7$	12.5	3.22	1.61E7
7	19.92	339.1247	$C_{20}H_{19}O_5$	11.5	2.63	2.65E7
8	20.13	381.1354	$C_{22}H_{21}O_6$	12.5	2.82	9.41E6
9	21.33	421.1669	$C_{25}H_{25}O_6$	13.5	2.94	5.20E6
10	21.85	353.1403	$C_{21}H_{21}O_5$	11.5	2.30	2.64E7
11	22.55	423.1824	$C_{25}H_{27}O_6$	12.5	2.57	2.30E7
		323.1298	$C_{20}H_{19}O_4$	11.5	2.90	
12	23.82	423.1827	$C_{25}H_{27}O_6$	12.5	2.57	2.66E6
		353.1405	$C_{21}H_{21}O_5$	11.5	2.98	
13	24.52	423.1829	$C_{25}H_{27}O_6$	12.5	3.80	2.73E6
14	25.68	407.1875	$C_{25}H_{27}O_5$	12.5	2.64	8.53E6
		377.1404	$C_{25}H_{21}O_5$	13.5	2.39	
15	28.72	381.1354	$C_{22}H_{21}O_6$	12.5	2.75	1.82E6
		329.1766	$C_{20}H_{25}O_4$	8.5	2.45	
16	29.73	417.1354	$C_{25}H_{21}O_6$	15.5	2.58	2.23E6
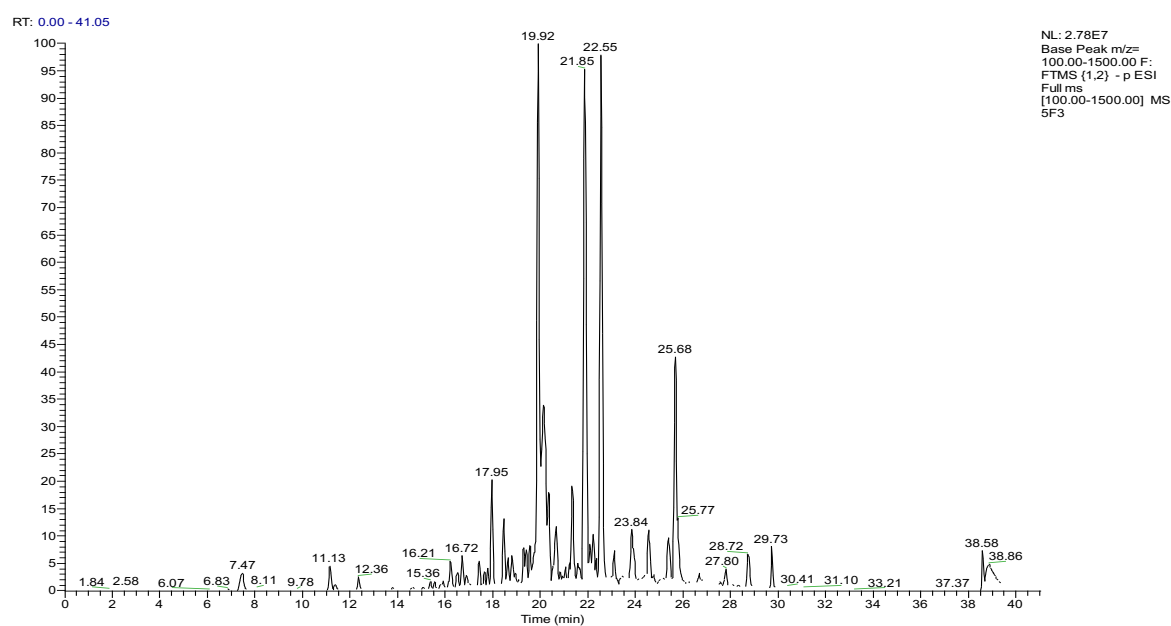
Figure 5-11: LC-MS spectral analysis of the fraction ZP-F3

133

Table 5-6: High resolution MS profiling of fraction 4 from CC of Zambian propolis sample using the negative ion masses in the LCMS

Peak no	RT (min)	M-1	Formula	RDB	Delta (ppm)	Intensity
1	14.57	399.1094	$C_{21}H_{19}O_8$	12.5	2.25	4.25E6
		369.0988	$C_{20}H_{17}O_7$	12.5	2.37	
2	16.75	455.1723	$C_{25}H_{27}O_8$	12.5	2.36	7.26E6
3	18.91	439.1772	$C_{25}H_{27}O_7$	12.5	2.33	1.58E7
4	20.33	339.1244	$C_{20}H_{19}O_5$	11.5	1.75	3.17E7
5	21.88	423.1823	$C_{25}H_{27}O_6$	12.5	2.29	2.59E7
		323.1297	$C_{20}H_{19}O_4$	11.5	2.43	
6	22.53	423.1825	$C_{25}H_{27}O_6$	12.5	2.80	1.31E7
7	25.78	339.1247	$C_{20}H_{19}O_5$	11.5	2.63	2.65E7
8	20.36	381.1354	$C_{22}H_{21}O_6$	12.5	2.82	9.41E6
9	21.33	421.1669	$C_{25}H_{25}O_6$	13.5	2.94	5.20E6
10	21.85	353.1403	$C_{21}H_{21}O_5$	11.5	2.30	2.64E7
11	22.53	423.1824	$C_{25}H_{27}O_6$	12.5	2.57	2.30E7
		323.1298	$C_{20}H_{19}O_4$	11.5	2.90	
12	24.52	423.1828	$C_{25}H_{27}O_6$	12.5	3.52	2.52E6
13	25.78	471.3490	$C_{30}H_{47}O_4$	7.5	2.22	1.03E7
		399.2552	$C_{25}H_{25}O_4$	8.5	2.77	
14	28.70	329.1765	$C_{20}H_{35}O_4$	8.5	2.15	2.54E6
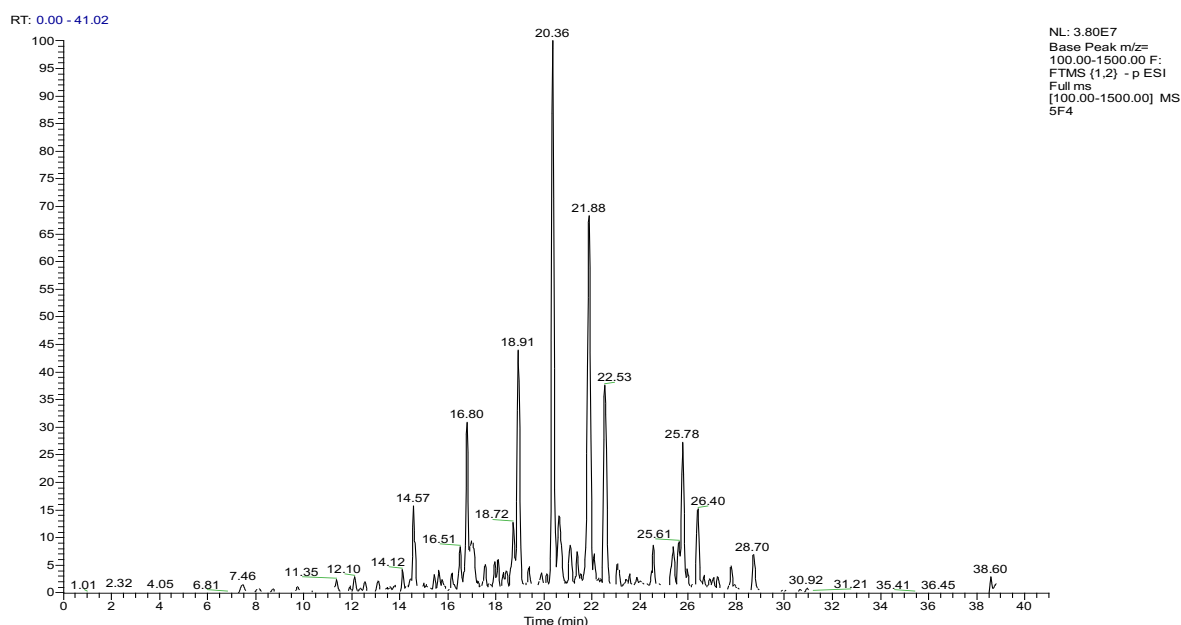
Figure 5-12: LC-MS spectral analysis of the fraction ZP-F4

The most abundant components in the Tanzania crude such as [M-H]$^-$ ion $C_{20}H_{19}O_4$ at m/z = 323.1298 and [M-H]$^-$ ion $C_{20}H_{19}O_5$ at m/z =339.1240 had the elemental compositions found in

134

TP-fractions 4. 4 as shown in **Table 5-7** and **Figure 5-13.** Therefore, TP-F4 were selected for further fractionation by repeated MPLC fallowed by SEC. Thus, the isolation was not completely based on bioassay guided isolation but partly on targeted isolation of specific components.

Table 5-7: High resolution MS profiling of fraction 4 from Tanzanian from CC using the negative ion masses in the LCMS

Peak no	RT (min)	M-1	Formula	RDB	Delta (ppm)	Intensity
1	11.53	455.1729	$C_{25}H_{27}O_8$	12.5	3.82	3.51E6
		329.2346	$C_{18}H_{33}O_5$	2.5	3.77	
2	12.52	339.1249	$C_{20}H_{19}O_5$	11.5	3.19	5.74E6
3	13.30	349.0619	$C_{21}H_{17}O_5$	13.5	4.22	4.66E6
4	15.62	455.1729	$C_{25}H_{27}O_8$	12.5	3.82	1.42E7
5	16.83	455.1729	$C_{25}H_{27}O_8$	12.5	3.43	2.93E7
6	18.46	439.1776	$C_{25}H_{27}O_7$	12.5	3.22	1.61E7
7	18.89	383.1153	$C_{21}H_{19}O_7$	12.5	4.37	5.69E6
		323.1304	$C_{20}H_{19}O_4$	12.5	4.69	
8	19.91	439.1776	$C_{25}H_{27}O_7$	12.5	2.54	7.88E7
		367.1197	$C_{21}H_{19}O_6$	12.5	2.58	
9	20.34	339.1249	$C_{20}H_{19}O_5$	11.5	3.19	6.64E6
10	21.88	423.1832	$C_{25}H_{27}O_6$	12.5	4.53	4.93E6
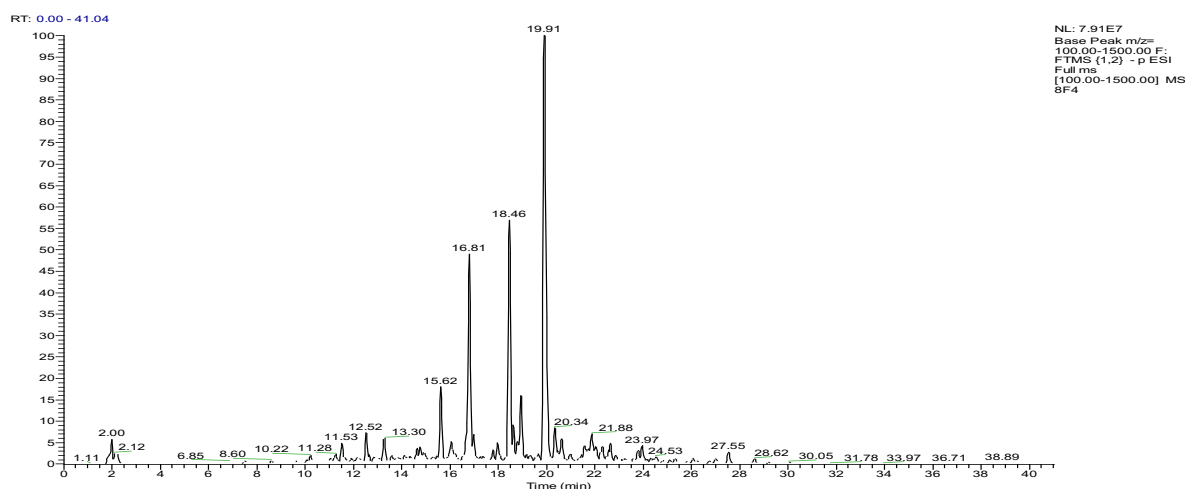
Figure 5-13: LC-MS spectral analysis of the fraction TP-F4

5.3.6 Analysis results of fractions from Zambia and Tanzania propolis

Solid phase extraction SPE was performed using a C-18 nonpolar stationary phase to purify compound in ZP-F(3+4)-20 that was isolated from Zambian propolis. Progress of purification

was monitored with proton NMR and high-resolution LC-MS. According to ^{1}HNMR in **Figure 5-14**, SPE seemed to be very useful for washing off the more polar impurities, while the compound of interest was eluted in the same degree of purity in both of solvent system 50:50 and 20:80 (methanol/water). Nevertheless, the fatty acid impurities remained in the stationary phase and only eluted with (50:50) water/acetone.
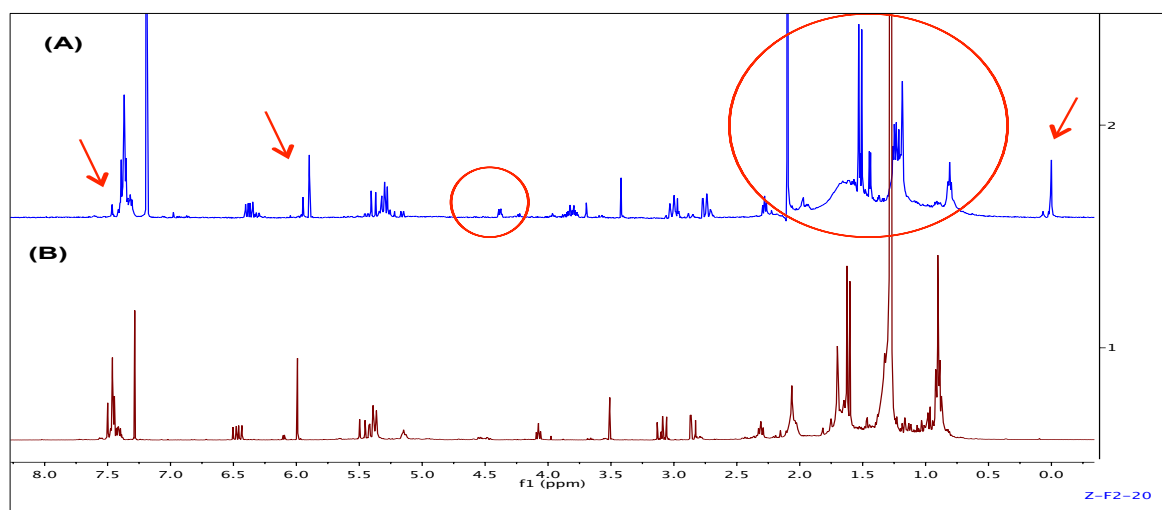
Figure 5-14:1H NMR spectra of (A) Purified ZP-F(3+4)-20 conducted from LC, (B); Further purification of the Purified compound ZP-F(3+4)-20 elution from SPE (50:50) MeOH/water. The arrows and circles identifying some impurities like fatty acids and water which disappeared after purification by SPE

The compound in ZP-F (3+4)-20 was obtained as a needle shaped white crystals with a yield of (46.8 mg), from the ethanol extract of the Zambian propolis by successive column chromatography over silica gel with hexane:ethyl acetate (40:60). On TLC plate it showed up as a single spot under UV light (254 or 365nm), also manifested a purple brownish color on spraying with p-anisaldehyde-sulphuric acid reagent and subsequent heating. Referring to **Figure 5-15**, It gave an R_f of 0.49, which is obviously higher than the R_f value of the other purified compound in fraction ZP-F(3+4)-70= 0.24 on TLC plate were elution with the mobile phase hexane:ethyl acetate (30:70), gave evidence that the purified compound in ZP-F(3+4)-20 is less polar than the other pure compound in fraction ZP-F(3+4)-70.
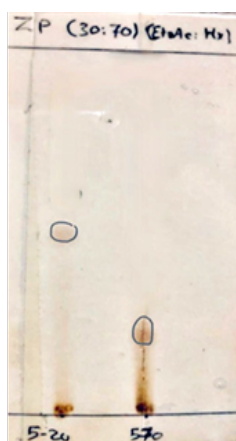
Figure 5-15: TLC plate after developing with the mobile phase Hx: EtOAc (70:30%) and spraying with p-anisaldehyde-sulphuric acid and heating, showed up single point for ZP-F(3+4)-20 and ZP- F(3+4)-70, displayed that R$_f$ value of compound in fraction ZP-F(3+4)-70 is less than ZP-F(3+4)-20

It is obvious from the IR Spectra **Figure 5-16** that factions ZP-F(3+4)-20 and ZP-F(3+4)-70 were indistinguishable, indicated that these compounds have the same substructure and we need NMR or Mass spectroscopy to discriminate between these two compounds. Moreover, the fraction TP-F4-(7-9) had the same substructure of other related fractions with a high degree of similarity in both functional groups and fingerprint regions.
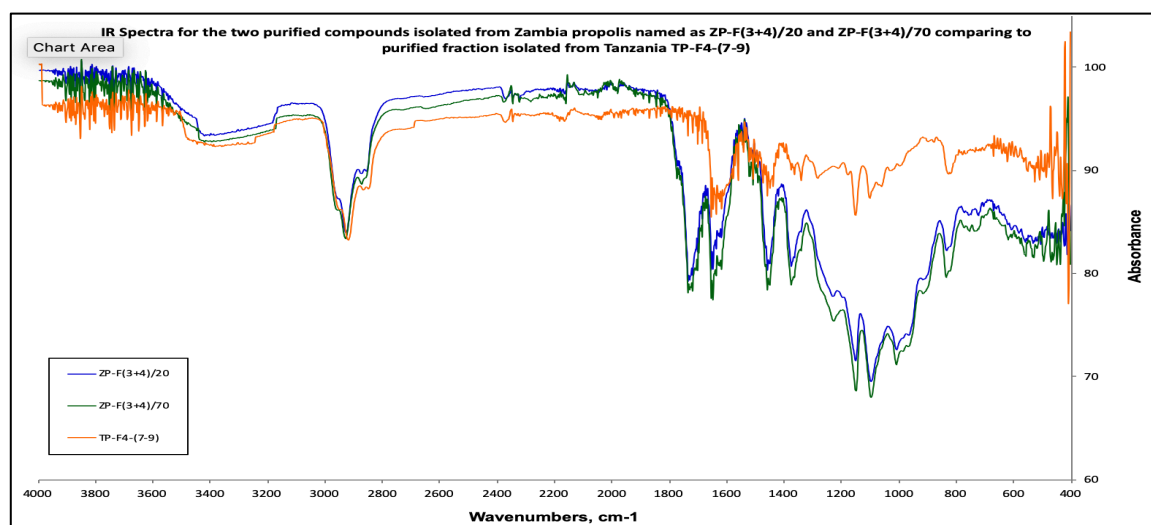
Figure 5-16: IR Spectra for the two purified compounds isolated from Zambia propolis named as ZP-F(3+4)-20 (green color in the graph) and ZP-F(3+4)-70 (blue color in the graph) comparing to purified fraction isolated from Tanzania TP-F4-(7-9) (Orange color in the graph).

5.3.6.1 Characterization of ZP 5-20 as 6-(1,1-dimethylallyl)pinocembrin (13)

Compound 13 was obtained from the combined fractions 3 and 4 from open column chromatography of the ethanol extract of Zambian propolis, with further purification as detailed in **section 5.3.1** The mass spectrum of the compound gave an $[M-H]^-$ ion at m/z = 323.1291 (Calc. for $C_{20}H_{19}O_4$, 323.1283) (**Figure 5-17**). The proton NMR spectrum (**Figure 5-21**) showed ten distinct signals and a multiple integrated for the 5 protons of a mono-substituted benzene ring. The most deshielded proton was at δ_H 13.13 ppm usually observed for the H-bonded 5-hydroxyl group of flavonoids. The aliphatic protons at 5.41, 3.08 and 2.84 indicated the compound is a flavanone as these signals are typical of the H-2, H-3a and H-3b of a flavanone moiety. The other aliphatic proton signals observed must be from a side chain on the flavanone moiety. The aromatic proton singlet at 5.99 ppm indicates the side chain must be on ring A of the flavanone and probably at position C-6 or C-8. A vinyl group on the side chain was revealed by the protons at 6.47 (dd, J = 17.8, 10.5 Hz), 5.38 (dd, J = 10.5, 0.9 Hz) and 5.48 (dd, J = 17.8, 0.9 Hz) in addition to a two methyl singlet, hence the side chain must be isopentyl. The ^{13}C spectrum (**Figure 5-22**) showed signals for a carbonyl carbon at δ_C 196.1 expected for the saturated ketone of a flavanone. There were 12 aromatic carbon signals, five aliphatic carbons and two olefinic carbons at 113.4 and 149.7 ppm. The structure of the compound was further deduced from correlations in its 2D NMR (**Figures 23 to 25**). From the HMBC spectrum, the 5-OH proton showed $^2J/^3J$ correlations to C-5, C-6 and C-10 and the methyl protons of the side chain also showed ^3J correlations to C-6 hence the side chain must be at position C-6. Similarly, the 7-OH proton showed correlations to C-6, C-7 and C-8. From the HSQC spectrum C-8 has the proton singlet at 5.99 ppm attached to it, thus confirming the substitution of the side chain at C-6 and not at C-8. The $^2J/^3J$ correlations, in the HMBC spectrum, from H-2 and H-3 to the carbonyl carbon confirm the flavanone moiety and other correlations from these protons to aromatic ring carbons indicate the phenyl ring is at C-2. Using these correlations, the chemical shifts for the protons and carbons were fully assigned as given in **Table 5-8**. This novel compound was characterized to be 6-(1,1-dimethylallyl)pinocembrin (**Figure 5-18**) . **Figure 5-19** shows MS^2 spectrum of compound 13 at 35V collision energy, the fragments at *m/z* 219.07, and 245.08 are consistent with a fragment containing ring A, while the fragment at *m/z* 267.10 consists of both rings A and B. A proposed fragmentation scheme is shown in **Figures 5-19** and **5-20**. The IR spectrum showed absorption bands at 3225 (-OH) 1720, 1700 (C=O), 1450 (C=C) cm^{-1}, and 1650, 1471 cm^{-1} for the presence

of aromatic rings.The physicochemical characteristics of this novel compound 1,1-Dimethylallyl pinocembrin were analyzed by ultraviolet (UV), fourier-transform infrared spectroscopy (FTIR), melting point assay, and Liquid Chromatography/Mass Spectrometry/Mass Spectrometry (LC/MS/MS). Its melting point (uncorrected) was between m.p 158-160°C while the UV spectrum gave absorption maxima at λ 296 nm. These values were close in value to their related compounds in comparing to the literature (Yang et al., 2018, Ching et al., 2007).
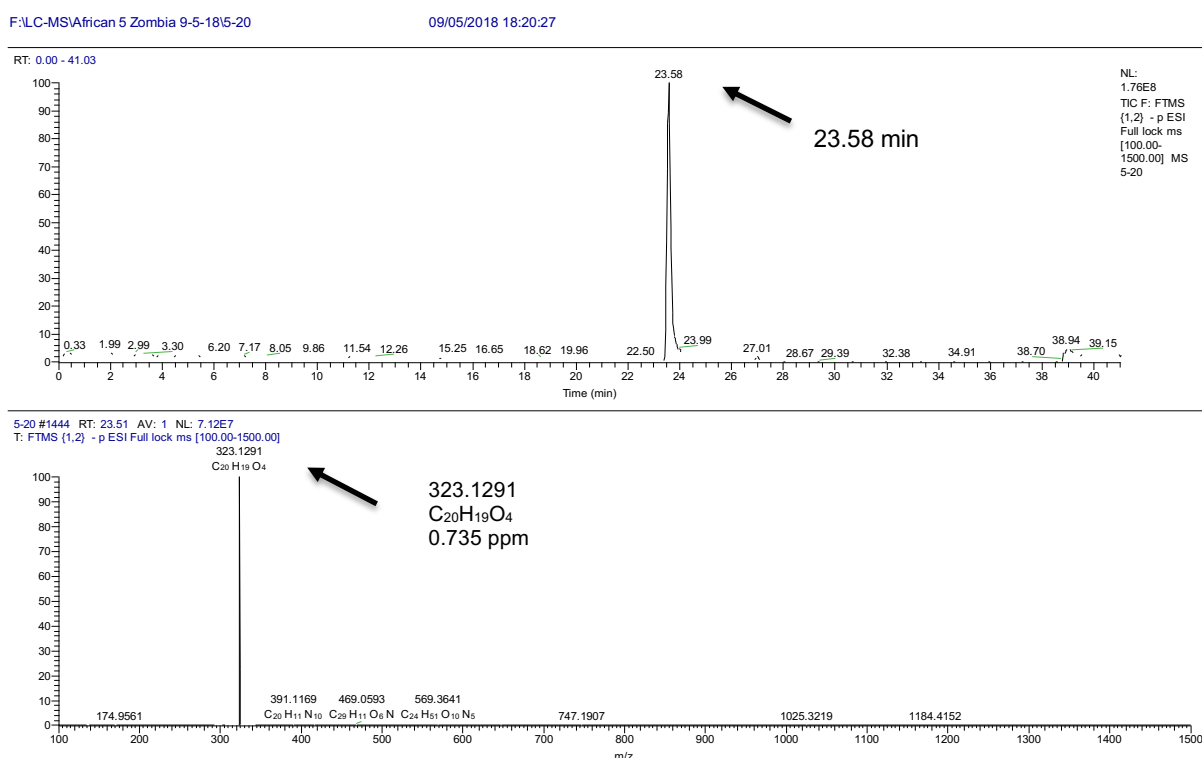
Figure 5-17: Mass ion chromatograms for the purified compound (13) found in fraction ZP-F(3+4)-20 ,the mass spectrum shows the ion mass [M-H] - m/z 323.1291 (C20H19O4, 0.735 ppm) at RT=23.58 (min) over the mass range of 100.00-1500.00 by using (LTQ) Orbitrap Mass Spectrometry (negative ion masses)
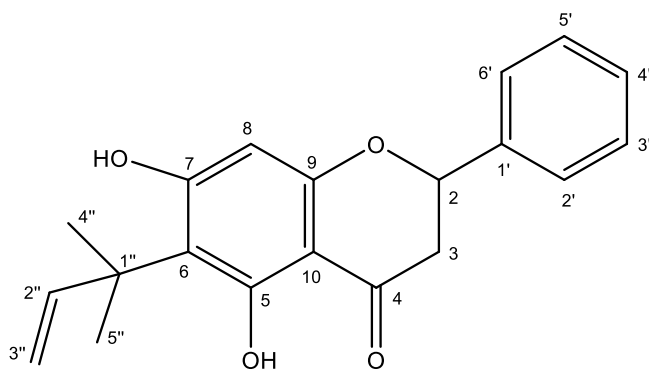
Chemical Formula: $C_{20}H_{20}O_4$

Figure 5-18: Structure of 6-(1,1-dimethylallyl) pinocembrin
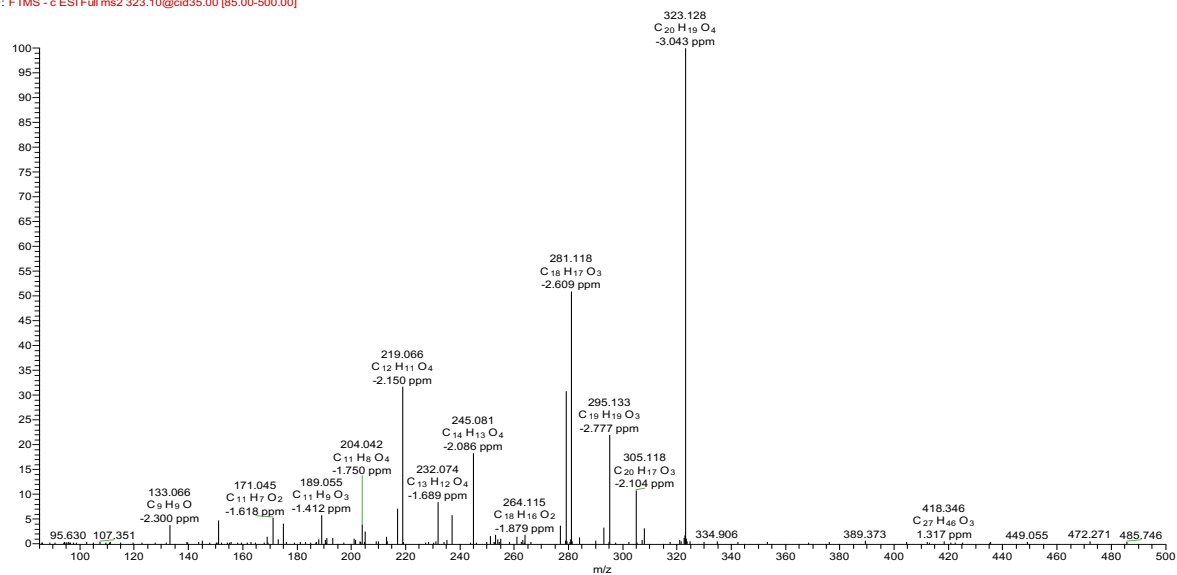
Figure 5-19: MS² spectrum of compound 13 over the mass range of 100.00-500, obtained on an LTQ Orbitrap at a collision energy of 35V (negative ion masses).

Chemical Formula: $C_{18}H_{17}O_3^-$
Exact Mass: 281.1183

Chemical Formula: $C_{20}H_{19}O_4^-$
Exact Mass: 323.1289

Chemical Formula: $C_{12}H_{11}O_4^{•-}$
Exact Mass: 219.0663

Chemical Formula: $C_{14}H_{13}O_4^-$
Exact Mass: 245.0819
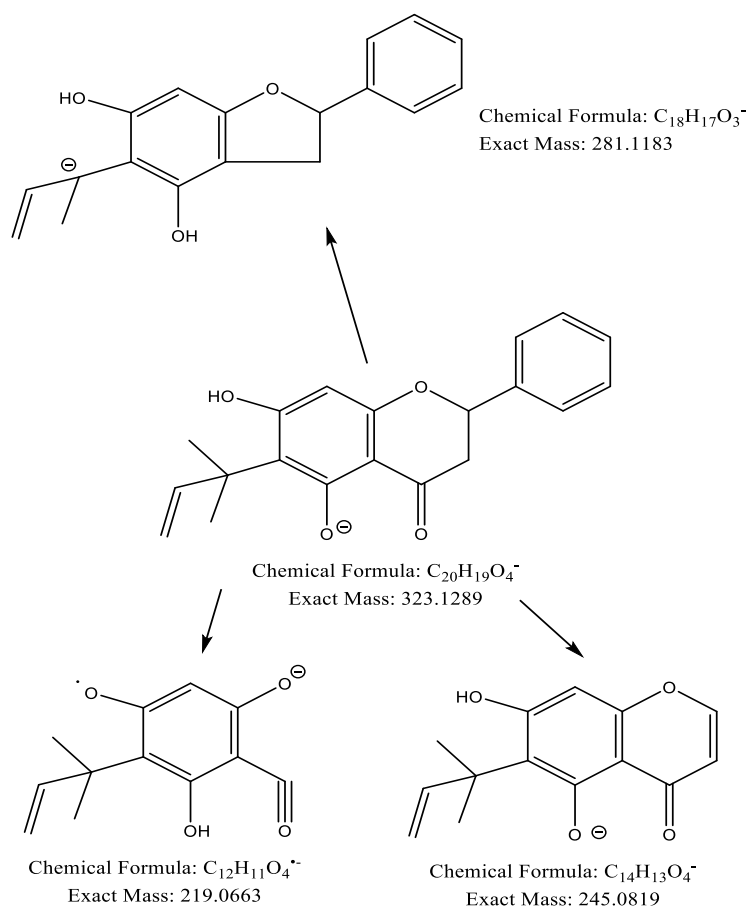
Figure 5-20: Suggested scheme for MS² fragmentation of compound 13

140

Table 5-8: ¹H (400MHz), ¹³C (100MHz) data of the compound (13) 6-(1,1-dimethylallyl) pinocembrin in fraction ZP-F(3+4)-20

Position	Proton δ ppm (mult, J Hz)	Carbon δ ppm (mult)	COSY	HMBC
2	5.37 (1H, dd, J = 5.8, 1.0)	78.7 (CH)	H-3	C-1', C-2', C-6'
3	2.85 (1H, dd, J = 17.1, 3.1) 3.10 (1H, dd, J = 17.2, 12.9)	43.5 (CH$_2$)	H-2, H-3	C-2, C-4
4	-	196.0 (C)	-	-
5	-	163.4 (C)	-	-
6	-	111.7 (C)	-	-
7	-	164.6 (C)	-	-
8	5.99 (1H, s)	96.8 (CH)	-	C-6, C-7, C-9, C-10
9	-	160.8 (C)	-	-
10	-	103.1 (C)	-	-
1'	-	138.5 (C)	-	-
2'	7.46 (1H, d, J = 1.1)	126.1 (CH)	H-3'	C-2, C-4', C-6'
3'	7.45 (1H, m)	128.8 (CH)	H-2'	C-1'
4'	7.42 (1H, m)	128.8 (CH)		C-2', C-6'
5'	7.45 (1H, m)	128.8 (CH)		C-1'
6'	7.47 (1H, d, J = 2.7)	126.1 (CH)		C-2, C-2', C-4'
1"	-	40.7 (C)		-
2"	6.47 (1H, dd, J = 17.8, 10.5)	149.7 (CH)	H-3"	C-1", C-4", C-5"
3"	5.39 (1H, d, J = 1.1) 5.48 (1H, dd, J = 17.8, 0.9)	113.4 (CH$_2$)	H-2"	C-1", C-2"
4"	1.62 (s)	27.3 (CH$_3$)	-	C-1", C-2", C-6
5"	1.60 (s)	26.6 (CH$_3$)	-	C-1", C-2", C-6
5-OH	13.13 (s)	-	-	C-5, C-6, C-10
7-OH	7.50 (s)	-	-	C-6, C-7, C-8
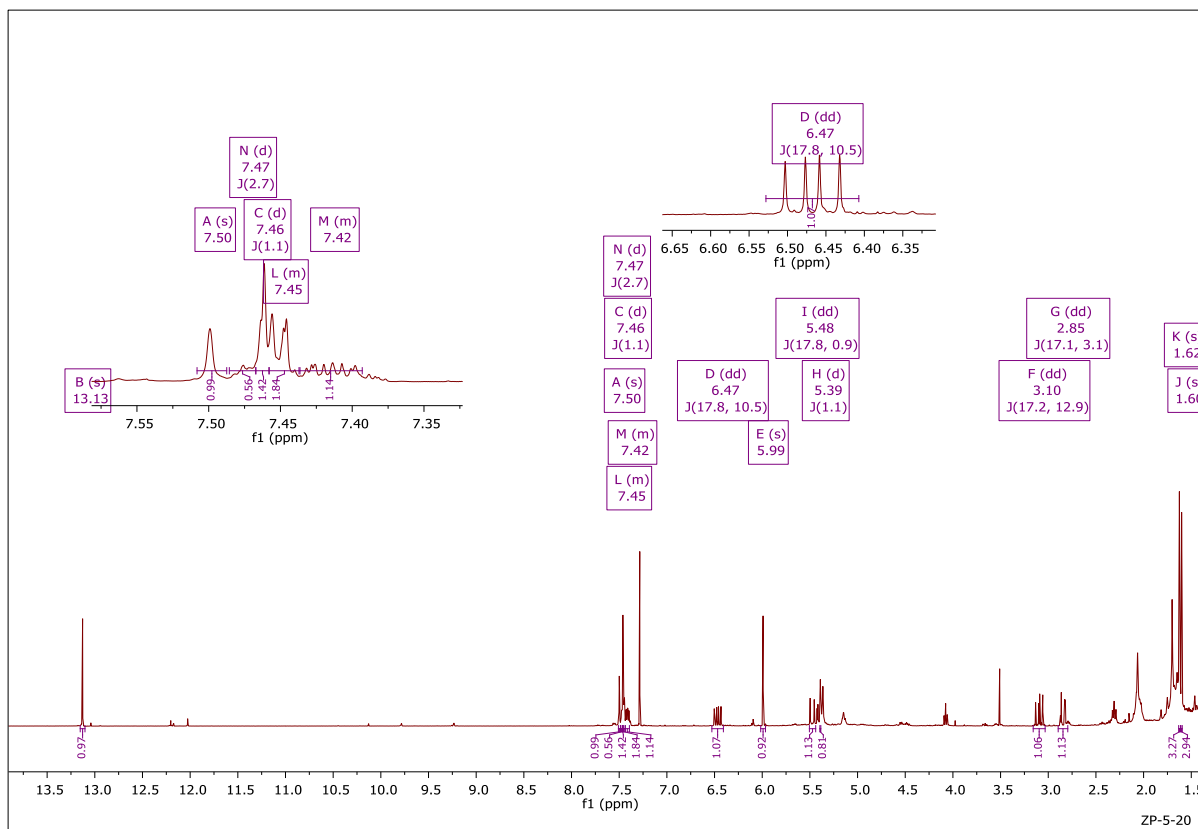
Figure 5-21: ^{1}H NMR (500 MHz) spectrum of the compound 13 labelled as ZP-F(3+4)-20 in CDCl$_3$
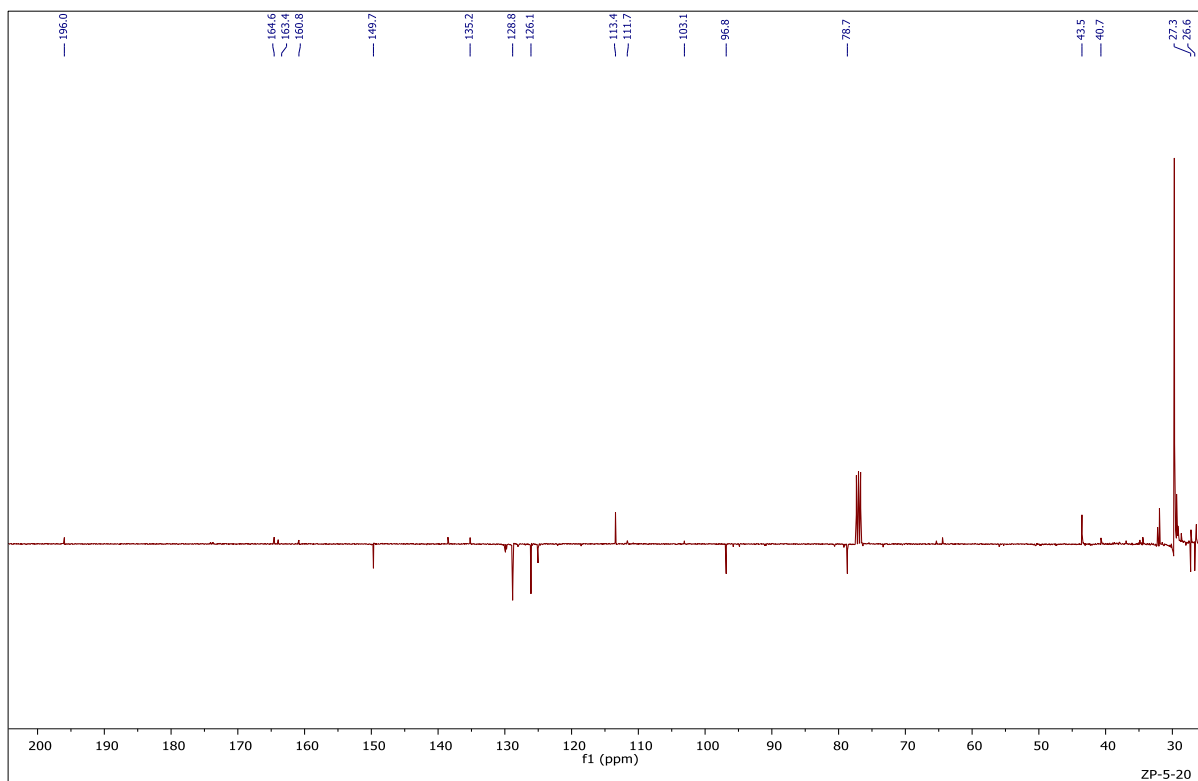
Figure 5-22: ^{13}C NMR (100 MHz) spectra of the compound (13) labelled as ZP-F(3+4)-20 in CDCl$_3$
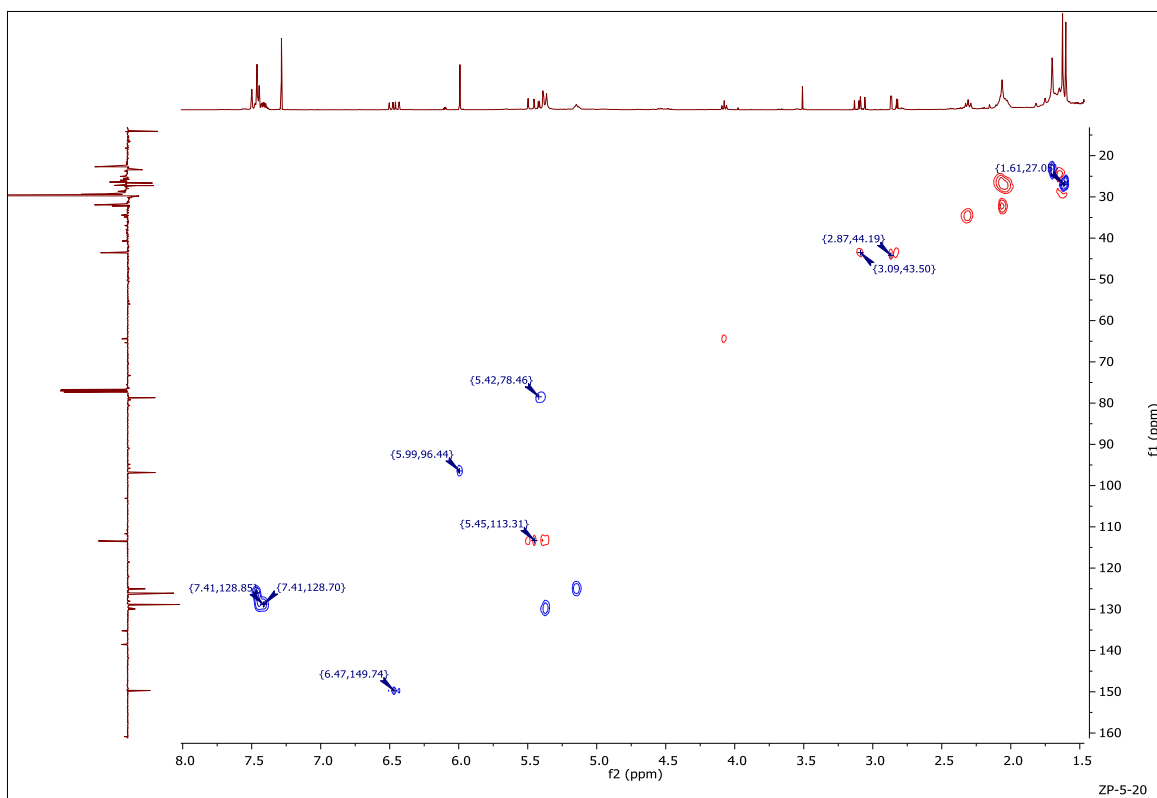
Figure 5-23: HSQC (500 MHz) Spectrum of the compound (13) labelled as ZP-F(3+4)-20 in CDCL₃.
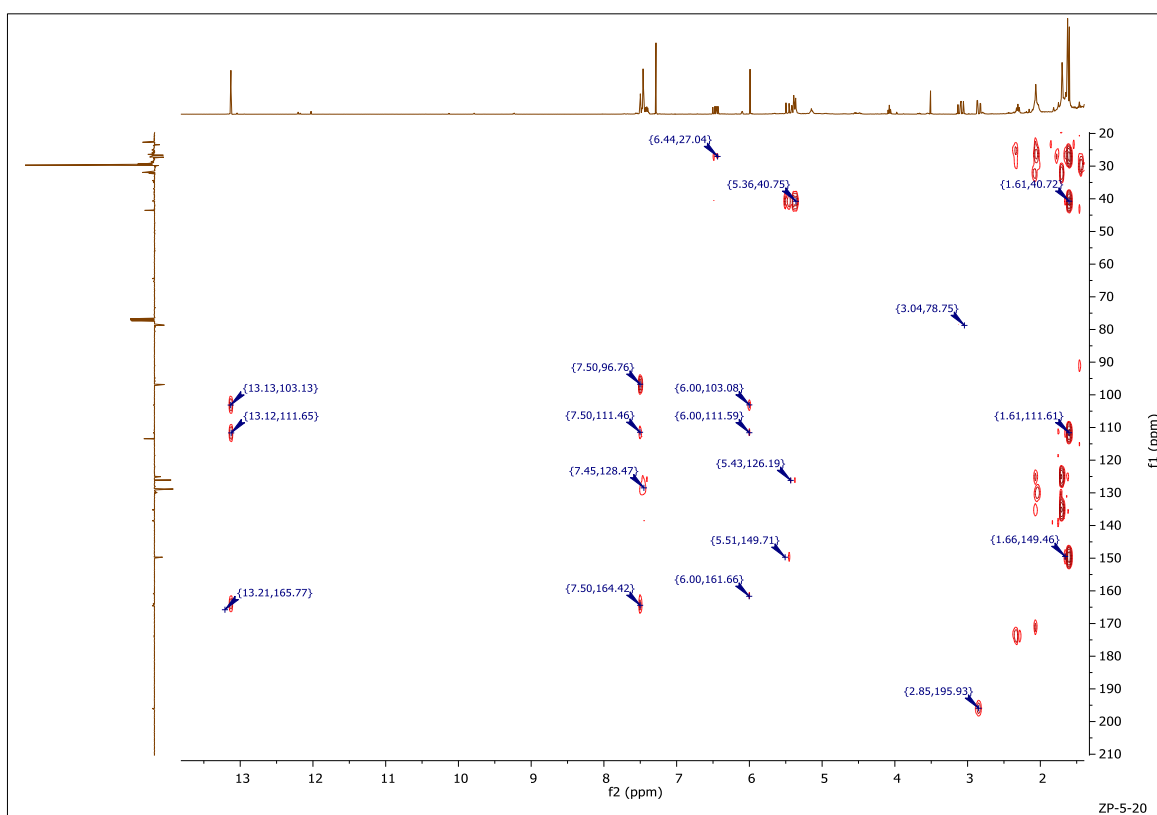
Figure 5-24: HMBC (500 MHz) Spectrum of the compound (13) labelled as ZP-F(3+4)-20 in CDCl₃
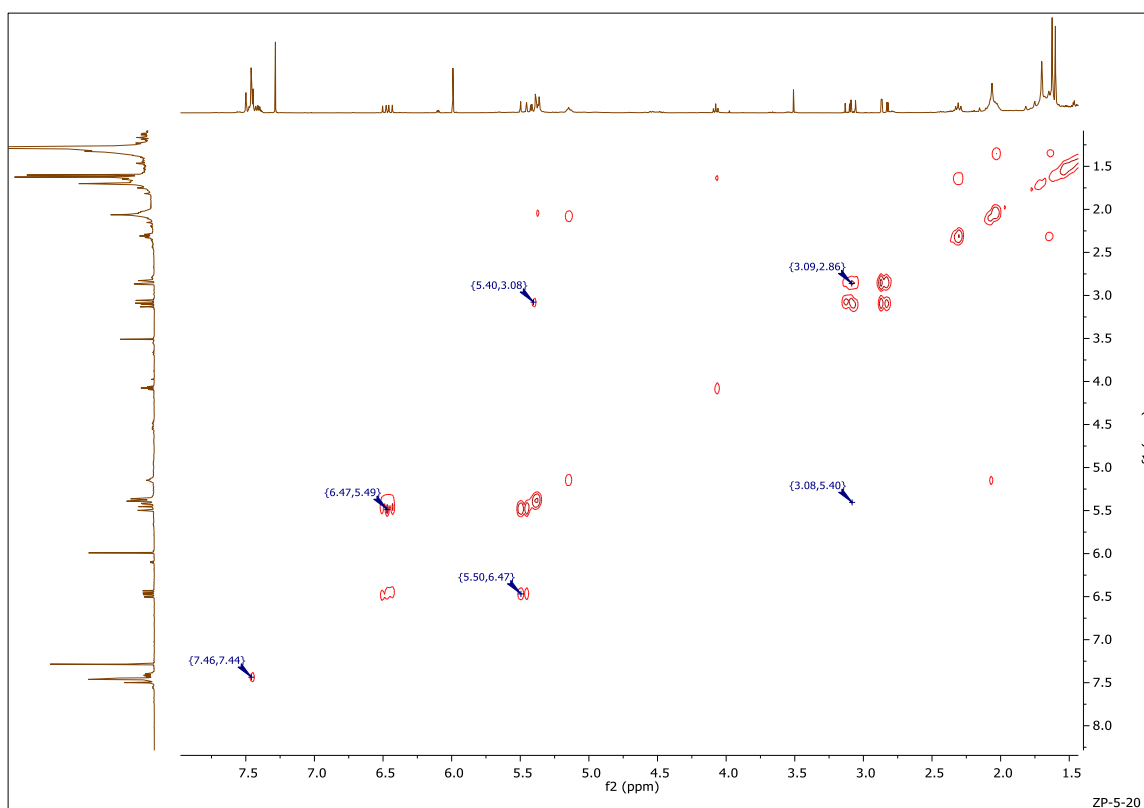
Figure 5-25: COSY (500 MHz) Spectrum of Compound (13) labelled as ZP-F(3+4)-20 in CDCl₃.

5.3.6.2 Characterization of the compound in fraction ZP-F(3+4)-70 as 6-(1,1-dimethylallyl)eriodictyol (14)

A compound was also obtained from fractions 3 and 4 of the ethanol extract of the Zambian propolis. The mass spectrum (**Figure 5-26**) gave an [M-H]⁻ ion at 339.1240 (Calc for $C_{20}H_{19}O_5$, 339.1233). Its proton spectrum was similar to that of compound 13 except for two aromatic doublets at δ_H 6.87 (2H, d, $J = 8.6$ Hz) and 7.31 (2H, d, $J = 8.6$ Hz) replacing the 5H aromatic multiples in compound 13 (**Figure 5-28**). The carbon signals were also identical except for the signals at δ_c115.8 (2xCH), 128.0 (2xCH) and 156.5 (C) replacing the carbon signals of the phenyl group in 13 (**Figure 5-29**). Therefore C-4' must be substituted with a hydroxyl group. This was further confirmed by the 16-mass unit difference of compound **14** with compound **13**. The correlations in its 2D NMR spectra (**Figures 30 to 32**) were similar to those of compound **13** and correlations from the protons in ring B confirmed the –OH attachment to C-4'. The full chemical shift assignments were thus made from the 2D spectra as shown in **Table 5-9** and were confirmed by comparison with literature reports (Seo et al., 1997). and the structure was assigned as 6-(1,1-dimethylallyl) eriodictyol (**Figure 5-27**).

RT: 0.00 - 41.05

NL: 4.97E8
Base Peak m/z=
100.00-1500.00 F:
FTMS {1,2} - p ESI
Full lock ms
[100.00-1500.00] MS
5-70

19.49

19.49 min

5-70 #1356 RT: 19.49 AV: 1 NL: 4.91E8
T: FTMS {1,2} - p ESI Full lock ms [100.00-1500.00]

339.1238
$C_{20}H_{19}O_5$

339.1238
$C_{20}H_{19}O_5$
-0.050 ppm

383.1136
$C_{21}H_{19}O_7$

439.1760   503.3382
$C_{25}H_{27}O_7$ $C_{30}H_{47}O_6$

679.2546
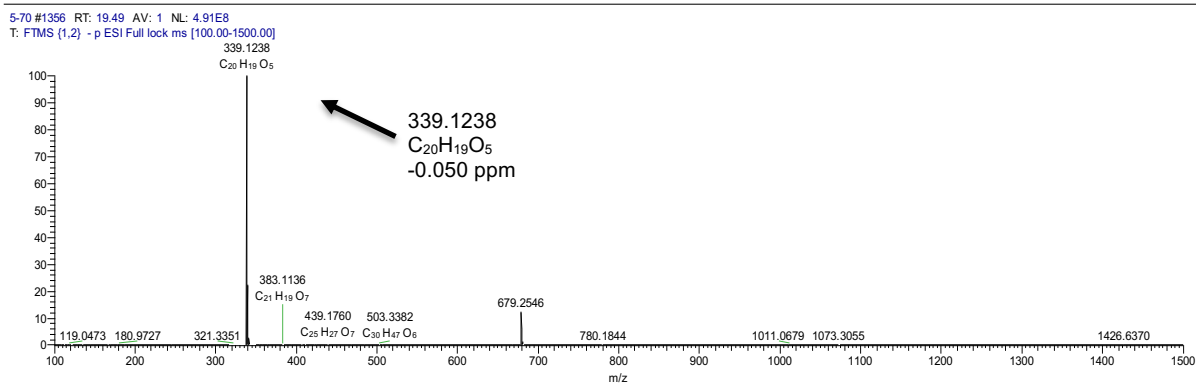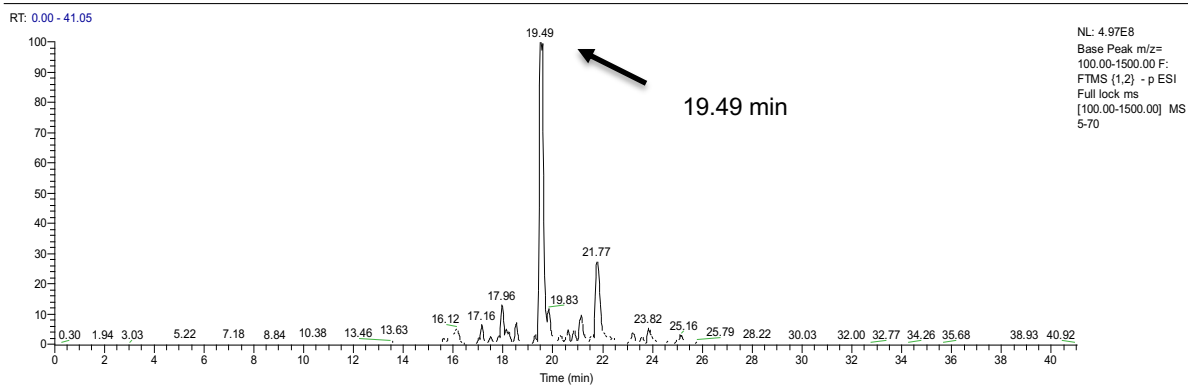
Figure 5-26: Mass ion chromatograms for the purified compound found in fraction ZP-F(3+4)-70. The mass spectrum shows the ion mass [M-H] - m/z 339.1238 (C20H19O5, - 0.050 ppm) at RT=19.49 (min) over the mass range of 100.00-1500.00 by using (LTQ) Orbitrap Mass Spectrometry (negative ion)

Chemical Formula: $C_{20}H_{20}O_5$
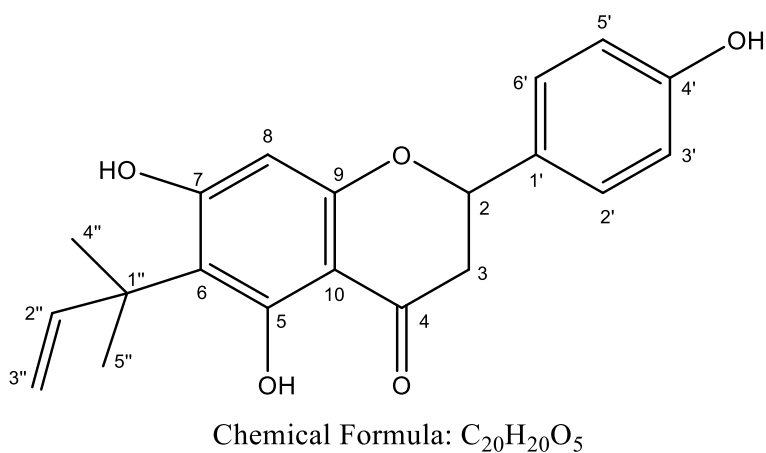
Figure 5-27: structure of 6-(1,1-dimethylallyl) eriodictyol

Table 5-9: ^{1}H (400MHz), ^{13}C (100MHz) data of the compound (14) 6-(1,1 Dimethylallyl)pinocembrin in fraction ZP-F(3+4)-70

Position	Experimental	
	Proton δ ppm (mult, *J* Hz)	Carbon δ ppm (mult)
2	5.30 (1H, dd, *J* = 12.9, 3.0)	78.6 (CH)
3	2.77 (1H, dd, *J* = 17.3, 3.0) 3.07 (1H, dd, *J* = 17.1, 12.9)	43.5 (CH$_2$)
4	-	196.4 (C)
5	-	163.2 (C)
6	-	113.4 (C)
7	-	164.7 (C)
8	5.94 (1H, s)	96.9 (CH)
9	-	161.1 (C)
10	-	103.8 (C)
1'	-	130.5 (C)
2'	7.30 (1H, m)	128.0 (CH)
3'	6.87 (1H, d, *J* = 8.6)	115.8 (CH)
4'	-	156.5 (CH)
5'	6.87 (1H, d, *J* = 8.6)	115.8 (CH)
6'	7.30 (1H, m)	128.0 (CH)
1"	-	43.0 (C)
2"	6.44 (1H, dd, *J* = 17.9, 10.5)	149.8 (CH)
3"	5.35 (1H, dd, *J* = 10.5, 1.0) 5.45 (1H, dd, *J* = 17.9, 1.0)	113.4 (CH$_2$)
4"	1.59 (s)	27.4 (CH$_3$)
5"	1.57 (s)	26.8 (CH$_3$)
5-OH	13.10 (s)	-
7-OH	7.46 (s)	-
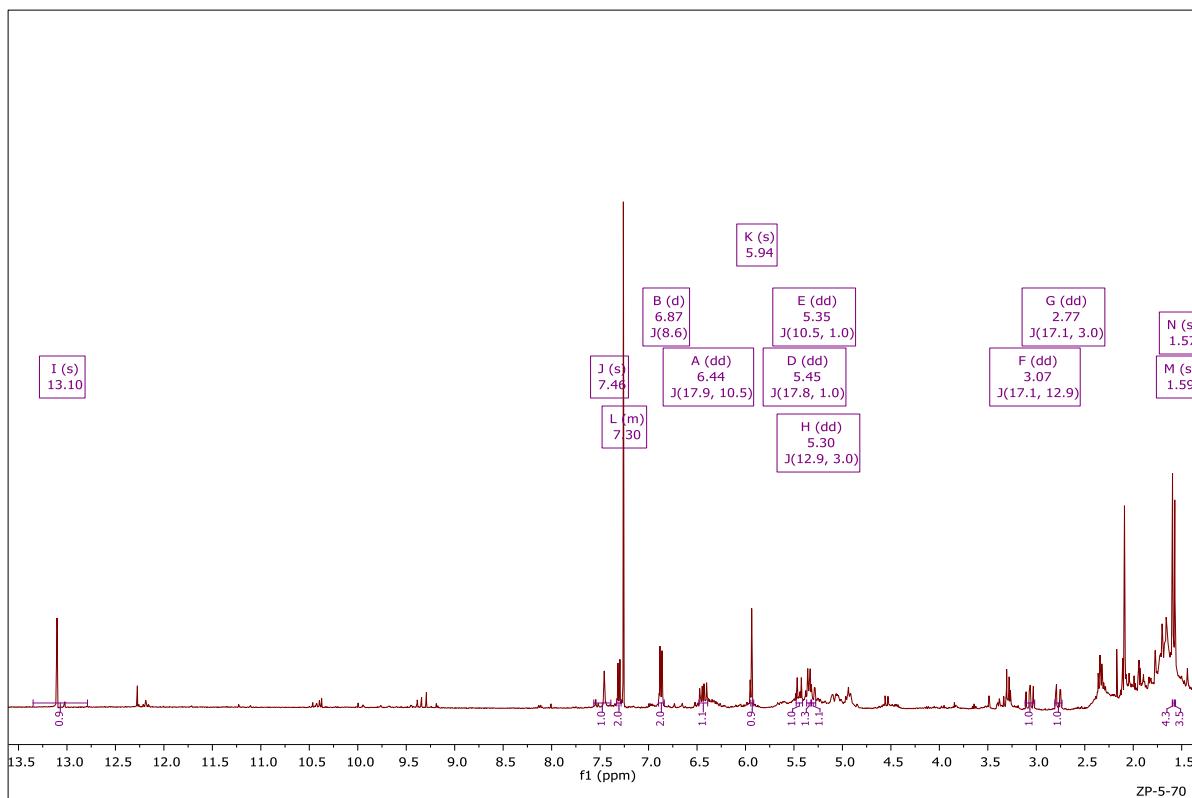
Figure 5-28: ^{1}H NMR (400 MHz) spectra of the compound (14) labelled as ZP-F(3+4)-70 in CDCl$_3$.
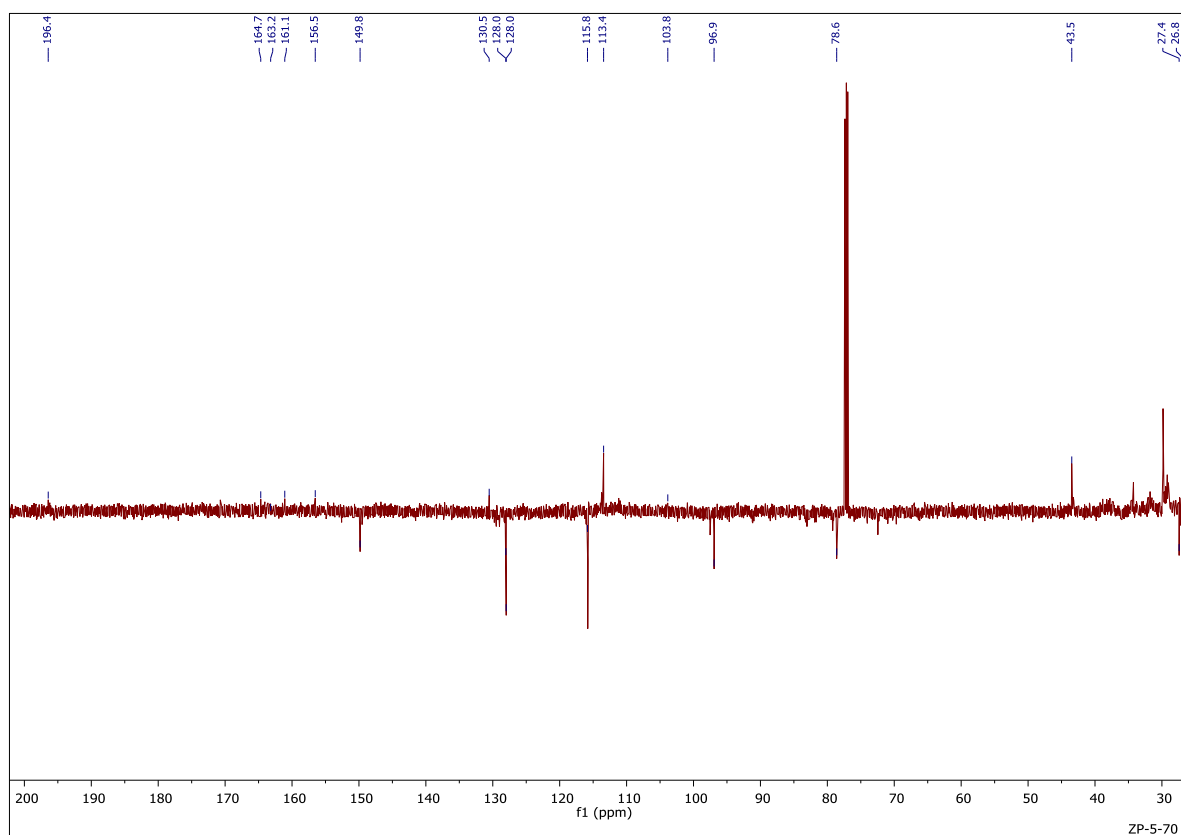
Figure 5-29: ^{13}C NMR (100 MHz) spectra of the compound (14) labelled as ZP-F(3+4)-70 in CDCl$_3$
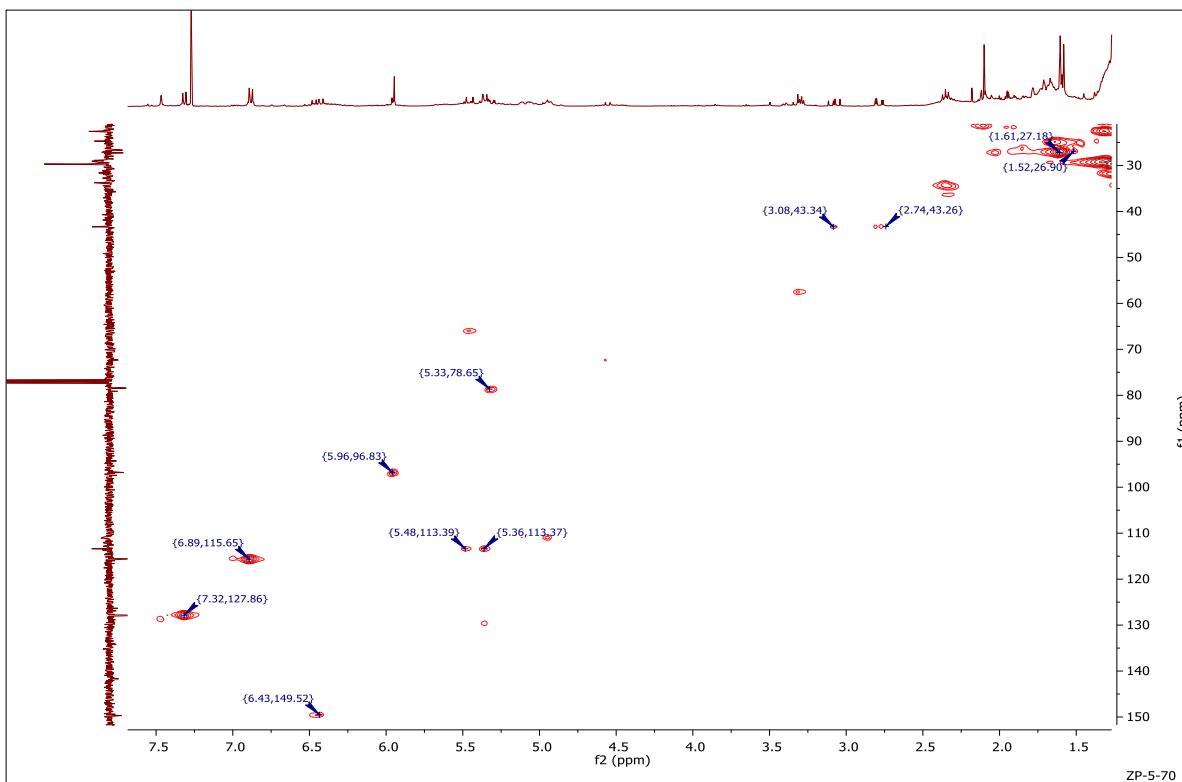
Figure 5-30: HSQC (400 MHz) Spectrum of the compound (14) labelled as ZP-F(3+4)-70 in CDCl₃.
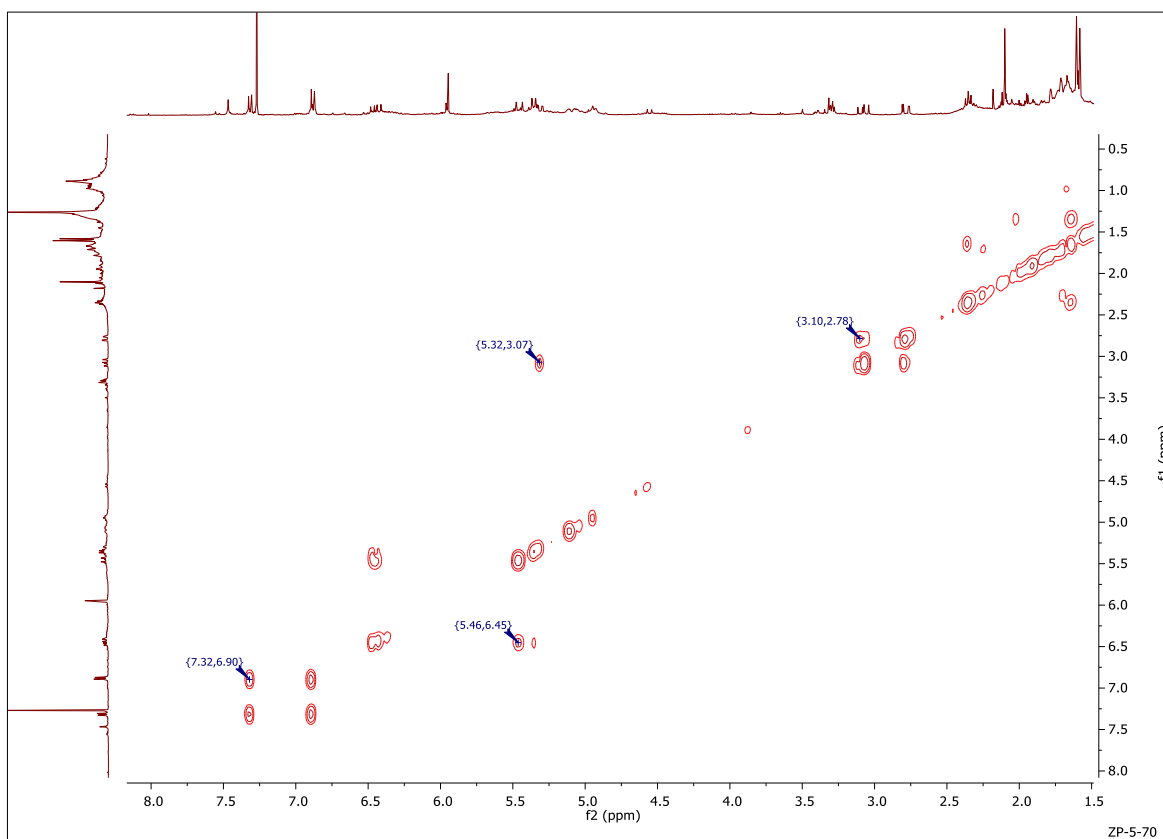
Figure 5-31: COSY (600 MHz) Spectrum of Compound (14) labelled as ZP-F(3+4)-70 in CDCl₃.
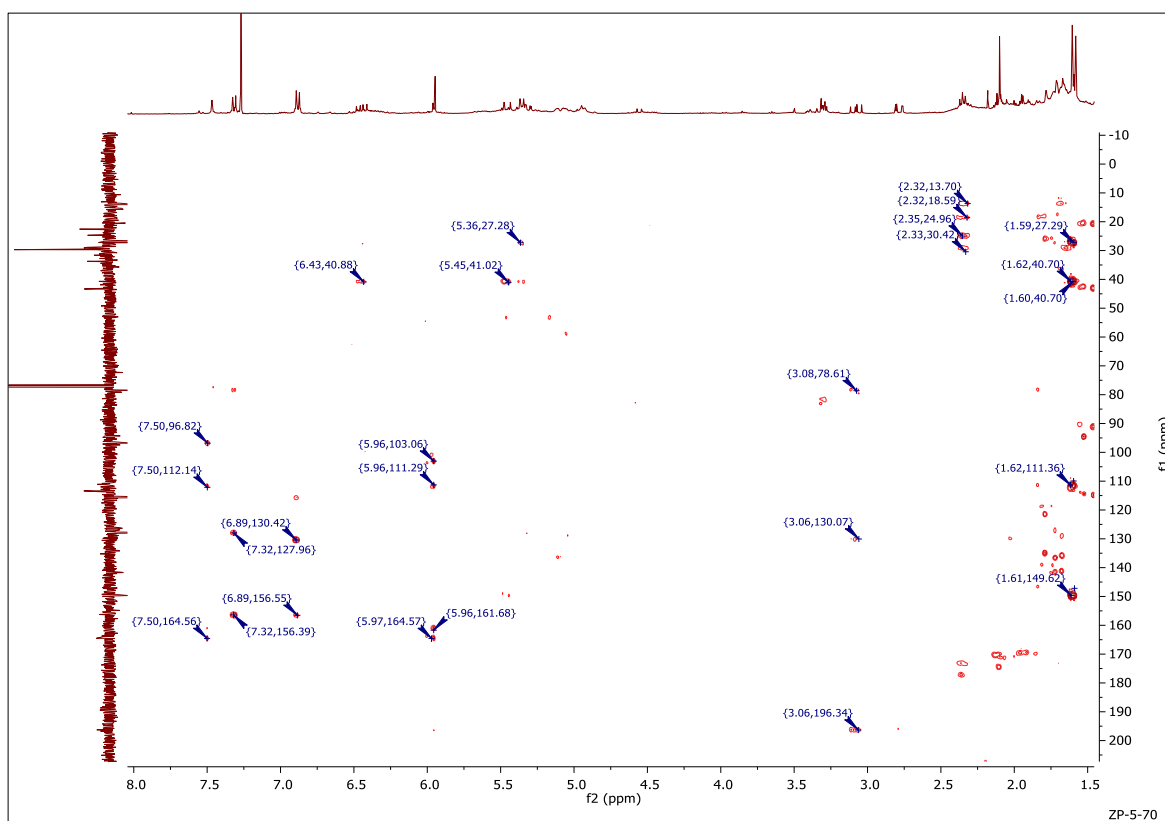
Figure 5-32: HMBC (400 MHz) Spectrum of the compound (14) labelled as ZP-F(3+4)-70 in CDCl₃

5.3.6.3 Characterization of TP-F4-(7-9) as 5-Hydroxy-4",4"-dimethyl-5"-methyl-5"-*H*-dihydrofurano[2",3",6,7]flavanone (15)

Compound **15** was obtained as a mixture which by comparing ring B protons in the NMR can be estimated to be composed of 52.4% compound **15** with 47.6% compound **14**. The LC-MS analysis of TP-F4-(7-9) in **Figure 5-33** exhibited multiple pseudo-molecular ion peaks, the main two characteristic peaks in negative mode were found at 339.1246 $C_{20}H_{19}O_5$, (Calc. 339.1233) and 323.1298 $C_{20}H_{19}O_4$, (Calc. 323.1283). For the compound isolated the IR spectrum showed the presence of an OH group at 3225 cm^{-1} carbonyl group (1700, 1650 cm-1) and 1650, 1500 cm^{-1} for the presence of aromatic rings. The proton spectrum is corresponding closely to those of compounds **13** and **14**, the major difference between their spectra was the absence of the isopentenyl side chain. This was replaced by a saturated furan ring fused to ring A of the flavanone at positions C-6 and C-7. The oxymethine furan proton was observed at δ_H 4.46 ppm while the three methyl groups on the furan ring were at 1.18, 1.43 and 1.36 ppm (**Figure 5-37**). The carbon spectrum (Dept-q) showed 20 carbon signals with three methyls, two oxygenated methines, one methylene, one carbonyl and 12 aromatic carbons

(**Figure 5-38**). The structure was confirmed using correlations in its 2D spectra (**Figures 5-39 to 5-41**) as follows; the furan proton (H-2") showed ^3J correlations to C-6 and C-7 in the HMBC spectrum thus confirming the furan ring being fused at those positions. Similar correlations for the 5-OH indicated C-6 to be a quaternary carbon, hence further confirming the furan ring being fused at C-6 and C-7. Also, the signals for H-3 protons were observed at δH3-a 2.73 (1H, dt, J =16.8, 4.2) and δH3-b 3.19 (1H, dd, J =17.0 ,13.1) that are coupled to each other as a 1H-1H COSY experiment. Furthermore, the signals of vicinal protons CH_3 were detected as doublets at δ_H 1.43 (3H, d, J =7.0, H-3") and δH 2" that are coupled to each other as a 1H-1H COSY experiment, showed (**Figure 5-40**).

Its chemical shift values were fully assigned as given in **Table 5-10**. The structure was a assigned as the novel compound 5-Hydroxy-4″,4″-dimethyl-5″-methyl-5″-H-dihydrofurano 312 [2″,3″,6,7]flavanone (**Figure 5-34**). The NMR assignments were further confirmed by comparison with the closely related compound iolated by Seo *et al* (Seo *et al*, 1997). The proton and carbon spectra were similar to those obtained by Seo et al where the compound they isolated differs from compound 3 in that the B ring is substituted with hydroxyl at position C-4 (Seo et al, 1997). Thuis, the carbon shifts obtained for compound 15 in rings A, C and the furan ring were similar to those in their compound 15 but the carbon signals in ring B were generally at lower shift values. In the proton spectrum there was an obvious envelope for the aromatic protons at δ_H 6.90 ppm. The MS^2 spectrum was consistent with the proposed structure and is shown in **figure 5-35** along with a proposed fragmentation scheme in **figure 5-36**
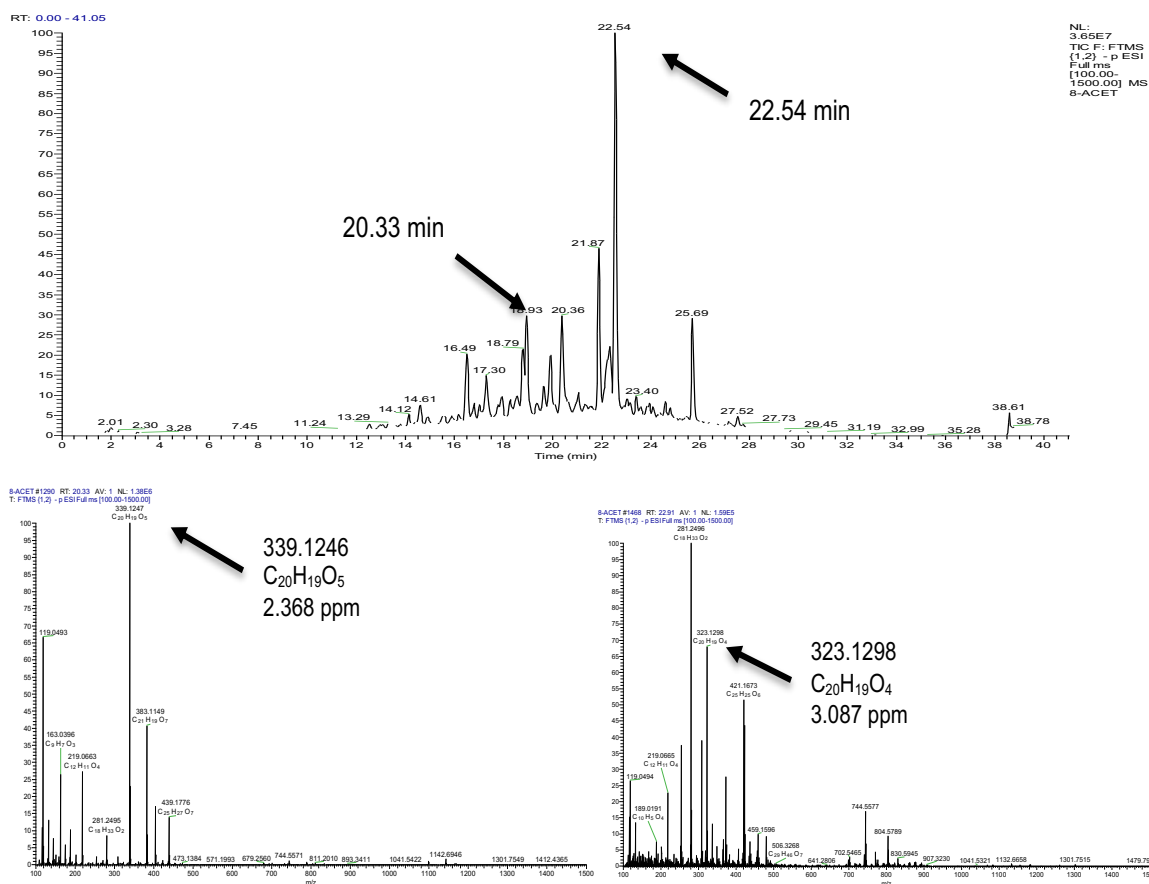
Figure 5-33: Mass ion chromatograms for the major compound (15) found in fraction TP-F4-(7-9). The mass spectrum shows the ion mass [M-H] - m/z 339.1246 (C20H19O5, 2.368 ppm) at RT=20.33 (min) and another ion mass [M-H] - m/z 323.1298 (C20H19O4, 3.087 ppm) at RT=22.54 (min) over the mass range of 100.00-1500.00 by using (LTQ) Orbitrap Mass Spectrometry (negative ion masses)

Chemical Formula: $C_{20}H_{20}O_4$
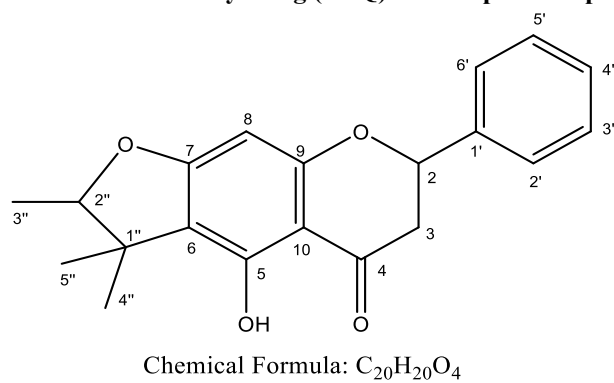
Figure 5-34: Structure of compound (15)
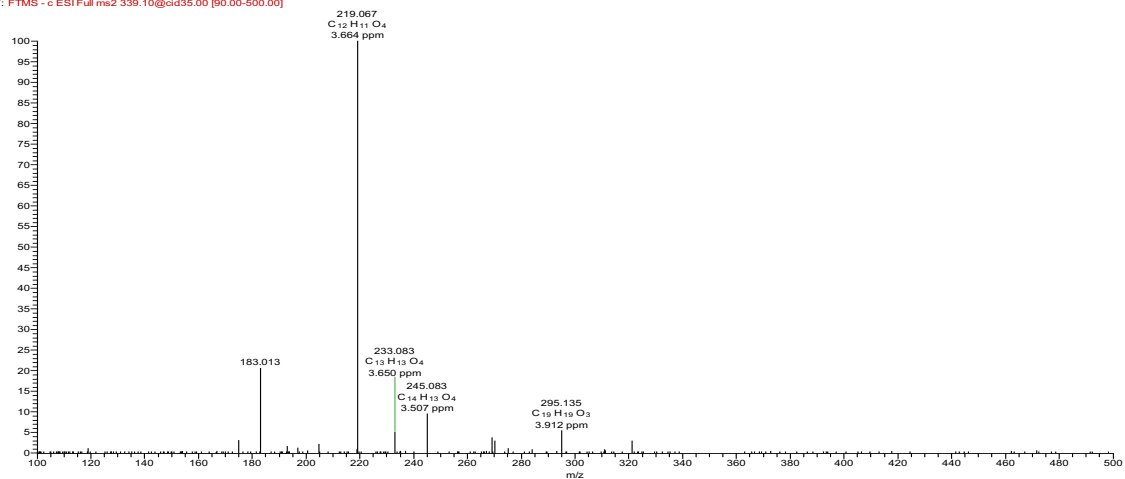
Figure 5-35: MS² spectrum of compound 15 over the mass range of 100.00-500. Obtained on an LTQ Orbitrap at a collision energy of 35V (negative ion masses)
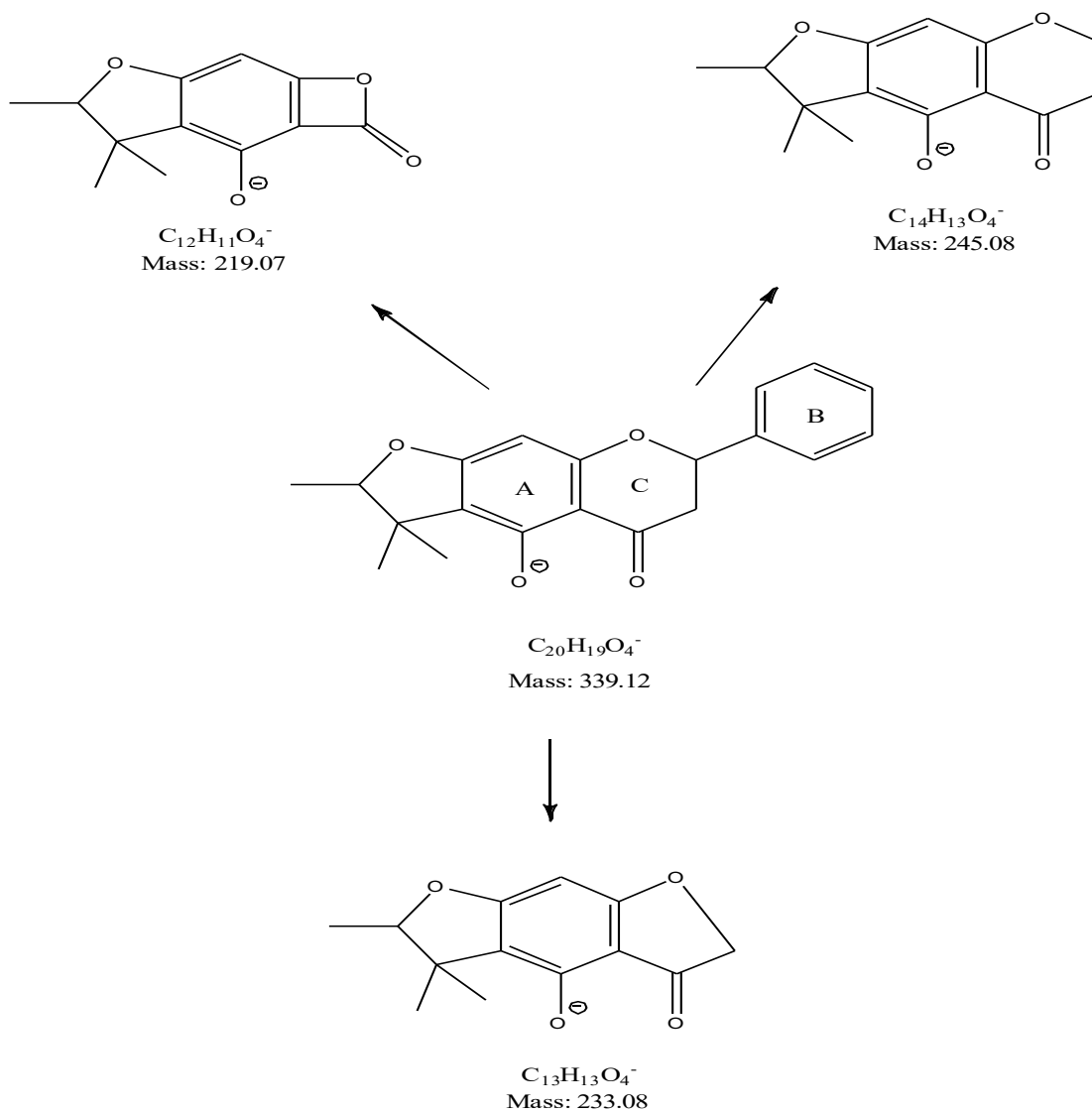
Figure 5-36: Suggested scheme for MS² fragmentation of compound 15

Table 5-10: ¹H (400MHz), ¹³C (100MHz) data of the compound (3) 5-Hydroxy-4",4"-dimethyl-5"-methyl-5"-*H*-dihydrofurano[2",3",6,7]flavone in fraction TP-F4-(7-9)

Position	Proton δ ppm (mult, *J* Hz)	Carbon δ ppm (mult)	COSY	HMBC
2	5.43 (1H, dd, *J* =13.0,3.0)	79.8 (CH)	H-3b	C-3
3	2.73(1H, dt, *J* =16.8, 4.2) 3.19 (1H, dd, *J* =17.0 ,13.1)	43.3 (CH₂)	H-3a- H-3b H-2	C-2, C-4
4	-	197.1 (C)	-	-
5	-	103.3 (C)	-	-
6	-	114.3 (C)	-	-
7	-	163.6 (C)	-	-
8	5.89 (1H, s)	90.9 (CH)	-	C-6, C-10
1'	-	129.7 (C)	-	-
2'	7.39 (1H, dd, *J* = 8.7, 2.8)	128.8 (CH)	H-3'	C-2, C-6'
3'	6.90 (1H, m)	115.9 (CH)	H-2'	C-1', C-5'
4'	6.90 (1H, m)	115.9 (CH)		C-2', C-3', C-5, C-6'
5'	6.90 (1H, m)	115.9 (CH)	H-6'	C-1' C-3'
6'	7.39 (1H, dd, *J* = 8.7, 2.8)	128.8 (CH)	H-5'	C-2, C-2'
1"	-	42.5 (C)	-	-
2"	4.46 (1H, q, *J* = 6.5)	91.4 (CH)	H-3''	
3"	1.36 (3H, d, *J* =7.0)	25.3 (CH3)	H-2''	C-1'', C-2''
4"	1.43 (3H, s)	14.2 (CH3)		C-1'', C-2'', C-6
5"	1.18 (3H, s)	20.7 (CH3)		C-1'', C-2'' C-4'', C-6
5-OH	12.45 (s)	96.5 (C)		C-6, C-9, C-10
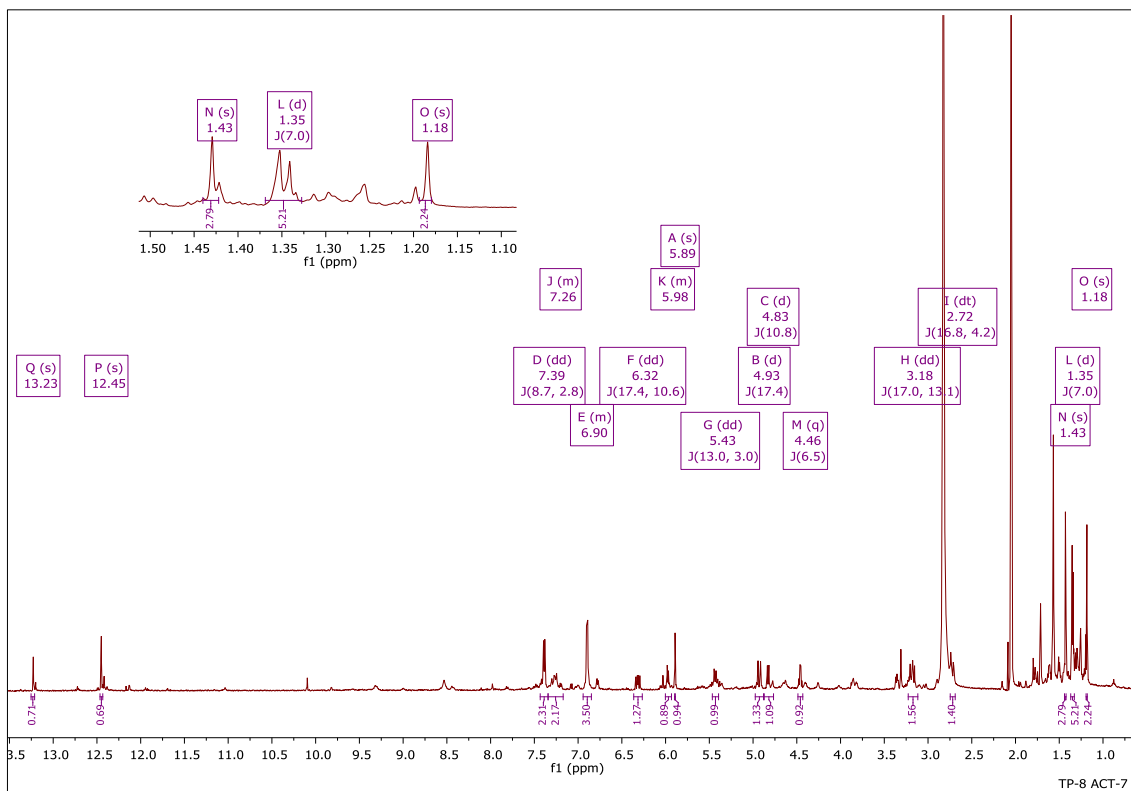
Figure 5-37: ^{1}H NMR (400 MHz) spectra of the compound (15) labelled as TP-F4-(7-9) in Aceton-d$_6$.
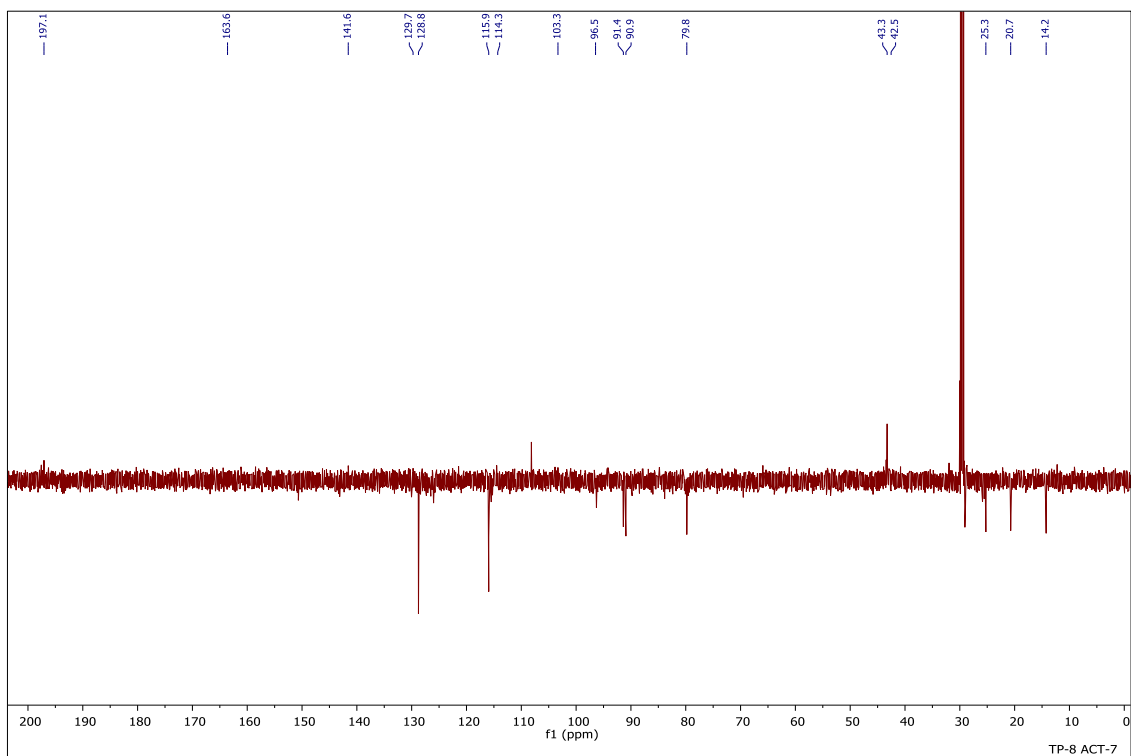
Figure 5-38: ^{13}C NMR (100 MHz) spectra of the compound (15) labelled as TP-F4-(7-9) in Aceton-d$_6$
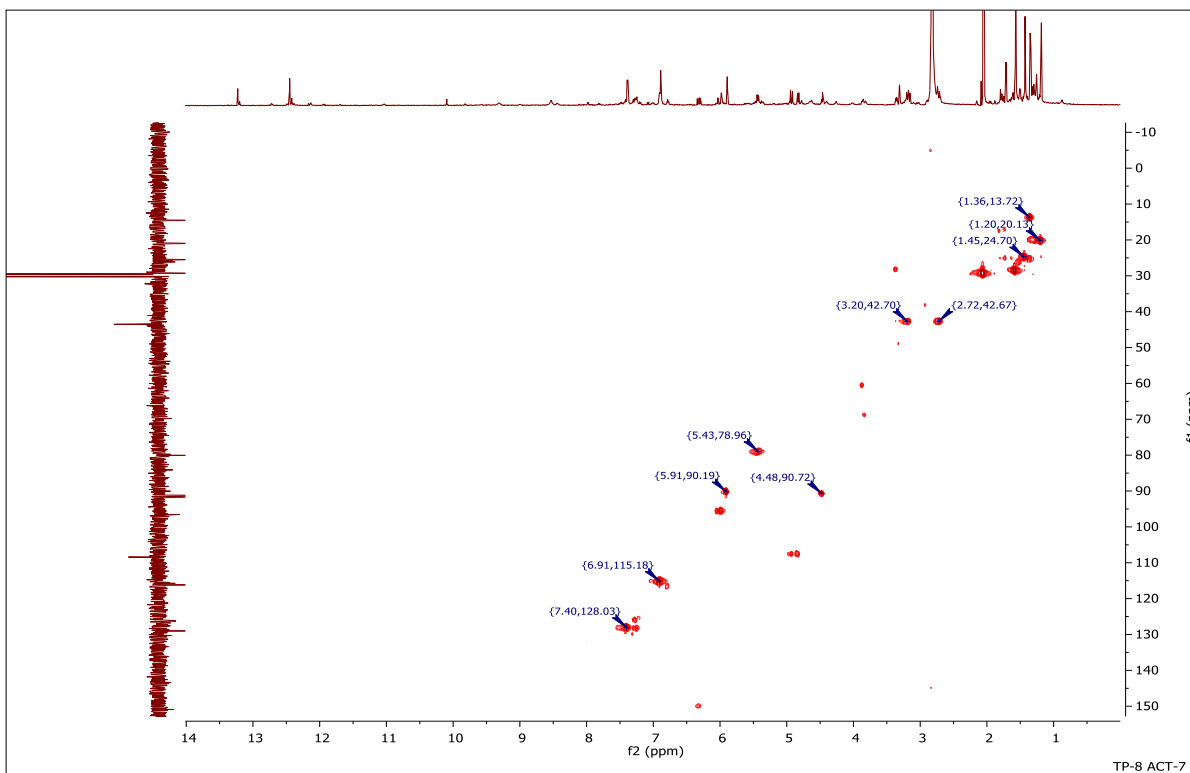
Figure 5-39: HSQC (400 MHz) Spectrum of the compound (15) labelled as TP-F4-(7-9) in Aceton-d$_6$
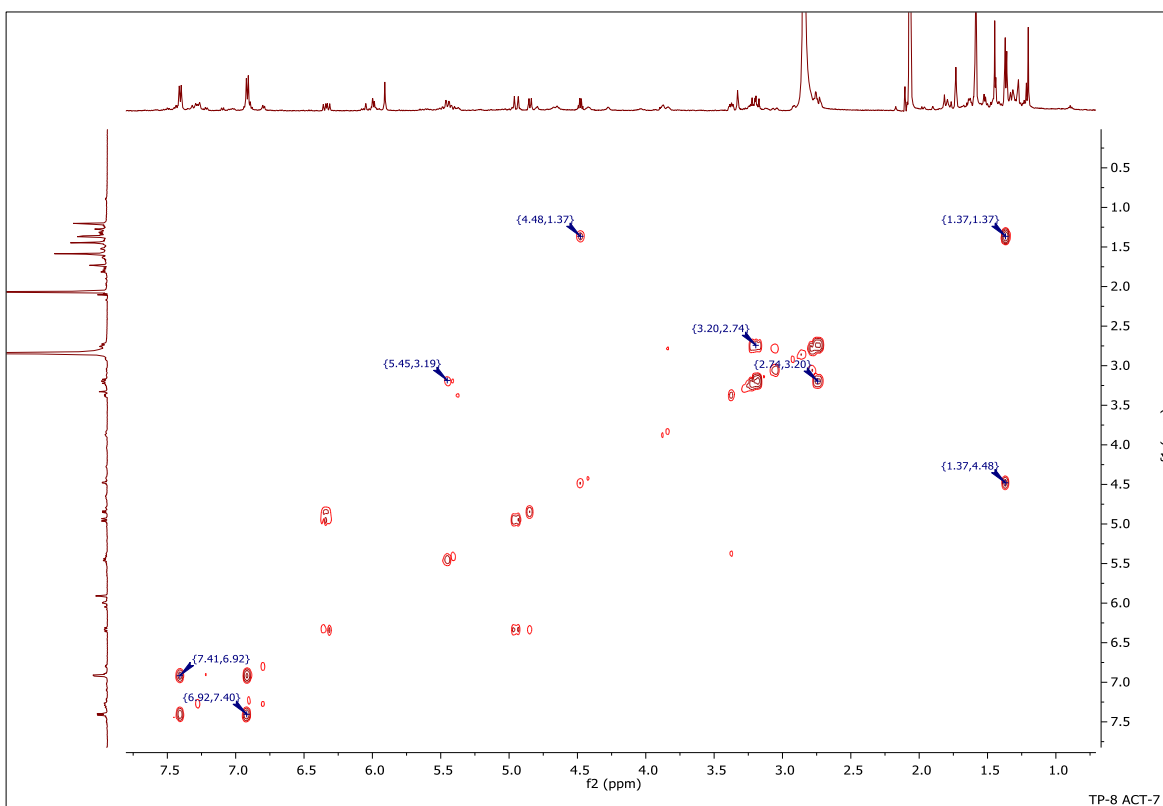
Figure 5-40: COSY (600 MHz) Spectrum of Compound (15) labelled as TP-F4-(7-9) in Aceton-d$_6$
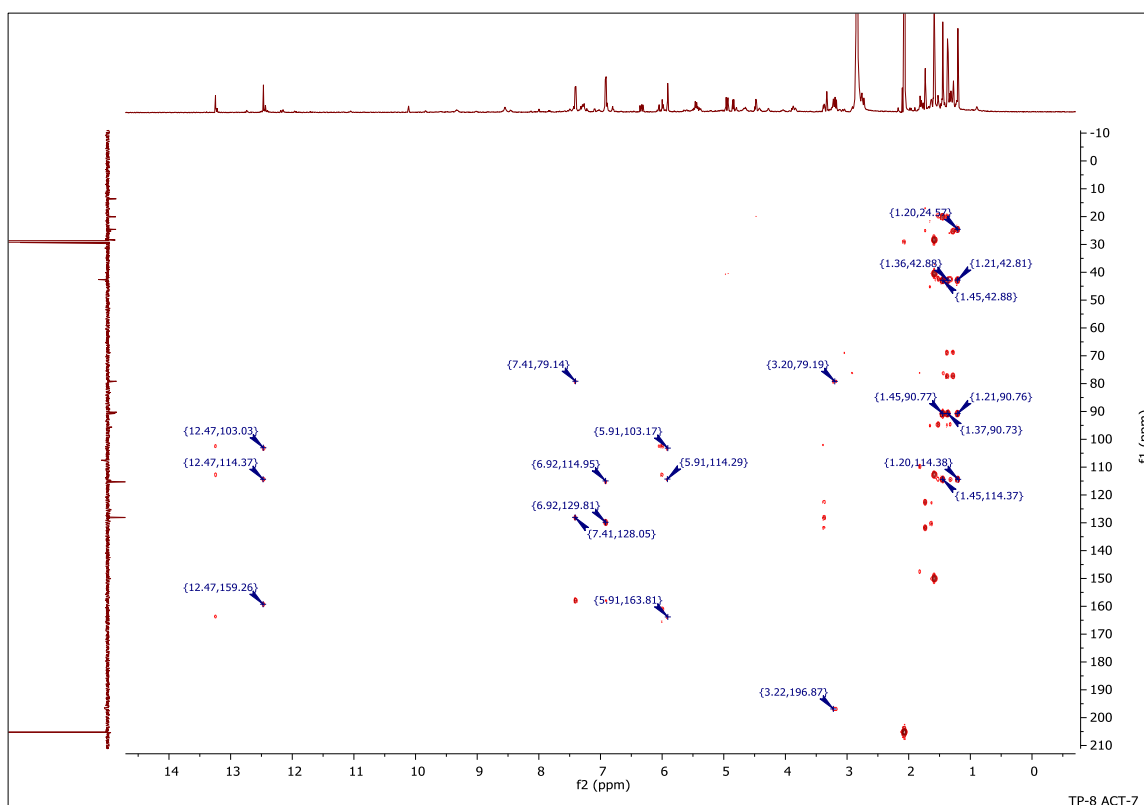
Figure 5-41: HMBC (400 MHz) Spectrum of the compound (15) labelled as TP-F4-(7-9) in Aceton-*d₆*

5.3.7 *In-vitro* Antitrypanosomal activity and cross-resistance studies of Zambian and Tanzanian propolis

The isolated compounds were also tested on the same drug sensitive and multi-drug resistant clones of *T. b. brucei* and *T. congolense*. The results are presented in the **Table 5-11**. Compound **14** from Zambian propolis displayed the highest activity against *T. b. brucei*, with an EC_{50} value of 2.24 µg/mL. Compounds **15+14** and **13** also displayed activity below 5 µg/mL, with EC_{50} values of 3.02 and 4.01 µg/mL, respectively. The EC_{50} values for the multidrug resistant strain B48 were within 1~1.2-fold ($P > 0.05$), thus the compounds were not cross-resistant with first-line HAT treatments pentamidine and melarsoprol (Bridges et al., 2007). The RF for pentamidine, included as control, was 144 ($P = 0.0003$; **Table 5-11**). Like the fractions tested above, the purified compounds displayed somewhat less potent activity against *T. congolense* than against *T. brucei* under the assay conditions, with EC_{50} values of 7.35, 10.47 and 13.77 µg/mL for compounds **14, 13**, and **15+14**, respectively. Again, no cross-resistance was observed with the main AAT treatment, diminazene aceturate (RF~1; $P > 0.05$; compared to RF = 9.8 for diminazene) **Table 5-12.**

Table 5-11: EC$_{50}$ values of purified compounds isolated from ZP and TP propolis samples against _T. brucei_ (n=3).

Purified Compounds	_T. b. brucei_ s427 WT		_T. b. brucei_ B48			
	EC$_{50}$ ± SEM (µg/mL)	EC$_{50}$ ± SEM (µM)	EC$_{50}$ ± SEM (µg/mL)	EC$_{50}$± SEM (µM)	RF	_P_
(13)	4.01 ± 0.26	12.4 ± 0.78	4.94 ± 0.22	15.3 ± 0.69	1.23	0.051
(14)	2.24 ± 0.13	6.58 ± 0.39	2.28 ± 0.16	6.69 ± 0.48	1.02	0.87
(15+14)	3.02 ± 0.27	-	3.61 ± 0.23	-	1.20	0.17
Pentamidine		0.0034 ± 0.0004		0.4929 ± 0.04	144.08	0.0003

The EC$_{50}$ values are the average and SEM of at least 3 independent determinations. RF= Resistance factor, being EC$_{50}$(WT)/EC$_{50}$(B48). Statistical significance was determined using an unpaired two-tailed Student's t-test comparing the EC$_{50}$ values of the resistant strain with those obtained for the control strain s427.

Table 5-12: EC$_{50}$ values of purified compounds isolated from ZP and TP propolis samples on T. congolense IL300, and a T. congolense cell line resistant to diminazene (n=3).

Purified Compounds	_Trypanosoma congolense_ IL3000		_Trypanosoma congolense_ 6C3			
	EC$_{50}$ ± SEM (µg/mL)	EC$_{50}$ ± SEM (µM)	EC$_{50}$ ± SEM (µg/mL)	EC$_{50}$ ± SEM (µM)	RF	_P_
(13)	10.47 ± 0.96	32.30 ± 2.96	9.03 ± 0.43	27.85 ± 1.33	0.86	0.2430
(14)	7.35 ± 0.71	21.61 ± 2.08	5.69 ± 0.61	16.74 ± 1.79	0.77	0.1506
(15+14)	13.77 ± 1.26	-	12.94 ± 1.04	-	0.94	0.6383
Diminazene	0.15 ± 0.03			1.45 ± 0.04	9.81	<0.0001

The EC$_{50}$ values are the average and SEM of at least 3 independent determinations. RF= Resistance factor, being EC$_{50}$(WT)/EC$_{50}$(B48). Statistical significance was determined using an unpaired two-tailed Student's t-test comparing the EC$_{50}$ values of the resistant strain with those obtained for the control strain s427.

5.3.8 _In vitro_ cytotoxicity of Zambian and Tanzanian propolis on mammalian cells

The purified compounds and the most active fractions that were isolated from Tanzanian and Zambian propolis were tested _in vitro_ on a Human U937 cell line and a murine RAW 246.7 cell line using the resazurin assay. The results showed very low levels of toxicity, with similar EC$_{50}$ values for both cell lines (**Table 5-13**). As the fractions and isolated compounds were more active against _T. b. brucei_ than against _T. congolense_, the Selectivity Index (SI), being the ratio of the mammalian cell line EC$_{50}$ and the parasite cell line EC$_{50}$, was higher for _T. b. brucei_, with values for the isolated compounds between 15 and 70, compared to 7 up to 17 for _T. congolense_. Interestingly, as the crude fractions displayed both higher trypanocidal activity

and lower toxicity, the SI values for the fractions were much higher and were >100 for Tanzanian crude propolis relative to both *Trypanosoma* species (**Table 5-13**).

Table 5-13: EC$_{50}$ of cytotoxicity of Zambian and Tanzanian propolis samples and the purified compounds against U937 cell line and RAW 246.7 cell line.

Sample/ Compound	U937				RAW 246.7			
	EC$_{50}$± SEM (µg/mL)	EC$_{50}$± SEM (µM)	Selectivity Index (SI)		EC$_{50}$± SEM (µg/mL)	EC$_{50}$± SEM (µM)	Selectivity Index (SI)	
			Tbb427WT	TcoIL3000			Tbb427 WT	TcoIL3000
ZP crude	166.2 ± 3.3	--	40.1	11.5	199.5 ± 1.7	--	48.2	13.9
ZP-F2+F3	71.6 ± 2.8	--	70.2	13.0	74.9 ± 2.8	--	73.4	13.6
(13)	59.9 ± 5.2	184.7 ± 16.2	14.9	6,6	60.7 ± 1.4	187.3 ± 4.4	15.1	6.7
(14)	51.2 ± 3.1	150.5 ± 9.2	22.8	9.0	79.9 ± 5.6	235.0 ± 16.4	35.7	14.0
TP crude	148.0 ± 2.4	--	123.4	101.4	91.3 ± 3.2	--	76.1	62.6
TP-F4	98.2 ± 4.8	--	41.6	16.6	114.4 ± 5.9	--	48.5	19.3
(15+14)	90.5 ± 4.2	-	30.0	7.0	97.5 ± 7.9	-	3 2.3	7.5

All EC$_{50}$ values are the average and SEM of at least 3 independent experiments. SI = EC$_{50}$(mammalian cell line) / EC$_{50}$(*Trypanosoma* species*)*.

Chapter Six

6 Chemical Characterisation of Nigerian Red Propolis and *In-vitro* Studies of Antitrypanosomal Activities and Cross-Resistance

6.1 Introduction

Propolis samples from Nigeria have been previously investigated for their major constituents. One of study identified phenolic compounds including calycosin, liquiritigenen, pinocembrin, vestitol, medicarpin, prenylnaringenin, and macarangin, in addition to xanthones and some triterpenes in the samples. The results of *in vitro* anti-trypanosomiasis assays of Nigerian propolis indicated high activity against *Trypanosoma brucei* and other protozoa (Omar et al., 2017). A recent study also investigated the chemical composition Nigerian propolis by means of combined chromatographic and spectroscopic techniques and identified isoflavonoids, diarylpropanes and flavanones. A study also tested the antioxidant activity and α-amylase and α-glucosidase inhibition of Nigerian propolis *in vitro* and the results suggested that Nigerian propolis could be a good raw material for nutraceuticals and food products (Alaribe et al., 2019). Other studies investigated the anti-*helicobacter pylori* activity *in vitro*, and found potent inhibitory activity of Nigerian propolis and thus it could also be a promising antibiotic agent against *H. pylori* (Chinwe et al., 2013)

6.2   Method of extraction

The raw Nigerian propolis sample was extracted using ethanol. The crude extract weighted approximately 12g, was treated with solvents and mixtures of solvents of varying polarities and in different proportions, using of ethyl acetate and hexane in a ratio of 1: 6, and dichloromethane and hexane in a ratio of 1: 6 respectively. The resulting fractions (RN-DCM crude, RN-DCM-ppt, RNE (EtOAc) crude ppt and RN-Hx) were monitored and profiled using 1H NMR Figures 6-2 to 6-5. **Figure 6-1** shows the protocol used for fractionation of the extract of red Nigerian propolis. General details of the apparatus used, and the materials are given in chapter 2.

6.3   Results and Discussion

6.3.1 Extraction, Isolation and purification of compounds (16, 17, 18, 19 and 20) from Nigerian Red propolis

It is clear that propolis samples from Nigeria are rich with a variety of compounds. Therefore, the present study is on the isolation of compounds from a sample of Nigerian propolis using a different extraction and isolation methods. The resulting fractions (RN-DCM crude, RN-DCM-ppt, RNE (EtOAc) crude ppt and RN-Hx) were monitored and profiled using 1H NMR Figures 6-2 to 6-5. Then CC was used to isolate pure compounds from RN-DCM crude as the following: 7-O-methylvestitol (16), neovestitol (17). Also, another CC was conducted to isolate pure compounds from RN-E as the following: vestitol (18), medicarpin (19), and 7-hydroxyflavanone (20). The compounds obtained were tested for activity against BSF T. b. brucei s427 WT and T. b. brucei B48; BSF T. congolense Tc-IL3000 WT and T. congolense 6C3, and for their cytotoxicity on U937 and RAW 246.7 cell lines. Figures 6-1 shows workflows for the extraction and fractionation of the Nigerian propolis sample
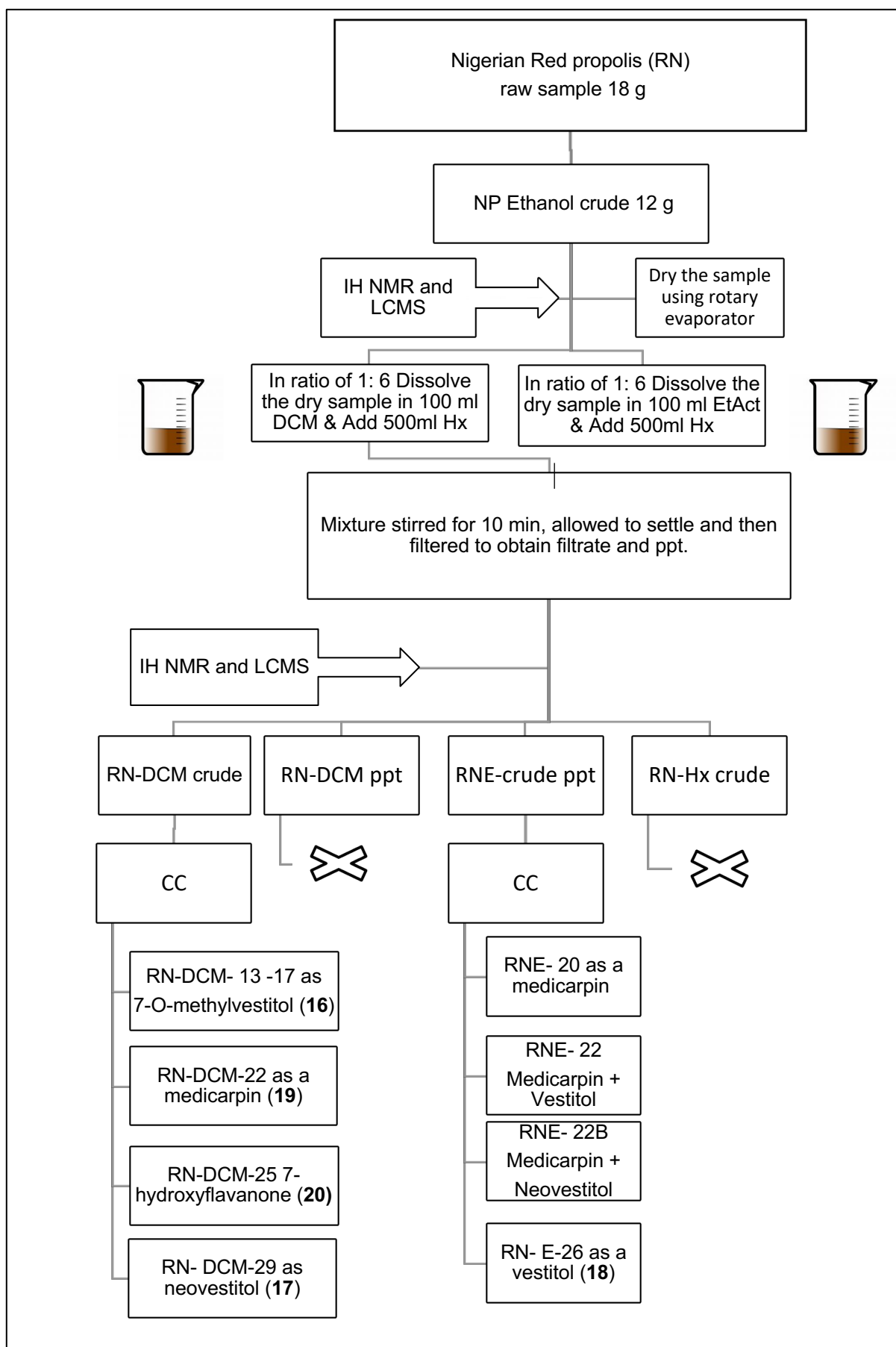
Figure 6-1: Workflow of Nigerian propolis analysis

6.3.2 Chemical profiling of the crude red Nigerian Propolis (RN)
6.3.2.1 Characterization of ethanol extract Nigerian Propolis using 1HNMR

The proton nmr (**Figure 6-2**) of the ethanolic Nigerian propolis extract showed the presence of triterpenoids with methyl group signals observed between δ_H 0.18 and 2.56 ppm. The triterpenoids must be of the cycloartane type as there were cyclopropane protons at 0.30 and 0.49 ppm which could imply mangiferolic/isomangiferolic acid or cycloartenol. There was little evidence for the presence of flavonoids containing the 5-OH chelated to a 4-C=O at 13.58 ppm which could also possibly be some xanthones with similar H-bonded –OH protons. The NMR spectrum also showed the presence of oxygenated methine or methylene protons between 4.00 and 5.20 ppm indicating the presence of lignans or flavans/isoflavans and the presence of aromatic and olefinic protons between 6.12 and 7.14 ppm was confirmation of the aromatic moieties in the flavonoids, lignans, flavans and isoflavans. There was also evidence for the presence of phenolic hydroxyls (between 0.89 and 9.69 ppm) and methoxy protons at 3.68 and 3.66 ppm implying the substitution of hydroxyl and methoxy groups in the aromatic rings.

E35249.1.fid — Person sameah alenezi — Nigeria crude
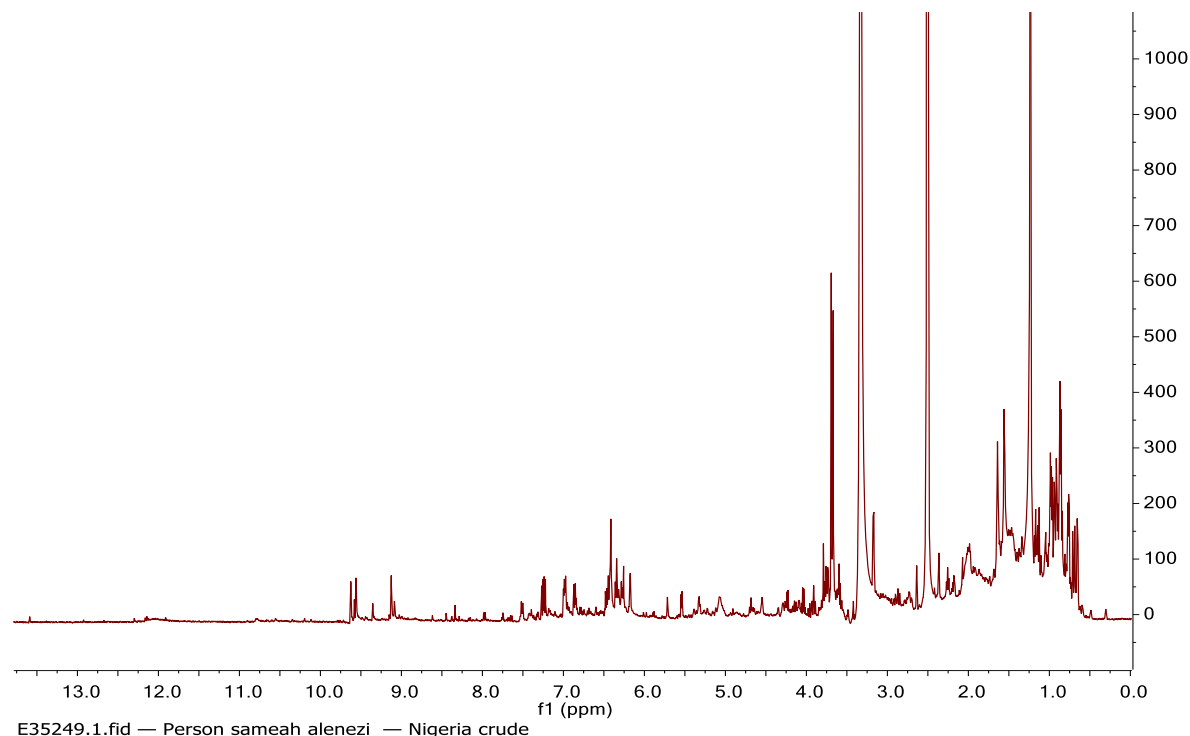
Figure 6-2: ^{1}H NMR (500 MHz) spectrum of the ethanolic crude RN propolis sample in DMSO-d_6

6.3.2.2 Characterization of Nigerian Propolis crude extracts using 1HNMR

The ethanolic extract of the Nigerian propolis was further fractionated as described in **Figure 6.1.** Based on HNMR results of the fractionations of the ethanolic crude extract of the Nigerian sample into four crudes called RN-DCM, RN-DCM-ppt , RNE (RN-EtOAc) and RN-H$_x$ (**Figures 6-3 to 6-6**), the RN-DCM (the supernatant) and RN-E (RN-EtOAc- the precipitate) were selected for further fractionation since they appeared to be rich in phenolic compounds. The profiling of the selected Nigerian propolis crudes were carried out on HPLC-MS. The profiling of the RN-DCM and RN-EtOAc crudes by LC-MS in (**Table 6-1, Figure 6-7)** and (**Table 6-2, Figure 6-8)** suggested a high content of flavonoids, lignans or any other phenolic compounds with varying degrees of oxygenation.
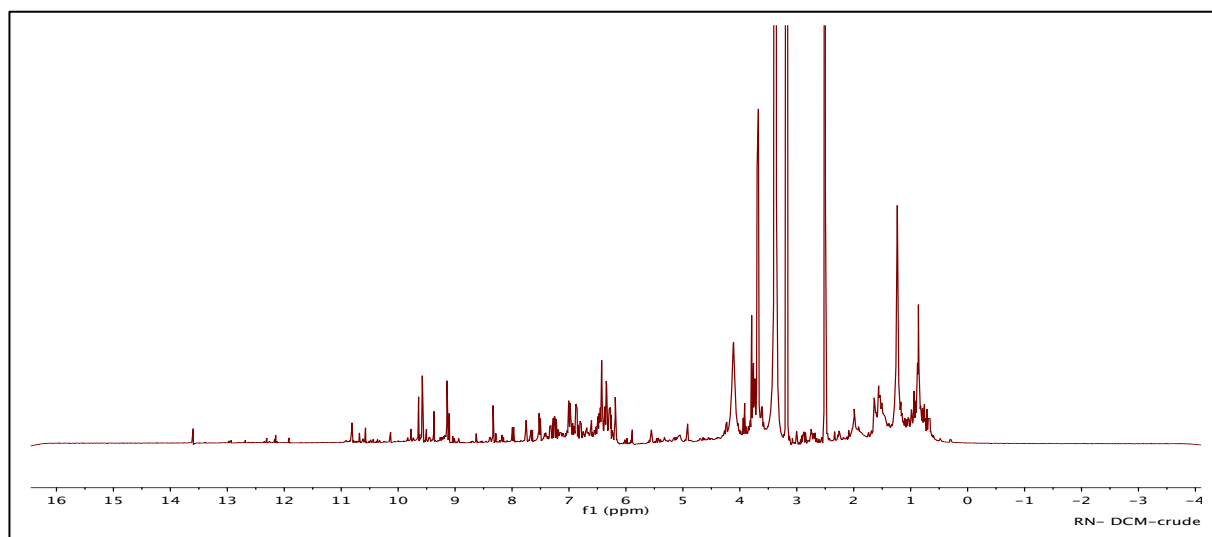
Figure 6-3: ^{1}H NMR (500 MHz) of the DCM crude RN propolis sample (supernatant prepared as described in figure 6.1) in DMSO-*d₆*
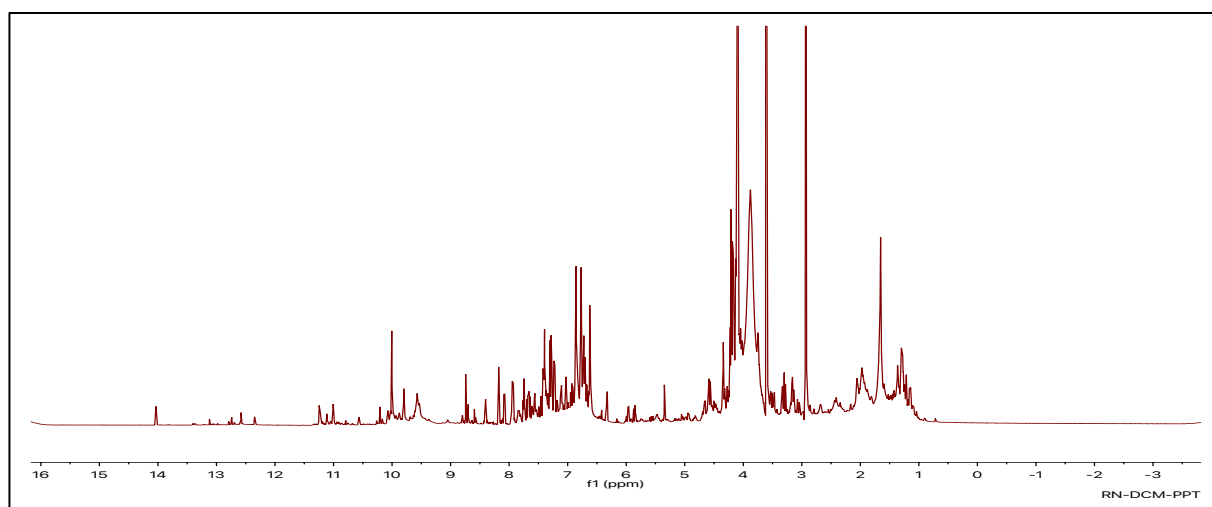
Figure 6-4: ^{1}H NMR (500 MHz) of the DCM-ppt crude RN propolis sample (precipitate prepared as described in figure 6.1) in DMSO-*d₆*
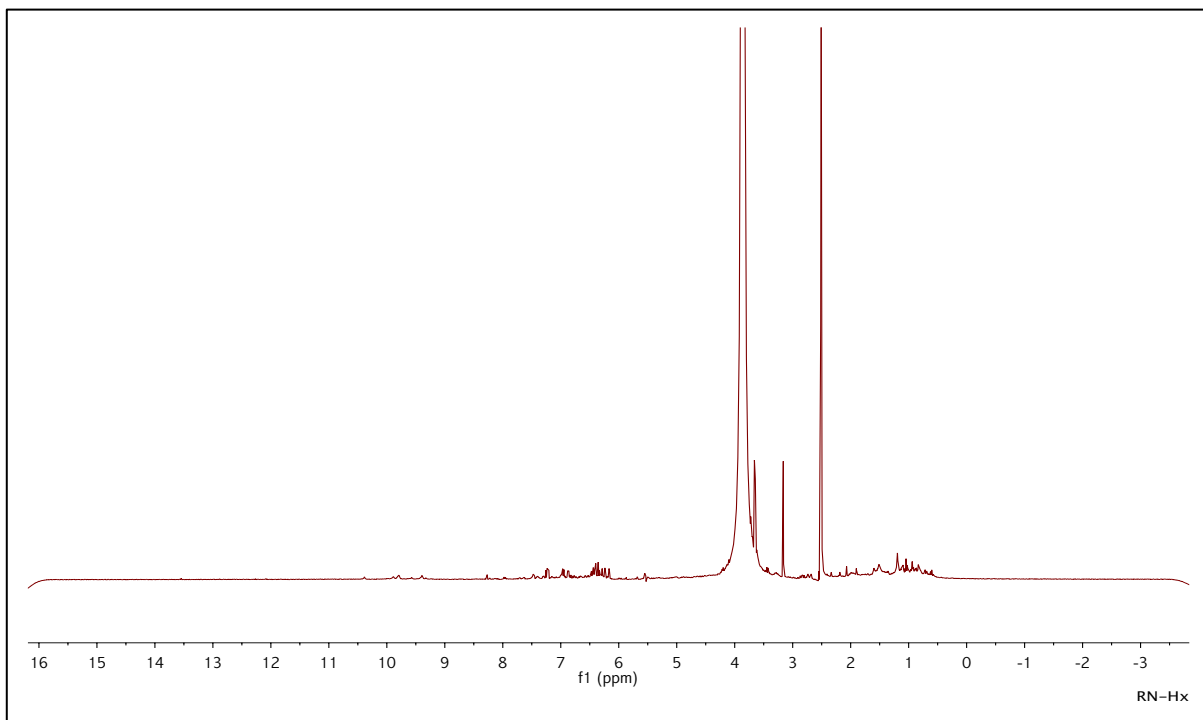
Figure 6-5: ^{1}H NMR (500 MHz) of the Hx extract of RN propolis sample (supernatant prepared as described in figure 6.1) in DMSO-*d₆*
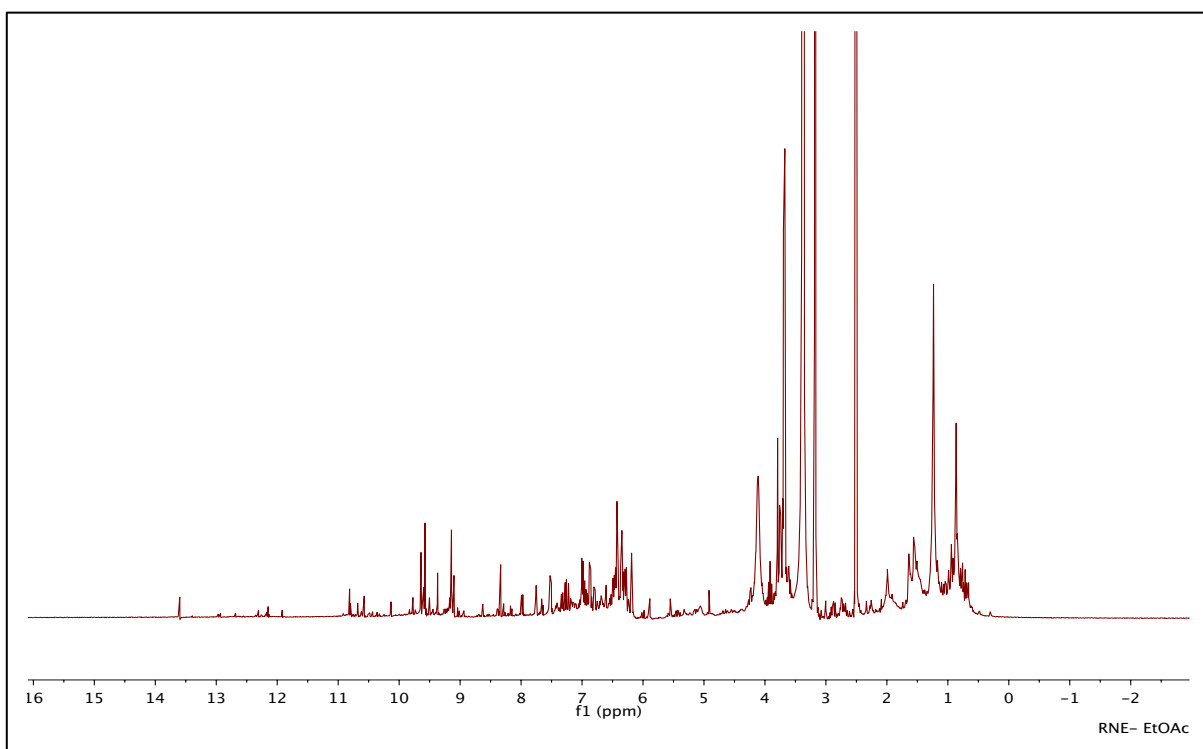
Figure 6-6: ^{1}H NMR (500 MHz) of the EtOAc extract of RN propolis sample (precipitate prepared as described in figure 6.1) in DMSO-*d₆*

6.3.2.3 Characterization of Nigerian Propolis crude RN-DCM extract using LC-MS (negative ion)
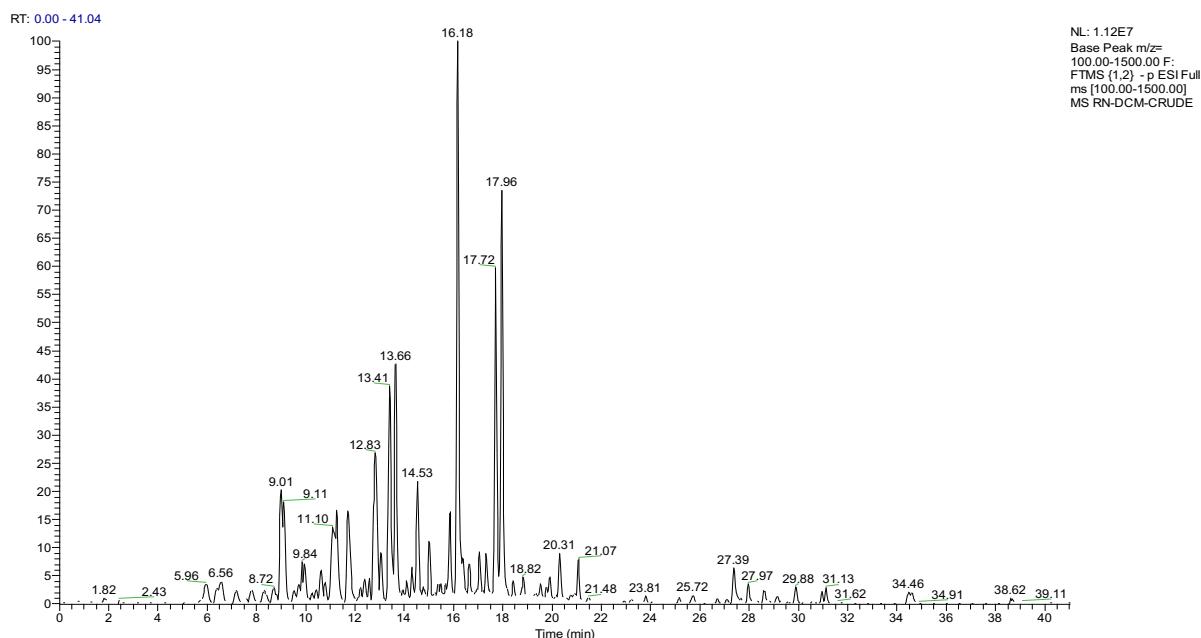
Figure 6-7: LC-MS spectral analysis of the RN-DCM crude

Table 6-1: High resolution MS profiling of RN-DCM crude using the negative ion masses in the LCMS

Peak no	RT (min)	M-1	Formula	RDB	Delta (ppm)	Intensity
1	9.01	315.0867	$C_{17}H_{15}O_6$	10.5	-2.25	1.78E6
2	11.24	271.0608	$C_{16}H_{11}O_5$	10.5	-1.61	1.67 E6
3	12.83	255.0659	$C_{15}H_{11}O_4$	10.5	-1.65	2.21E6
		301.0712	$C_{16}H_{13}O_6$	10.5	-1.96	
4	13.41	267.0657	$C_{16}H_{11}O_4$	11.5	-2.29	3.91E6
5	13.66	267.0660	$C_{16}H_{11}O_4$	11.5	-1.31	3.51E6
6	14.53	271.0971	$C_{16}H_{15}O_4$	9.5	-1.85	2.34E6
7	15.87	271.0971	$C_{16}H_{15}O_4$	9.5	-1.85	1.82E6
8	16.18	269.0814	$C_{16}H_{13}O_4$	10.5	-2.13	1.11E7
9	17.72	255.0656	$C_{15}H_{11}O_4$	10.5	-2.12	6.68E6
10	17.96	266.0579	$C_{16}H_{10}O_4$	12.0	-2.02	8.20E6
11	18.82	285.1128	$C_{17}H_{17}O_4$	9.5	-1.446	5.24E5
12	20.31	240.0422	$C_{14}H_8O_4$	11.0	-2.49	7.35E5
			$C_{16}H_{15}O_4$	9.5	-0.97	

6.3.2.4 Characterization of Nigerian Propolis crude RN-E extract using LC-MS (negative ion)
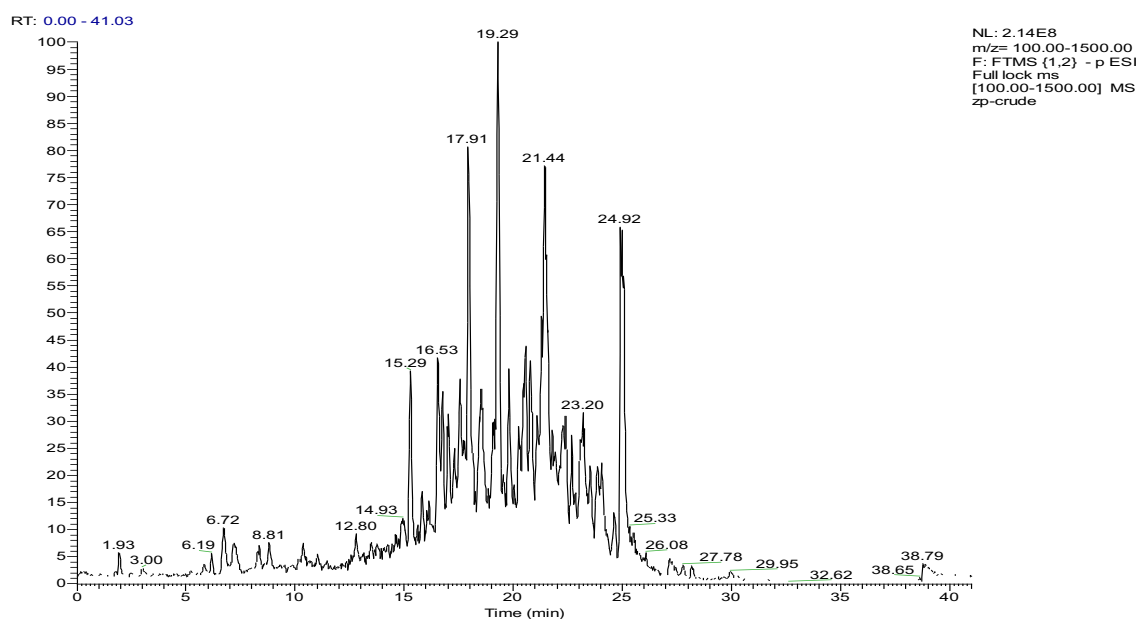
Figure 6-8: LC-MS spectral analysis of the RN-E crude

Table 6-2: High resolution MS profiling of RN-E crude using the negative ion masses in the LCMS

Peak no	RT (min)	M-1	Formula	RDB	Delta (ppm)	Intensity
1	6.72	287.0562	$C_{15}H_{11}O_6$	10.5	0.45	7.93E6
		329.1607	$C_{16}H_{25}O_7$	4.5	0.41	
2	15.29	323.1291	$C_{20}H_{19}O_4$	11.5	0.55	2.37E7
3	15.84	439.1763	$C_{25}H_{27}O_7$	12.5	0.24	1.36E7
4	16.53	455.1715	$C_{25}H_{27}O_8$	12.5	0.88	1.88E7
5	17.52	339.1240	$C_{20}H_{19}O_5$	12.5	0.48	2.76E7
6	17.91	383.1141	$C_{21}H_{19}O_7$	12.5	1.16	9.84E7
7	18.56	395.1138	$C_{22}H_{19}O_7$	13.5	0.36	2.32E7
		339.1240	$C_{20}H_{19}O_5$	11.5	0.66	
8	19.29	381.1346	$C_{25}H_{21}O_6$	12.5	0.57	5.77E7
		319.2280	$C_{20}H_{31}O_3$	5.5	0.41	
9	19.82	417.2288	$C_{24}H_{33}O_6$	8.5	1.33	1.72E7
		485.3277	$C_{30}H_{45}O_5$	8.5	0.87	
10	20.78	339.1240	$C_{20}H_{19}O_5$	11.5	0.57	2.36E7
		483.2025	$C_{27}H_{31}O_8$	12.5	0.54	
11	21.44	367.1190	$C_{21}H_{19}O_6$	12.5	0.76	7.76E7
		339.1241	$C_{20}H_{19}O_5$	11.5	1.04	
12	23.20	423.1818	$C_{25}H_{27}O_6$	12.5	1.20	3.62E7
13	23.52	423.1815	$C_{25}H_{27}O_6$	12.5	0.49	1.46E7
		323.1291	$C_{20}H_{19}O_4$	11.5	0.64	
14	24.92	407.1865	$C_{25}H_{27}O_5$	12.5	0.30	6.65E7

6.3.2.5 Characterization of RN-DCM- 13 -17 as 7-O-methylvestitol (16)

The compound was obtained from the ethanol extract of the Nigerian red propolis sample using column chromatography of RN-DCM crude as indicated on a schematic diagram **Figure 6-1**. Fractions 13-17 were combined based on TLC. The LC-MS chromatogram gave a peak at 18.75 min and an [M-H]$^-$ ion at m/z 285.1126 corresponding to $C_{17}H_{17}O_4$ (Calc 285.1127) in the negative mode, and an [M+H]$^+$ ion at m/z 287.1269 ($C_{17}H_{19}O_4$, calc 287.1283) in the positive mode (**Figure 6-10**). This indicated the molecular formula to be $C_{17}H_{18}O_4$. ESI-MS/MS (negative mode), also provided fragments masses at *m/z* 121.0290 ($C_7H_5O_2$), *m/z* 123.0473 ($C_7H_7O_2$), *m/z* 135.0446 ($C_8H_7O_2$). The fragment at *m/z* 135.0446 is consistent with a fragment from the B ring while the fragment at *m/z* 123.0473 is obtainable from ring A. The proton nmr in CDCl$_3$ (**Figure 6-11**) gave two sets of ABX coupled aromatic protons at δ_H 7.01 (d, *J* = 8.5 Hz), 6.47 (dd, *J* = 8.4, 2.6 Hz) and 6.36 (d, *J* = 2.5 Hz), and the other set at 6.98 (d, *J* = 8.3 Hz), 6.47 (dd, *J* = 8.4, 2.6 Hz) and 6.42 (d, *J* = 2.6 Hz) inferring two tri-substituted aromatic rings in the compound. The rest of the signals were for five aliphatic coupled (COSY) protons at 4.34 (ddd *J* = 10.5, 3.5, 2.0 Hz) 4.05 (m), 3.51 (m), 3.01 (ddd, *J* = 15.7, 10.5, 1.1) and 2.94 (ddd, *J* = 15.8, 5.4, 1.9 Hz). The ^{13}C Dept-q spectrum showed the presence of 17 signals comprising of 12 aromatic, three aliphatic and two methoxy carbons. Four of the aromatic carbons were phenolic. One of the aliphatic carbons was an oxymethylene at δ_C 69.6 ppm (**Figure 6-12**). The structure was elucidated based on its 2D NMR spectra (**Figures 6-13 to 6-15**) as follows: Correlations from the two aromatic doublets identified the rings and their substitutions. The aromatic rings had one methoxy group each, both at 3.77 ppm. The aliphatic protons at δ_H 2.93 and 3.01 showed long range ^3J correlations to the two aromatic rings hence each of the rings must be 3-bonds away from the CH$_2$. This implies an isoflavan type moiety and was confirmed by other correlations from the rest of the protons in the HMBC spectrum (**Figure 6-14**) and literature reports (Piccinelli et al., 2005, Campo Fernández et al., 2008). Thus, enabled the identification of the compound as 7-O-methylvestitol (**Figure 6-9**). The chemical shifts for the protons and carbons were fully assigned as given in **Table 6-3**.
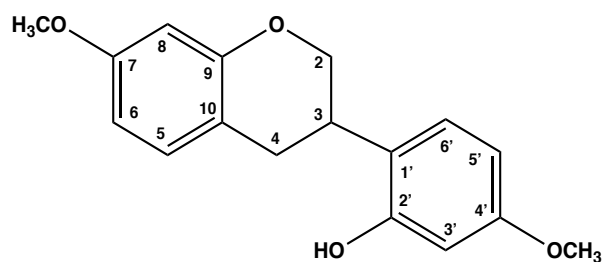
Chemical Formula: $C_{17}H_{18}O_4$

Figure 6-9: Structure of 7-O-methylvestitol (16)
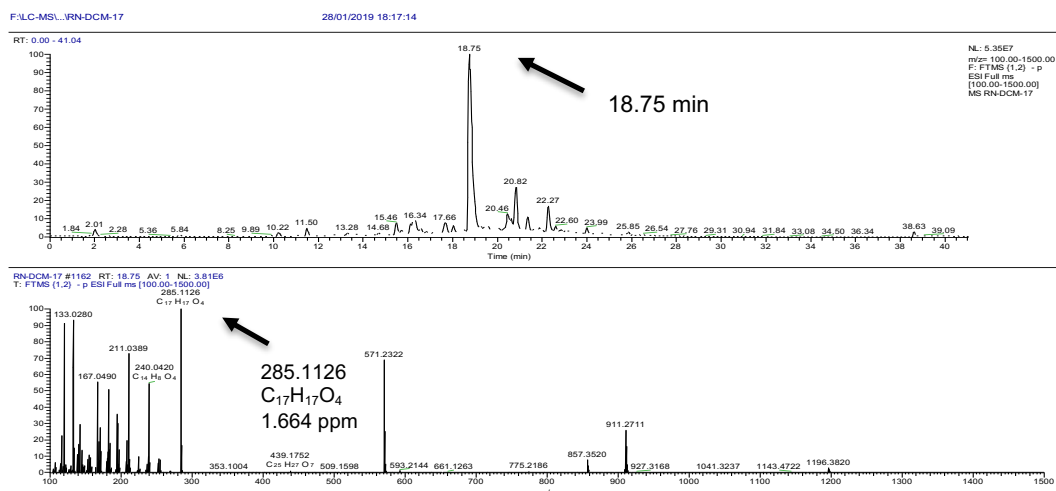
Figure 6-10: LC-MS chromatogram (ESI negative mode) for compound 16.

Table 6-3: ^{1}H and ^{13}C data of compound 16

Position	Proton δ ppm (mult, *J* Hz)	Carbon δ ppm (mult)
2	4.34 (1H, ddd *J* = 10.47, 3.46, 1.98) 4.05 (1H, m)	69.9 (CH$_2$)
3	3.51 (1H, m)	31.7 (CH)
4	3.01 (1H, ddd *J* = 15.73, 10.54, 1.08) 2.91 (1H, ddd *J* = 15.82, 5.40, 1.92)	30.3 (CH$_2$)
5	7.01 1H, d *J* = 8.52)	128.2 (CH)
6	* 6.47 (1H, dd *J* = 8.40, 2.56)	107.2 (CH)
7	-	159.0 (C)
8	6.36 (1H, d *J* = 2.52)	102.1 (CH)
9	-	155.0 (C)
10	-	119.9 (C)
1'	-	114.4 (C)
2'	-	154.2 (CH)
3'	6.42 (1H, d, *J* = 2.58)	101.4 (CH)
4'	-	159.3 (CH)
5'	* 6.47 1H, dd *J* = 8.40, 2.56)	106.1 (CH)
6'	6.98 (1H, dd, *J* = 8.28, 1.00)	130.2 (CH)
7-OCH$_3$	3.77 (3H, s)	55.3 (CH$_3$)
4'- OCH$_3$	3.77 (3H, s)	55.3 (CH$_3$)

169
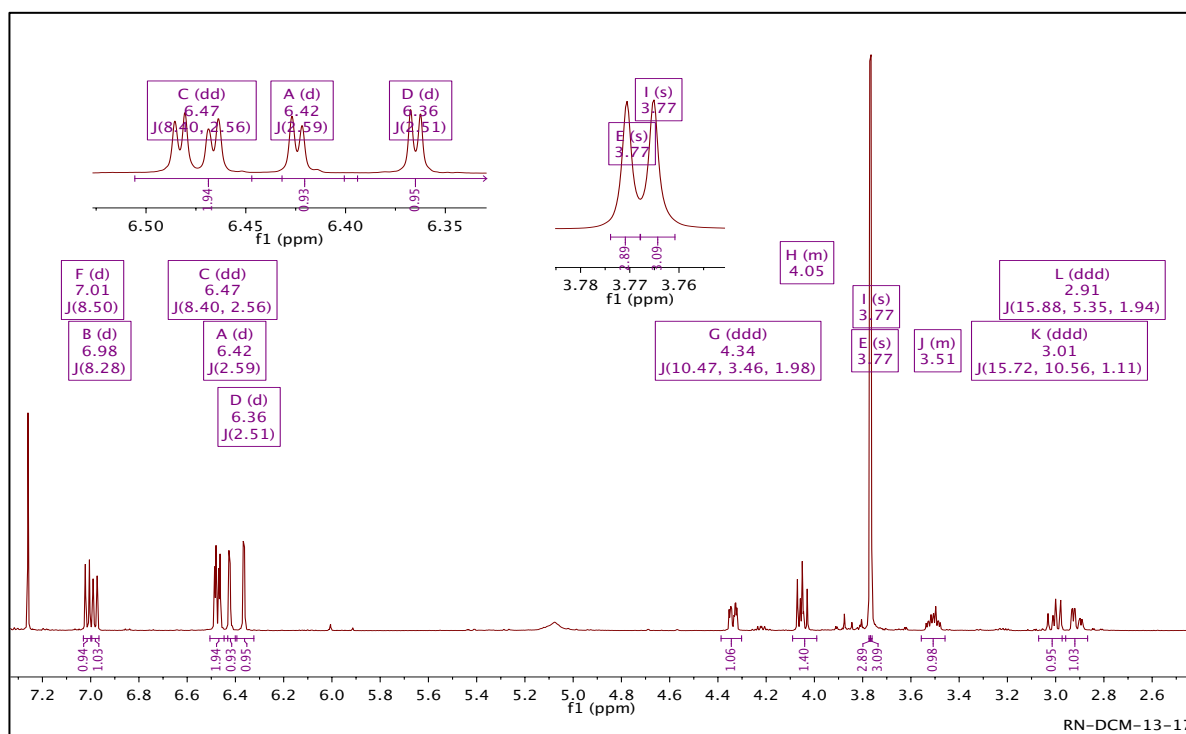
Figure 6-11:^{1}**H NMR (500 MHz) spectrum of compound 16 in CDCl₃**
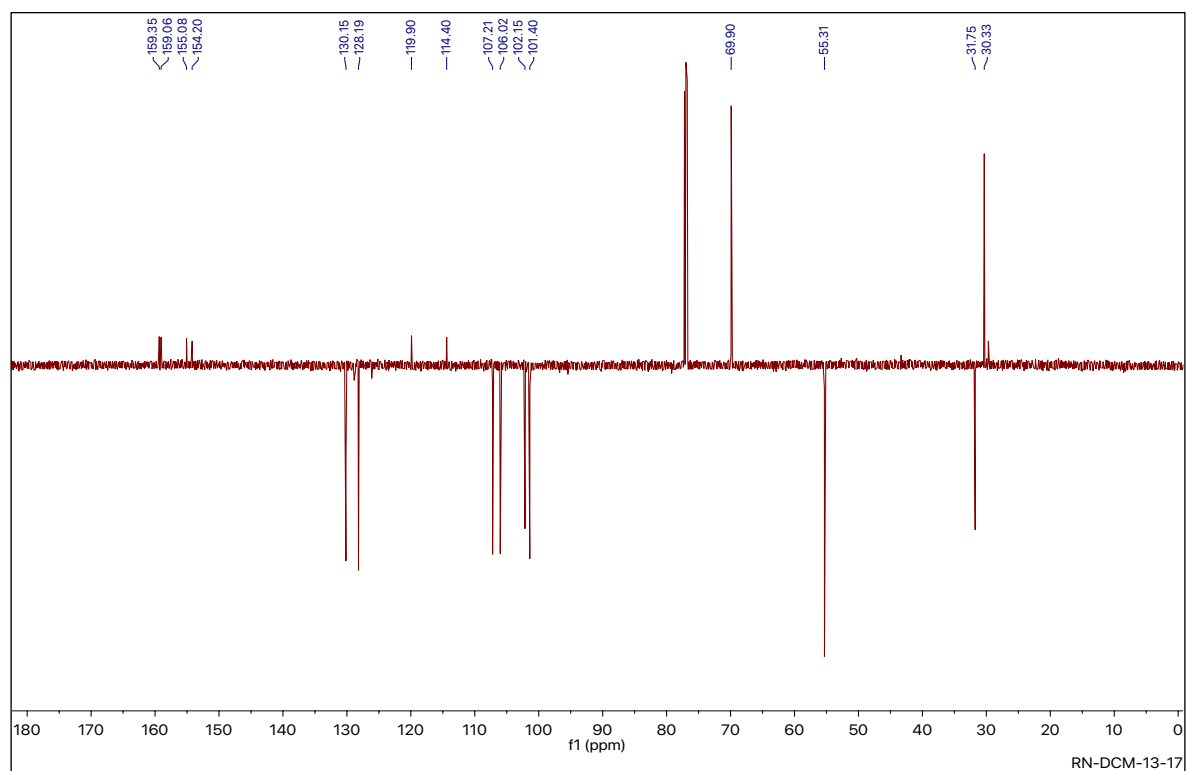
Figure 6-12: ^{13}C NMR (100 MHz) spectrum of the compound 16 in CDCl₃
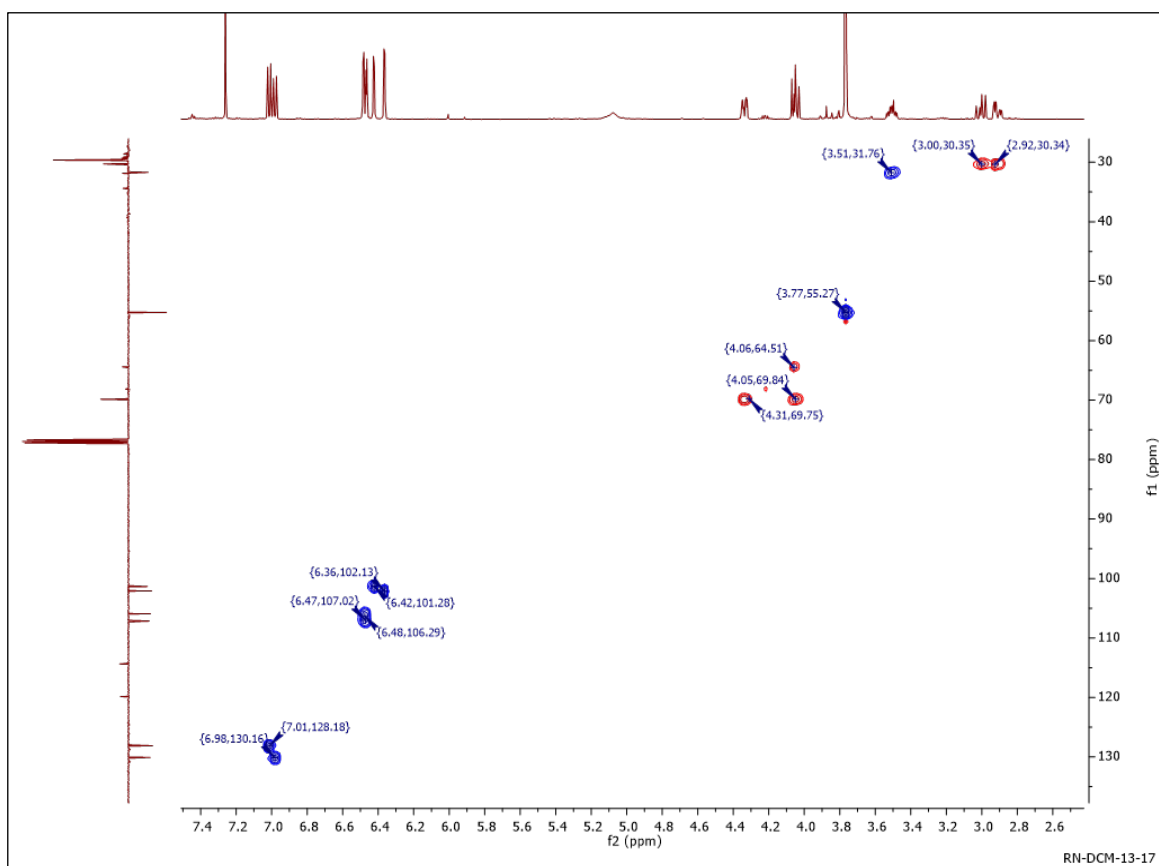
Figure 6-13: HSQC (500 MHz) spectrum of the compound 16 in CDCl₃
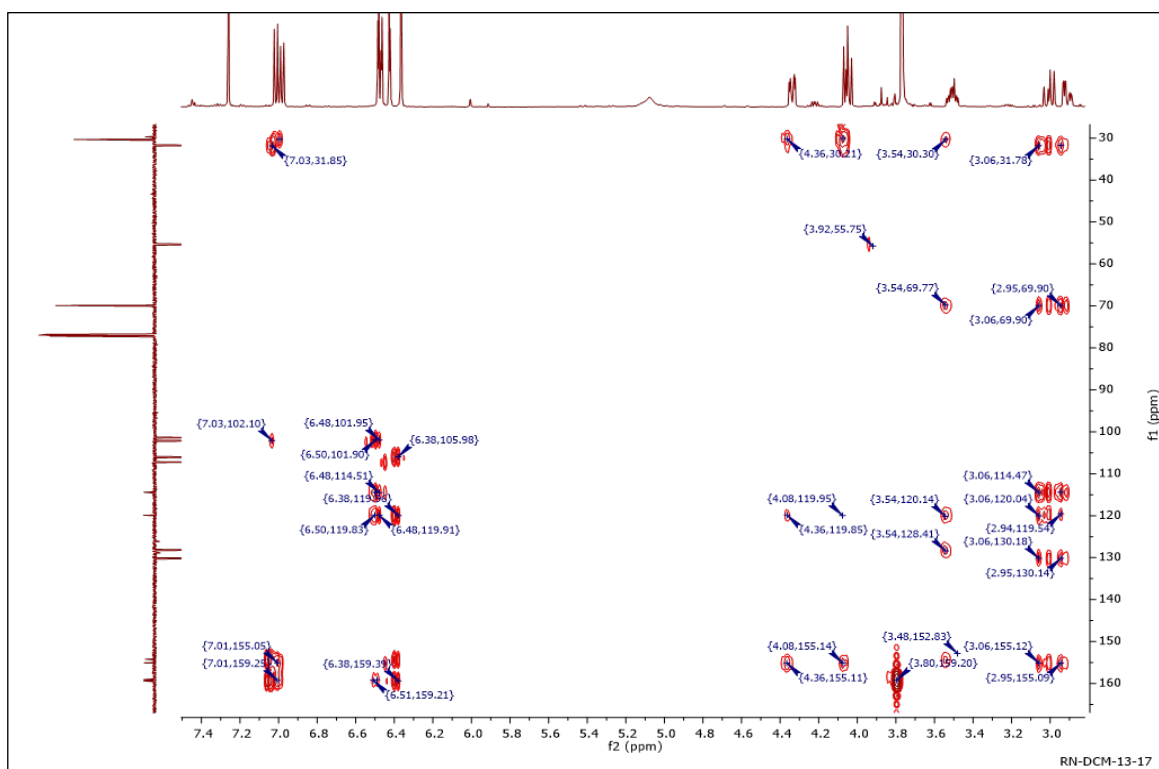
Figure 6-14: HMBC (500 MHz) spectrum of the compound 16 in CDCl₃.
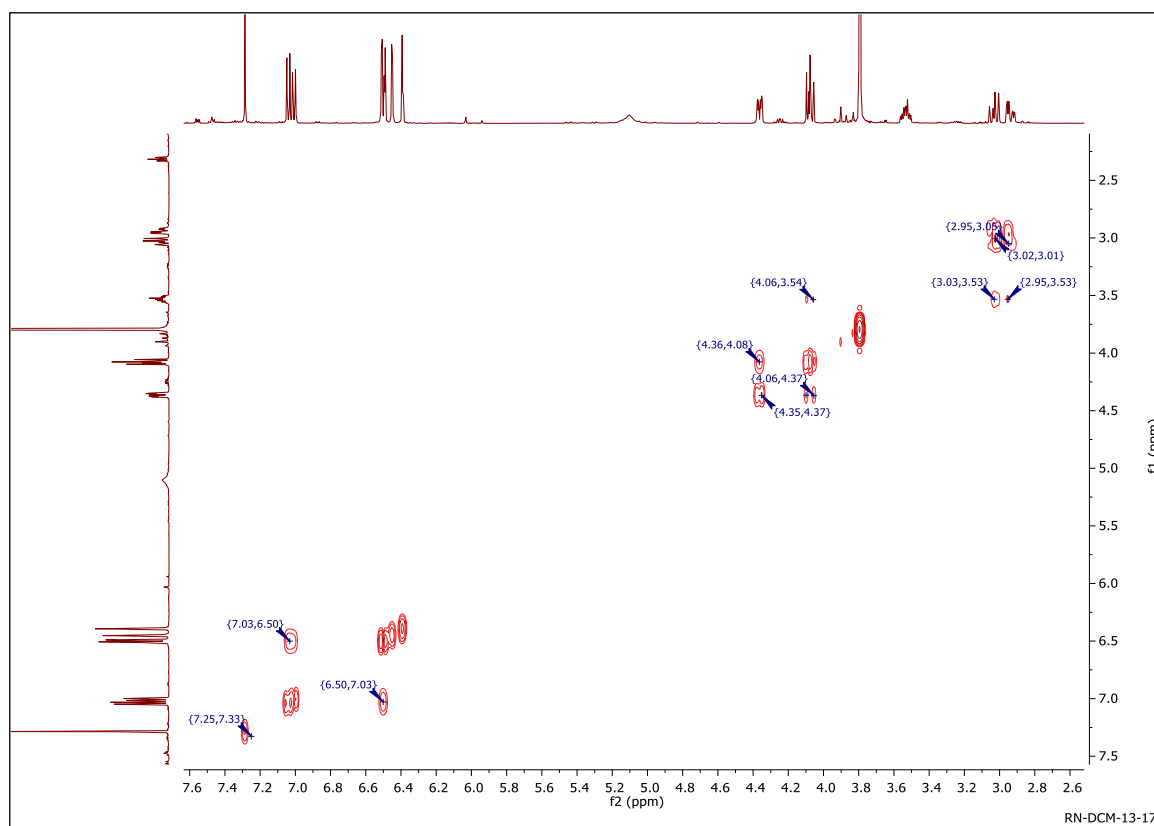
Figure 6-15: COSY (500 MHz) Spectrum of Compound 16 in CDCl₃.

6.3.2.6 Characterization of RN- DCM-29 as of neovestitol (17)

RN- DCM-29 was isolated from ethanol extract of Nigerian propolis. LC-MS (ESI) gave a peak at Rt = at 13.38 min in the positive mode was found at *m/z* [M+H]⁺ m/z 273.1113 ($C_{16}H_{17}O_4$ calc 273.1127), while in the negative mode an [M-H]⁻ was observed at m/z 271.0970 ($C_{16}H_{15}O_4$, calc 271.0970). This confirmed a molecular formula of $C_{16}H_{16}O_4$ (**Figure 6-17**).

The 1H NMR spectrum of RN- DCM-29 (**Figure 6-18**) showed two similar sets of aromatic protons for two trisubstituted benzene rings at δ (ppm) 6.38 (1H, dd *J* = 8.2, 2.5), 6.52 (1H, d *J* = 2.6) and 7.07 (1H, d *J* = 8.5) for one aromatic ring. While the other aromatic ring protons appeared at δ (ppm) 6.31 (1H, d *J* = 2.4), 6.44 (1H, dd *J* = 8.5, 2.6) and 6.91 (1H, d *J* = 8.2). Two oxymethylene protons, one methine and two methylene protons were observed at 4.26 ((1H, ddd, *J* =10.3, 3.5, 2.0 Hz), 4.00 (1H, t, *J* =10.1 Hz), 3.50 (1H, tt, *J* = 10.4, 4.3 Hz), 2.98 (1H, dd, *J* = 15.6, 11.0 Hz) and 2.82 (1H, ddd, *J* = 15.6, 5.3, 1.9 Hz), respectively. One of the aromatic rings had one-methoxy groups at 3.74 ppm. The ¹³C spectrum (**Figure 6-19**) gave 16 signals made up of six aromatic CH, two aliphatic CH_2 and one CH, one methoxy and six quaternary carbons (including four phenolic ones). The proton and carbon spectra were similar to that of compound 16 and therefore they must be analogues. Analysis of its 2D spectra

172

(**Figures 6-20** to **6-22**) confirmed the compound to be neovestitol (**17**) as shown in **Figure 6-16** and was supported by literature (Campo Fernández et al., 2008). The chemical shifts for the protons and carbons were fully assigned as given in **Table 6-4.**

Chemical Formula: $C_{16}H_{16}O_4$
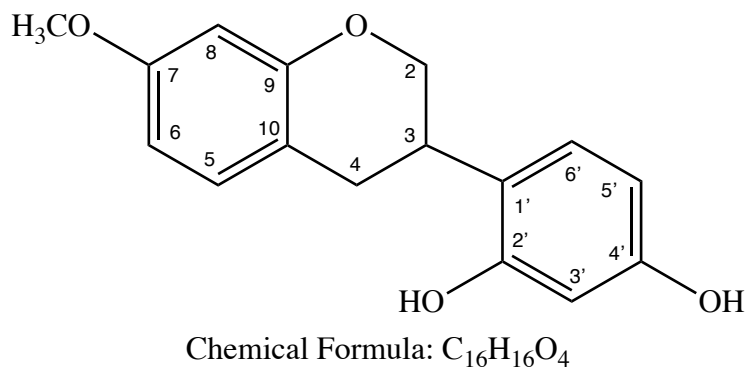
Figure 6-16: Structure of 7,4′-dihydroxy-2′-methoxyisoflavan (neovestitol)
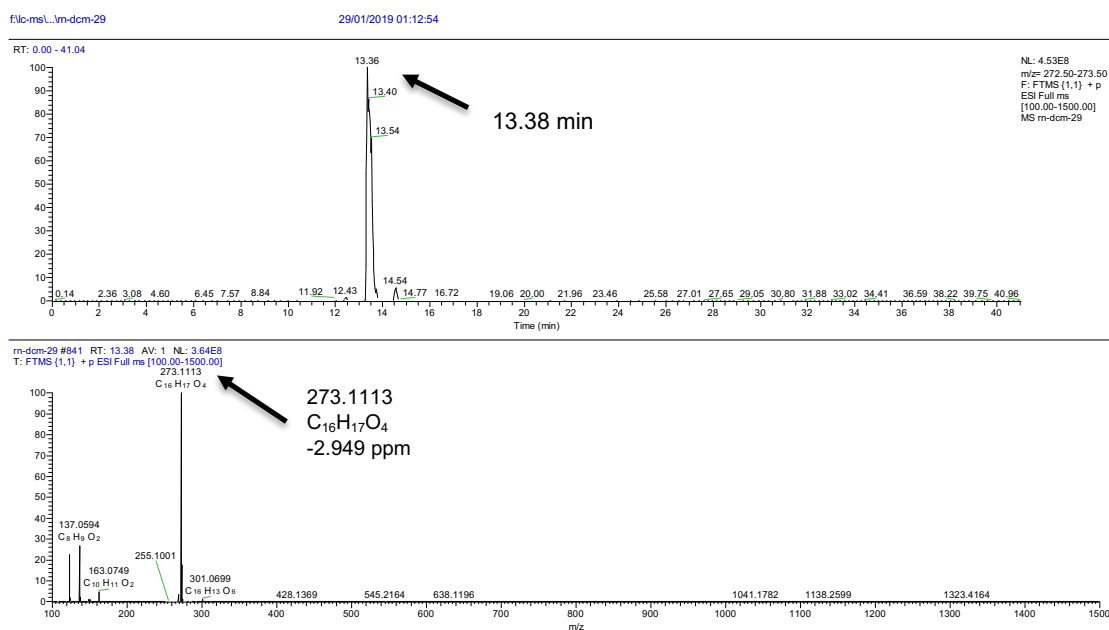
Figure 6-17: LC-MS chromatogram (ESI positive mode) for compound 17

Table 6-4: ^1H and ^{13}C data of compound 17

Position	Proton δ ppm (mult, J Hz)	Carbon δ ppm (mult)
2	4.26 (1H, ddd J =10.3, 3.5, 2.0) 4.00 (1H, t J =10.1)	69.6 (CH$_2$)
3	3.50 (1H, tt J = 10.4, 4.3)	31.8 (CH)
4	2.98 (1H, dd J = 15.6, 11.0) 2.82 (1H, ddd J = 15.6, 5.3, 1.9)	30.2 (CH$_2$)
5	7.07 (1H, d J = 8.5)	127.9 (CH)
6	6.38 (1H, dd J = 8.2, 2.5)	107.9 (CH)
7	-	159.5 (C)
8	6.52 (1H, d J = 2.6)	101.6 (CH)
9	-	156.6 (C)
10	-	113.4 (C)
1'	-	120.1 (C)
2'	-	155.2 (CH)
3'	6.31 (1H, d J = 2.4)	102.8 (CH)
4'	-	155.8 (CH)
5'	6.44 (1H, dd J = 8.5, 2.6)	104.8 (CH)
6'	6.91 (1H, d J = 8.2)	130.1 (CH)
7- OCH$_3$	3.74 (3H, s)	54.5 (CH$_3$)
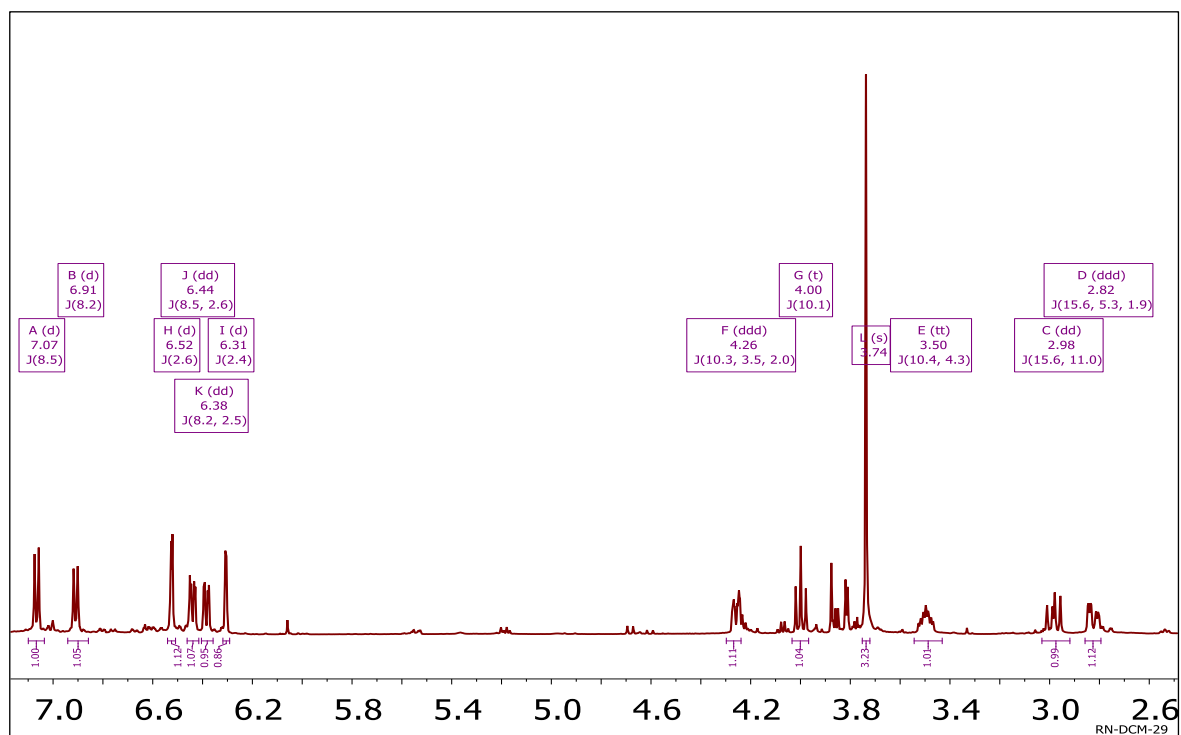
Figure 6-18: ^1H NMR (500 MHz) spectra of compound 17 in acetone-d$_6$

174
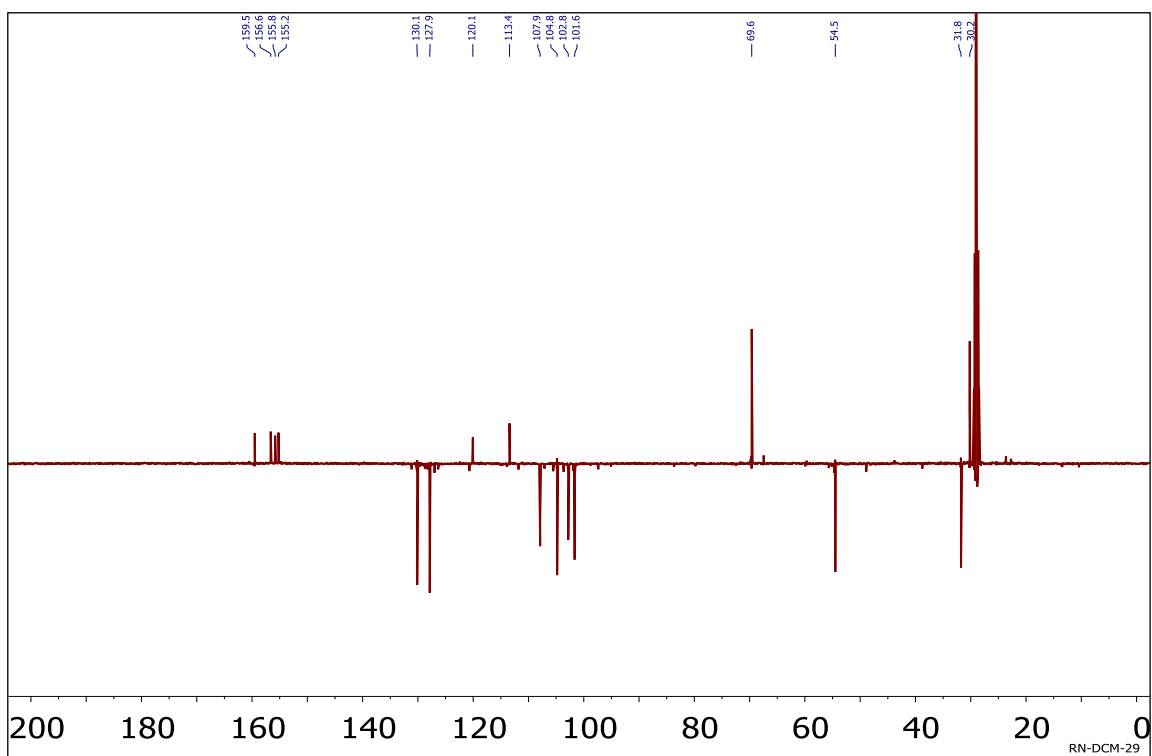
Figure 6-19: ^{13}CNMR (100 MHz) spectra of the compound 17 in acetone-d$_6$
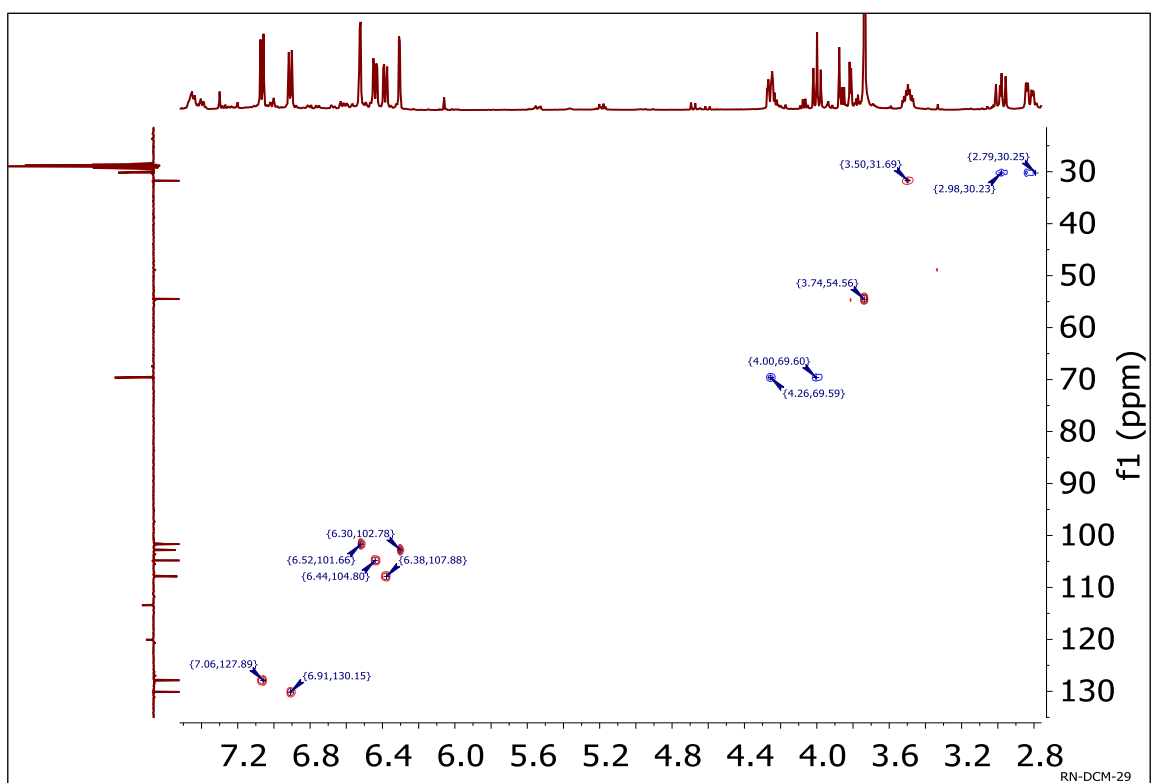
Figure 6-20: HSQC (500 MHz) spectrum of the compound 17 in acetone-d$_6$
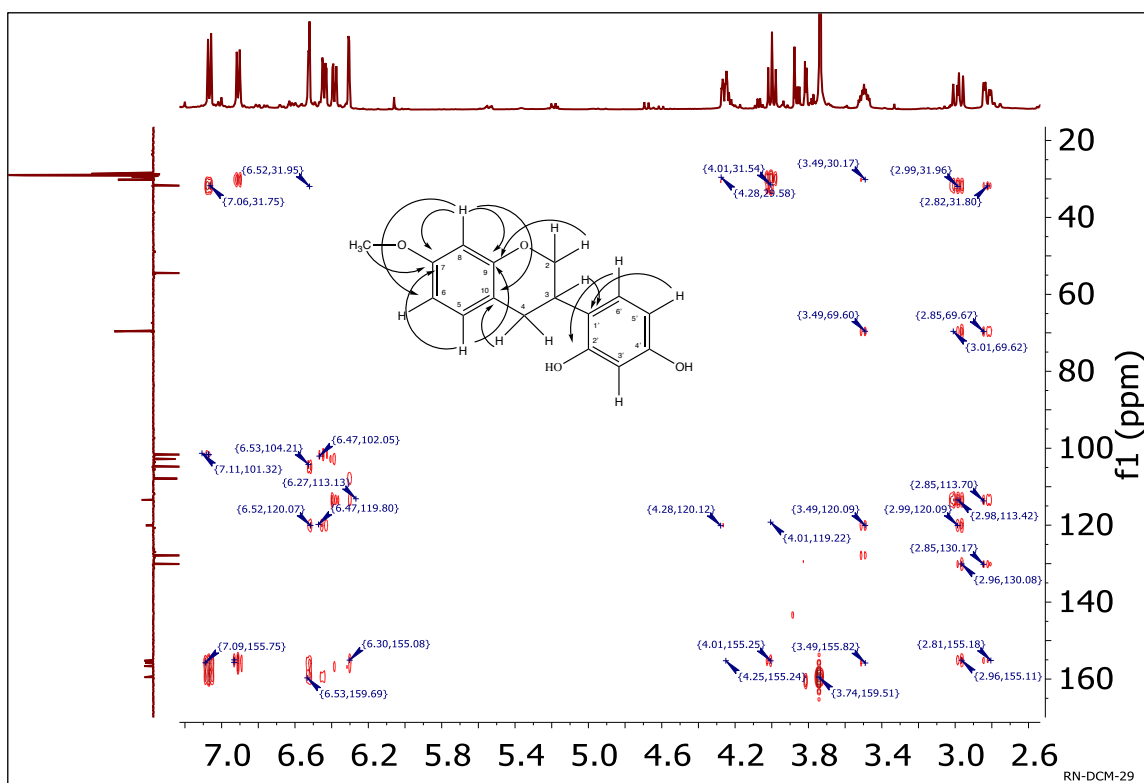
Figure 6-21: HMBC (500 MHz) Spectrum of the compound 17 in acetone-d₆
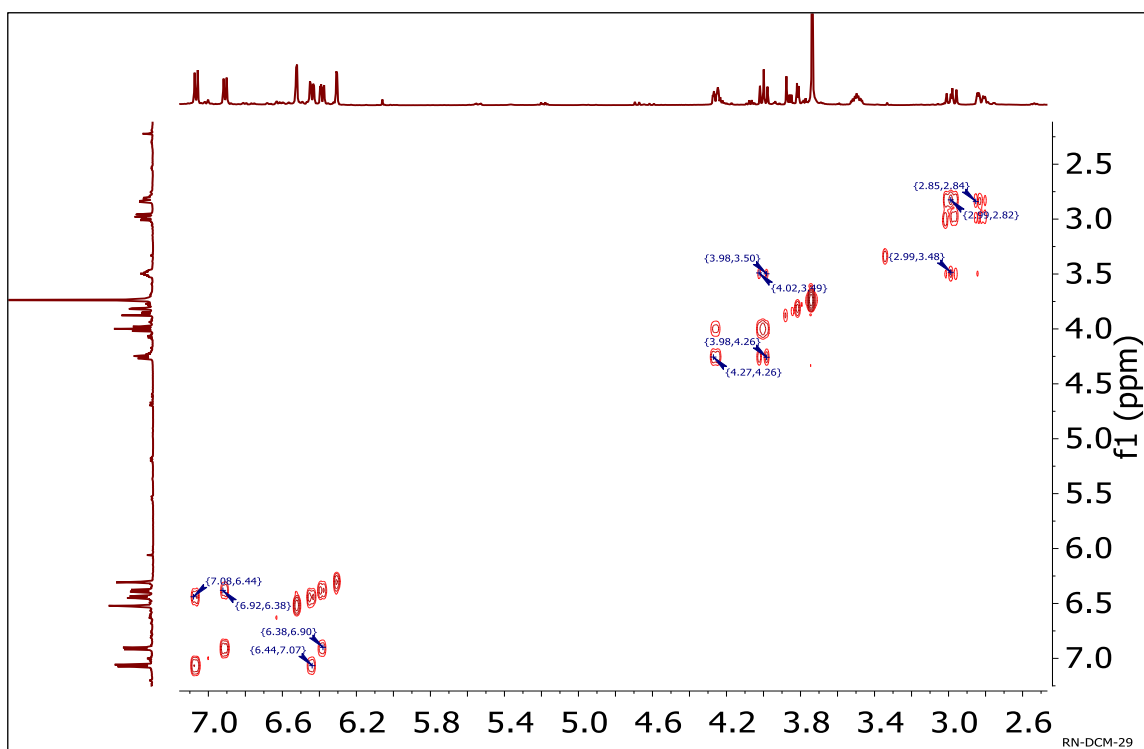
Figure 6-22: COSY (500 MHz) Spectrum of the compound 17 in acetone-d₆

6.3.2.7 Characterization of vestitol in fraction RN- E-26 (18)

RN- E-26 was isolated from ethanol extract of Nigerian propolis. In LC-MS ESI, a peak at Rt = 13.61min was observed and an $[M+H]^+$ ion at m/z 273.1112 corresponding to $C_{16}H_{17}O_4$, (Calc 273.1126) while in the negative mode, a peak at 13.49 min and an $[M-H]^-$ ion at m/z 271.0971 corresponding to $C_{16}H_{15}O_4$ (Calc 271.0970) and confirmed a molecular formula of $C_{16}H_{16}O_4$ (**Figure 6-24**). The proton and carbon spectra (**Figures 6-25** and **6-26**) for the compound were similar to compound **16** and **17** with one methoxy group substituted on one of the aromatic rings at 3.76 ppm. The structure was elucidated based on its 2D NMR spectrum as follows; correlations from the two deshelled aromatic doublets identified the two aromatic rings and their substitutions. The key HMBC correlations for the structure were the correlations from H-6' observed at δ_H 7.00 (d $J = 8.5$) display correlation with C-3 δ_C 31.9 ppm (CH), C-2' δ_C 154.5 ppm (C) and C-4' δ_C 159.5 ppm (C). While, H-5 observed at δ_H 6.93 (dq, $J = 7.97$, 1.08) showing correlation with C-4 δ_C 30.5 ppm (CH$_2$), C-7 δ_C 155.0 ppm (**Figure 6-27**). Further analysis of its NMR data and comparison to compound **16** and **17** enabled the identification of the compound as vestitol **18** as shown in **Figure 6-23** (Campo Fernández et al., 2008). The chemical shifts for the protons and carbons were fully assigned as given in **Table 6-5.**

Chemical Formula: $C_{16}H_{16}O_4$
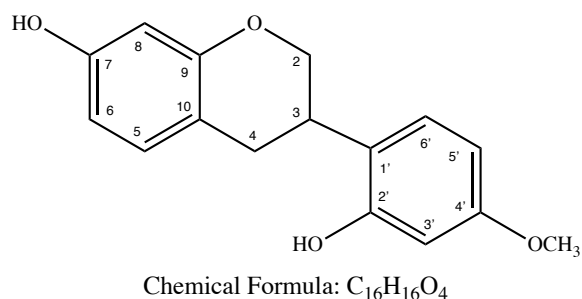
Figure 6-23: Structure of vestitol
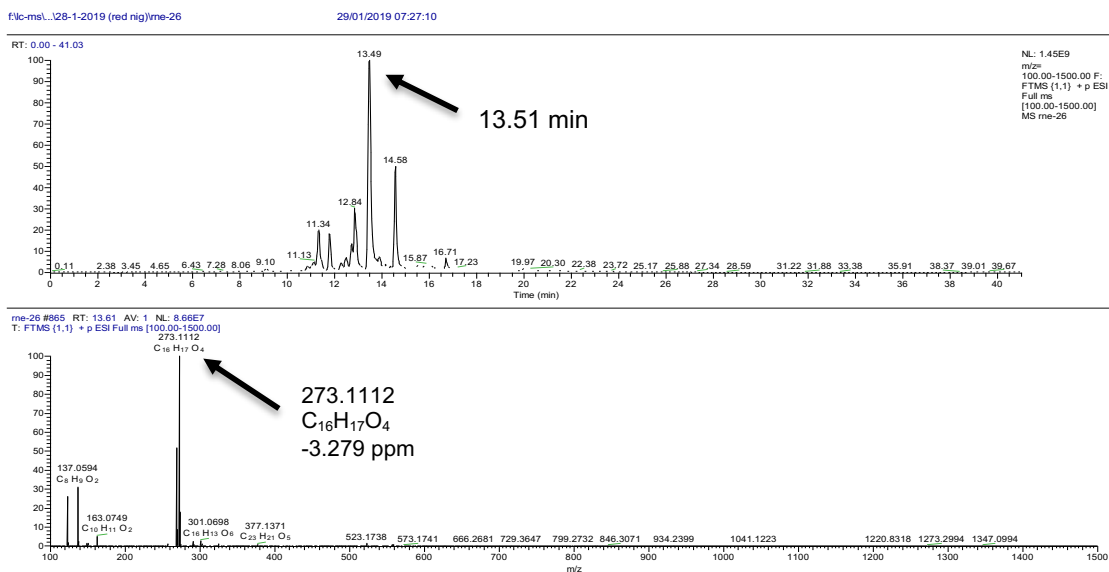
Figure 6-24: : LC-MS chromatogram (ESI positive mode) for compound 18

Table 6-5: ^{1}H and ^{13}C data of compound 18

Position	Proton δ ppm (mult, *J* Hz)	Carbon δ ppm (mult)
2	4.33 (1H, ddd *J* =10.4, 3.5, 2.0) 4.03 (1H, t *J* =10.1)	70.1 (CH$_2$)
3	3.50 (1H, m)	31.9 (CH)
4	2.98 (1H, dd *J* = 15.8, 10.4) 2.89 (1H, dd *J* = 15.8, 5.4, 2.0)	30.5 (CH$_2$)
5	6.93 (1H, dq, *J* = 7.97, 1.08)	130.6 (CH)
6	6.39 (1H, dd *J* = 8.5, 2.6)	108.2 (CH)
7	-	155.0 (C)
8	6.37 (1H, d *J* = 2.5)	102.3 (CH)
9	-	155.2 (C)
10	-	114.8 (C)
1'	-	120.1 (C)
2'	-	154.5 (C)
3'	6.36 (1H, d *J* = 2.6)	103.4 (CH)
4'	-	159.5 (C)
5'	6.47 (1H, dd *J* = 8.5, 2.5)	106.1 (CH)
6'	7.00 (1H, m d *J* = 8.5)	128.3 (CH)
4'- OCH$_3$	3.76 (3H, s)	55.5 (CH$_3$)
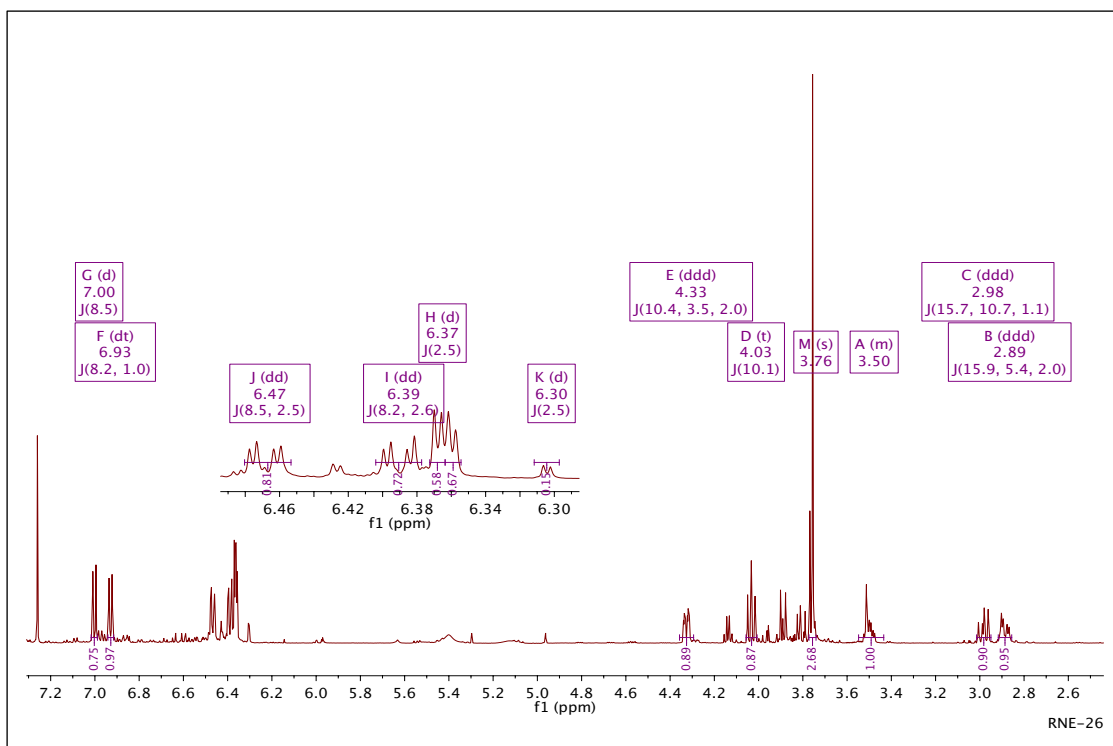
Figure 6-25: ^{1}H NMR (500 MHz) spectra of the compound 18 in CDCl$_3$.
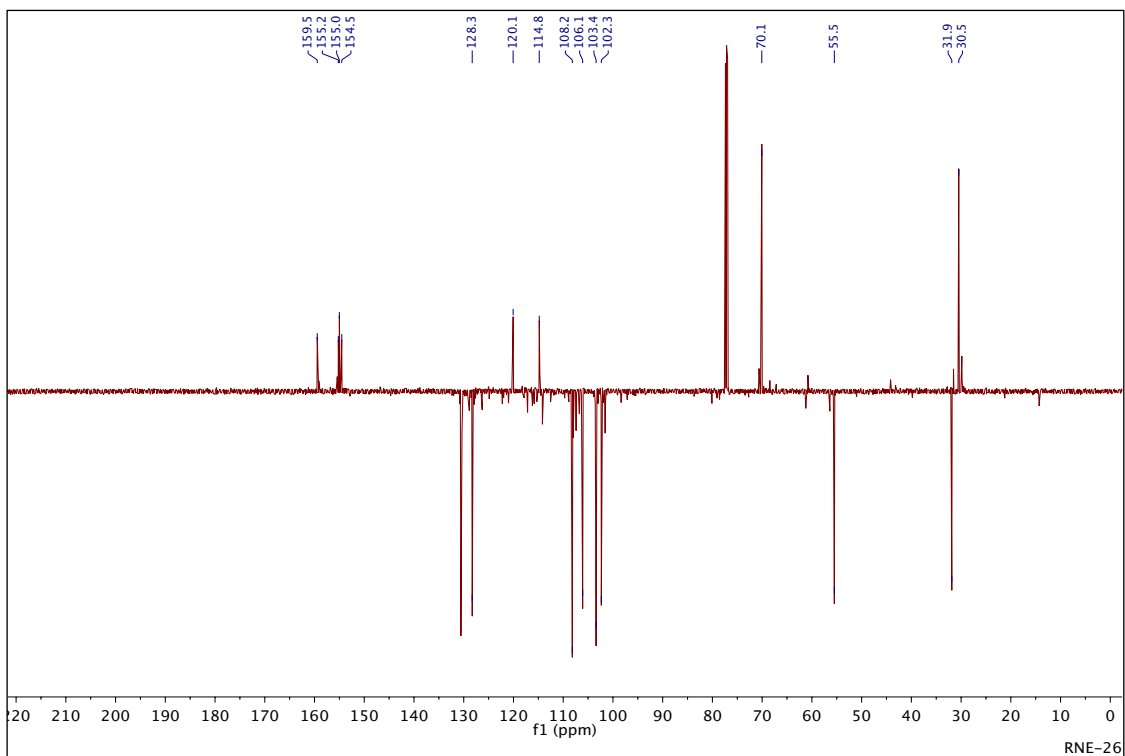
Figure 6-26: ^{13}C NMR (100 MHz) spectra of the compound 18 in CDCl$_3$.
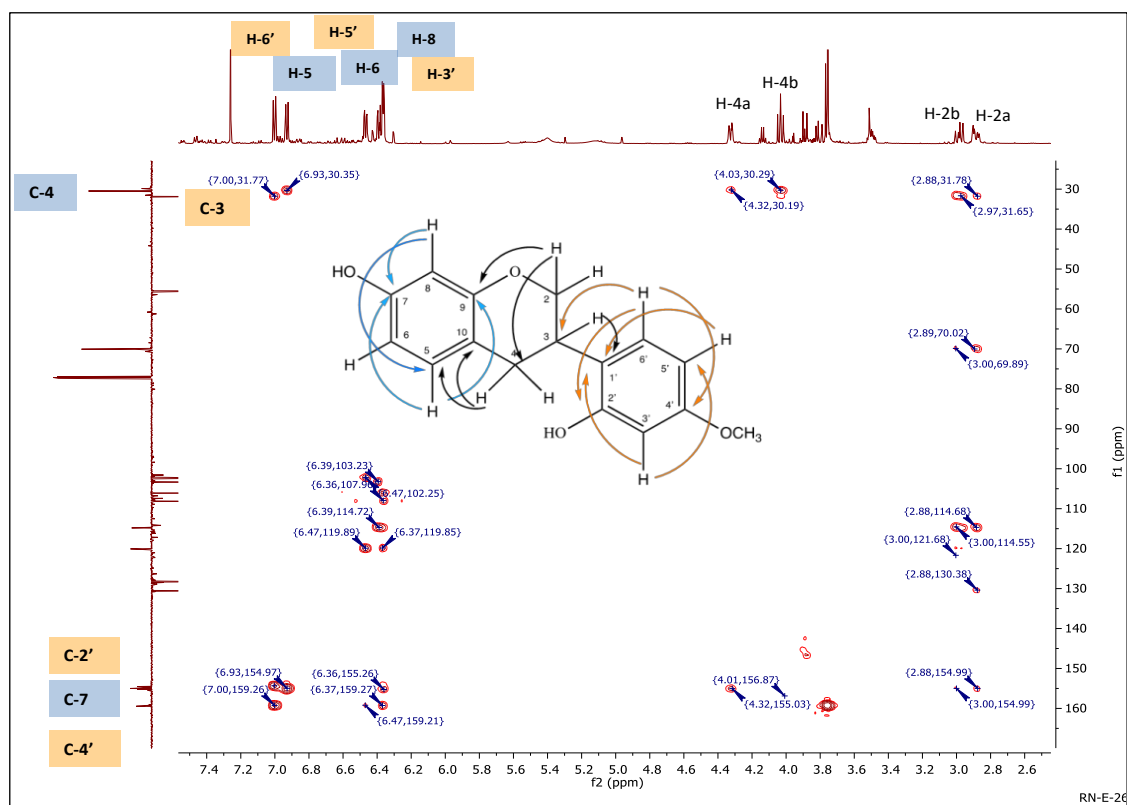
Figure 6-27: HMBC (400 MHz) Spectrum of the compound 18 in CDCl₃.

6.3.2.8 Characterization of RN-DCM-22 as a medicarpin (19)

The LC-MS data afforded a peak at 15.41 min and an ion $[M+H]^+$ at *m/z* 271.0955 ($C_{16}H_{15}O_4$) (Calc 271.0970) and a peak at 11.52 min and an $[M-H]^-$ ion at *m/z* 269.0817 corresponding to $C_{16}H_{13}O_4$ (Calc. 269.0813), hence the molecular formula $C_{16}H_{14}O_4$ (**Figure 6-29**).

In its proton spectrum (**Figure 6-30**) the compound showed signals for two oxymethylene protons at δ_H (ppm) 4.26 (ddd, *J* = 11.04, 5.1, 0.7 Hz) and 3.65 (t, *J* =11.0 Hz), one methine proton at 3.56 (t, *J* =11.0 Hz) and an oxymethine proton at 5.52 (d, *J* = 6.8 Hz). The proton spectrum of the compound showed two sets of aromatic ABX spin systems and confirmed the presence of two trisubstituted benzene rings. The first set were at δ_H 7.41 (m), 6.57 (dd, *J* = 8.4, 2.5 Hz) and 6.44 (d, *J* = 2.5 Hz). The second set of the aromatic ABX protons were at 7.15 (m), and 6.48 (m) integrated for two protons. From ^{13}C spectrum (**Figure 6-31**), 16 carbon signals were observed made up of six aromatic CH, one aliphatic CH_2, two aliphatic CH, one methoxy and six quaternary carbons (including four phenolic ones). The compound is similar to compounds **16-18**, however, in compounds **16-18**, C-2' is –OH substituted and the chemical shift is around δ_C 154.5 but in this compound, the shift is 160.8 hence C-2' must have an ether

linkage just as for a methoxy substituted aromatic carbon. According to the literature data when there is a 'free' OH its carbon attachment resonates at around 156ppm whereas when it cyclises to an ether heterocycle or is alkylated (i.e. made into an ether, e.g. OMe) the carbon resonates at around 160+ppm. Analysis of its 2D spectra (COSY, HSQC and HMBC) as shown in **Figures 6-32** and **6-34**, indicated the compound to be medicarpin (**19**) (**Figure 6-28**), and the structure was confirmed by literature reports (Piccinelli et al., 2005, Campo Fernández et al., 2008). The chemical shifts for the protons and carbons were fully assigned as given in **Table 6-6.**
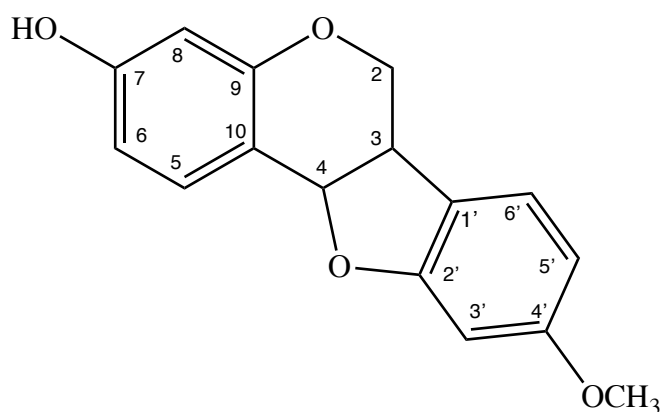
Chemical Formula: $C_{16}H_{14}O_4$

Figure 6-28: Structure of medicarpin
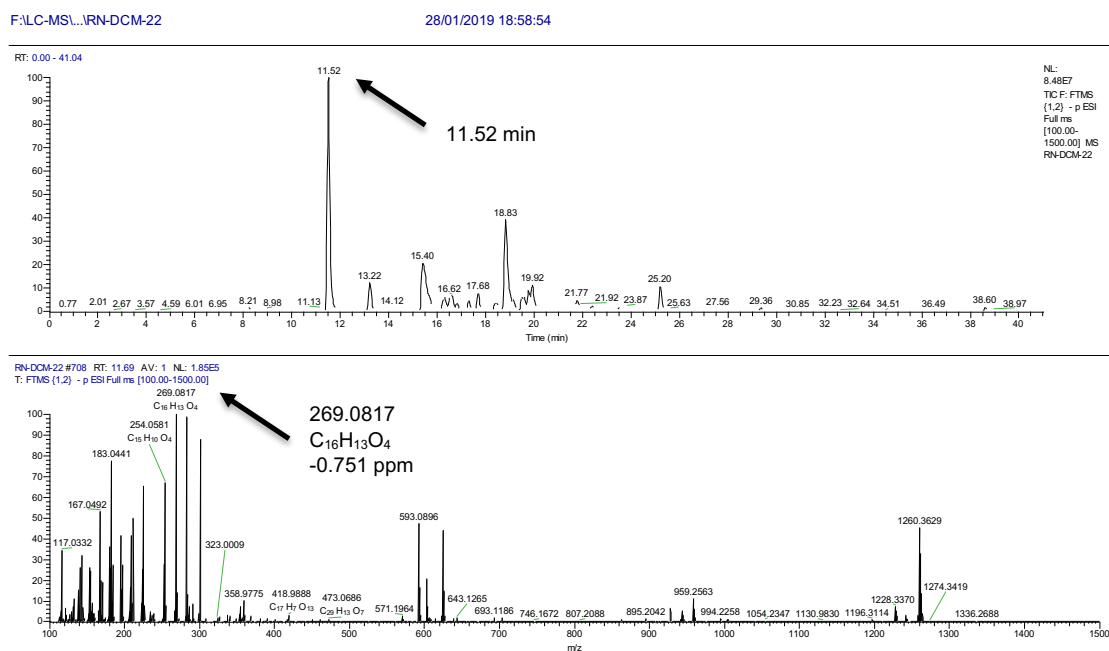
Figure 6-29: LC-MS chromatogram (ESI negative mode) for compound 19.

Table 6-6: ^{1}H and ^{13}C data of compound 19

Position	Proton δ ppm (mult, *J* Hz)	Carbon δ ppm (mult)
2	4.26 (1H, ddd *J* =11.04, 5.1, 0.7) 3.65 (1H, t *J* =11.0)	66.7 (CH$_2$)
3	3.56 (1H, t *J* =11.0)	39.6 (CH)
4	5.52 (1H, d *J* = 6.8)	78.7 (CH)
5	7.41 (1H, m)	132.3 (CH)
6	6.57 (1H, dd *J* = 8.4, 2.5)	110 (CH)
7	-	157.3 (CH)
8	6.44 (1H, d *J* = 2.5)	103.8 (CH)
9	-	156.8 (C)
10	-	112.7 (C)
1'	-	119.3 (C)
2'	-	160.8 (CH)
3'	6.48 (1H, m)	97.1 (CH)
4'	-	161.2 (C)
5'	6.48 (1H, m)	106.6 (CH)
6'	7.15 (1H, m)	124.9 (CH)
4'-OCH$_3$	3.79 (3H, s)	55.7 (CH$_3$)
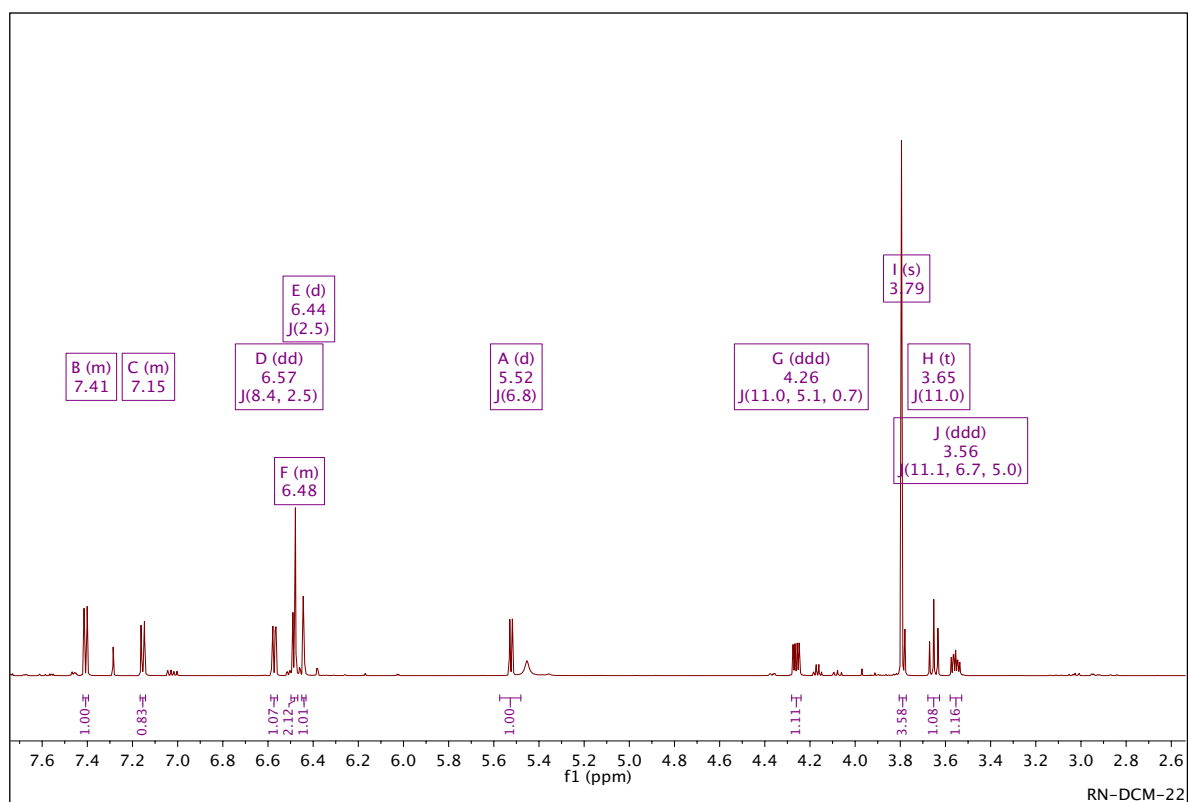
Figure 6-30: ^{1}H NMR (500 MHz) spectra of the compound 19 in CDCl$_3$

182
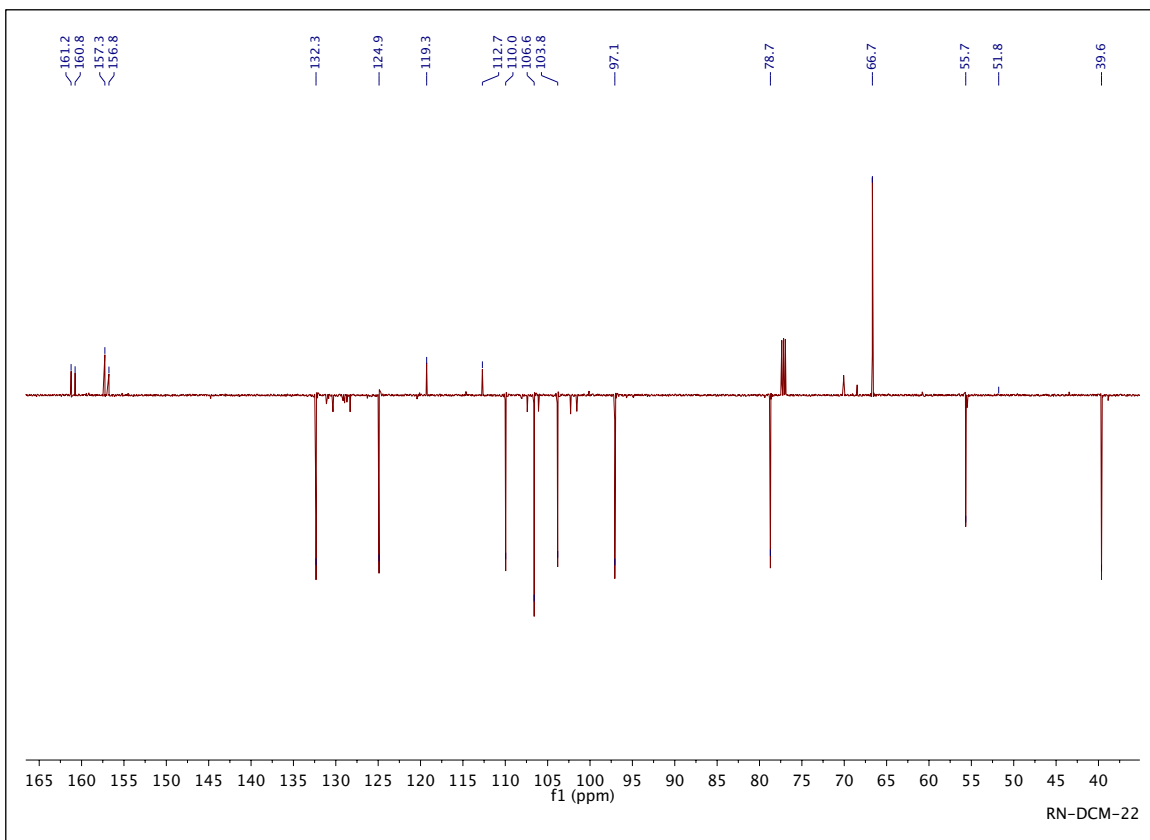
Figure 6-31: ^{13}C NMR (100 MHz) spectra of the compound 19 in CDCl$_3$
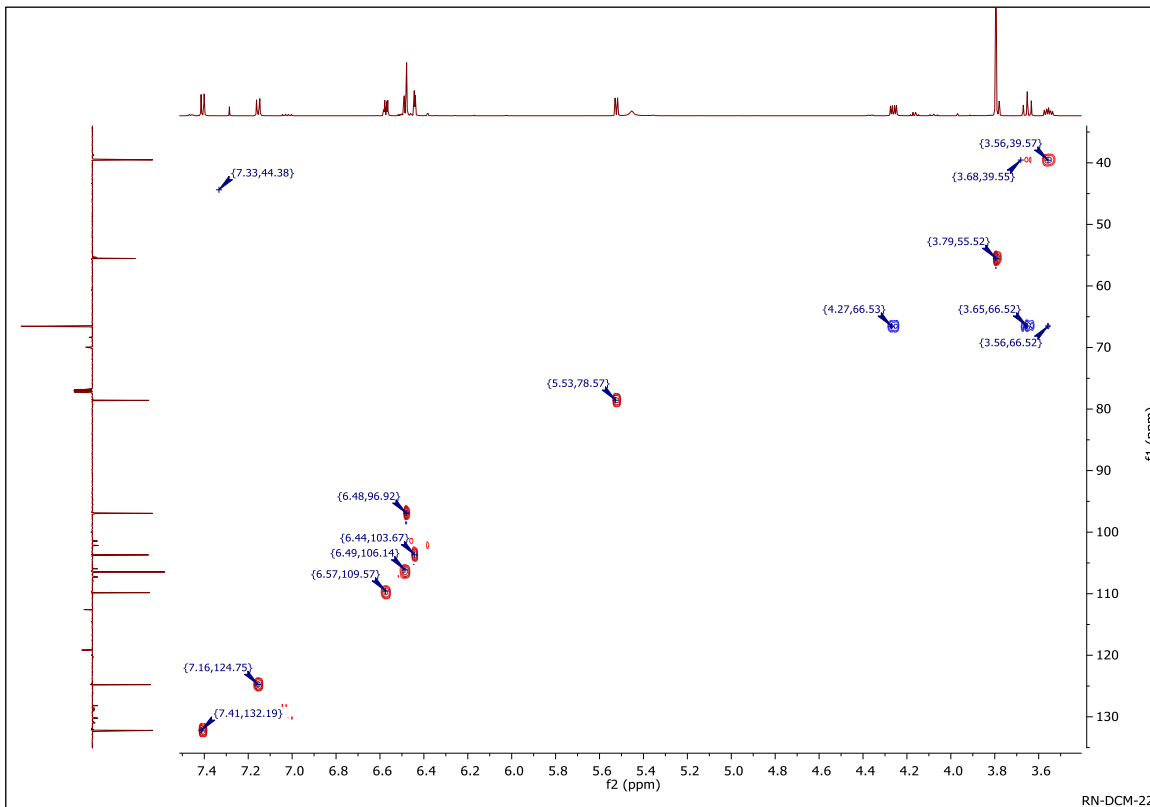
Figure 6-32: HSQC (500 MHz) spectra of the compound 19 in CDCl$_3$
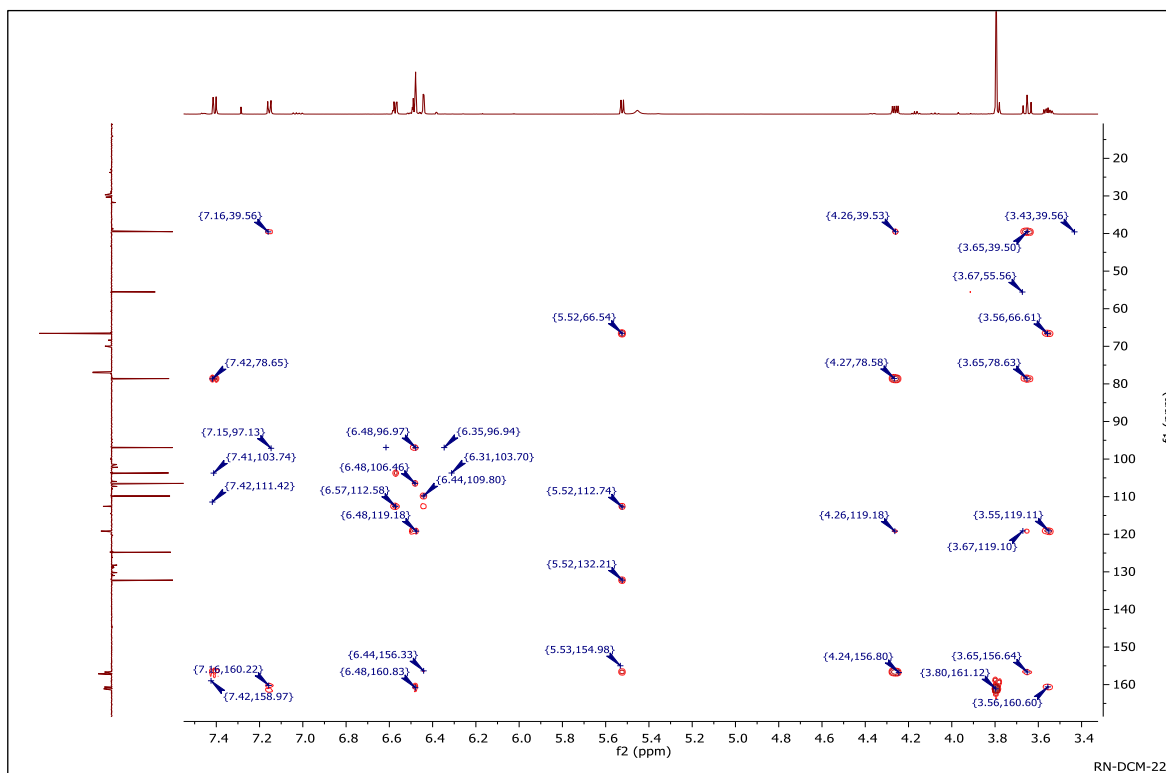
Figure 6-33: HMBC (500 MHz) spectra of the compound 19 in CDCl₃
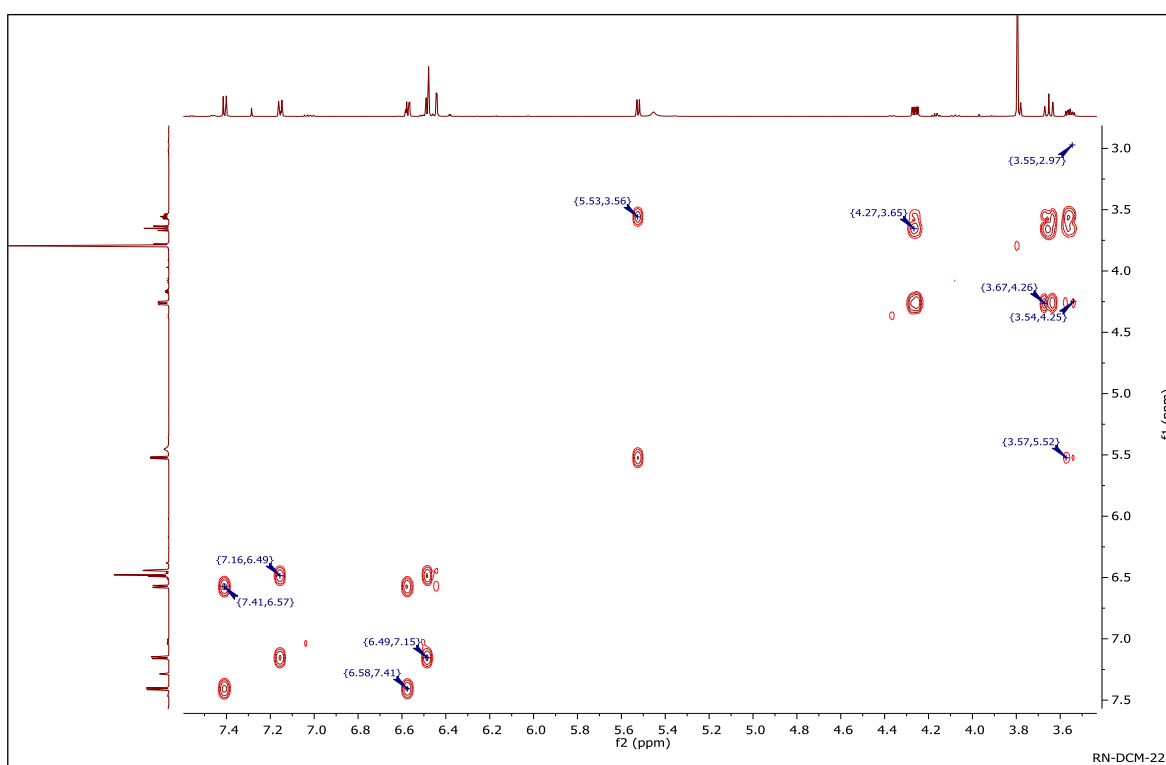
Figure 6-34: COSY (500 MHz) spectra of the compound 19 in CDCl₃

6.3.2.9 Characterization of RN-DCM-25 7-hydroxyflavanone (20)

LC-MS data afforded multiple peaks. one at 14.13 min and an ion [M+H] [+] at *m/z* 241.0848 ($C_{15}H_{13}O_3$) (Calc 241.0864) and another peak at 15.49 min and an [M+H][+] ion at *m/z* 271.0956 corresponding to $C_{16}H_{15}O_4$ (Calc. 271.0970), hence the molecular formula $C_{16}H_{14}O_4$ **(Figure 6-36)** .

The 1H NMR spectrum of RN-DCM-25 (**Figure 6-37**) showed more than two sets of aromatic protons which indicated the presence of two compounds in the fraction. The ^{1}H-^{1}H COSY (**Figure 6-41**.), HSQC (**Figure 6-39**), and HMBC (**Figure 6-40**.), were used to confirm the structures of the two compounds. The ^{1}H-^{1}H COSY and HMBC correlation patterns observed for the minor compound in RN-DCM-25 were identical to those of compound **19** hence it was identified as medicarpin. The other aromatic ABX spin system comprising of a proton at 7.85 (d, *J*= 8.7 Hz) for (H-5), 6.55 (1H, td, *J* = 7.5, 6.5, 2.3 Hz) for (H-6) and 6.42 (1H, d, *J* = 2.4 Hz) for (H-8). In addition, a set of five aromatic protons were observed at 7.44 (4H) and 7.38 (1H). Three coupled aliphatic protons were also observed at 5.46 (1H, dd, *J* =13.2, 2.8 Hz), 2.84 (1H, dd, *J* =16.9, 2.9 Hz) and 3.05 (1H, dd, *J* =17.0, 13.3 Hz). Their chemical shift values were indicative of proximity to a carbonyl or electron withdrawing group. The ^{13}C spectrum (**Figure 6-38)** showed 16 carbons for medicarpin and 15 carbon signals for the major compound made up of one carbonyl at δ_C 191.5, 12 aromatic carbons and two oxygenated aliphatic carbons at 80.0 and 44.4 ppm. Using its 2D (COSY, HSQC and HMBC) spectra, the structure was determined to be 7-Hydroxyflavanone (**20**) as shown in **Figure 6-35**, and was confirmed by literature reports (Kostrzewa-Susłow and Janeczko, 2012)
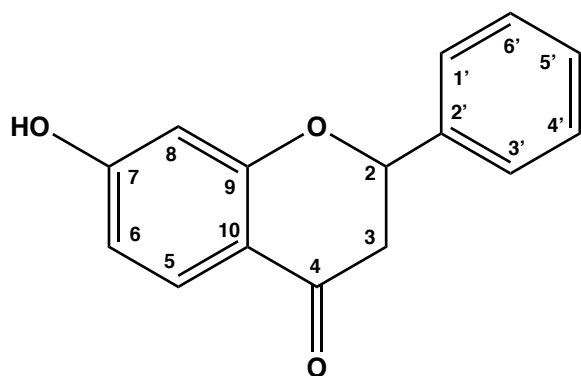
Chemical Formula: $C_{15}H_{12}O_3$

Figure 6-35: structure of 7-hydroxyflavanone
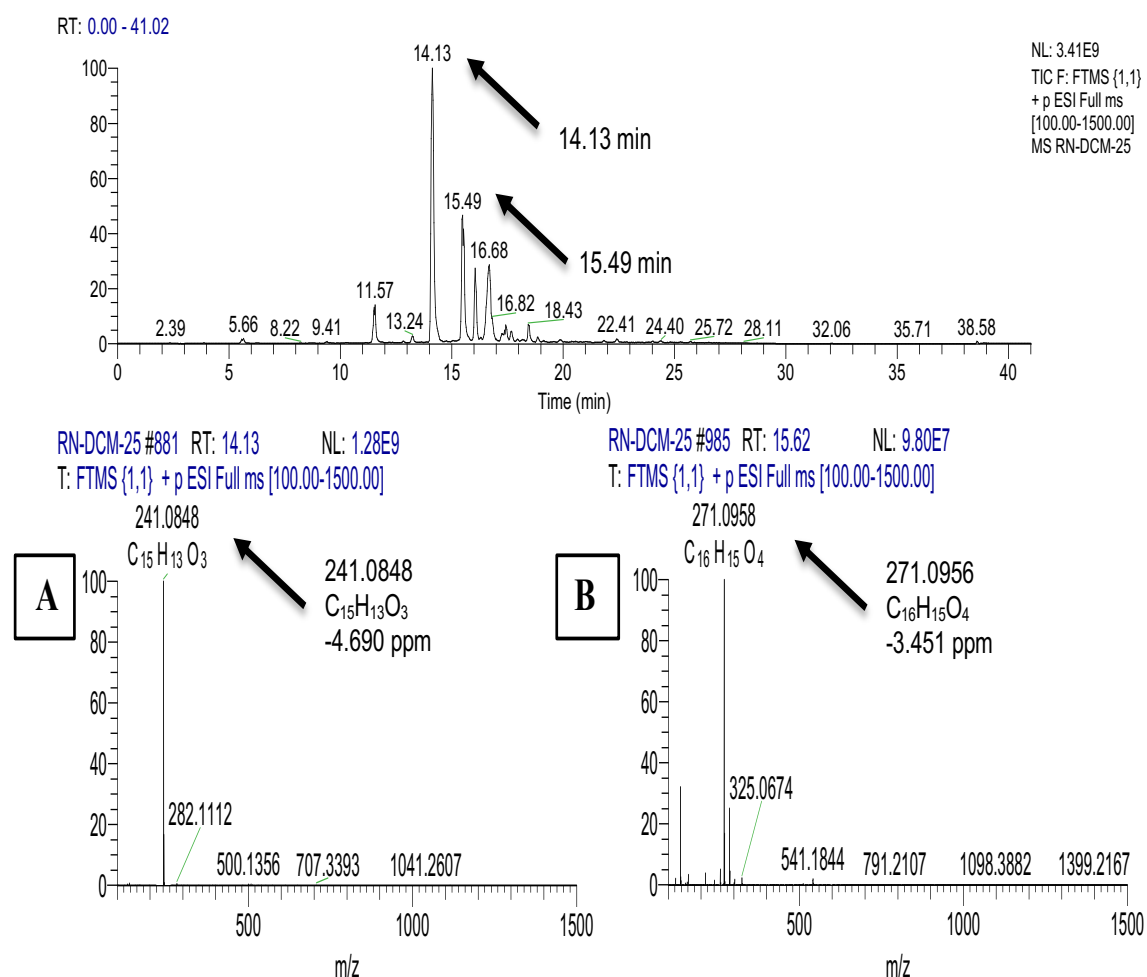
Figure 6-36: LC-MS chromatogram (ESI positive mode) of fraction RN-DCM-25 showed the two purified compounds (A) compound 20 mass spectrum shows the ion mass *m/z* 241.0848 [M + H]+] ($C_{15}H_{13}O_3$, -4.690 ppm) at RT=14.13 (min) and (B) compound 19 shows the ion mass *m/z* 271.0956 [M + H]+ ($C_{16}H_{15}O_4$, -3.451 ppm) at RT=15.49 (min), over the mass range of 100.00-1500.00

Table 6-7: ¹H and ¹³C data of compound 20

Position	Proton δ ppm (mult, *J* Hz)	Carbon δ ppm (mult)
2	5.46 (1H, dd *J* =13.2, 2.8)	80.0 (CH)
3	3.05 (1H, dd *J* =17.0, 13.3) 2.84 (1H, dd *J* =16.9, 2.9)	44.4 (CH_2)
4	-	191.5 (C)
5	7.85 (1H, d *J* = 8.7)	129.5 (CH)
6	6.55 (1H, td J = 7.5, 6.5, 2.3)	111.0 (CH)
7	-	163.7 (C)
8	6.42 (1H, d *J* = 2.4)	103.6 (CH)
9	-	163.9 (C)
10	-	114.9 (C)
1'	-	138.8 (C)
2'	7.44 (1H, m)	126.3 (CH)
3'	7.44 (1H, m)	129.0 (CH)
4'	7.38 (1H, m)	128.9 (CH)
5'	7.44 (1H, m)	128.9 (CH)
6'	7.44 (1H, m)	126.3 (CH)
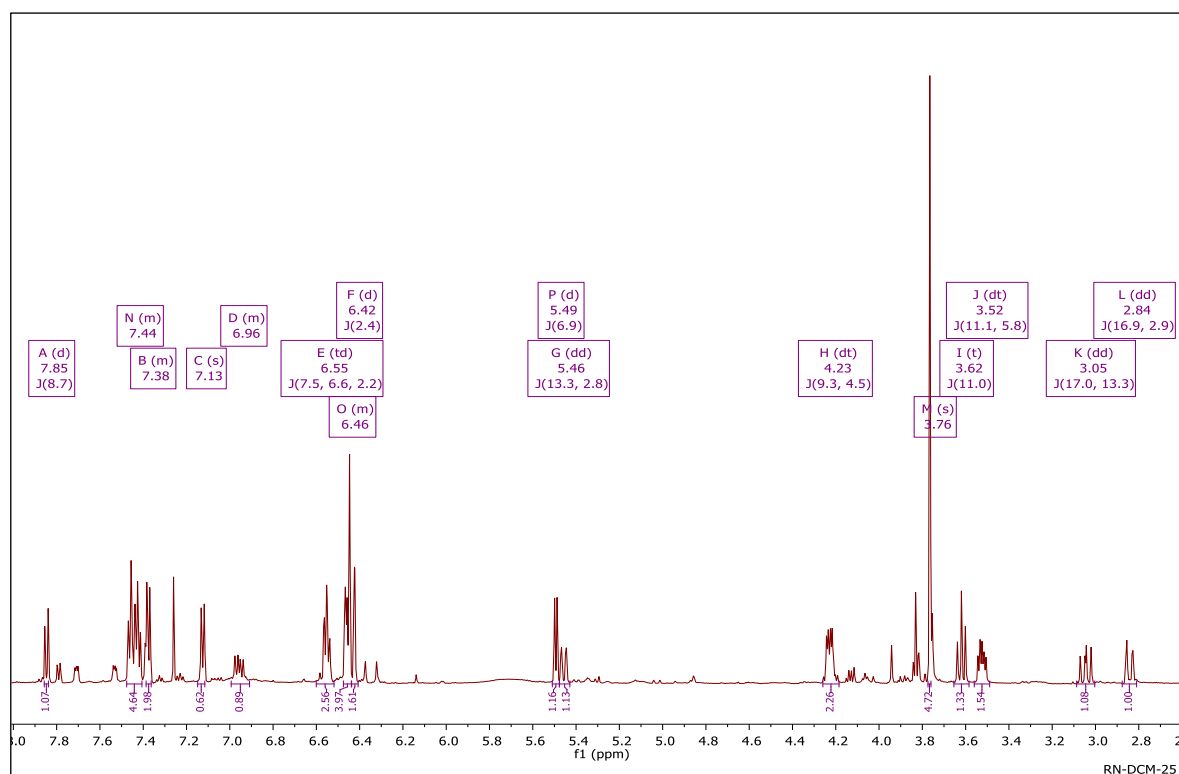
Figure 6-37: ¹H NMR (500 MHz) spectra of the compound 20 in CDCl₃
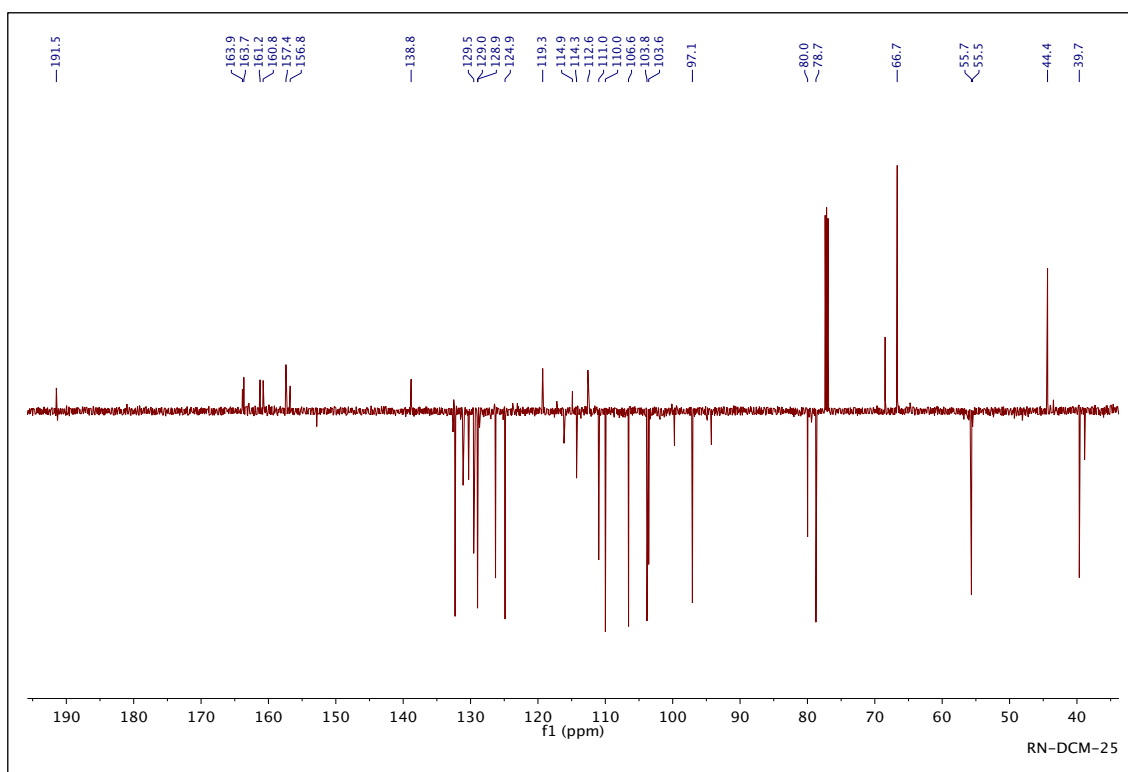
Figure 6-38: ^{13}C NMR (100 MHz) spectra of the compound 20 in CDCl$_3$
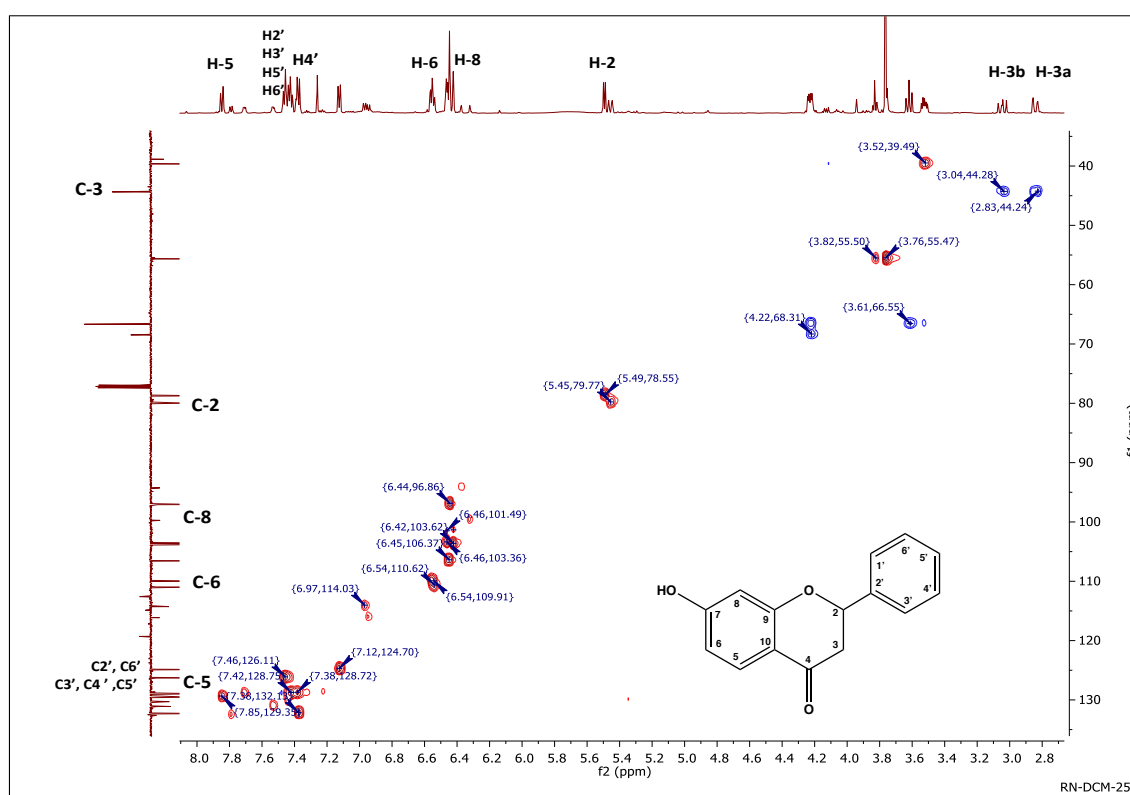
Figure 6-39: HSQC (500 MHz) spectra of the compound 20 in CDCl$_3$
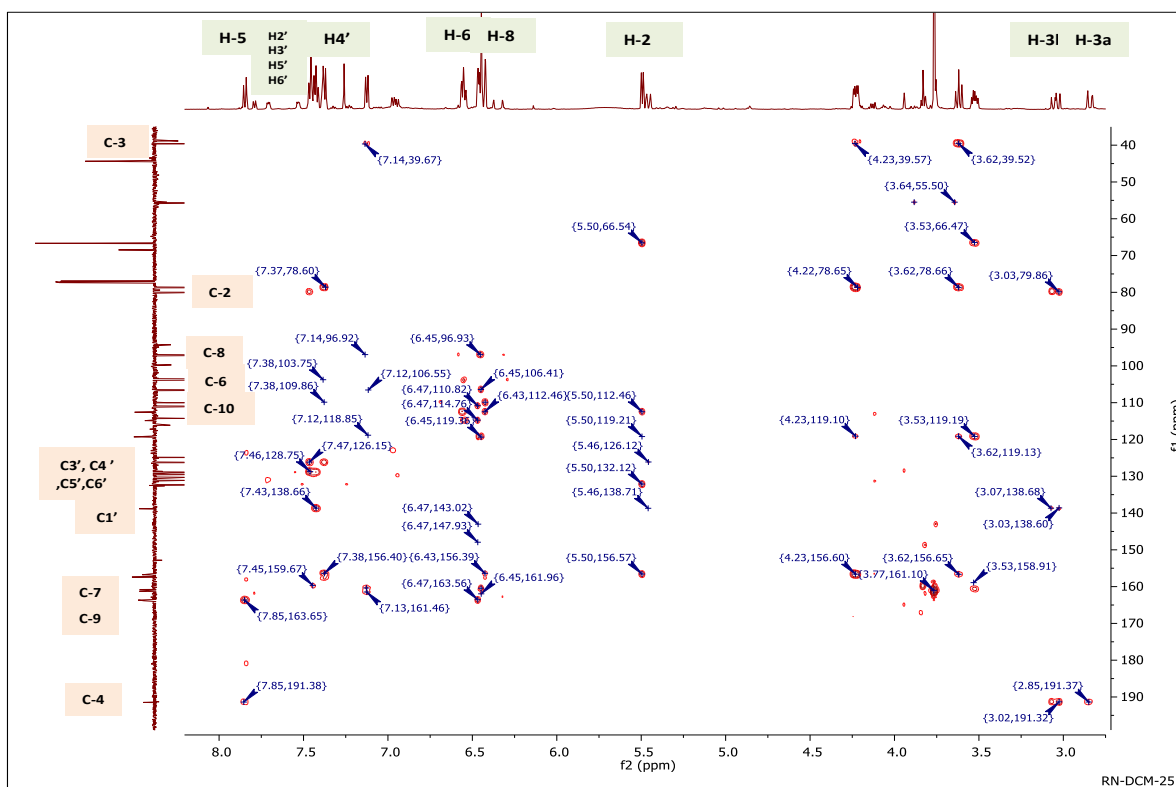
Figure 6-40: HMBC (500 MHz) spectra of the compound 20 in CDCl₃
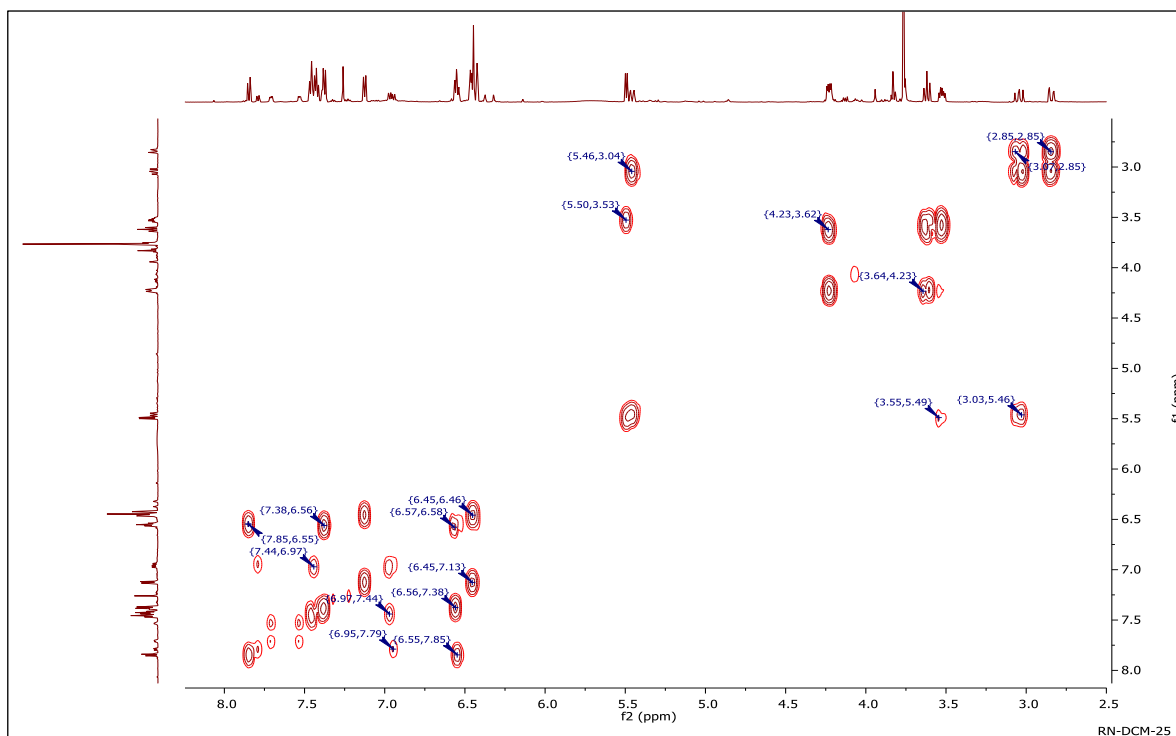
Figure 6-41: COSY (500 MHz) spectra of the compound 20 in CDCl₃

189

6.3.3 *In-vitro* Antitrypanosomal activity and cross-resistance studies of Nigerian propolis extracts and its fractions

The purified compounds isolated from RN propolis sample were tested against BSF *T. b. brucei* s427 WT and *T. b. brucei* B48; BSF *T. congolense Tc*-IL3000 WT and *T. congolense* 6C3, in order to assess their antiparasitic activity and the potential for cross-resistance with existing drugs. All EC_{50} values were shown in **Tables 6-8** and **6-9** as averages in μg/mL and μM of at least 3 independent determinations. RN-DCM crude showed relatively high activity against *T.brucei* with EC_{50} value of 1.66 μg/mL, while the purified compounds exhibited lower activities than the RN-DCM- crude as shown in **Tables 6-8**. A notable observation was that P values for all the fractions, apart from RN-Hx, were ($P > 0.05$; Student's unpaired, two tailed t-test) with a Resistance Factor (RF) of < 2 compared to a 225 fold resistance for pentamidine ($P<0.0001$), therefore there was no cross-resistance with pentamidine.

EC_{50} values for *T. congolense* IL3000 WT and its resistant cell line to diminazene. *T. congolense* 6C3 were shown in **Tables 6-9**. The most active fractions were RN-DCM Crude and RNE- 26 with EC_{50} 4.00 and 4.36 μg/mL, respectively. Neither the RN extracts nor purified compounds excepted cross resistance with resistance cell line to current AAT treatment such as diminazen *T. congolense* 6C3, where the P values > 0.05; Student's unpaired, two tailed t-test) with a Resistance Factor (RF) of 0.49 compared to 14-fold resistance for diminazene ($P<0.0001$). The assays precision was achieved for all samples where <30 % RSD.

Table 6-8: EC_{50} values of RN propolis and its purified compounds on *T. brucei. S427* wild-type, and B48 (n=3).

| Samples | T. brucei S427WT | | | | T. brucei B48 (Pentamidine Resistance) | | | | | |
	Mean of EC_{50} (μg/mL)	Mean of EC_{50} (μM)	SD	RSD%	Mean of EC_{50} (μg/mL)	Mean of EC_{50} (μM)	RF	t-test	SD	RSD%
RN-DCM-Crude	1.66	-	0.13	8.10	2.22		1.34	0.062	0.35	15.89
RN-DCM 13 To 17 (**16**)	3.44	12.01	0.66	19.33	4.66	16.30	1.36	0.159	1.04	22.22
RN-DCM-22 (**19**)	7.93	29.34	0.56	7.00	8.90	32.97	1.12	0.102	0.57	6.46
RN-DCM-25 (**19+20**)	7.73	-	1.52	19.66	9.14	-	1.18	0.219	0.72	7.87
RN-DCM-26	10.35	-	1.29	12.44	12.72	-	1.23	0.061	0.93	7.28
RN-DCM-27 to 28	5.05	-	0.95	18.84	6.62	-	1.31	0.210	1.54	23.30
RN-DCM-29 (**17**)	5.69	18.57	0.94	16.46	7.88	28.97	1.39	0.103	1.54	19.52

RN-DCM-30	4.52	-	0.31	6.76	5.77	-	1.27	0.076	0.85	14.74
RNE-Crude	2.53	-	0.47	18.39	2.93	-	1.16	0.454	0.71	24.06
RNE- 20	5.81	-	1.46	25.10	8.02	-	1.38	0.107	1.13	14.10
RNE- 22	3.03	-	0.35	11.41	3.91	-	1.29	0.015	0.14	3.46
RNE- 22B	4.68	-	0.4	8.51	6.95	-	1.49	0.003	0.49	7.10
RNE- 26 (**18**)	3.86	14.16	0.54	13.92	4.75	17.43	1.23	0.088	0.43	9.00
RN-Hx crude	2.51	-	0.58	23.14	4.92	-	1.96	0.005	0.46	9.27
Pentamidine	-	0.0022	0.0019	86.39	0.49	0.49	224.76	0.0002	0.07	13.90

Table 6-9: EC$_{50}$ values of RN propolis extracts and its purified compounds on *T. congolense* IL300, and the *T. congolense* resistance cell line to diminazene (n=3).

Samples	Trypanosoma congolense IL300				Trypanosoma congolense Diminazene Resistance					
	Mean of EC$_{50}$ (µg/mL)	Mean of EC$_{50}$ (µM)	SD	RSD%	Mean of EC$_{50}$ (µg/mL)	Mean of EC$_{50}$ (µM)	RF	t-test	SD	RSD%
RN-DCM-Crude	4.00		0.72	18.09	4.68		1.17	0.250	0.50	10.72
RN-DCM 13 To 17 (**16**)	12.11	42.34	1.58	13.02	12.51	43.73	1.03	0.790	1.86	14.82
RN-DCM- 22 (**19**)	8.69	32.16	0.91	10.50	7.45	27.58	0.86	0.195	1.03	13.88
RN-DCM- 25 (**19+20**)	7.78	N/A	0.85	10.94	7.93	N/A	1.02	0.854	1.08	13.56
RN-DCM- 26	11.74	N/A	3.43	29.22	13.06	N/A	1.11	0.615	2.42	18.54
RN-DCM- 27 to 28	12.40	N/A	1.58	12.78	12.65	N/A	1.02	0.844	1.36	10.78
RN-DCM- 29 (**17**)	7.51	27.58	1.58	21.10	7.10	26.09	0.95	0.621	0.49	6.85
RN-DCM- 30	12.93	N/A	1.23	9.48	13.73	N/A	1.06	0.644	2.12	15.47
RNE-Crude	6.70	N/A	1.83	27.22	6.74	N/A	1.01	0.968	0.95	14.06
RNE- 20	11.73	N/A	2.87	24.47	11.00	N/A	0.94	0.787	3.27	29.71
RNE- 22	7.88	N/A	0.66	8.36	8.65	N/A	1.10	0.362	1.11	12.80
RNE- 22B	7.10	N/A	1.70	23.99	8.71	N/A	1.23	0.243	1.11	12.70
RNE- 26 (**18**)	4.36	16.02	0.46	10.59	4.47	16.42	1.02	0.844	0.75	16.81
RN-Hx crude	14.66	N/A	2.65	18.05	13.16	N/A	0.90	0.571	3.26	24.76
Diminazene	-	0.2558	0.03	10.99	-	3.69	14.42	0.002	0.84	22.67

6.3.4 *In vitro* cytotoxicity of Nigerian Propolis extracts and its fractions on mammalian cells

The RN crudes and its purified compounds were tested *in vitro* for their cytotoxicity activities against human cell line U937 and murine cell line Raw 246.7, the cell viability was determined using resazurin assay. The toxicity results in **Table 6-10** showed that the RN-DCM- 22 displayed the least IC$_{50}$ record however, crude extracts RN-DCM, RNE, RN-Hx showed low toxicity to these cell lines. Thus, RN crude extracts displayed remarkable selectivity against kinetoplastid parasites compared to the mammalian cells. An assay precision of <11 % RSD was achieved for all samples.

Table 6-10: IC$_{50}$ of Cytotoxicity of RN propolis samples and its purified compounds against U937 cell line and RAW 246.7 cell line.

Samples	U937					RAW 246.7				
	Mean of IC$_{50}$ (μg/mL)	Mean of IC$_{50}$ (μM)	SD	RSD%	SI=U 937/T.b.bWT	Mean of IC$_{50}$ (μg/mL)	Mean of IC$_{50}$ (μM)	SD	RSD %	SI = RAW 246.7/T.C
RN-DCM-Crude	85.99		7.31	8.50	51.74	103.79		5.93	5.71	25.97
RN-DCM 13 To 17 (**16**)	44.38	155.1	3.40	7.66	12.92	55.27	193.15	5.93	10.72	4.56
RN-DCM- 22 (**19**)	42.38	156.81	6.37	15.04	5.34	47.46	175.60	3.36	7.07	5.46
RN-DCM- 25 (**19+20**)	46.83		6.81	14.55	6.06	119.93		5.53	4.61	15.42
RN-DCM- 26	85.09		8.74	10.27	8.22	121.70		3.95	3.25	10.37
RN-DCM- 27 to 28	58.41		2.25	3.84	11.56	85.46		8.12	9.50	6.89
RN-DCM- 29 (**17**)	51.23	188.25	5.72	11.17	9.00	53.97	198.32	6.43	11.92	7.19
RN-DCM- 30	52.69		5.97	11.32	11.65	54.36		6.32	11.63	4.21
RNE-Crude	129.6		5.12	3.95	51.23	133.33		7.32	5.49	19.89
RNE- 20	55.75		10.80	19.38	9.60	79.10		8.27	10.46	6.74
RNE- 22	51.36		8.81	17.15	16.96	46.63		4.63	9.93	5.91
RNE- 22B	45.93		3.34	7.27	9.82	47.86		3.11	6.50	6.74
RNE- 26 (**18**)	64.95	238.68	4.11	6.33	16.84	61.44	225.65	4.15	6.75	14.08
RN-Hx crude	119.5		8.23	6.88	47.55	154.07		11.80	7.66	10.51

Chapter Seven

7 General Discussion, Conclusion and Future Work

Generally, propolis is composed of a wide range of secondary metabolites that are variable even if the samples are collected from the same geographic region. The diversity of the propolis components is related to the miscellaneous of the plant species that are collected by bees in that particular zone (Bankova, 2005, Miguel and Antunes, 2011, Toreti et al., 2013, Huang et al., 2014). Consequently, the biological activities of propolis are diverse. In addition, not all the compounds in propolis have been identified even in the commonly used temperate propolis. Therefore, presently, there is a hinderance in the achievement of the therapeutic standardisation (Sforcin, 2016, de la Cruz-Cervantes et al., 2018). Thus, more studies are necessary to investigate and identify other propolis components. In addition, the biological activities of each type of propolis need to be correlated with their chemical composition, additional tests are required to fully investigate the biological effects of many types of propolis sample.

This thesis investigated the chemical compositions of a wide range of propolis samples derived from different African and Pacific Ocean locations by applying the tools of metabolomics and then evaluating for activity against selected kinetoplastid parasites. This chapter summarizes the findings from chapters 3, 4, 5 and 6. The primary aim was to describe comprehensive of the chemical profile of the samples by applying MzMine, SIMCA-P and PCA analysis based to LC-MS data obtained for the propolis samples. The results demonstrated the applicability of the method since it was able to classify the 25 samples tested into five different groups according to their chemical profile.

From the outset, the main objectives of this project were to study the most bioactive samples that had sufficient weight for preparative scale fractionation among in each cluster. However, the group the New Zealand sample was excluded although it displayed high activity, in view of the fact that, the chemical and biological activity was well studied previously in the literature, and also, because of the long time taken to complete the isolation processes and structure elucidation of the biologically active compounds.

The isolation and identification process without a biologicallly guided assay can be geared towards obtaining a biologically active or inactive compound. Thus, target samples with biological activity is significant and dictates the separation and purification process. Since, the isolation and identification processes for the sample of interest mainly depend on profiling of the target fraction and identifying the secondary metabolites. Hence, the target of the separation must be established before the selection of the separation technique. Thus, knowing the series

of compounds as well as the nature of the propolis sample aids in the effective fractionation. Meanwell, the isolation and identification of the compounds depends significantly on the techniques used.

The propolis extracts and fractions of the interest samples and their purified compounds were evaluated for biological activity *in vitro* against selected kinetoplastid parasites. Active principles were isolated by bioassay-led fractionation, testing for trypanocidal activity, and identified using NMR and mass spectrometry. The last objective was to determine the cytotoxicity of the propolis samples, and the purified compounds isolated from Papua New Guinea, Zambian, Tanzanian and Nigerian propolis samples on two cell lines U937 and RAW246.7 was achieved via the resazurin assay.

The study of PNG propolis identified and characterized 12 triterpenoid compounds. The PNG extract and its fractions displayed high levels of anti-protozoal activity and showed low toxicity on both U937 cell growth and RAW 26.7, the crude extract exhibited a higher f Selectivity Index than the isolated compounds. While other studies of propolis identified and characterized two novel flavanones and one known flavanone isolated from Tanzanian and Zambian propolis. All flavanones demonstrated antitrypanosomal activity against drug-susceptible and drug-resistant *T. b. brucei* and *T. congolense*. Interestingly, the Tanzanian propolis extract was found to be more active than its fractions and purified compounds in these assays. The Nigerian propolis analysis yield of five known compounds a flavanone, isoflavan and isoflavonoids. The Nigerian extracts and its purified compounds were tested *in vitro* for their cytotoxicity activities. The Nigerian propolis extract was found to have greater antitrypanosomal activity than its fractions and isolated compounds. Also, Nigerian propolis extracts and the purified compounds showed low toxicity on both U937 cell growth and RAW 26.7 cell lines. Thus, Nigerian crudes displayed remarkable selectivity against kinetoplastid parasites compared to the mammalian cells.

These findings are in line with previous reports of greater antitrypanosomal activity of crude propolis extracts from Nigeria and Libya compared with their isolated phytochemicals ((Siheri et al., 2014, Siheri et al., 2016b); Omar et al., 2017). Taken together, these results consistently point to the possibility of a synergistic effect between the compounds in propolis with respect to antitrypanosomal activity. In fact, this makes the use of propolis to treat diseases caused by kinetoplastid parasites more attractive since a whole propolis extract would be decidedly

cheaper to produce but could require standardization. The use of proton NMR with pattern analysis might be a useful tool in this respect.

Propolis, whatever its origin, appears to always exhibit high levels of anti-trypanosomatid activity, particularly exhibited by flavonoids (Siheri et al., 2016b, Alotaibi et al., 2019, Omar et al., 2016). This is believed to be a self-selecting feature due to the bee's vulnerability to certain trypanosomatid parasites. The Scottish honey bee microbiome contains high levels of genetic material derived from the trypanosomatid *Lotmarim passim* (Regan et al., 2018) and this organism has been found to be widespread in other bee populations (Schwarz et al., 2015, Castelli et al., 2019, Ravoet et al., 2015). Thus far there is no evidence that bees ingest propolis but since the spread of the protozoal infection occurs via insect feces (RUIZ-GONZÁLEZ and Brown, 2006), coating the surfaces in the hive with propolis that is active against trypanosomatids could prevent transmission. Interestingly, it has recently been reported that feeding propolis to bees also reduces infection with the microsporidium bee parasite *Nosema ceranae* (Mura et al., 2020). In addition, it has observed that propolis has beneficial effects in stablising the honey be microbiome (Saelao et al. 2020). East African propolis, like propolis from other African locations, has promising anti-kinetoplastid properties that should be prioritized for further development as antiparasitic agents. Despite the great variation in its chemical components, propolis from different geographic regions showed promising activity against kinetoplastid parasites. The crudes displaying remarkable selectivity index's against kinetoplastid parasites compared to the mammalian cells

We propose that the anti-kinetoplastid activity happens because of the synergic activity of components within the mixture. The crude extracts tend to have lower toxicity against the mammalian cell lines and that is lost when individual compounds are separated and purified. However, the problem of the standardization of propolis has been unsolvable until now due to the high diversity of the propolis components and the challenge, in establishing a clear relationship between specific types of propolis and different biological activities (Bankova, 2005). The presence of a specific compound in the extract as a major component could lead to the expectation of particular bioactivity which is not in the mixture as a whole (Sforcin and Bankova, 2011; Toreti et al., 2013; Mendonça et al., 2015).

Finally, This study has filled many gaps identified at the beginning of the project such as a shortage of literature available on the study of African and Pacific Ocean propolis and proved

the usefulness of metabolomics tools along with LC-MS data inorder chemically profile propolis, compare different types and associate composition with bioactivity.. Also, the Isolation and structure elucidation of 20 compounds was carried out with two of them being novel. The biological effects of these samples have been evaluated in protozoa and the cytotoxicity against two cell lines was determined. The the selectivity index of propolis extracts and purified compounds against trypanosoma species and Crithidia could be determined.

Future Work:

There is still a lot of work to be done by researchers to achieve a reliable standardization of propolis. One approach to this would be to use proton NMR, which is more reliably quantitative than MS for complex mixtures, to set a quality standard for propolis from particular sources. Variations in overall composition could then be linked variations in biological activity. A future plan will be to continue work on different propolis samples from different geographical regions in order to chemically profile various types of propolis and investigate them for other pharmacological activities. Analyzing different samples by applying metabolic tools and identification of target novel compounds might aid in uncovering new bioactive components which aid in the understanding this exceptional natural product. It would also be of interest to test extracts, fractions and compounds against a wider panel of protozoal pathogens such as Leishmania, malaria and trichomoniasis in order to find one potential drug targets that might be able to treat different types of trypanosomes (broad-spectrum treatment). More structure-activity relationship analysis is required to optimise these natural compounds as leads for synthetic compounds.

References

ACHCAR, F., FADDA, A., HAANSTRA, J. R., KERKHOVEN, E. J., KIM, D.-H., LEROUX, A. E., PAPAMARKOU, T., ROJAS, F., BAKKER, B. M. & BARRETT, M. P. 2014. The silicon trypanosome: a test case of iterative model extension in systems biology. *Advances in Microbial Physiology.* Elsevier.

ALARIBE, C. S., ESPOSITO, T., SANSONE, F., SUNDAY, A., PAGANO, I., PICCINELLI, A. L., CELANO, R., CUESTA RUBIO, O., COKER, H. A. & NABAVI, S. M. 2019. Nigerian propolis: chemical composition, antioxidant activity and α-amylase and α-glucosidase inhibition. *Natural Product Research*, 1-5.

ALENCAR, S. M., OLDONI, T. L., CASTRO, M. L., CABRAL, I. S., COSTA-NETO, C. M., CURY, J. A., ROSALEN, P. L. & IKEGAKI, M. 2007. Chemical composition and biological activity of a new type of Brazilian propolis: red propolis. *J Ethnopharmacol,* 113, 278-83.

ALMUTAIRI, S., EAPEN, B., CHUNDI, S. M., AKHALIL, A., SIHERI, W., CLEMENTS, C., FEARNLEY, J., WATSON, D. G. & EDRADA-EBEL, R. 2014. New anti-trypanosomal active prenylated compounds from African propolis. *Phytochemistry Letters,* 10, 35-39.

ALOTAIBI, A., EBILOMA, G. U., WILLIAMS, R., ALENEZI, S., DONACHIE, A.-M., GUILLAUME, S., IGOLI, J. O., FEARNLEY, J., DE KONING, H. P. & WATSON, D. G. 2019. European propolis is highly active against trypanosomatids including Crithidia fasciculata. *Scientific Reports,* 9, 1-10.

ASFARAM, S., FAKHAR, M., KEIGHOBADI, M. & AKHTARI, J. 2020. Promising Anti-Protozoan Activities of Propolis (Bee Glue) as Natural Product: A Review. *Acta Parasitologica*, 1-12.

AYUPOVA, D., DOBHAL, G., LAUFERSKY, G., NANN, T. & GOREHAM, R. V. 2019. An in vitro investigation of cytotoxic effects of InP/ZnS quantum dots with different surface chemistries. *Nanomaterials,* 9, 135.

BANKOVA, V. 2005. Chemical diversity of propolis and the problem of standardization. *Journal of ethnopharmacology,* 100, 114-117.

BANKOVA, V., POPOVA, M. & TRUSHEVA, B. 2014. Propolis volatile compounds: chemical diversity and biological activity: a review. *Chemistry Central Journal,* 8, 28.

BANSKOTA, A. H., TEZUKA, Y. & KADOTA, S. 2001. Recent progress in pharmacological research of propolis. *Phytotherapy Research,* 15, 561-571.

BARRETT, M. P., BAKKER, B. M. & BREITLING, R. 2010. Metabolomic systems biology of trypanosomes. *Parasitology,* 137, 1285-1290.

BARRETT, M. P., BURCHMORE, R. J., STICH, A., LAZZARI, J. O., FRASCH, A. C., CAZZULO, J. J. & KRISHNA, S. 2003. The trypanosomiases. *The Lancet,* 362, 1469-1480.

BARTH, H. G., JACKSON, C. & BOYES, B. E. 1994. Size exclusion chromatography. *Analytical chemistry,* 66, 595-620.

BASIM, E., BASIM, H. & ÖZCAN, M. 2006. Antibacterial activities of Turkish pollen and propolis extracts against plant bacterial pathogens. *Journal of Food Engineering,* 77, 992-996.

BITTENCOURT, M. L., RIBEIRO, P. R., FRANCO, R. L., HILHORST, H. W., DE CASTRO, R. D. & FERNANDEZ, L. G. 2015. Metabolite profiling, antioxidant and antibacterial activities of Brazilian propolis: Use of correlation and multivariate analyses to identify potential bioactive compounds. *Food Research International,* 76, 449-457.

BLICHARSKA, N. & SEIDEL, V. 2019. Chemical diversity and biological activity of african propolis. *Progress in the Chemistry of Organic Natural Products 109.* Springer.

BOGDANOV, S. 2012. Propolis: Composition, Healt, medicine: A Review. Obtenido de Propolis: composition, health, medicine: a review.: www ….

BOITEAU, P. & CHANEZ, M. 1967. Isolation of madecassic acid, a new triterpene acid from Madagascan Centella asiatica. *Comptes Rendus de l Academie des Sciences. Serie D, Sciences Naturelles (Paris),* 264**,** 407-410.

BREITMAIER, E. 2002. *Structure Elucidation By NMR In Organic Chemistry: A Practical Guide.*, Wiley.

BRIDGES, D. J., GOULD, M. K., NERIMA, B., MÄSER, P., BURCHMORE, R. J. & DE KONING, H. P. 2007. Loss of the high affinity pentamidine transporter is responsible for high levels of cross-resistance between arsenical and diamidine drugs in African trypanosomes. *Molecular pharmacology*.

BURDOCK, G. 1998a. Review of the biological properties and toxicity of bee propolis (propolis). *Food and Chemical toxicology,* 36**,** 347-363.

BURDOCK, G. A. 1998b. Review of the biological properties and toxicity of bee propolis (propolis). *Food Chem Toxicol,* 36**,** 347-63.

BÜSCHER, P., CECCHI, G., JAMONNEAU, V. & PRIOTTO, G. 2017. Human african trypanosomiasis. *The Lancet,* 390**,** 2397-2409.

CAMPO FERNÁNDEZ, M., CUESTA-RUBIO, O., ROSADO PEREZ, A. S., MONTES DE OCA PORTO, R., MÁRQUEZ HERNÁNDEZ, I., PICCINELLI, A. L. & RASTRELLI, L. 2008. GC-MS determination of isoflavonoids in seven red Cuban propolis samples. *Journal of agricultural and food chemistry,* 56**,** 9927-9932.

CAPEWELL, P., VEITCH, N. J., TURNER, C. M. R., RAPER, J., BERRIMAN, M., HAJDUK, S. L. & MACLEOD, A. 2011. Differences between Trypanosoma brucei gambiense groups 1 and 2 in their resistance to killing by trypanolytic factor 1. *PLoS Negl Trop Dis,* 5**,** e1287.

CASTELLI, L., BRANCHICCELA, B., INVERNIZZI, C., TOMASCO, I., BASUALDO, M., RODRIGUEZ, M., ZUNINO, P. & ANTÚNEZ, K. 2019. Detection of Lotmaria passim in Africanized and European honey bees from Uruguay, Argentina and Chile. *Journal of invertebrate pathology,* 160**,** 95-97.

CERONE, M., ULIASSI, E., PRATI, F., EBILOMA, G. U., LEMGRUBER, L., BERGAMINI, C., WATSON, D. G., DE AM FERREIRA, T., ROTH CARDOSO, G. S. H. & SOARES ROMEIRO, L. A. 2019. Discovery of Sustainable Drugs for Neglected Tropical Diseases: Cashew Nut Shell Liquid (CNSL)‐Based Hybrids Target Mitochondrial Function and ATP Production in Trypanosoma brucei. *ChemMedChem,* 14**,** 621-635.

CHENG, Y., LIANG, Q., HU, P., WANG, Y., JUN, F. W. & LUO, G. 2010. Combination of normal-phase medium-pressure liquid chromatography and high-performance counter-current chromatography for preparation of ginsenoside-Ro from Panax ginseng with high recovery and efficiency. *Separation and purification technology,* 73**,** 397-402.

CHING, A. Y. L., WAH, T. S., SUKARI, M. A., LIAN, G. E. C., RAHMANI, M. & KHALID, K. 2007. Characterization of flavonoid derivatives from Boesenbergia rotunda (L.). *The Malaysian Journal of Analytical Sciences,* 11**,** 154-159.

CHINWE, S. A., RASTRELLI, L., SUNDAY, A., EMMANUEL, O., SOLA, I. & HERBERT, C. 2013. Anti-Helicobacter Pylori Activities of Nigerian Propolis (Bee Product). *Planta Medica,* 79**,** PM2.

CLAESON, P., TUCHINDA, F. & REUTRAKUL, V. 1993. Some empirical aspects on the practical use of flash chromatography and medium pressure liquid chromatography for

the isolation of biologically active compounds from plants. *Journal of the ScientiTc Society of Thailand,* 19**,** 73-86.

COUSTOU, V., GUEGAN, F., PLAZOLLES, N. & BALTZ, T. 2010. Complete in vitro life cycle of Trypanosoma congolense: development of genetic tools. *PLoS neglected tropical diseases,* 4**,** e618.

CRAGG, G. M. & NEWMAN, D. J. 2005. Biodiversity: A continuing source of novel drug leads. *Pure and applied chemistry,* 77**,** 7-24.

CUTILLAS, P. R. & TIMMS, J. F. 2010. *LC-MS/MS in proteomics: methods and applications*, Springer.

DE CASTRO, S. & HIGASHI, K. 1995. Effect of different formulations of propolis on mice infected with Trypanosoma cruzi. *Journal of ethnopharmacology,* 46**,** 55-58.

DE KONING, H. P., MACLEOD, A., BARRETT, M. P., COVER, B. & JARVIS, S. M. 2000. Further evidence for a link between melarsoprol resistance and P2 transporter function in African trypanosomes. *Molecular and biochemical parasitology,* 106**,** 181-185.

DE LIMA, G. G., DE SOUZA, R. O., BOZZI, A. D., POPLAWSKA, M. A., DEVINE, D. M. & NUGENT, M. J. 2016. Extraction Method Plays Critical Role in Antibacterial Activity of Propolis-Loaded Hydrogels. *Journal of pharmaceutical sciences,* 105**,** 1248-1257.

DE, P. T., URONES, J., MARCOS, I., BASABE, P., CUADRADO, M. S. & MORO, R. F. 1987. Triterpenes from Euphorbia broteri. *Phytochemistry,* 26**,** 1767-1776.

DEANS, S., SIMPSON, E., NOBLE, R., MACPHERSON, A. & PENZES, L. Natural antioxidants from Thymus vulgaris (thyme) volatile oil: the beneficial effects upon mammalian lipid metabolism. WOCMAP I-Medicinal and Aromatic Plants Conference: part 2 of 4 332, 1992. 177-182.

EMARA, S., AMER, S., ALI, A., ABOULEILA, Y., OGA, A. & MASUJIMA, T. 2017. Single-cell metabolomics. *Metabolomics: from fundamentals to clinical applications.* Springer.

ESCOBEDO‐MARTÍNEZ, C., CONCEPCIÓN LOZADA, M., HERNÁNDEZ‐ORTEGA, S., VILLARREAL, M. L., GNECCO, D., ENRÍQUEZ, R. G. & REYNOLDS, W. 2012. 1H and 13C NMR characterization of new cycloartane triterpenes from Mangifera indica. *Magnetic Resonance in Chemistry,* 50**,** 52-57.

FALCÃO, S. I., VALE, N., COS, P., GOMES, P., FREIRE, C., MAES, L. & VILAS‐BOAS, M. 2014. In vitro evaluation of portuguese propolis and floral sources for antiprotozoal, antibacterial and antifungal activity. *Phytotherapy research,* 28**,** 437-443.

FIELD, M. C., HORN, D., FAIRLAMB, A. H., FERGUSON, M. A., GRAY, D. W., READ, K. D., DE RYCKER, M., TORRIE, L. S., WYATT, P. G. & WYLLIE, S. 2017. Anti-trypanosomatid drug discovery: an ongoing challenge and a continuing need. *Nature Reviews Microbiology,* 15**,** 217.

FITZMAURICE, S., SIVAMANI, R. & ISSEROFF, R. 2011. Antioxidant therapies for wound healing: a clinical guide to currently commercially available products. *Skin pharmacology and physiology,* 24**,** 113-126.

FOKT, H., PEREIRA, A., FERREIRA, A., CUNHA, A. & AGUIAR, C. 2010. How do bees prevent hive infections? The antimicrobial properties of propolis. *Current Research, Technology and Education Topics in Applied Microbiology and Microbial Biotechnology,* 1**,** 481-493.

FRANCO, J. R., CECCHI, G., PRIOTTO, G., PAONE, M., DIARRA, A., GROUT, L., MATTIOLI, R. C. & ARGAW, D. 2017. Monitoring the elimination of human African trypanosomiasis: Update to 2014. *PLoS neglected tropical diseases,* 11**,** e0005585.

FREIRES, I. A., QUEIROZ, V. C. P. P., FURLETTI, V. F., IKEGAKI, M., DE ALENCAR, S. M., DUARTE, M. C. T. & ROSALEN, P. L. 2016. Chemical composition and

antifungal potential of Brazilian propolis against Candida spp. *Journal de Mycologie Médicale/Journal of Medical Mycology,* 26**,** 122-132.

FREITAS, S., SHINOHARA, L., SFORCIN, J. & GUIMARÃES, S. 2006. In vitro effects of propolis on Giardia duodenalis trophozoites. *Phytomedicine,* 13**,** 170-175.

FUCHINO, H., SATOH, T. & TANAKA, N. 1996. Chemical Evaluation of Betula Species in Japan. III. Constiutents of Betula maximowicziana. *Chemical and pharmaceutical bulletin,* 44**,** 1748-1753.

GHISALBERTI, E. 1979. Propolis: a review. *Bee world,* 60**,** 59-84.

GIORDANI, F., MORRISON, L. J., ROWAN, T. G., DE KONING, H. P. & BARRETT, M. P. 2016. The animal trypanosomiases and their chemotherapy: a review. *Parasitology,* 143**,** 1862-1889.

GOULD, M. K., VU, X. L., SEEBECK, T. & DE KONING, H. P. 2008. Propidium iodide-based methods for monitoring drug action in the kinetoplastidae: comparison with the Alamar Blue assay. *Analytical biochemistry,* 382**,** 87-93.

HAGE, D. S. 2018. Chromatography. *Principles and Applications of Clinical Mass Spectrometry.* Elsevier.

HAN, S., SUNG, K.-H., YIM, D., LEE, S., CHO, K., LEE, C.-K., HA, N.-J. & KIM, K. 2002. Activation of murine macrophage cell line RAW 264.7 by Korean propolis. *Archives of pharmacal research,* 25**,** 895-902.

HARVEY, A. L., EDRADA-EBEL, R. & QUINN, R. J. 2015. The re-emergence of natural products for drug discovery in the genomics era. *Nature reviews drug discovery,* 14**,** 111-129.

HO, C. S., LAM, C., CHAN, M., CHEUNG, R., LAW, L., LIT, L., NG, K., SUEN, M. & TAI, H. 2003. Electrospray ionisation mass spectrometry: principles and clinical applications. *The Clinical Biochemist Reviews,* 24**,** 3.

HOSOE, T., NOZAWA, K., UDAGAWA, S.-I., NAKAJIMA, S. & KAWAI, K.-I. 1990. An anthraquinone derivative from Dichotomophthora lutea. *Phytochemistry,* 29**,** 997-999.

HULPIA, F., MABILLE, D., CAMPAGNARO, G. D., SCHUMANN, G., MAES, L., RODITI, I., HOFER, A., DE KONING, H. P., CALJON, G. & VAN CALENBERGH, S. 2019. Combining tubercidin and cordycepin scaffolds results in highly active candidates to treat late-stage sleeping sickness. *Nature communications,* 10**,** 1-11.

ISLA, M. I., MORENO, M. N., SAMPIETRO, A. & VATTUONE, M. A. 2001. Antioxidant activity of Argentine propolis extracts. *Journal of Ethnopharmacology,* 76**,** 165-170.

ISLA, M. I., PAREDES-GUZMAN, J. F., NIEVA-MORENO, M. I., KOO, H. & PARK, Y. K. 2005. Some chemical composition and biological activity of northern Argentine propolis. *Journal of agricultural and food chemistry,* 53**,** 1166-1172.

JACKSON, C. M., ESNOUF, M. P., WINZOR, D. J. & DUEWER, D. L. 2007. Defining and measuring biological activity: applying the principles of metrology. *Accreditation and quality assurance,* 12**,** 283-294.

JAIN, A., YANG, G. & YALKOWSKY, S. H. 2004. Estimation of melting points of organic compounds. *Industrial & engineering chemistry research,* 43**,** 7618-7621.

KADDURAH-DAOUK, R., KRISTAL, B. S. & WEINSHILBOUM, R. M. 2008. Metabolomics: a global biochemical approach to drug response and disease. *Annual review of pharmacology and toxicology,* 48**,** 653-683.

KALOGEROPOULOS, N., KONTELES, S. J., TROULLIDOU, E., MOURTZINOS, I. & KARATHANOS, V. T. 2009. Chemical composition, antioxidant activity and antimicrobial properties of propolis extracts from Greece and Cyprus. *Food chemistry,* 116**,** 452-461.

KARDAR, M., ZHANG, T., COXON, G., WATSON, D., FEARNLEY, J. & SEIDEL, V. 2014. Characterisation of triterpenes and new phenolic lipids in Cameroonian propolis. *Phytochemistry,* 106**,** 156-163.

KENNEDY, P. G. 2013. Clinical features, diagnosis, and treatment of human African trypanosomiasis (sleeping sickness). *The Lancet Neurology,* 12**,** 186-194.

KIPANDULA, W., SMITH, T. K. & MACNEILL, S. A. 2017. Tandem affinity purification of exosome and replication factor C complexes from the non-human infectious kinetoplastid parasite Crithidia fasciculata. *Molecular and biochemical parasitology,* 217**,** 19-22.

KIPANDULA, W., YOUNG, S. A., MACNEILL, S. A. & SMITH, T. K. 2018. Screening of the MMV and GSK open access chemical boxes using a viability assay developed against the kinetoplastid Crithidia fasciculata. *Molecular and biochemical parasitology,* 222**,** 61-69.

KOSTRZEWA-SUSŁOW, E. & JANECZKO, T. 2012. Microbial transformations of 7-hydroxyflavanone. *The Scientific World Journal,* 2012.

KUJUMGIEV, A., TSVETKOVA, I., SERKEDJIEVA, Y., BANKOVA, V., CHRISTOV, R. & POPOV, S. 1999. Antibacterial, antifungal and antiviral activity of propolis of different geographic origin. *Journal of ethnopharmacology,* 64**,** 235-240.

KUMAZAWA, S., UEDA, R., HAMASAKA, T., FUKUMOTO, S., FUJIMOTO, T. & NAKAYAMA, T. 2007. Antioxidant prenylated flavonoids from propolis collected in Okinawa, Japan. *J. of Agricultural and Food Chemistry,* 55**,** 7722-7725.

KUROPATNICKI, A. K., SZLISZKA, E. & KROL, W. 2013. Historical aspects of propolis research in modern times. *Evidence-Based Complementary and Alternative Medicine,* 2013.

LA GRECA, F. & MAGEZ, S. 2011. Vaccination against trypanosomiasis: can it be done or is the trypanosome truly the ultimate immune destroyer and escape artist? *Human vaccines,* 7**,** 1225-1233.

LANGOUSIS, G. & HILL, K. L. 2014. Motility and more: the flagellum of Trypanosoma brucei. *Nature Reviews Microbiology,* 12**,** 505-518.

LUIS-VILLAROYA, A., ESPINA, L., GARCÍA-GONZALO, D., BAYARRI, S., PÉREZ, C. & PAGÁN, R. 2015. Bioactive properties of a propolis-based dietary supplement and its use in combination with mild heat for apple juice preservation. *International journal of food microbiology,* 205**,** 90-97.

MAMANI-MATSUDA, M., RAMBERT, J., MALVY, D., LEJOLY-BOISSEAU, H., DAULOUÈDE, S., THIOLAT, D., COVES, S., COURTOIS, P., VINCENDEAU, P. & MOSSALAYI, M. D. 2004. Quercetin induces apoptosis of Trypanosoma brucei gambiense and decreases the proinflammatory response of human macrophages. *Antimicrobial agents and chemotherapy,* 48**,** 924-929.

MARCUCCI, M. C. 1995. Propolis: chemical composition, biological properties and therapeutic activity. *Apidologie,* 26**,** 83-99.

MATOVU, E., STEWART, M. L., GEISER, F., BRUN, R., MÄSER, P., WALLACE, L. J., BURCHMORE, R. J., ENYARU, J. C., BARRETT, M. P. & KAMINSKY, R. 2003. Mechanisms of arsenical and diamidine uptake and resistance in Trypanosoma brucei. *Eukaryotic cell,* 2**,** 1003-1008.

MATSUDA, H., MORIKAWA, T., UEDA, H. & YOSHIKAWA, M. 2001. Medicinal foodstuffs. XXVII. Saponin constituents of gotu kola (2): structures of new ursane-and oleanane-type triterpene oligoglycosides, centellasaponins B, C, and D, from Centella asiatica cultivated in Sri Lanka. *Chemical and Pharmaceutical Bulletin,* 49**,** 1368-1371.

MEJANELLE, P., BLETON, J., GOURSAUD, S. & TCHAPLA, A. 1997. Identification of phenolic acids and inositols in balms and tissues from an Egyptian mummy. *Journal of Chromatography a,* 767**,** 177-186.

MELLO, B. C. & HUBINGER, M. D. 2012. Antioxidant activity and polyphenol contents in B razilian green propolis extracts prepared with the use of ethanol and water as solvents in different p H values. *International Journal of Food Science & Technology,* 47**,** 2510-2518.

MIGUEL, M. G. & ANTUNES, M. D. 2011. Is propolis safe as an alternative medicine? *Journal of pharmacy & bioallied sciences,* 3**,** 479.

MOUREY, T. H. & OPPENHEIMER, L. E. 1984. Principles of operation of an evaporative light-scattering detector for liquid chromatography. *Analytical Chemistry,* 56**,** 2427-2434.

MORAES, C. B., GIARDINI, M. A., KIM, H., FRANCO, C. H., ARAUJO-JUNIOR, A. M., SCHENKMAN, S., CHATELAIN, E. & FREITAS-JUNIOR, L. H. 2014. Nitroheterocyclic compounds are more efficacious than CYP51 inhibitors against Trypanosoma cruzi: implications for Chagas disease drug discovery and development. *Scientific reports,* 4**,** 4703.

MUNDAY, J. C., EZE, A. A., BAKER, N., GLOVER, L., CLUCAS, C., AGUINAGA ANDRÉS, D., NATTO, M. J., TEKA, I. A., MCDONALD, J. & LEE, R. S. 2014. Trypanosoma brucei aquaglyceroporin 2 is a high-affinity transporter for pentamidine and melaminophenyl arsenic drugs and the main genetic determinant of resistance to these drugs. *Journal of Antimicrobial Chemotherapy,* 69**,** 651-663.

MURA, A., PUSCEDDU, M., THEODOROU, P., ANGIONI, A., FLORIS, I., PAXTON, R. J. & SATTA, A. 2020. Propolis Consumption Reduces Nosema ceranae Infection of European Honey Bees (Apis mellifera). *Insects,* 11**,** 124.

NAGLE, A. S., KHARE, S., KUMAR, A. B., SUPEK, F., BUCHYNSKYY, A., MATHISON, C. J., CHENNAMANENI, N. K., PENDEM, N., BUCKNER, F. S. & GELB, M. H. 2014. Recent developments in drug discovery for leishmaniasis and human African trypanosomiasis. *Chemical reviews,* 114**,** 11305-11347.

NEWMAN, D. J. & CRAGG, G. M. 2020. Natural products as sources of new drugs over the nearly four decades from 01/1981 to 09/2019. *Journal of Natural Products,* 83**,** 770-803.

NGUYEN, H. X., NGUYEN, M. T., NGUYEN, N. T. & AWALE, S. 2017. Chemical constituents of propolis from vietnamese trigona minor and their antiausterity activity against the panc-1 human pancreatic cancer cell line. *Journal of natural products,* 80**,** 2345-2352.

NWODO, N. J., OKOYE, F. B. C., LAI, D., DEBBAB, A., BRUN, R. & PROKSCH, P. 2014. Two trypanocidal dipeptides from the roots of Zapoteca portoricensis (Fabaceae). *Molecules,* 19**,** 5470-5477.

OMAR, R., IGOLI, J. O., ZHANG, T., GRAY, A. I., EBILOMA, G. U., CLEMENTS, C. J., FEARNLEY, J., EBEL, R. E., PAGET, T. & DE KONING, H. P. 2017. The chemical characterization of Nigerian propolis samples and their activity against Trypanosoma brucei. *Scientific reports,* 7**,** 1-10.

OMAR, R. M., IGOLI, J., GRAY, A. I., EBILOMA, G. U., CLEMENTS, C., FEARNLEY, J., EDRADA EBEL, R. A., ZHANG, T., DE KONING, H. P. & WATSON, D. G. 2016. Chemical characterisation of Nigerian red propolis and its biological activity against Trypanosoma brucei. *Phytochemical Analysis,* 27**,** 107-115.

ORGANIZATION, W. H. 2019. *WHO interim guidelines for the treatment of gambiense human African trypanosomiasis*, World Health Organization.

ORSI, R. O., SFORCIN, J. M., FUNARI, S. R. & BANKOVA, V. 2005. Effects of Brazilian and Bulgarian propolis on bactericidal activity of macrophages against Salmonella typhimurium. *International Immunopharmacology,* 5**,** 359-368.

OTA, C., UNTERKIRCHER, C., FANTINATO, V. & SHIMIZU, M. 2001. Antifungal activity of propolis on different species of Candida. *Mycoses,* 44**,** 375-378.

ÖTLES, S. & KARTAL, C. 2016. Solid-Phase Extraction (SPE): Principles and applications in food samples. *Acta Scientiarum Polonorum Technologia Alimentaria,* 15**,** 5-15.

PARREIRA, N. A., MAGALHÃES, L. G., MORAIS, D. R., CAIXETA, S. C., DE SOUSA, J. P., BASTOS, J. K., CUNHA, W. R., SILVA, M. L., NANAYAKKARA, N. & RODRIGUES, V. 2010. Antiprotozoal, schistosomicidal, and antimicrobial activities of the essential oil from the leaves of Baccharis dracunculifolia. *Chemistry & biodiversity,* 7**,** 993-1001.

PASSMORE, J., LUKEY, P. & RESS, S. 2001. The human macrophage cell line U937 as an in vitro model for selective evaluation of mycobacterial antigen‐specific cytotoxic T‐cell function. *Immunology,* 102**,** 146-156.

PENA, I., MANZANO, M. P., CANTIZANI, J., KESSLER, A., ALONSO-PADILLA, J., BARDERA, A. I., ALVAREZ, E., COLMENAREJO, G., COTILLO, I. & ROQUERO, I. 2015. New compound sets identified from high throughput phenotypic screening against three kinetoplastid parasites: an open resource. *Scientific reports,* 5**,** 8771.

PICCINELLI, A. L., CAMPO FERNANDEZ, M., CUESTA-RUBIO, O., MÁRQUEZ HERNÁNDEZ, I., DE SIMONE, F. & RASTRELLI, L. 2005. Isoflavonoids isolated from Cuban propolis. *Journal of Agricultural and Food Chemistry,* 53**,** 9010-9016.

PICCINELLI, A. L., MENCHERINI, T., CELANO, R., MOUHOUBI, Z., TAMENDJARI, A., AQUINO, R. P. & RASTRELLI, L. 2013. Chemical composition and antioxidant activity of Algerian propolis. *Journal of agricultural and food chemistry,* 61**,** 5080-5088.

PLUSKAL, T., CASTILLO, S., VILLAR-BRIONES, A. & OREŠIČ, M. 2010. MZmine 2: modular framework for processing, visualizing, and analyzing mass spectrometry-based molecular profile data. *BMC bioinformatics,* 11**,** 395.

POPOVA, M., SILICI, S., KAFTANOGLU, O. & BANKOVA, V. 2005. Antibacterial activity of Turkish propolis and its qualitative and quantitative chemical composition. *Phytomedicine,* 12**,** 221-228.

PRAKASH, C. V. S. & PRAKASH, I. 2012. Isolation and structural characterization of Lupane triterpenes from Polypodium vulgare. *Research Journal of Pharmaceutical Sciences,* 1**,** 23-27.

RAVOET, J., MAHARRAMOV, J., MEEUS, I., DE SMET, L., WENSELEERS, T., SMAGGHE, G. & DE GRAAF, D. C. 2013. Comprehensive bee pathogen screening in Belgium reveals Crithidia mellificae as a new contributory factor to winter mortality. *PLoS One,* 8**,** e72443.

RAVOET, J., SCHWARZ, R. S., DESCAMPS, T., YAÑEZ, O., TOZKAR, C. O., MARTIN-HERNANDEZ, R., BARTOLOMÉ, C., DE SMET, L., HIGES, M. & WENSELEERS, T. 2015. Differential diagnosis of the honey bee trypanosomatids Crithidia mellificae and Lotmaria passim. *Journal of invertebrate pathology,* 130**,** 21-27.

REGAN, T., BARNETT, M. W., LAETSCH, D. R., BUSH, S. J., WRAGG, D., BUDGE, G. E., HIGHET, F., DAINAT, B., DE MIRANDA, J. R. & WATSON, M. 2018. Characterisation of the British honey bee metagenome. *Nature communications,* 9**,** 1-13.

RUIZ‑GONZÁLEZ, M. X. & BROWN, M. J. 2006. Honey bee and bumblebee trypanosomatids: specificity and potential for transmission. *Ecological Entomology,* 31**,** 616-622.

SALAS, A. L., ALBERTO, M. R., ZAMPINI, I. C., CUELLO, A. S., MALDONADO, L., RÍOS, J. L., SCHMEDA-HIRSCHMANN, G. & ISLA, M. I. 2016. Biological activities of polyphenols-enriched propolis from Argentina arid regions. *Phytomedicine,* 23**,** 27-31.

SALOMÃO, K., DE SOUZA, E., BARBOSA, H. & DE CASTRO, S. 2010. Propolis and derivatives of megazol: In vitro and in vivo activity on Trypanosoma cruzi, mechanism of action and selectivity. *International Journal of Infectious Diseases,* 14**,** e441-e442.

SANTOS, L. M., FONSECA, M. S., SOKOLONSKI, A. R., DEEGAN, K. R., ARAÚJO, R. P., UMSZA-GUEZ, M. A., BARBOSA, J. D., PORTELA, R. D. & MACHADO, B. A. 2020. Propolis: types, composition, biological activities, and veterinary product patent prospecting. *Journal of the Science of Food and Agriculture,* 100**,** 1369-1382.

SANTOS, V., PIMENTA, F., AGUIAR, M., DO CARMO, M., NAVES, M. & MESQUITA, R. 2005. Oral candidiasis treatment with Brazilian ethanol propolis extract. *Phytotherapy Research: An International Journal Devoted to Pharmacological and Toxicological Evaluation of Natural Product Derivatives,* 19**,** 652-654.

SARKER, S. D. & NAHAR, L. 2012. Natural Products Isolation.

SCHWARZ, R. S., BAUCHAN, G. R., MURPHY, C. A., RAVOET, J., DE GRAAF, D. C. & EVANS, J. D. 2015. Characterization of Two Species of Trypanosomatidae from the Honey Bee Apis mellifera: Crithidia mellificae Langridge and McGhee, and Lotmaria passim n. gen., n. sp. *Journal of Eukaryotic Microbiology,* 62**,** 567-583.

SEIDEL, V., PEYFOON, E., WATSON, D. G. & FEARNLEY, J. 2008. Comparative study of the antibacterial activity of propolis from different geographical and climatic zones. *Phytotherapy research,* 22**,** 1256-1263.

SEO, E.-K., SILVA, G., CHAI, H.-B., CHAGWEDERA, T., FARNSWORTH, N., CORDELL, G., PEZZUTO, J. & KINGHORN, A. 1997. Cytotoxic prenylated flavanones from Monotes engleri. *Phytochemistry,* 45**,** 509-515.

SFORCIN, J. 2007. Propolis and the immune system: a review. *Journal of ethnopharmacology,* 113, 1-14.

SFORCIN, J. M. 2016. Biological properties and therapeutic applications of propolis. *Phytotherapy research,* 30**,** 894-905.

SFORCIN, J. M. & BANKOVA, V. 2011. Propolis: is there a potential for the development of new drugs? *Journal of ethnopharmacology,* 133**,** 253-260.

SHIMADZU. 2007. *Principles and Practical Applications of Shimadzu ' s ELSD-LT 2 Evaporative Light Scattering Detector* [Online]. japan: Technical Repor t vol.6. Available: https://pdfs.semanticscholar.org/11fb/c2ccc3f655ec51ceda850e494fd2a7aa4b2f.pdf [Accessed].

SIHERI, W., EBILOMA, G. U., IGOLI, J. O., GRAY, A. I., BIDDAU, M., AKRACHALANONT, P., ALENEZI, S., ALWASHIH, M. A., EDRADA-EBEL, R. & MULLER, S. 2019. Isolation of a novel flavanonol and an alkylresorcinol with highly potent anti-trypanosomal activity from Libyan propolis. *Molecules,* 24**,** 1041.

SIHERI, W., IGOLI, J. O., GRAY, A. I., NASCIEMENTO, T. G., ZHANG, T., FEARNLEY, J., CLEMENTS, C. J., CARTER, K. C., CARRUTHERS, J. & EDRADA‑EBEL, R. 2014. The isolation of antiprotozoal compounds from Libyan propolis. *Phytotherapy research,* 28**,** 1756-1760.

SIHERI, W., ZHANG, T., EBILOMA, G. U., BIDDAU, M., WOODS, N., HUSSAIN, M. Y., CLEMENTS, C. J., FEARNLEY, J., EBEL, R. E. & PAGET, T. 2016a. Chemical and

antimicrobial profiling of propolis from different regions within Libya. *PloS one,* 11**,** e0155355.

SIHERI, W., ZHANG, T., EBILOMA, G. U., BIDDAU, M., WOODS, N., HUSSAIN, M. Y., CLEMENTS, C. J., FEARNLEY, J., EBEL, R. E. & PAGET, T. 2016b. Chemical and antimicrobial profiling of propolis from different regions within Libya. *PLoS One,* 11.

SILVA-CARVALHO, R., BALTAZAR, F. & ALMEIDA-AGUIAR, C. 2015. Propolis: a complex natural product with a plethora of biological activities that can be explored for drug development. *Evidence-based complementary and alternative medicine,* 2015.

STERNBERG, J. M. 2004. Human African trypanosomiasis: clinical presentation and immune response. *Parasite immunology,* 26**,** 469-476.

STUART, B. 2000. Infrared spectroscopy. *Kirk‐Othmer encyclopedia of chemical technology*.

STUART, K., BRUN, R., CROFT, S., FAIRLAMB, A., GÜRTLER, R. E., MCKERROW, J., REED, S. & TARLETON, R. 2008. Kinetoplastids: related protozoan pathogens, different diseases. *The Journal of clinical investigation,* 118**,** 1301-1310.

SWARTZ, M. 2010. HPLC detectors: a brief review. *Journal of Liquid Chromatography & Related Technologies,* 33**,** 1130-1150.

TAWFIKE, A. F., VIEGELMANN, C. & EDRADA-EBEL, R. 2013. Metabolomics and dereplication strategies in natural products. *Metabolomics Tools for Natural Product Discovery.* Springer.

TIJJANI, A., NDUKWE, I. & AYO, R. 2012. Isolation and characterization of lup-20 (29)-ene-3, 28-diol (Betulin) from the stem-bark of Adenium obesum (Apocynaceae). *Tropical Journal of Pharmaceutical Research,* 11**,** 259-262.

TORETI, V. C., SATO, H. H., PASTORE, G. M. & PARK, Y. K. 2013. Recent progress of propolis for its biological and chemical compositions and its botanical origin. *Evidence-Based Complementary and Alternative Medicine,* 2013.

TSICHRITZIS, F. & JAKUPOVIC, J. 1990. Diterpenes and other constituents fromRelhania species. *Phytochemistry,* 29**,** 3173-3187.

UGUR, A. & ARSLAN, T. 2004. An in vitro study on antimicrobial activity of propolis from Mugla province of Turkey. *Journal of Medicinal Food,* 7**,** 90-94.

VALENZUELA-BARRA, G., CASTRO, C., FIGUEROA, C., BARRIGA, A., SILVA, X., DE LAS HERAS, B., HORTELANO, S. & DELPORTE, C. 2015. Anti-inflammatory activity and phenolic profile of propolis from two locations in Región Metropolitana de Santiago, Chile. *Journal of ethnopharmacology,* 168**,** 37-44.

VODNALA, S. K., LUNDBÄCK, T., YEHESKIELI, E., SJÖBERG, B., GUSTAVSSON, A.-L., SVENSSON, R., OLIVERA, G. C., EZE, A. A., DE KONING, H. P. & HAMMARSTRÖM, L. G. 2013. Structure–activity relationships of synthetic cordycepin analogues as experimental therapeutics for African trypanosomiasis. *Journal of Medicinal Chemistry,* 56**,** 9861-9873.

WAGH, V. D. 2013. Propolis: a wonder bees product and its pharmacological potentials. *Advances in pharmacological sciences,* 2013.

WALLACE, F. G. 1966. The trypanosomatid parasites of insects and arachnids. *Experimental parasitology,* 18**,** 124-193.

WATSON, D. G. 2012. *Pharmaceutical Analysis: a Textbook for Pharmacy Students and Pharmaceutical Chemists,* London, Elsevier Health Sciences.

YANG, X., WANG, X., CHEN, X.-Y., JI, H.-Y., ZHANG, Y. & LIU, A.-J. 2018. Pinocembrin–Lecithin Complex: Characterization, Solubilization, and Antioxidant Activities. *Biomolecules,* 8**,** 41.

YARO, M., MUNYARD, K., STEAR, M. & GROTH, D. 2016. Combatting African animal trypanosomiasis (AAT) in livestock: the potential role of trypanotolerance. *Veterinary parasitology,* 225**,** 43-52.

ZHANG, T., OMAR, R., SIHERI, W., AL MUTAIRI, S., CLEMENTS, C., FEARNLEY, J., EDRADA-EBEL, R. & WATSON, D. 2014. Chromatographic analysis with different detectors in the chemical characterisation and dereplication of African propolis. *Talanta,* 120**,** 181-190.